The role of oxygen sensing pathways in infection and inflammation

Alfred Arthur Roger Thompson

Academic Unit of Respiratory Medicine,

Department of Infection and Immunity

Submitted towards the degree of Doctor of Philosophy,

September 2012

Acknowledgements

Summary

Many inflammatory diseases are characterised by persistent and inappropriate neutrophil activation, systemic or localised hypoxia and bacterial colonisation. Hypoxia represents an important regulator of inflammatory responses since it inhibits neutrophil apoptosis, a process central to timely resolution of inflammation. Furthermore, the oxygen sensing transcription factor, HIF-1α is a critical regulator of myeloid cell function and neutrophil survival in hypoxia. I show that HIF-2α has a distinct role from HIF-1α in regulating survival of inflammatory neutrophils. Specifically, HIF-2α was expressed in neutrophils from patients with chronic inflammatory diseases and was upregulated by inflammatory stimuli and in a mouse model of acute lung inflammation. Overexpression of HIF-2α inhibited constitutive apoptosis of human neutrophils *in vitro* and delayed resolution of inflammation in an *in vivo* model of zebrafish tailfin injury. By contrast, myeloid-specific deficiency of HIF-2α enhanced resolution of inflammation in a murine model of lung inflammation but did not impair essential neutrophil antimicrobial functions *in vitro* or *in vivo*. These findings implicate HIF-2α as a potential target for treating neutrophilic inflammation.

Infections frequently cause or complicate illnesses associated with arterial hypoxaemia and local tissue hypoxia. I investigated the effect of systemic hypoxia on host-pathogen interactions using a subcutaneous infection model in mice. Surprisingly ambient hypoxia transformed the local bacterial challenge into a phenotype of sickness behaviour and hypothermia. The mechanism responsible for this phenotype was not discovered but I found no evidence of bacteraemia, excessive cytokine production or lung injury in the hypoxic infected mice. However, there was significant circulatory dysfunction, with hypotension, bradycardia and impaired left ventricular function. These findings imply that hypoxia may adversely alter the host response to a minor bacterial challenge, leading to profound systemic illness. Interestingly, myeloid-cell deficiency of HIF-2α protected mice from the adverse systemic phenotype in this model, further supporting the potential utility of targeting HIF-2α in inflammatory disease.

Table of Contents

Table of Figures

Table of Tables

1 Introduction

1.1 Hypoxia

Oxygen is fundamentally important to living organisms. A shortage of oxygen, hypoxia, can occur systemically and at tissue or cellular levels. The millions of people who travel to high altitude each year experience whole body hypoxia as a consequence of the reduction in barometric pressure. The reduction in ambient oxygen tension feeds down the oxygen cascade as shown in Figure 1.1-1 resulting in lower levels of oxygen in body tissues. Even in health, oxygen tension at a tissue level varies depending upon the metabolic requirements of the tissue and the distance from the vascular supply (Arteel *et al.*, 1995; Maxwell *et al.*, 1989). Tissue values measured by microelectrode in rats breathing room air revealed mean values of 1.7 kPa of oxygen in the liver, 3.0 kPa in subcutaneous tissue and 4.9 kPa in the brain (Jamieson and van den Brenk, 1965). Indeed, relative hypoxia is often a physiological signal guiding important processes such as angiogenesis in wound healing (Knighton *et al.*, 1983) and maintaining pulmonary vasoconstriction *in utero* (Cassin *et al.*, 1964).

However, for most cells and tissues, severe or prolonged hypoxia will result in damage. The brain tolerates hypoxia poorly with neuronal damage occurring after 5 to 10 minutes of ischemic injury (Levy *et al.*, 1975). This is in part due to the high neuronal requirement for adenosine triphosphate (ATP), but hypoxic cellular injury is not only a result of cellular energy depletion but also due to cellular acidosis and the generation of damaging free radicals (Chen *et al.*, 2011; Erecińska and Silver, 2001; Perlman, 2007).

In disease, oxygen tensions in tissue can fall substantially. For example, lung disease leads to systemic hypoxaemia through impaired gas exchange and inadequate arterial oxygenation while vascular disease interrupts normal blood supply and results in local tissue ischemia (Agusti *et al.*, 2003). Furthermore, increased demand for oxygen will occur in infected or inflamed tissue (Kempf *et al.*, 2005).
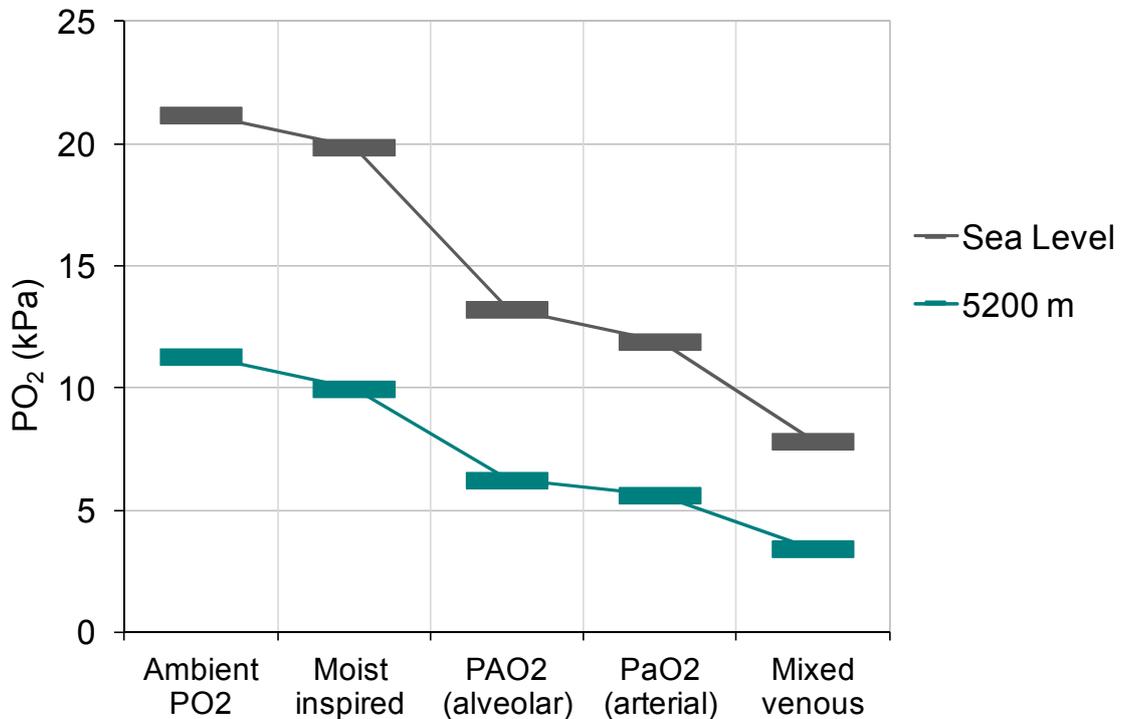
Figure 1.1-1. The oxygen cascade.

A diagram showing oxygen tensions at each step of the oxygen cascade from ambient oxygen tension to mixed venous blood oxygen tension. With ascent to altitude, barometric pressure decreases and ambient partial pressure of oxygen falls. This diagram shows calculated oxygen tensions at 5200 m and sea level. At 5200 m the ambient partial pressure of oxygen is approximately 11 kPa, compared to that at sea level where the ambient oxygen tension is 21 kPa. Adaptation to hypoxia increases ventilation, reducing the effect of dead space ventilation thus increasing the alveolar oxygen tension. Cardiac output also increases, maximising arterial oxygen tension.

The calculator used to draw this cascade was authored by JK Baillie and is available at www.altitude.org,

1.1.1 Hypoxia and disease

In the context of human disease, hypoxia is an important factor in the pathogenesis and prognosis of many conditions.

1.1.1.1 *Altitude*

In otherwise healthy humans resident at sea level, acute ascent to an altitude of 5200 m, with the corresponding drop in oxygen tensions shown in Figure 1.1-1, results in an incidence of acute mountain sickness (AMS) that approaches 60% (Dorward *et al.*, 2007). AMS is a self-limiting disorder characterised by headache and non-specific symptoms of fatigue, nausea and dizziness (Hackett and Roach, 2001). However, life-threatening pathologies such as high altitude pulmonary oedema (HAPE) and high altitude cerebral oedema (HACE) may also occur following acute ascent, with HAPE having a reported incidence of up to 2% at 4000 m (Hackett and Roach, 2001; Schoene, 2008). The pathogenesis of these disorders is incompletely understood but adequate acclimatisation effectively ameliorates the risk of these conditions (Bartsch, 1999; Basnyat and Murdoch, 2003). Such a strategy cannot be employed to prevent the hypoxic complications of sea level diseases.

1.1.1.2 *Lung disease*

Chronic respiratory conditions were reported by 6.4% of UK adults in 2004, with an estimated 3 million patients in the UK having chronic obstructive pulmonary disease (BTS, 2006; HealthcareCommission, 2006). Lung disease may lead to alveolar hypoxia through hypoventilation or increased dead space and arterial hypoxia through a reduction in the diffusing capacity for oxygen (Wagner and West, 2005). Indeed patients with advanced chronic obstructive pulmonary disease (COPD) frequently have arterial oxygen tensions less than 7.3 kPa, evidenced by the 865,000 prescriptions for oxygen issued in primary care in 2004 (BTS, 2006). This threshold of arterial oxygen tension used as an indication for long term oxygen treatment was extrapolated from data acquired during two major trials of domiciliary oxygen

treatment. The MRC trial of domiciliary oxygen use demonstrated a reduction in mortality in hypoxaemic patients receiving oxygen treatment for more than 15 hours per day (MRC, 1981) and in a similar cohort of patients the NOTT trial showed a significant mortality benefit from continuous rather than nocturnal oxygen therapy (NOTT, 1980). Interestingly, the physiological benefits of receiving this supplemental oxygen were not clear but reductions in haematocrit and improvements in pulmonary haemodynamic measurements were demonstrated (MRC, 1981; NOTT, 1980). Other studies have shown that low arterial oxygen tension and mixed venous oxygen saturation in COPD patients predict poor outcome and risk of acute exacerbation requiring hospitalization (Kawakami *et al.*, 1983; Kessler *et al.*, 1999).

COPD and other chronic lung conditions such as cystic fibrosis may also predispose to areas of local tissue hypoxia within the lung (Hamedani *et al.*, 2011). Airway obstruction, mucus hypersecretion and bacterial colonization will reduce oxygen tension. Indeed, pO_2 measurements as low as 0.33 kPa were reported in infected mucopurulent collections in the airways of patients with cystic fibrosis (Hamedani *et al.*, 2011; Worlitzsch *et al.*, 2002).

1.1.1.3 Critical care

Acute or chronic lung diseases are often contributing factors in the hypoxaemia frequently evident in critically ill patients (Simpson *et al.*, 2005). Patients with acute respiratory distress syndrome (ARDS) or pneumonia may be hypoxaemic despite aggressive ventilation, with ventilation potentially perpetuating lung injury (ARDSN, 2000; Matthay and Zemans, 2011). Sepsis, the presence of the systemic inflammatory response syndrome (SIRS) due to infection (Bone *et al.*, 1992), is another important cause of admissions to critical care. Due to the high prevalence of respiratory infection underlying the diagnosis of sepsis and the frequency of respiratory failure associated with it, hypoxaemia is common in this disorder (Alberti *et al.*, 2002; Martin *et al.*, 2003; Stearns-Kurosawa *et al.*, 2011). In sepsis, tissue hypoxia in sepsis may result from impaired oxygen extraction and abnormalities of the microcirculation even

with normal arterial oxygenation (Anning *et al.*, 1999; Spronk *et al.*, 2004). Importantly, in the context of severe sepsis, respiratory failure was an independent predictor of mortality (Guidet *et al.*, 2005).

1.1.1.4   Local hypoxia

While causes of systemic hypoxaemia may result in widespread tissue hypoxia, more localised reductions in oxygen tension are also found in the context of infection, inflammation and cancer and have been implicated in disease pathogenesis and severity. In a rabbit model of empyema, oxygen tensions of less than 3kPa were found in the infected empyema cavity (Shohet *et al.*, 1987) while in a mouse model of inflammatory bowel disease the gut epithelium, which is relatively hypoxic in health, displays evidence of significantly greater hypoxia when inflamed (Karhausen *et al.*, 2004). Synovial fluid from inflamed human joints had oxygen tensions of less than 3kPa (Ng *et al.*, 2010). Interestingly, the study by Ng et al. found a direct correlation between synovitis and oxygen tension and higher levels of inflammatory cytokines in hypoxic synovial fluid (Ng *et al.*, 2010). Tumours often have necrotic centres with penumbral hypoxia and hypoxia has been implicated in cancer metastasis, poor prognosis and resistance to radiotherapy (Brahimi-Horn *et al.*; Vaupel, 2004; Vaupel *et al.*, 1991; Welsh and Powis, 2003).

1.1.2 Adaptation to hypoxia

Over the course of evolution, mechanisms of compensating for oxygen deprivation have developed. In humans, hypoxia rapidly induces an increase in heart rate and ventilation to maintain oxygen delivery (Honig and Tenney, 1957; Keys *et al.*, 1943; Rahn and Otis, 1949). If hypoxia is sustained for days, erythropoesis will occur. Indeed the erythropoetic effect of high altitude, first observed by Viault, is perhaps the best known adaptation to systemic hypoxia (Viault, 1890). After 23 days at 4392 m, with an ambient oxygen tension equivalent to 60 % of that at sea level, he found a rise of 3 million red cells per cubic millimetre of his blood (Viault, 1890). Investigation of the regulation of erythropoietin (EPO), the hormone responsible for Viault's observation, led to the discovery of one of the key regulators of cellular adaptation to hypoxia, the nuclear transcription factor, hypoxia inducible factor (HIF) (Semenza and Wang, 1992). HIF and the regulatory components of the HIF pathway are not unique to mammals. Homologs of HIF have been found in corals, nematodes, beetles and flies, demonstrating the importance of this ancient pathway in oxygen sensing across diverse species and habitats (Hampton-Smith and Peet, 2009; Taylor and McElwain, 2010).

In mammals, HIF is a heterodimeric protein consisting of α and β subunits (Wang and Semenza, 1995). The β subunit, the aryl hydrocarbon receptor nuclear transporter (ARNT), is constitutively expressed while the α subunits are regulated by a family of oxygen-sensitive enzymes (Bruick and McKnight, 2001; Epstein *et al.*, 2001; Wang *et al.*, 1995) Under hypoxic conditions these enzymes are inhibited, HIF-α subunits accumulate, translocate to the nucleus and dimerize with ARNT. HIF dimers bind to genes that contain the core DNA sequence, 5'-RCGTG-3', known as the hypoxic response element (HRE) (Semenza *et al.*, 1996). HIF target genes have a broad range of functions, but many aim to preserve cell survival or restore oxygen delivery (Kaelin and Ratcliffe, 2008).

1.1.3   Hypoxia and the innate immune system

Of the three known HIF-α subunits, HIF-1α has been studied in most detail and its role extends far beyond controlling cellular adaptation to hypoxia. Cramer *et al.* showed that HIF-1α is a critical regulator of the innate immune system (Cramer *et al.*, 2003).   Although sites of inflammation are often hypoxic, HIF-1α can be stabilised in myeloid cells activated by bacterial stimuli independent of oxygen tension (Peyssonnaux *et al.*, 2005) .

I will now discuss the importance of hypoxia and oxygen-sensing pathways in the innate immune system, specifically focussing on neutrophils.   These short-lived effector cells undergo apoptosis to safely dispose of their potent cytotoxic armaments, but if neutrophil survival is prolonged, resolution of inflammation is delayed resulting in damage to surrounding tissues (Dransfield and Rossi, 2004; Rossi *et al.*, 2006; Savill, 1997). Hypoxia, in contrast to its effects on many other cells, is a profound neutrophil survival stimulus (Walmsley *et al.*, 2005). However, the effects of hypoxia on neutrophil pro-inflammatory functions are not well characterised. HIF-1α has been implicated in the control of neutrophil survival and function but the role of the structurally related transcription factor, HIF-2α, is not known (Walmsley *et al.*, 2005). I will therefore discuss the biology of HIF-2α and the evidence that it has a role distinct from HIF-1α will be explored.   The wider interactions between hypoxia and the host response to bacterial infection will also be considered and I will conclude this chapter with a description of the aims of the experimental work in this thesis.

1.2   Neutrophilic inflammation

Neutrophils are vital components of the innate immune system and the first cells to migrate to sites of inflammation or tissue damage. They are recruited by the release of chemoattractants from activated macrophages, epithelial cells and bacteria, and transmigrate across the capillary epithelium to enter the injured or infected tissue (Kelly *et al.*, 2007; Nourshargh and Williams, 1995). Neutrophils have impressive cytotoxic abilities including phagocytosis, the respiratory burst and the release of granule proteases (Borregaard *et al.*, 2007; Dinauer, 2005; Dransfield and Rossi, 2004). Furthermore, through the secretion of inflammatory mediators, neutrophils are capable of modulating the immune response (Borregaard *et al.*, 2007; Dransfield and Rossi, 2004). Neutrophils are short-lived and undergo constitutive apoptosis (Savill *et al.*, 1989). Apoptosis allows neutrophils to retain their granule contents and reduces chemotaxis, phagocytosis and the respiratory burst (Whyte *et al.*, 1993). Apoptosis also promotes recognition and removal of neutrophils by macrophages which then restore normal tissue homeostasis (Savill *et al.*, 1989).   Inhibition of apoptosis will therefore impair the resolution of inflammation and may result in tissue damage (see Figure 1.2-1) (Rossi *et al.*, 2006; Savill, 1997; Vissers and Wilkie, 2007). Indeed, persistent neutrophilic inflammation has been implicated in numerous disease processes including COPD (Quint and Wedzicha, 2007), asthma (Barnes, 2007), lung fibrosis (Gharaee-Kermani *et al.*, 2007), cystic fibrosis (Elizur *et al.*, 2008), inflammatory bowel disease (Taylor and Colgan, 2007), inflammatory arthritis (Cross *et al.*, 2006) and atherosclerosis (Zernecke *et al.*, 2008).
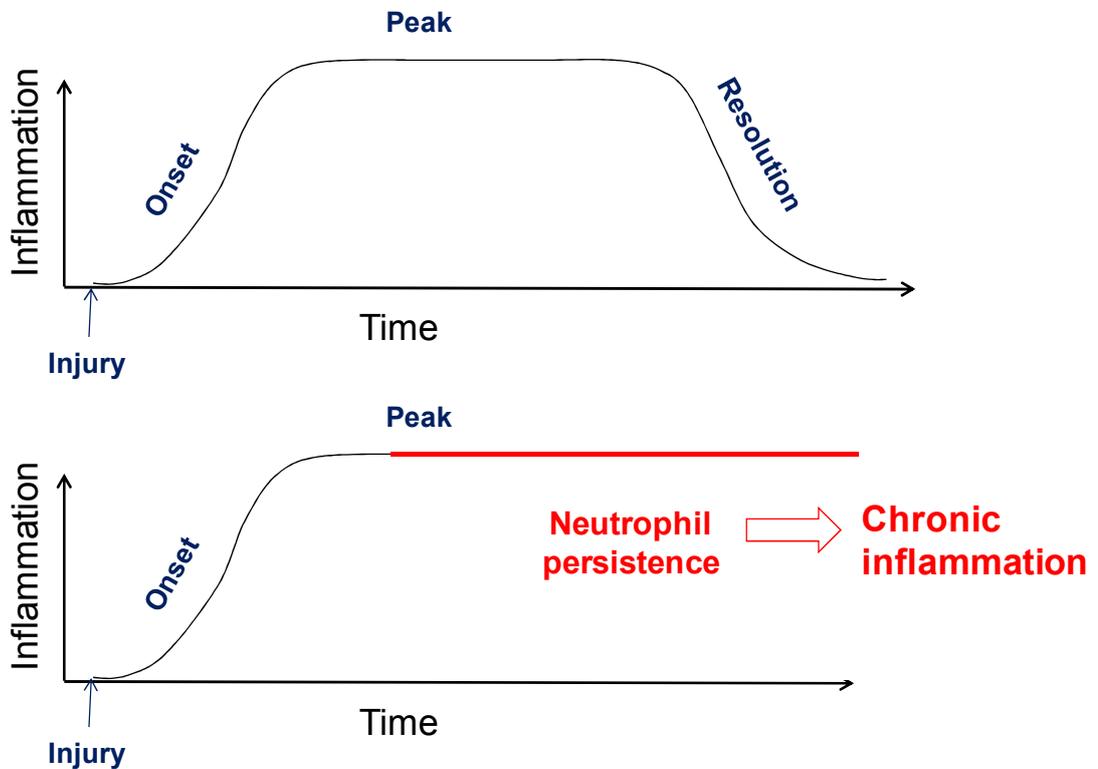
Figure 1.2-1. Neutrophilic inflammation.

A diagram showing the phases of neutrophilic inflammation. Following an injurious stimulus, neutrophils are recruited and perform their anti-microbial and immunomodulatory functions. In the top panel the resolution of this acute inflammatory response requires timely neutrophil apoptosis followed by clearance by macrophages and the restoration of normal tissue homeostasis. The bottom panel depicts delayed apoptosis favouring persistence of neutrophils and leading to chronic inflammation. This schematic was based on a diagram from Serhan *et al.* (2007).

1.2.1   Neutrophil apoptosis

Timely neutrophil death and clearance are essential for the resolution of inflammation and safe disposal of the neutrophils' potentially damaging contents (Haslett, 1999). Neutrophils are inherently short-lived being genetically programmed to undergo spontaneous apoptosis even at sites of inflammation (Savill *et al.*, 1989). Apoptotic neutrophils display characteristic morphological features such as nuclear fragmentation, chromatin condensation and cell shrinkage and biochemical changes such as the exposure of phosphatidylserine on the outer plasma membrane and cleavage of DNA and chromatin (Martin *et al.*, 1995; Savill *et al.*, 1989). Apoptosis is thus clearly distinct from necrosis, which is characterised by increased cell volume, loss of membrane integrity and cell lysis (Wyllie *et al.*, 1980).

Neutrophil apoptosis is not only triggered by classical intrinsic and extrinsic pathways, but the involvement of reactive oxygen species and granule proteases has also been demonstrated. The intrinsic pathway is characterised by mitochondrial outer membrane permeabilisation resulting in release of cytochrome C and leading to assembly of the apoptosome with subsequent caspase 9 activation (Green and Kroemer, 2004). The integrity of the mitochondrial outer membrane is controlled by the BCL-2 family of proteins. Neutrophils express both anti-apoptotic (MCL-1, BCL-XL, A1) and pro-apoptotic (BAX, BAK) members of this family (Bianchi *et al.*, 2006; Witko-Sarsat *et al.*, 2011). The apoptosis inducers, BAX and BAK, insert into the mitochondrial membrane but are inhibited when in complex with anti-apoptotic BCL-2 family members. Interestingly, the expression of anti-apoptotic BCL-2 family members is lower in mature neutrophils than in neutrophil precursors (Geering and Simon, 2011; Theilgaard-Monch *et al.*, 2005). Thus this pathway is implicated in the control of constitutive apoptosis characteristic of mature neutrophils.

Extrinsic signals triggering apoptosis are typified by death receptor pathway signalling. Ligation of receptors by Fas ligand (FasL), TNF-related apoptosis inducing ligand (TRAIL) and,

under certain conditions, tumour necrosis factor (TNF)-α induce neutrophil apoptosis via the generation of a death-induced signalling complex (DISC) and subsequent caspase 8 activation. Importantly, inflammatory neutrophils retain susceptibility to apoptosis triggered by extrinsic stimuli (Renshaw *et al.*, 2000). Both intrinsic and extrinsic pathways culminate in downstream activation of effector caspases which lead to apoptosis (Kothakota *et al.*, 1997).

An important feature of neutrophil anti-bacterial function is their capacity to produce reactive oxygen species (ROS). ROS have been implicated in the activation of the intrinsic apoptosis pathway (Arruda *et al.*, 2006) and they may also activate the extrinsic pathway independently of receptor ligation (Scheel-Toellner *et al.*, 2004). ROS may also directly lead to neutrophil apoptosis by damaging DNA and activating the pro-apoptotic p53 pathway (Ye *et al.*, 1999). Evidence of their role in spontaneous neutrophil apoptosis comes from experiments using antioxidants, which delay constitutive apoptosis, but importantly also from patients with chronic granulomatous disease (Kasahara *et al.*, 1997). These patients have defects in NADPH-oxidase that lead to impaired or absent ROS production and, as a result, increased susceptibility to bacterial and fungal infections (Dinauer, 2005). Neutrophils from these patients have significantly lower rates of constitutive apoptosis (Kasahara *et al.*, 1997).

While neutrophils undergo apoptosis constitutively, numerous stimuli prolong their lifespan. Inflammatory stimuli are key mediators of delayed neutrophil apoptosis. As neutrophils migrate into inflamed or infected tissue bacterial and viral stimuli, signalling via toll-like receptors, promote neutrophil survival (Francois *et al.*, 2005). Furthermore, inflammatory cytokines including IL-1β, IFN-γ, G-CSF and GM-CSF also delay neutrophil apoptosis (Colotta *et al.*, 1992; Maianski *et al.*, 2004b). Signals from the local inflammatory microenvironment are therefore of critical importance in the regulation of neutrophil persistence. Another such signal, characteristic of inflammatory sites, is hypoxia.

1.2.2 Hypoxia enhances neutrophil survival

Hypoxia is a characteristic feature of inflammatory sites and many tumours (Bertout *et al.*, 2008; Brahimi-Horn *et al.*, 2007). Neutrophils need to function at these hypoxic sites and are well adapted for this purpose by relying mainly on glycolysis to generate ATP (Levene and Meyer, 1912; Maianski *et al.*, 2004a; Sbarra and Karnovsky, 1959). Indeed, in contrast to its effects on many other cell types, hypoxia is a profound neutrophil survival stimulus (Hannah *et al.*, 1995).

1.2.3 Neutrophil survival in hypoxia requires HIF-1α

Walmsley *et al.* demonstrated that HIF-1α was necessary for inhibition of neutrophil apoptosis by hypoxia (Walmsley *et al.*, 2005). HIF-1α deficient bone marrow-derived neutrophils showed markedly reduced survival in anoxia, while the HIF stabiliser, dimethyloxalylglycine (DMOG) promoted survival (Walmsley *et al.*, 2005). Supernatant transfer experiments also demonstrated hypoxic induction of a pro-survival factor, identified as macrophage inflammatory protein-1β (Walmsley *et al.*, 2005). In contrast to the direct survival effect of hypoxia, this transferrable effect was dependent on phosphoinositide 3-kinase signalling.

1.2.4 Neutrophil function in hypoxia

The effects of hypoxia on neutrophil function have been less well characterised. Experimental conditions in published studies have varied widely making conclusions difficult. This is because the method of neutrophil isolation and even the anticoagulant used influences neutrophil function and must always be considered when interpreting *ex vivo* data (Dransfield and Rossi, 2004; Engstad *et al.*, 1997; Freitas *et al.*, 2008; Haslett *et al.*, 1985).

Existing data suggest that neutrophil function is preserved and possibly enhanced by hypoxia. Neutrophils isolated from the blood of healthy volunteers following an acute episode of systemic hypoxaemia (arterial oxygen saturation <70%) showed enhanced elastase release in response to the bacterial peptide, N-formyl-L-methionyl-L-leucyl-L-phenylalanine (fMLP) (Tamura *et al.*, 2002). Wang *et al.* exposed subjects to normobaric hypoxia for 2 hours and found, using *ex vivo* assays, that 12% oxygen resulted in enhanced chemotaxis, respiratory burst and phagocytosis (Wang and Liu, 2009). However, in theory the effects observed in both of these studies could have been due to reoxygenation of the neutrophils during isolation.

1.2.4.1 *Phagocytosis*

Neutrophils cultured in hypoxic conditions (PO_2 in media ≈3kPa), for 1 hour demonstrated increased phagocytosis of heat-inactivated *Streptococcus pneumoniae* compared to those cultured in normoxia (PO_2 ≈20kPa) (Walmsley *et al.*, 2006). Similar findings were reported when whole blood was rendered hypoxaemic *in vitro* (PO_2<2kPa) (Simms and D'Amico, 1994). The percentage of neutrophils positive for opsonised fluorescent microspheres was significantly greater than in normoxic venous blood (PO_2 8-10kPa) (Simms and D'Amico, 1994).

1.2.4.2 *Chemotaxis and transmigration*

Previous studies on the effect of hypoxia on neutrophil chemotaxis have yielded conflicting results. Studies using Boyden chambers suggested that neutrophil chemotaxis was inhibited at oxygen tensions of around 3kPa but Wang et al. found that chemotaxis was enhanced following systemic exposure to hypoxia (Rotstein *et al.*, 1988; Wang and Liu, 2009). Differences in the experimental protocols and chemoattractant used may explain these differences. For example Wang et al. isolated neutrophils from subjects exposed to hypoxia and used fMLP as the chemoattractant, but the assay was carried out in normoxic conditions (Wang and Liu, 2009). More recent data revealed no difference in chemotaxis of human neutrophils through a 5 µm filter under hypoxic conditions (PO_2 in media ≈3kPa) (McGovern *et*

al., 2011). Furthermore hypoxia had no effect on the expression of chemokine receptors or on the capacity for neutrophils to undergo shape change (McGovern *et al.*, 2011). However, hypoxia led to the upregulation of the adhesion molecule CD11b and has been shown to enhance transmigration across the endothelium of blood vessels through both neutrophil and endothelial cell receptor regulation (Colgan *et al.*, 1996; Kong *et al.*, 2004; Meyer *et al.*, 2007). Consistent with hypoxia enhancing the mechanisms responsible for transmigration, culture in hypoxia for 4 hours enhanced elastase release from primed neutrophils stimulated with fMLP (McGovern *et al.*, 2011; Tamura *et al.*, 2002). While enhanced elastase release may facilitate tissue infiltration and elastase is important for host defence in gram negative sepsis, it also has the potential to damage healthy tissue and has been implicated in the pathogenesis of lung injury (Belaaouaj *et al.*, 1998; Kaynar *et al.*, 2008; Lee and Downey, 2001).

1.2.4.3   *Respiratory burst*

While phagocytosis and chemotaxis appear to be preserved in hypoxic conditions, defects in neutrophil respiratory burst have been observed. The respiratory burst is the chemical generation of free radicals by the multi-component phagocyte NADPH oxidase enzyme and is an important anti-microbial function of neutrophils (Roos *et al.*, 2003). McGovern et al. demonstrated that extracellular superoxide generation by primed neutrophils in response to stimulation with fMLP was reduced in hypoxia. Neutrophils stimulated with phorbol 12-myristate 13-acetate (PMA) also had impaired generation of extracellular superoxide and intracellular oxidant generation was significantly reduced with either PMA or opsonized zymosan stimulation (McGovern *et al.*, 2011). Importantly, the profound impairment of respiratory burst was not associated with a reduction in NADPH-oxidase components in hypoxia (McGovern *et al.*, 2011). Pyocyanin, a phenazine pigment exotoxin secreted by *Pseudomonas aeruginosa*, induces an accumulation of intracellular oxidants independent of NADPH-oxidase but involving direct oxidation of NADPH and NADH (Muller *et al.*, 1989; O'Malley *et al.*, 2004; Prince *et al.*, 2008; Reszka *et al.*, 2004). ROS generation in response to

pyocyanin was significantly inhibited in hypoxia indicating that impaired ROS production in hypoxia was independent of NADPH-oxidase (McGovern *et al.*, 2011). This and the fact that restoration of oxygen tension to normoxic levels reinstated the ability of neutrophils to produce ROS suggest it is the lack of molecular oxygen that leads to deficiency of ROS production in hypoxia. Critically, hypoxia impaired the ability of neutrophils to kill certain bacteria. Killing of *Staphylococcus aureus*, but not *Escherichia coli,* was impaired in hypoxia (McGovern *et al.*, 2011). The selective defect in killing of *S. aureus* was mirrored by NADPH-oxidase inhibition, suggesting that while killing of *S. aureus* requires intact ROS generation, other ROS-independent mechanisms are sufficient for effective killing of *E. coli* (McGovern *et al.*, 2011).

1.2.5   HIF-1α is a key regulator of myeloid cell function

Although the effect of hypoxia on neutrophil function requires further study, the oxygen sensing transcription factor HIF-1α has been shown to be a key regulator of myeloid cell function and survival. As discussed above, Walmsley *et al.* showed that HIF-1α was essential for neutrophil survival in hypoxia (Walmsley *et al.*, 2005). Furthermore, using mice with targeted deletion of the HIF-1α or VHL genes in myeloid cells (macrophages and neutrophils), Randall Johnson's group elegantly demonstrated that HIF-1α is vital to the innate immune response.

Cramer *et al.* showed that HIF-1α deficient myeloid cells had reduced levels of intracellular ATP in normoxic culture (Cramer *et al.*, 2003). Functions dependent on ATP generation such as macrophage motility and invasion were significantly inhibited (Cramer *et al.*, 2003). Although macrophage phagocytosis was not affected, bactericidal capacity was markedly reduced (Cramer *et al.*, 2003). HIF-1α deficiency did not impair neutrophil transmigration across a pulmonary endothelial cell monolayer or respiratory burst but significant reductions in granule

protease production and levels of cathelecidin-related antimicrobial peptide were demonstrated (Peyssonnaux *et al.*, 2005). These studies also demonstrated that bacteria and LPS led to stabilisation of HIF-1α protein in macrophages independent of oxygen tension (Peyssonnaux *et al.*, 2005). A summary of myeloid cell functions dependent upon HIF-1α is shown in Figure 1.2-2.

Importantly, these *in vitro* findings were substantiated by *in vivo* models of infection and inflammation. Cutaneous myeloid cell infiltration and tissue oedema in an *in vivo* model of acute inflammation was greatly reduced in HIF-1α deficient mice, but was increased in VHL deficient mice (Cramer *et al.*, 2003). Group A streptococcal skin infection was also more severe in HIF-1α deficient mice, with larger necrotic lesions and greater weight loss than wild-type mice (Peyssonnaux *et al.*, 2005). Interestingly, HIF-1α deficient mice were less susceptible to LPS-induced sepsis with less clinical evidence of haemodynamic compromise and reduced mortality (Peyssonnaux *et al.*, 2007). HIF-1α deficient mice in this model produced lower levels of the inflammatory cytokines, tumour necrosis factor-α (TNF-α) and interleukin-6 (Peyssonnaux *et al.*, 2007).

Other groups have also shown that HIF-1α activation modifies the immune response. Vissers *et al.* isolated neutrophils from mice lacking ascorbate oxidase (Vissers and Wilkie, 2007). These ascorbate deficient neutrophils had elevated levels of HIF-1α and, consistent with the findings in hypoxia, had delayed rates of apoptosis (Vissers and Wilkie, 2007). Furthermore, ascorbate deficient neutrophils aged *in vitro* were not phagocytosed by macrophages and an *in vivo* model suggested that resolution of inflammation was delayed (Vissers and Wilkie, 2007).

The mechanism by which HIF-1α regulates innate immune cell function may extend beyond its direct ability to modulate gene expression. For example, there is also evidence of important cross-talk between HIF-1α and another transcription factor, nuclear factor kappa-light-chain-enhancer of activated B cells (NF-κB)(Rius *et al.,* 2008; Taylor, 2008). NF-κB is itself a master-

regulator of inflammation and is implicated in the control of neutrophil apoptosis and function (Hsu *et al.*, 2011; Ward *et al.*, 1999). As will be discussed later, NF-κB regulates HIF-1α transcription and may itself be regulated by HIF-1α (van Uden *et al.*, 2008; Walmsley *et al.*, 2005).
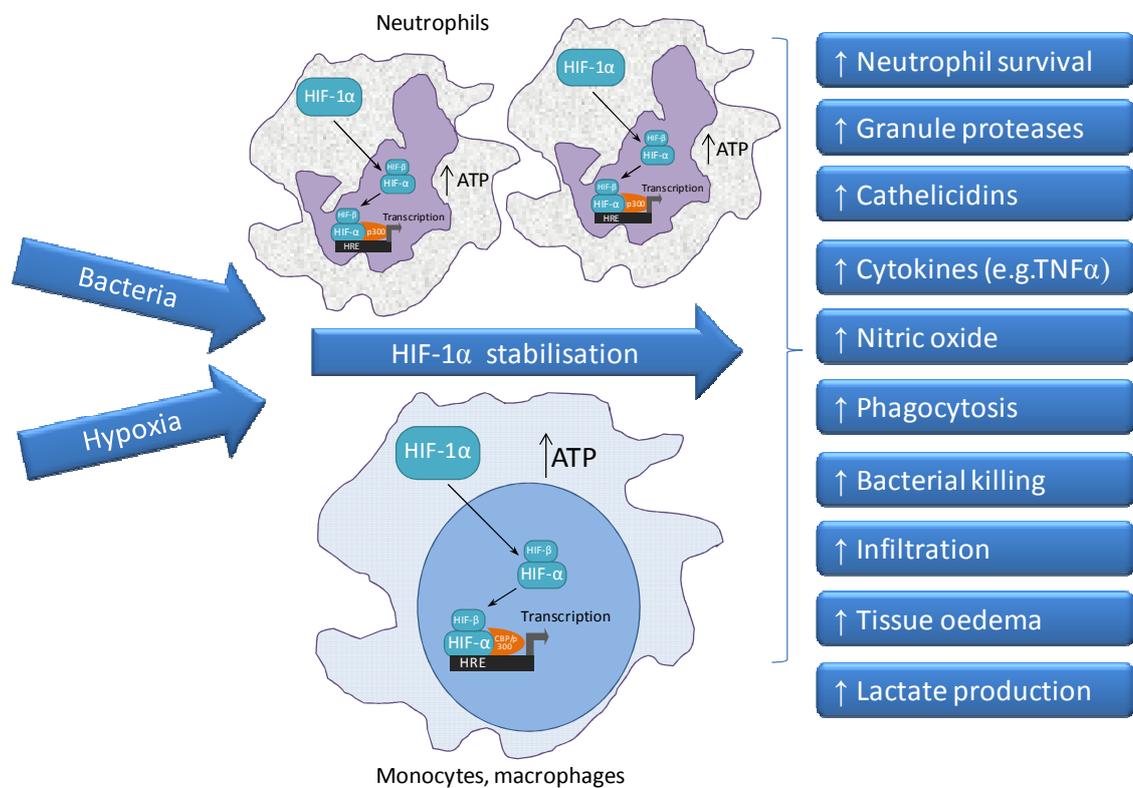
Figure 1.2-2. HIF-1α is a key regulator of myeloid cell function.

Bacterial stimuli, hypoxia or both lead to stabilization of HIF-1α subunits in innate immune cells. As a result transcription of hypoxia responsive genes is upregulated and in turn glycolytic activity of the cells is enhanced. Studies have shown increases in a range of myeloid cell functions listed on the right hand side of the figure.

Furthermore patients with activation of HIF-pathways, for example patients with heterozygous mutation of the *VHL* gene (encoding the von Hippel Lindau protein responsible for HIF-α degradation) have been shown to exhibit a distinct neutrophil phenotype compared to healthy controls with delayed rates of constitutive apoptosis and enhanced phagocytic capacity (Walmsley *et al.*, 2006). This provides direct evidence that the HIF pathway influences human neutrophil survival and function.

1.2.6   Evidence of a distinct role for HIF-2α in myeloid cells

Recent evidence has emerged that suggests that another HIF-α subunit, HIF-2α has a distinct role from HIF-1α in controlling nitric oxide (NO) homeostasis in macrophages. Takeda et al. showed that murine bone marrow derived macrophages (BMDMs) polarised to the M1 phenotype (or classically activated) using lipopolysaccharide or Th1 cytokines such as interferon-gamma upregulated HIF-1α expression (Takeda *et al.*, 2010). On the other hand, BMDMs polarised to the M2 phenotype (or alternatively activated) using Th2 cytokines such as interleukin-4 or interleukin-13 upregulated HIF-2α expression. Interestingly, this differential activation of the HIF-α subunits led to differences in NO synthesis. Inducible nitric oxide synthase (iNOS), the enzyme responsible for NO synthesis from L-arginine and a known HIF-1α target gene (Peyssonnaux *et al.*, 2005), was upregulated in M1 polarised macrophages while arginase-1, an enzyme which competes for L-arginine, was upregulated in M2 polarised macrophages under the regulation of HIF-2α (Takeda *et al.*, 2010).

Given the importance of the HIF pathway in myeloid cells and emerging evidence of a distinct role for the structurally similar HIF-2α subunit, the biology of the HIF-α subunits will be discussed and known differences between HIF-1α and HIF-2α reviewed.

1.3 HIF-α subunits – regulation and roles

Three HIF-α subunits have been identified and while the most studied to date has been HIF-1α, emerging evidence has a distinct role for the structurally similar HIF-2α subunit.   HIF-2α, also known as EPAS-1, HIF-1α-like factor (HLF), HIF-related factor (HRF) and member of PAS superfamily 2 (MOP2), was identified by several groups searching for novel proteins similar to HIF-1α (Ema *et al.*, 1997; Flamme *et al.*, 1997; Tian *et al.*, 1997). The structure of the HIF-α and β subunits is shown in Figure 1.3-1.

1.3.1 Regulation of HIF-α subunits

HIF-α subunits are predominantly regulated at the protein level by a family of hydroxylase enzymes (HIF-hydroxylases) which require oxygen, 2-oxoglutarate, iron (Fe(II)) and for maximal activity, ascorbate (Bruick and McKnight, 2001; Knowles et al., 2003; Lando et al., 2002). The concentration of oxygen required for half-maximal activity of these enzymes (KM 90-230 µM) is well above that in human tissues (10-30 µM), so the activity of the HIF-hydroxylases will fluctuate across the physiological range of oxygen tension *in vivo* (Ehrismann et al., 2007; Tuckerman et al., 2004). However, as the expression of HIF-α subunits varies in different cell types even when oxygen is available, activity of the HIF-hydroxylases at a given oxygen tension may be limited by other factors.
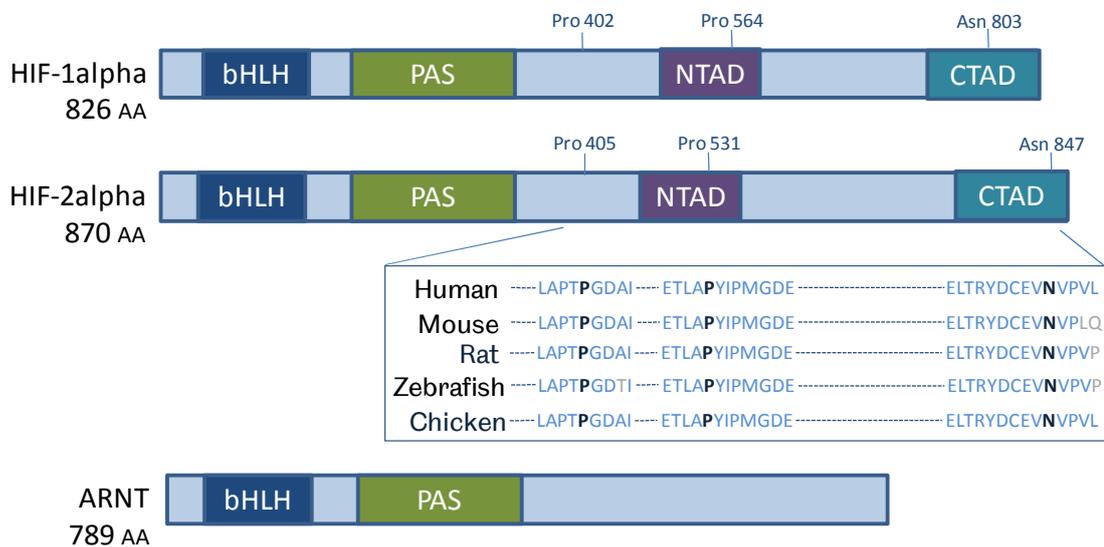
Figure 1.3-1. Structure of HIF-α and HIF-β subunits.

A schematic drawing of the structures of HIF-1α, HIF-2α and HIF-β subunits. HIF-3α is not included. HIF-α subunits contain basic-helix-loop-helix (bHLH) and period-ARNT-sim (PAS) domains and their amino acid sequences display a high degree of homology (Hu *et al.*, 2003; Tian *et al.*, 1997). In humans, the bHLH DNA binding domain of HIF-2α is 85% similar to HIF-1α and the PAS domains, important for dimerization with ARNT, are 70% similar (Hu *et al.*, 2003). HIF-α subunits have two transcriptional activation domains (TADs) termed the N-terminal TAD (N-TAD) and C-terminal TAD (C-TAD) (O'Rourke *et al.*, 1999; Patel and Simon, 2008). The inset shows the conservation across species of the asparaginyl (Asn) and prolyl (Pro) residues on HIF-2α that are hydroxylated by factor inhibiting-HIF (FIH) and the prolyl hydroxylase (PHD) enzymes respectively.

1.3.1.1   The prolyl hydroxylases (PHDs)

Hydroxylation of highly conserved prolyl residues (see Figure 1.3-1) by prolyl hydroxylase domain-containing enzymes (PHDs) allows HIF-α subunits to bind to the von Hippel Lindau protein (pVHL) (Ivan *et al.*, 2001; Jaakkola *et al.*, 2001; Masson *et al.*, 2001). The pVHL forms part of an E3 ubiquitin ligase complex and binding of this complex leads to ubiquitination of the HIF-α subunit, marking it for proteasomal destruction; see Figure 1.3-2 (Maxwell *et al.*, 1999). Four PHD enzymes have been identified (PHD1-4) (Bruick and McKnight, 2001; Epstein *et al.*, 2001; Koivunen *et al.*, 2007). They are widely expressed but for each enzyme levels of RNA may vary considerably according to cell type and the pattern of localisation within a cell is distinct (Kaelin and Ratcliffe, 2008; Lieb *et al.*, 2002; Metzen *et al.*, 2003). *In vitro* experiments have suggested that PHD-2 is the main regulator of HIF-1α, but this may be because PHD-2 is the most abundant PHD in most cells under normoxic culture conditions (Appelhoff *et al.*, 2004; Berra *et al.*, 2003).

Importantly, differences in substrate specificity of the PHD enzymes have been described. For example, data suggest that PHD-3 preferentially degrades HIF-2α (Appelhoff *et al.*, 2004). In normoxic conditions, suppression of PHD-3 stabilised HIF-2α to a greater extent than HIF-1α and suppression of PHD-2 did not prevent degradation of HIF-2α following re-oxygenation of hypoxic cells (Appelhoff *et al.*, 2004). Thus, as the PHD enzymes catalyse only the forward reaction, the relative abundance of the different enzymes within a cell may be a key mechanism by which differential regulation of the HIF-α subunits occurs.
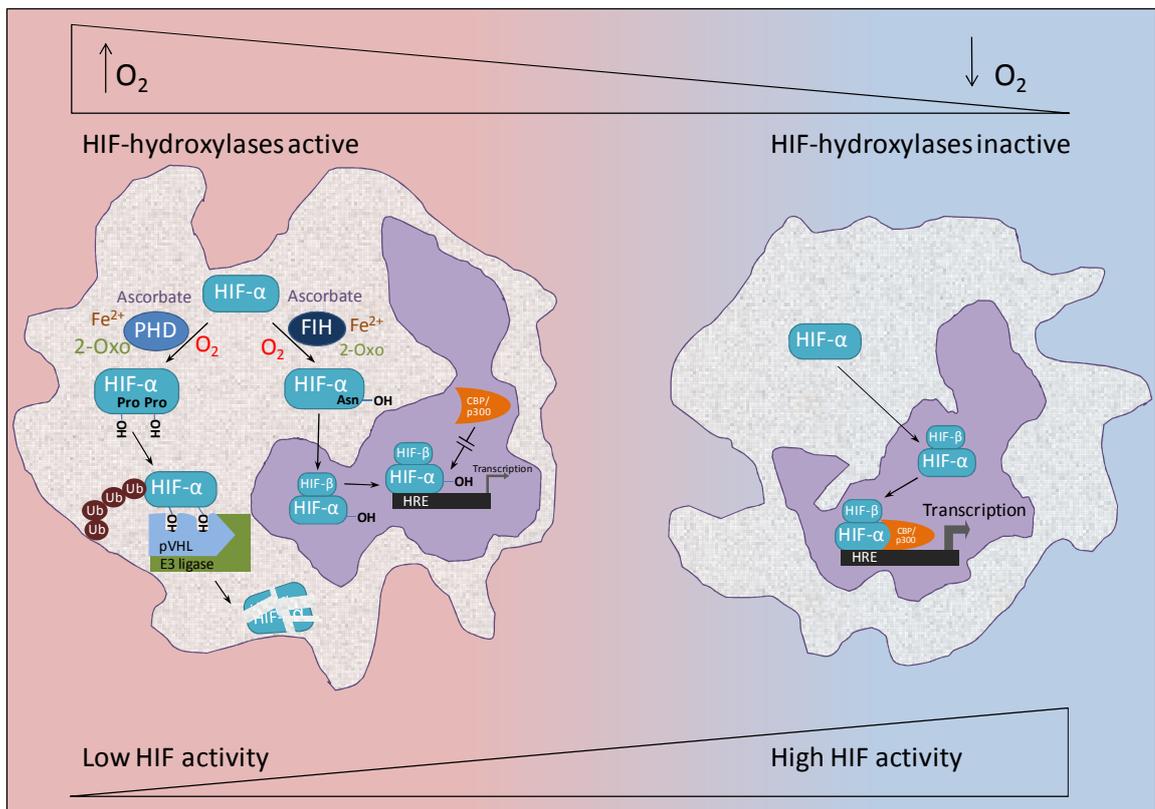
Figure 1.3-2. Post-translational regulation of HIF-α subunits.

In normoxia, HIF-α subunits are subject to hydroxylation by prolyl hydroxylase (PHD) enzymes and factor inhibiting-HIF (FIH). These enzymes require oxygen (O_2) and 2-oxolglutarate (2-Oxo) as substrates and their activity also depends on availability of iron (Fe^{2+}) and ascorbate. PHD enzymes hydroxylate prolyl (Pro) residues allowing the von Hippel Lindau protein (pVHL) to bind to the HIF-α subunits. An E3 ligase complex then forms leading to ubiquitination (Ub) and subsequently degradation by the proteasome. FIH hydroxylates (OH) an asparaginyl (Asn) residue in the C-terminal transactivation domain (CTAD), preventing recruitment of the co-activators CBP/p300 and thus inhibiting transcription of HIF-target genes. In hypoxia, the HIF-hydroxylases are less active allowing stable HIF-α subunits to dimerize with HIF-β, bind to hypoxic response elements (HRE), recruit the co-activators and upregulate transcription.

1.3.1.2 Factor inhibiting HIF (FIH)

One asparaginyl hydroxylase has been identified in humans, factor-inhibiting HIF (FIH) (Lando *et al.*, 2002). Hydroxylation of a conserved asparaginyl residue in the CTAD prevents interaction with the co-activators, creb-binding protein (CBP)/p300 and therefore deactivates HIF-mediated transcription; see Figure 1.3-2 (Lando *et al.*, 2002).

FIH hydroxylates ankyrin repeat domains, which exist in many proteins (Cockman *et al.*, 2009). FIH may therefore be competitively inhibited by these proteins depending upon their hydroxylation status (Cockman *et al.*, 2009; Webb *et al.*, 2009). However, FIH may play a less important role in HIF-2α regulation as its CTAD has been shown in vitro to be more resistant to the effect of FIH than the CTAD of HIF-1α (Bracken *et al.*, 2006; Yan *et al.*, 2007).

1.3.1.3 Regulation of the HIF-hydroxylases

The finding of stable HIF-α subunits in cells where oxygen is readily available suggests other factors involved in HIF-hydroxylase activity may become limiting (Maxwell, 2005; Schofield and Ratcliffe, 2004). For example, iron chelation is known to limit HIF-hydroxylase activity, but more recent data have shown that non-hypoxic stabilisation of HIF-1α in a myeloid cell line was associated with changes in the intracellular labile iron pool and could be suppressed with iron supplementation (Epstein *et al.*, 2001; Knowles *et al.*, 2006; Knowles *et al.*, 2003). Ascorbate supplementation also de-stabilised HIF-1α in this context and in a number of normoxic tumour cell lines in which HIF-1α was stable (Knowles *et al.*, 2003).

Negative feedback occurs through HIF-dependent expression of PHD-2 and PHD-3. This dampens the HIF pathway in chronic hypoxia and enables rapid deactivation of HIF-α when normoxic conditions are restored (Appelhoff *et al.*, 2004; Aprelikova *et al.*, 2006; D'Angelo *et al.*, 2003). Succinate (a product of the hydroxylase reaction) can competitively compete with the substrate, 2-oxoglutarate, reducing HIF-hydroxylase activity (Selak *et al.*, 2005). Thus disorders of succinate metabolism, such as the mutations in the succinate dehydrogenase

gene found in some types of cancer, may explain the activation of HIF-α subunits in those tumours (Mole, 2009; Selak *et al.*, 2005).

Nitric oxide (NO) may inhibit HIF-hydroxylase activity by competing with oxygen to bind to Fe(II). However, the role of NO is complex as it has paradoxical effects on HIF-α subunit stability which depend on NO dose, ambient oxygen concentration and interaction with reactive oxygen species (Berchner-Pfannschmidt *et al.*, 2010).

1.3.1.4 *Hydroxylase-independent regulation of HIF-α subunit stability*

Multiple HIF-hydroxylase independent mechanisms control HIF-α stability. Firstly, de-ubiquitination of hydroxylated HIF-1α subunits by the pVHL-interacting deubiquitinating enzyme, VDU2, may rescue them from degradation (Li *et al.*, 2005). Secondly, conjugation with small ubiquitin-like modifier (SUMO) may regulate HIF-α subunits. This process, known as SUMOylation, is not fully understood. On the one hand reports have suggested SUMOylation of HIF-1α leads to its stabilisation while on the other hand several studies have shown enhanced degradation (Bae *et al.*, 2004; Cheng *et al.*, 2007). Thirdly, receptor of activated protein kinase C (RACK-1) mediated recruitment of the E3 ligase complex and finally, phosphorylation by glycogen synthase kinase 3 (GSK3) both lead to proteasomal degradation of HIF-1α (Flugel *et al.*, 2007; Liu *et al.*, 2007).

None of the above studies showed whether these additional methods of regulation are important for HIF-2α, but three novel mechanisms resulting in differential regulation of the two α subunits have been recently identified. Firstly, binding of heat shock protein 70 (Hsp70) to the HIF-1α subunit, led to its degradation in a process independent of pVHL but involving recruitment of the E3 ubiquitin ligase, carboxyl terminus of Hsc70-interacting protein (CHIP) (Luo *et al.*, 2009). In these *in vitro* experiments, HIF-2α levels were not affected by overexpression or knockdown of Hsp70 or CHIP (Luo et al., 2009). Secondly, hypoxia-associated factor (HAF), another E3 ubiquitin ligase, also selectively regulated HIF-1α subunits

but not HIF-2α (Nakayama *et al.*, 2004). Finally, the integration site 6 (Int6) protein has been shown to regulate HIF-2α but not HIF-1α in a pVHL and oxygen independent manner (Chen *et al.*, 2007).

1.3.1.5   Reactive oxygen species (ROS)

Many studies have demonstrated that changes in ROS levels within cells can alter HIF-α protein levels (Acker *et al.*, 2006; Guzy *et al.*, 2005; Hagen *et al.*, 2003; Mansfield *et al.*, 2005). However the exact role of ROS, particularly in hypoxia, remains controversial with apparent inconsistencies in experimental findings. For example, inhibition of ROS production by the mitochondrial transport chain has been shown to prevent HIF-1α and HIF-2α stabilisation while others found no effect (Doege *et al.*, 2005; Guzy *et al.*, 2005; Mansfield *et al.*, 2005; Maxwell *et al.*, 1999). As ambient oxygen tension influenced the results, a proposed explanation was that when oxygen was in short supply, mitochondrial inhibition led to a redistribution of oxygen within the cell and resulted in increased oxygen availability for the PHD enzymes (Doege *et al.*, 2005; Hagen *et al.*, 2003). However, Bell *et al.* used cells with a defect in complex III of the mitochondrial transport chain that prevented utilisation of oxygen but permitted generation of ROS in hypoxic conditions (Bell *et al.*, 2007). HIF-1α stabilisation occurred in these circumstances but could be prevented by antioxidants. These results argue against the redistribution of intracellular oxygen levels and suggest ROS may be acting via other mechanisms. For example, ROS may influence available levels of Fe(II) and thus limit PHD enzyme activity (Mole, 2009).

1.3.1.6   Transcription and translation

If protein synthesis were to overwhelm the post-translational eliminatory mechanisms or if oxygen-sensitive enzyme activity was limited, transcription and translation could play a role in HIF-α regulation (Schofield and Ratcliffe, 2004).

One important factor implicated in the control of HIF-1α transcription, and a key player in the inflammatory response, is the oxygen sensitive transcription factor, NFκB (Rius *et al.*, 2008). I*n vitro* studies have shown that HIF-1α mRNA levels are regulated by members of the NFκB pathway via binding of NFκB to the HIF-1α promoter (Belaiba *et al.*, 2007; van Uden *et al.*, 2008). A recent study showed that IKKβ, a component of the NFκB signalling pathway, is necessary *in vitro* and *in vivo* for HIF-1α mRNA expression (Rius *et al.*, 2008). Furthermore lipopolysaccharide, an activator of NFκB, upregulated HIF-1α protein levels in hypoxic macrophages (Rius *et al.*, 2008). Interestingly, Rius *et al.* found no regulatory effect of IKKβ on HIF-2α. In HIF-1α deficient neutrophils, hypoxic induction of NFκB mRNA was markedly reduced, suggesting that HIF-1α also exerts control on the NFκB pathway (Walmsley *et al.*, 2005).

Protein synthesis is usually inhibited in hypoxia but HIF-α subunits are in a minority of essential proteins whose production is preserved (Fahling, 2009; Lang *et al.*, 2002; Nakayama *et al.*, 2004). Increased translation of HIF-1α has been reported as a method of increasing levels of the transcription factor in hypoxic and normoxic conditions, while Sanchez et al. showed that inhibition of HIF-2α synthesis can occur via binding of iron-regulatory proteins (IRPs) to an iron response element in the 5'-untranslated region of HIF-2α mRNA (Laughner *et al.*, 2001; Pore *et al.*, 2006; Sanchez *et al.*, 2007).

1.3.2 Roles of HIF-1α and HIF-2α

Despite the similarities in their structure and regulation, HIF-2α has a distinct role from HIF-1α. Some differences in post-translational regulation have been described above and there are notable differences in expression, target genes, transcriptional regulation and function.

1.3.2.1 *Expression*

Ema *et al.* showed HIF-2α mRNA expression in most major organs of mice, most abundantly in the lung, heart and brain (Ema *et al.*, 1997). *In situ* hybridization studies confirmed expression in alveolar epithelial cells, cardiomyocytes and vascular endothelial cells (Ema *et al.*, 1997; Flamme *et al.*, 1997; Tian *et al.*, 1997). Wiesener *et al.* examined protein expression and immunoblotting revealed low or undetectable HIF-2α in tissues isolated from normoxic rats (Wiesener *et al.*, 2003). However, marked widespread upregulation of HIF-2α expression occurred following exposure of the animals to normobaric hypoxia (8%) or carbon monoxide. The induction of HIF-2α varied between tissues and interestingly, even within tissues. For example, in the liver, increased staining for HIF-2α was seen in hepatocytes closest to the central vein compared to staining around the portal triad, consistent with known *in vivo* oxygen gradients (Wiesener *et al.*, 2003).

In contrast with these *in vivo* data, some studies have shown expression of HIF-2α protein in normoxia. Primary cultures of human pulmonary artery fibroblasts and several cell lines including bovine arterial endothelial cells and human mammary epithelial cells expressed HIF-2α (Ban *et al.*, 1994; Eul *et al.*, 2006; Wiesener *et al.*, 1998). Rius *et al.* showed presence of HIF-2α in murine BMDMs but Fang *et al.* did not find normoxic expression in human monocyte-derived macrophages (Fang *et al.*, 2009; Rius *et al.*, 2008). Recent evidence suggests that the method of isolation is important in determining HIF-2α expression in mononuclear cells but whether there is a true species difference in expression is as yet unknown (Takeda *et al.*, 2010).

Key differences between HIF-1α and HIF-2α expression have been identified. Firstly, in the kidney and brain, HIF-1α and HIF-2α were expressed in different cell populations following hypoxic exposure (Wiesener *et al.*, 2003). Secondly, *in vitro* and *in vivo* studies showed that HIF-2α protein was stabilised at higher oxygen concentrations than HIF-1α (Stroka *et al.*, 2001; Wiesener *et al.*, 2003; Wiesener *et al.*, 1998). Thirdly, hypoxic induction of HIF-2α was sustained for longer than HIF-1α (Stroka *et al.*, 2001; Wiesener *et al.*, 2003). Indeed, more recently these differences have been mirrored in the stability of *HIF1A* and *HIF2A* mRNA, with *HIF2A* mRNA being more stable than that of *HIF1A* (Takeda *et al.*, 2010)*. Finally, the cellular localisation of the two transcription factors was different, with HIF-2α only being observed in cell nuclei but HIF-1α being found in both cytoplasm and nucleus (Stroka *et al.*, 2001; Wiesener *et al.*, 2003).

1.3.2.2   Target genes

More than 600 DNA binding sites for HIF-α subunits have been identified in the genome (Mole *et al.*, 2009). The majority bound only HIF-1α but a significant number also bound both α subunits with a minority binding only HIF-2α (Mole *et al.*, 2009). Other studies using gene array analysis also showed that HIF-1α regulates substantially more genes than HIF-2α in hypoxia or in response to iron chelation (Elvidge *et al.*, 2006; Wiesener *et al.*, 2003). Furthermore, despite high affinity binding to HREs, several studies have suggested that HIF-2α does not always activate transcription (Hu *et al.*, 2006; Mole *et al.*, 2009). Nonetheless, compelling data suggest HIF-2α is the key regulator of several genes.

Among the genes that HIF-2α has been shown to preferentially regulate are transforming growth factor-α; the stem cell factor, Oct-4; the iron transporter, divalent metal transporter-1 (DMT-1); and the adenosine A_{2A} receptor (Ahmad *et al.*, 2009; Covello *et al.*, 2006; Mastrogiannaki *et al.*, 2009). HIF-1α uniquely regulates carbonic anhydrase-9; PHD-2; and glycolytic enzymes, such as hexokinase-2, phosphoglycerate kinase and lactate

dehydrogenase-A (Aprelikova *et al.*, 2006; Hu *et al.*, 2003; Raval *et al.*, 2005). Both HIF-1α and HIF-2α have been shown to play a role in the regulation of PHD-3; adrenomedullin; vascular endothelial growth factor (VEGF); and glucose transporter-1 (Aprelikova *et al.*, 2006; Hu *et al.*, 2003).

Recent data suggest that HIF-2α is the dominant regulator of EPO *in vivo* (Gruber *et al.*, 2007). In postembryonic mice deletion of HIF-2α using a conditional knockout system led to anaemia and decreased levels of circulating EPO while deletion of HIF-1α had no effect (Gruber *et al.*, 2007)). Evidence does suggest that HIF-1α plays a role in EPO regulation during development (Yoon *et al.*, 2006).

Although predominance of one α subunit over another has been demonstrated for certain target genes, this preferential regulation may be context-dependent (Holmquist-Mengelbier *et al.*, 2006). For example, in neuroblastoma cells VEGF was regulated by HIF-1α after acute exposure to 1% oxygen, but following more prolonged and milder (5%) hypoxia, HIF-2α was the main inducer of VEGF (Holmquist-Mengelbier *et al.*, 2006). Differential regulation may also occur. In renal cell carcinoma cells deficient in pVHL, the pro-apoptotic protein, BNIP3 was upregulated by augmenting expression of HIF-1α but downregulated by HIF-2α (Raval *et al.*, 2005).

Further cell-type specific differences between HIF-1α and HIF-2α were demonstrated in mouse embryo fibroblasts (Park *et al.*, 2003). These cells expressed HIF-2α protein in normoxia but it did not activate known target genes, even in hypoxic conditions, unless ectopically overexpressed (Park *et al.*, 2003). Experiments revealed that HIF-2α could not translocate to the nucleus, but the reason for this was not elucidated (Park *et al.*, 2003).

1.3.2.3 Factors affecting HIF-2α target gene specificity

Experiments using mutant HIF-α proteins have shown that it is not the DNA-binding region that confers target gene specificity. Interestingly, replacement of the N-TAD of HIF-2α with that of HIF-1α can switch target gene specificity but both C-TAD and N-TAD regions are needed for full transcriptional activity (Hu *et al.*, 2003; Lau *et al.*, 2007).

Multiple co-activators have been implicated in the control of transcriptional activity of both HIF-1α and HIF-2α including CREB-binding protein (CBP)/p300 and steroid receptor co-activator (SRC1), but other transcription factors may determine target gene specificity (Carrero *et al.*, 2000). Binding sites for members of the E-twenty six (ETS) family of transcription factors have been identified on genes preferentially regulated by HIF-2α (Aprelikova *et al.*, 2006). Using siRNA to knockdown ELK-1, an ETS family member, prevented hypoxic induction of some but not all HIF-2α target genes (Aprelikova *et al.*, 2006; Hu *et al.*, 2007).

Bracken *et al.* showed that HIF-2α but not HIF-1α interacts with IKK-gamma, also known as NFκB essential modulator (NEMO) (Bracken *et al.*, 2005). In normoxic human embryonic kidney cells, overexpression of NEMO resulted in enhanced HIF-2α transcriptional activity and conversely knockdown of NEMO reduced activity (Bracken *et al.*, 2005).

1.3.2.4 Function

Key roles for HIF-2α in catecholamine homeostasis, lung maturation and vascular remodelling have been demonstrated by a variety of transgenic animal models, while roles in tumourigenesis and erythrocytosis are evident not only from experimental models but from human diseases.

1.3.2.4.1 HIF-2α in embryogenesis

Mice with homozygous deletion of HIF-2α (HIF2-α$^{-/-}$) die either *in utero* or shortly after birth (Compernolle *et al.*, 2002; Tian *et al.*, 1998). Embryonic lethality is thought to result from a deficiency of foetal catecholamines leading to circulatory failure (Tian *et al.*, 1998). However,

mice with a different genetic background displayed vascular disorganisation, particularly in the yolk sac (Peng *et al.*, 2000). Endothelial-specific expression of HIF-2α in this model restored vascular development, but embryonic mortality remained high (Peng *et al.*, 2000). A third group investigated HIF-2α$^{-/-}$ mice that survived to term (Compernolle *et al.*, 2002). These pups died of respiratory failure within a few hours due to insufficient surfactant and immature lungs (Compernolle *et al.*, 2002). These findings contrast with HIF-1α$^{-/-}$ mice, which die during mid-gestation due to abnormal vascularisation (Ryan *et al.*, 1998).

1.3.2.4.2 Tumourigenesis

HIF-α subunits are stable in many tumours but there are marked differences in the function of HIF-2α compared to HIF-1α. In the tumour syndrome, von Hippel Lindau (VHL) disease, mutations in the pVHL gene are associated with the development of clear-cell renal cell carcinomas, haemangioblastomas and pheochromocytomas (Mole and Ratcliffe, 2008). Loss of functional pVHL leads to accumulation of both α subunits, but HIF-2α has been implicated in the promotion of renal cell tumour growth while HIF-1α overexpression in renal cancer xenografts actually inhibited growth (Holmquist-Mengelbier *et al.*, 2006; Patel and Simon, 2008; Raval *et al.*, 2005). Consistent with these findings, HIF-2α expression in other types of cancer (breast cancer, non-small cell lung cancer, neuroblastoma and teratomas) correlated with advanced stage or an aggressive phenotype (Covello *et al.*, 2006; Holmquist-Mengelbier *et al.*, 2006; Kim *et al.*, 2009). Furthermore, inhibition of HIF-2α in lung carcinoma and clear cell renal cancer cells, led to increased tumour cell death and enhanced the response to radiation treatment (Bertout *et al.*, 2008). In contrast, loss of HIF-2α expression in colon tumours was correlated with advanced tumour stage and colon cancer cell xenografts deficient in HIF-2α exhibited enhanced growth (Imamura *et al.*, 2009).

1.3.2.4.3 Erythrocytosis

Mutations of several key regulatory components of the HIF pathway lead to the development of familial erythrocytosis (Lee, 2008). For example, a mutation in the *VHL* gene leads to an autosomal recessive form of erythrocytosis that is endemic to Chuvashia, Chuvash polycythaemia (Lee, 2008; Sergeyeva *et al.*, 1997)). Affected individuals have a homozygous missense mutation in the *VHL* gene leading to an amino acid substitution (Arg200Trp) that impairs interaction between the VHL protein and HIF-α subunits, inhibiting ubiquitination and therefore stabilising HIF-α subunits in non-hypoxic conditions (Ang *et al.*, 2002).

As discussed above (Section 1.3.2.2), evidence has emerged to suggest that HIF-2α is the dominant HIF-α subunit regulating EPO production. Studies of familial erythrocytosis have also supported this conclusion. Percy *et al.* identified a family with a gain-of-function mutation (G1609→T) in the HIF-2α gene (*HIF2A)*(Percy *et al.*, 2008b). This mutation led to a replacement of glycine by tryptophan at amino acid 537 close to the hydroxylation target, Pro531. Hydroxylation of the Gly537→Trp HIF-2α by PHD-2 was reduced but not to the same extent as a direct mutation at Pro531 (Percy *et al.*, 2008b).

In summary, I have described the biology of HIF-1α and HIF-2α, providing evidence that they may be differentially regulated and have distinct roles in many cell types. Both transcription factors have important roles in innate immune cell function but the role of HIF-2α in neutrophils requires further exploration.

1.4   Aims of the thesis

Hypoxia is a common finding at sites of inflammation but also more globally in patients with lung disease or critical illness. The oxygen sensing transcription factor, HIF-1α is a critical regulator of innate immunity. Neutrophils are profoundly influenced by this transcription factor, depending on it for survival in hypoxia and production of ATP and important antimicrobial enzymes and proteins. Although HIF-α subunits have some similarities, there is compelling evidence that HIF-1α and HIF-2α have distinct roles and that these roles vary according to cell type or microenvironment. It is unknown whether HIF-2α has a unique role in neutrophils.

Infections frequently cause or complicate illnesses associated with arterial hypoxaemia and local tissue hypoxia. In these contexts, the effects of local versus systemic HIF activation are not well characterised.

Therefore, in this thesis I aim to investigate:

i)   The regulation and expression of HIF-2α in neutrophils

ii)   The functional consequences of HIF-2α overexpression and HIF-2α deficiency in neutrophils

iii)   Host-pathogen interactions in hypoxia using a subcutaneous infection model

iv)   The influence of HIF-1α or HIF-2α deficiency on host responses in the context of HIF-pathway activation by the combination of bacteria and hypoxia.

2 Methods

2.1 Ethical approval

The taking of blood samples from healthy volunteers and from patients with inflammatory arthritis was approved by the Sheffield Research Ethics Committee. Volunteers gave full informed consent to participate. Ethical approval to study neutrophils from patients with gain-of-function mutations in the *HIF2A* gene was given by the Oxfordshire Clinical Research Ethics Committee and use of the human lung tissue was approved by the ethics committee of the Helsinki University Central Hospital, Helsinki, Finland.

2.2 Human neutrophil isolation

Neutrophils were isolated from peripheral blood using dextran sedimentation with discontinuous plasma-Percoll gradients. This method causes less activation of neutrophils than other methods of isolation (Haslett *et al.*, 1985). Percoll® (Sigma-Aldrich Company Ltd., Gillingham, UK) consists of polyvinylpyrrolidone coated colloidal silica particles ranging in diameter from 15-30 nm (23% w/w in water) (Sigma-Aldrich, 1998a). Materials used for neutrophil isolation were warmed to 37˚C in a water bath before use and centrifugation was carried out at room temperature. Sterile technique was employed throughout within a Class II microbiological safety cabinet (Walker, Glossop, UK).

Peripheral blood was drawn using a 21 gauge needle and decanted into a 50 ml falcon tube containing tri-sodium citrate (Martindale Pharmaceuticals, Romford, UK) as an anticoagulant (4.4 ml 3.8% tri-sodium citrate for 35.6 ml blood). Tubes were gently mixed then spun at 1200 rpm (270 g) for 20 minutes (MSE centrifuge, Sanyo, Loughborough, UK). The plasma phase was aspirated into clean falcon tubes, taking care not to disrupt the buffy coat layer, and spun at 2000 rpm (1155g) for 20 minutes to form platelet poor plasma (PPP). To the lower cell-rich

layer remaining after the first spin, 6 ml of 6% dextran (Sigma-Aldrich Company Ltd., Gillingham, UK) were added and topped up to 50 ml with sterile 0.9% saline. This was mixed by gently inverting the tubes, air bubbles were removed and the contents were allowed to settle for 20-30 minutes allowing red cell sedimentation to occur.

When a clear interface was achieved, the upper leukocyte-rich layer was transferred to clean falcon tubes and spun at 1000 rpm (185 g) for 6 minutes. Discontinuous plasma-Percoll gradients were prepared by overlaying 2 ml of 42% Percoll/58% PPP onto 2 ml of 51% Percoll/49% PPP in 15 ml tubes. Leukocytes (from up to 80 ml of blood) were re-suspended in 1.5 ml PPP and layered on top of the upper phase of the plasma-Percoll gradient. These tubes were immediately spun at 1100 rpm (225 g) for 11 minutes with zero brake.

Three layers of cells are produced using this method. Erythrocytes pellet at the bottom of the 15 ml tubes. Above this, between the 51% and 42% plasma-Percoll layers, a band of neutrophils and eosinophils is formed. A further band, at the interface of the 42% Percoll and plasma layers, contains peripheral blood mononuclear cells (PBMCs). The PBMCs were carefully removed using a Pasteur pipette and then the granulocytes were transferred into 25% PPP (10 ml PPP + 30 ml Hanks buffered salt solution (HBSS) without Ca^{2+}/Mg^{2+} (Gibco®, Invitrogen Ltd., Paisley, UK)), counted using a haemocytometer and spun at 1500 rpm (420 g) for 6 minutes. The supernatant was discarded and the cells were re-suspended to give $5x10^6$ neutrophils per ml in RPMI 1640 (Gibco®, Invitrogen Ltd., Paisley, UK) containing 1% penicillin and streptomycin and 10% foetal bovine serum (FBS).

Neutrophil purity was measured by examination of cytocentrifuge slides prepared using freshly isolated cells (see Section 2.7.1) and was routinely >95% with eosinophils as the main contaminating cell type (see Figure 2.2-1).

2.2.1 Ultrapure human neutrophils

To further purify human neutrophils, contaminating cells were removed by magnetic selection (Sabroe *et al.*, 2002). Following density gradient purification, the harvested and counted granulocytes were resuspended in 1 ml of column buffer (HBSS containing 2% FBS). For every $100x10^6$ granulocytes, 70 µl of a custom antibody cocktail (StemCell Technologies, Grenoble, France) containing antibodies to CD36, CD2, CD3, CD19, CD56, and glycophorin A were added and the cells were incubated for 15 minutes at room temperature. Magnetic colloid (50 µl per $100x10^6$ granulocytes, Miltenyi Biotec Ltd., Bisley, UK) was then added before further 15 minutes incubation at room temperature, swirling intermittently. During the incubation a MACS® LS column (Miltenyi Biotec Ltd.) was primed with 3 mls column buffer. The cells were then added to the column, collecting the effluent in a falcon tube. A further 9 mls of column buffer were then added to the column in 3 aliquots collecting a total of 10 mls of effluent. The negatively selected cells that passed through the column were then pelleted at 1500 rpm (420 g) for 6 minutes and resuspended in neutrophil media (RPMI 1640 containing 1% penicillin and streptomycin and 10% FBS), counted and diluted in media to a final concentration of $5x10^6$/ml. Neutrophil purity following negative magnetic selection was greater than 99% (see Figure 2.2-1).

A

B
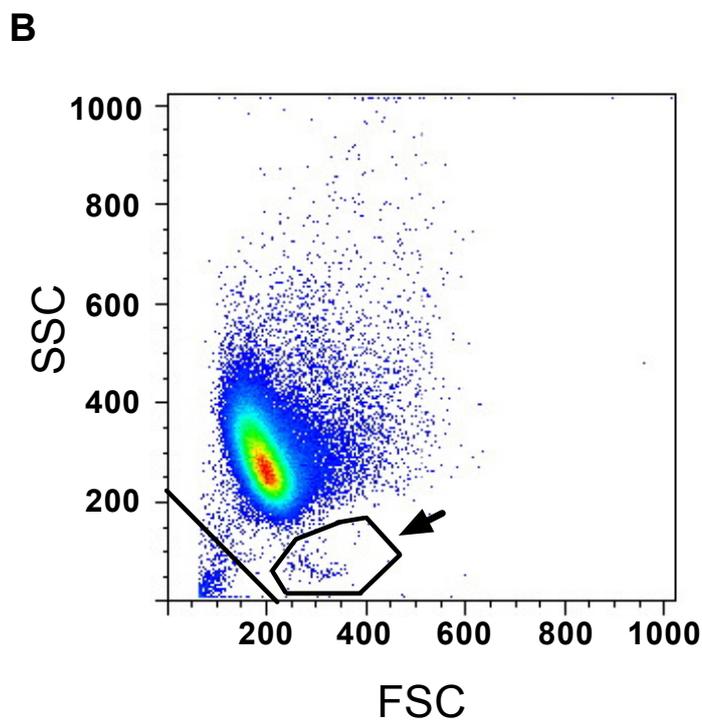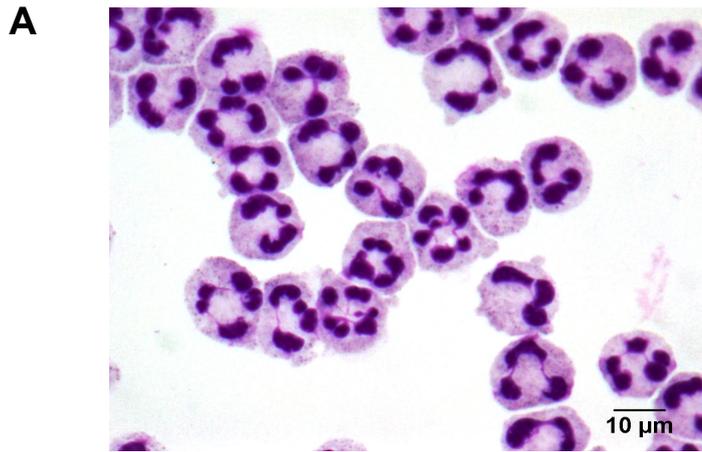
Figure 2.2-1. Human neutrophil isolation.

(A) Photographic image of freshly isolated human neutrophils on a cytocentrifugation slide. Original magnification x1000. (B) Representative side scatter (SSC) versus forward scatter (FSC) flow cytometry plot of an ultrapure neutrophil isolation. The plot shows 10,000 events with gate indicating contaminating PBMCs which represented 0.08% of the total population. Debris to the left of the diagonal black line was excluded.

2.3   Human neutrophil culture

Human neutrophils were cultured at a concentration of 5×10^6/ml on 96-well non-tissue culture treated polyvinyl chloride plates (BD Falcon™, BD Biosciences, Becton Dickinson Ltd., Oxford, UK).   Normoxic cell culture was carried out at 37°C in a humidified incubator with 5% supplemental CO_2 (Sanyo Electric Co Ltd., Japan). Hypoxic cell culture was established by re-suspending cells in media that had been pre-equilibrated in 1% O_2, 5% CO_2 using an Invivo$_2$ 400 hypoxic work station (Ruskinn, Bridgend, UK).   The PO_2, PCO_2 and pH of the hypoxic media were measured weekly using a blood gas analyser (ABL5, Radiometer, Copenhagen, Denmark) to confirm the delivery of a consistent hypoxic environment (see Table 2.3-1).   Neutrophils were cultured in the presence or absence of 10 ng/ml LPS from *E coli.* (Serotype R515(RE), TLR*grade*™, Alexis® biochemicals, Lausen, Switzerland), the hydroxylase inhibitor, dimethyloxalylglycine (DMOG 1-1000 µM, Frontier Scientific Europe, Carnforth, UK), heat killed *Staphylococcus aureus* (SH1000, kind gift from Professor Simon Foster, University of Sheffield) or *Streptococcus pneumoniae* (serotype 2 strain D39, NCTC 7466, Health Protection Agency Culture Collections, Salisbury, UK).

	pH	PO$_2$ (kPa)	PCO$_2$ (kPa)
Normoxia **n=4**	7.37 +/- 0.03	19.02 +/-0.17	4.66 +/- 0.16
Hypoxia **n=10**	7.34 +/- 0.01	3.54 +/- 0.15	4.55 +/- 0.07

Table 2.3-1. Gas tensions in culture media.

Gas tension and pH values in neutrophil culture media equilibrated in either normoxia (atmospheric oxygen, 5% CO_2) or hypoxia (1% O_2, 5% CO_2). Data are mean and SEM.

2.4 Human neutrophil RNA preparation

Neutrophils (5×10^6) were lysed with 750 µl of TRI® reagent (Sigma-Aldrich Company Ltd., Gillingham, UK). To isolate RNA, 200 µl of chloroform was added and after 15 minutes incubation at room temperature the sample was centrifuged at 14,000 g for 15 minutes at $4\,^{\circ}$C (Eppendorf 5417R, Hamburg, Germany). The clear aqueous RNA layer was transferred to a clean eppendorf tube and 500 µl of isopropanol were added. Following 10 minutes incubation at room temperature the sample was again centrifuged at 14,000 g for 15 minutes at $4\,^{\circ}$C. The supernatant was discarded and 1 ml of 75% ethanol was added before centrifugation at 9000 g for 5 minutes at $4\,^{\circ}$C. The supernatant was discarded and the pellet air-dried before being re-suspended in 10 µl of RNase-free water. A NanoDrop™ 1000 spectrophotometer (Fisher Scientific UK Ltd., Loughborough, UK) was used to assess RNA quantity and purity.

2.4.1 DNase treatment of RNA

Contaminating genomic DNA was removed from RNA samples using a DNase digestion kit (DNA-*free*™, Ambion, Huntingdon, UK). RNA samples were diluted to achieve a nucleic acid concentration of approximately 200 ng/µl. DNase I buffer (10x) was added to the RNA samples at a 1 in 10 dilution then 1 µl of DNase I enzyme was added for every 10 µg of nucleic acid. Samples were incubated for 30 minutes at 37˚C before addition of DNase inactivation reagent. A minimum of 2 µl or 0.1 volumes of inactivation reagent were added to the RNA samples which were then spun at 10,000g for 90 seconds to pellet the inactivation beads. A NanoDrop™ 1000 spectrophotometer (Fisher Scientific UK Ltd., Loughborough, UK) was used to again assess RNA quantity and purity.

2.4.2 Random hexamer cDNA synthesis from human RNA aliquots

Avian myeloblastosis virus (AMV) reverse transcriptase and random primers were used to generate cDNA from the RNA aliquots. Every 1 µg RNA was made up to 12.4 µl with RNase-free water and a cocktail of primers, enzyme and dNTP was added (see Appendix I). Samples

were run on a DNA *Engine*™(PTC-200, MJ Research, Watertown, USA) at 23 ^{o}C for 5 minutes, then 42 ^{o}C for 2 hours, followed by 99 ^{o}C for 2 minutes to heat inactivate the enzyme and stored at –20 ^{o}C until required.

2.4.3   Polymerase chain reaction

Custom primers were designed for *HIF2A* (see Appendix II)*.* These were used to amplify human neutrophil cDNA in polymerase chain reactions using GoTaq® Flexi DNA Polymerase (Promega UK, Southampton).   The components of the mastermix for these reactions and the cycling conditions are shown in Appendix III.   Negative controls with H_2O in place of sample were performed routinely.

2.4.4   Sequencing

PCR products were run at 100 volts (PowerPac 300, Bio-Rad Laboratories) on 1.5% agarose gels.   Gels were prepared using electrophoresis grade agarose (Melford Laboratories Ltd., Ipswich, UK) and TAE buffer (40 mM Tris-base (Fisher Bioreagents, Fisher Scientific, New Jersey, USA), 20 mM acetic acid (Fisher Scientific), 1mM EDTA (Sigma-Aldrich Ltd.)) and heated in a microwave to dissolve.   Ethidium bromide (1 µl per 50 ml) was added to the liquid agarose/TAE before pouring into a gel tank and allowing to set. A 100 bp ladder (Hyperladder IV™, Bioline Reagents Ltd., London, UK) was used to confirm the size of the resulting product and this was localized using an ultraviolet transilluminator (UVP Chromato-Vue, San Gabriel, USA) or imaging system (ChemiDoc XRS+, Bio-Rad Laboratories Ltd., Hemel Hempstead, UK). The PCR product was subsequently extracted from the agarose gel with a scalpel and purified using a QIAquick PCR purification kit (QIAGEN, Crawley, UK). Sequencing was performed by the genetics core facility (University of Sheffield) using BigDye® 3.1 sequencing kits on a 3730 DNA Analyser (Applied Biosystems, Foster, USA).   Sequences were visualized using Finch TV software (Version 1.4.0, Geospiza Inc.) and alignment with known mRNA sequences analysed by NCBI nucleotide BLAST (http://blast.ncbi.nlm.nih.gov/).

2.4.5 Real-time polymerase chain reaction (RT-PCR)

Real-time PCR allows detection and quantification of specific sequences in a sample of DNA. TaqMan® oligonucleotide probes use a high energy reporter dye at the 5'-end and a quencher molecule at the 3'-end. The probe is designed to anneal to a specific sequence between the forward and reverse primers and is cleaved when the DNA polymerase starts to copy the cDNA. This releases the fluorophore from the quencher molecule and fluorescent resonance energy transfer (FRET) is detected in real time. Identification of the exponential phase of the PCR reaction enables accurate quantification and comparison of samples.

2.4.6 TaqMan® protocol

TaqMan® gene expression assays (Applied Biosystems, Foster, USA) were used for target assay and endogenous control assay reactions. Each product contained sequence-specific primers and a 6-FAM dye-labelled probe. Beta-actin was selected as the endogenous control as it is highly expressed and expression is not altered by hypoxia. This enabled relative quantification following RT-PCR reactions. When commercially available assays were not available (*HIF2A*, *PHD3*), probes and primers were designed and then manufactured by Sigma-Aldrich. Primer and probe sequences for each assay are shown in Appendix II.

Pre-optimised cDNA samples were diluted to give standards in order to create a standard curve for each gene of interest. On the same 384-well plate, 1 µl of cDNA samples and standards were added in duplicate to 19 µl of master mix (see Appendix I). The thermal cycler conditions used were 2 minutes at 50 ^{o}C, 10 minutes at 95 ^{o}C then each of 40 cycles 15 seconds at 95°C to denature and 1 minute at 60°C to anneal and extend.

Average threshold cycle values were obtained for each sample using SDS2.2.1 software (Applied Biosystems). Standards curves were plotted using an arbitrary value of 10000 for the top standard followed by the appropriate dilution series against average threshold cycle values. Samples were then quantified using the standard curve. The values obtained were

normalised to values for beta-actin expression in the same samples using the following

equation: Normalised value = Gene-of-interest expression / beta-actin expression

2.5 Western blotting

2.5.1 Preparation of human neutrophil lysates for protein separation

Following culture for the appropriate time period, neutrophils were gently harvested from the

culture plates and spun at 2000 rpm for 2 minutes. Hypoxic samples were harvested into

eppendorf tubes within the hypoxic workstation and maintained on ice for the duration of the

lysis protocol to minimise degradation of oxygen-sensitive proteins. The cells were washed in

ice cold phosphate buffered saline (PBS) (Gibco®, Invitrogen Ltd., Paisley, UK) before being

washed in 1ml of sonication lysis buffer (see Appendix IV). The supernatant was discarded and

cells re-suspended in 100 µl of sonication lysis buffer and incubated on ice for 10 minutes.

Cells were then sonicated in a Bioruptor™ iced water bath (Diagenode Europe SA, Liège,

Belgium) using 30 second on-off high power cycles for 10 minutes. The whole cell lysates were

centrifuged at 12,000 g for 10 minutes at 4°C. The supernatant was removed into fresh 1.5ml

tubes and an equal volume of 2X SDS lysis buffer was added to each aliquot (see Appendix IV).

Samples were boiled for 5 minutes at 100°C then stored at -80°C.

2.5.2 Protein separation

Proteins were separated by sodium dodecyl sulphate polyacrylamide electrophoresis (SDS-

PAGE) using the Bio-Rad mini PROTEAN®II electrophoresis cell system (Bio-Rad laboratories,

Hemel Hempstead, UK). Glass plates were cleaned with distilled water and 70% industrial

methylated spirits, before being assembled in a horizontal casting stand 1.5 mm apart.

Resolving gels (8% for HIF-alpha western blots) were prepared (See Appendix V), and

transferred to the casts using a Pasteur pipette. The resolving gel was overlaid with

isopropanol to prevent evaporation until set. The isopropanol was then decanted and the gel washed with distilled water. A 5% stacking gel was poured on top of the resolving gel and a 10-well 1.5 mm thick comb carefully inserted to avoid air bubbles. After the stacking gel had set the comb was carefully removed and the glass plates were placed in a gel running tank and immersed with SDS-PAGE running buffer (See Appendix V). Neutrophil cell lysates were heated to 100°C for 2-5 minutes before being loaded into individual lanes with one or two lanes containing rainbow markers (Bio-Rad Laboratories). The gel was run at 180 volts (PowerPac 300, Bio-Rad Laboratories) until the blue dye front reached the bottom of the gel.

2.5.3 Protein Transfer

Following separation by SDS-PAGE as described above, the gel apparatus was disassembled. The glass plates were carefully separated and the stacking gel was removed. Using flat-ended tweezers, the resolving gel was lifted off the glass and placed onto blotting paper soaked in transfer buffer (see Appendix V).

A piece of PVDF Immobilon-P transfer membrane (Millipore, Bedford, USA) was activated by soaking in methanol for 2 minutes and then placed in transfer buffer. In a tray containing transfer buffer, a gel-holding transfer cassette was opened and a fibre pad soaked in transfer buffer was placed on the black side of the cassette. Two pieces of blotting paper (Whatman® 3mm chromatography paper, Whatman International, Maidstone, UK) were then placed on top of this followed by the resolving gel and then the activated membrane. Two further pieces of blotting paper and another fibre pad were applied on top before the gel holding cassette was closed and placed in a tank filled with ice-cold transfer buffer. Transfer of protein to the membrane was performed using a Bio-Rad Mini Trans-Blot® cell at 100 volts for 70 minutes. Loading and transfer success was assessed by Ponceau S solution staining (Sigma-Aldrich Company Ltd., Gillingham, UK). Membranes were stained for 30 seconds, before rinsing in distilled water.

2.5.4   Immunoblotting and Detection

After transfer, the membrane was blocked in blocking buffer (see Appendix V) for 1 hour on an orbital shaker. This minimised non-specific binding of antibodies to the membrane. The membrane was transferred to a 50 ml tube and the primary antibody, diluted in 4 ml of blocking buffer, was added. The dilutions at which the antibodies were used are shown in Appendix VI. The membrane was incubated overnight at 4°C on a rolling platform. After incubation with the primary antibody, the membrane was washed for 30 minutes in Tris-buffered saline supplemented with Tween 20 (see Appendix V) before being incubated for one hour at room temperature with the appropriate HRP-conjugated secondary antibody diluted in 4 ml of blocking buffer. The membrane was then washed again as before. Labelled proteins were detected using the Enhanced Chemi-Luminescent™ (ECL) system (EZ-ECL, Geneflow Ltd., Fradley, UK). The ECL-treated membranes were placed between two pieces of acetate. Air bubbles and excess ECL were removed before the membrane was placed in a developing cassette (Amersham Hypercassette™, GE Healthcare Ltd. Little Chalfont, UK) and exposed to X-ray film (Amersham Hyperfilm™) in a dark room. Exposed x-ray films were developed, washed and air-dried.

2.6   Immunohistochemistry

Lung tissue sections were from non-smokers and patients with COPD undergoing resection of hamartomas and kindly provided by Professor Vuokko Kinnula (Department of Medicine and Pathology, Helsinki University Central Hospital, Finland).   Immunohistochemistry was kindly performed by Yvonne Stephenson.

2.6.1 Staining of tissue sections

Slides were dewaxed twice in xylene, leaving slides in the xylene for 5 minutes each time. Slides were then placed in 95% ethanol for 2 minutes followed by 70% ethanol for 2 minutes before being washed well in water. Endogenous peroxidases were quenched by adding 3% H_2O_2 in methanol for 20 minutes then slides were washed again with water. Non-specific antibody binding was blocked by incubating in Power Block™ (Biogenex, Fremont, USA) for 10 minutes. Slides were washed 3 times in water then incubated in primary antibody for 30 minutes.   The primary antibodies were diluted in TBST (see Appendix IX for dilutions).   An appropriate isotype control antibody was used alongside each primary antibody. Following 3 washes in TBST, slides were incubated with ImmPRESS™ reagent (ImmPRESS™ universal polymer detection kit, Vector Laboratories Ltd, Peterborough, UK).   The ImmPRESS™ reagent consists of a peroxidase coupled to anti-mouse and anti-rabbit IgG secondary antibodies. Slides were washed 3 times in TBST before adding diaminobenzidine (DAB) substrate from the DAB peroxidase substrate kit (Vector Laboratories Ltd.).   The peroxidase in the ImmPRESS™ kit reacts with the DAB substrate producing a dark brown reaction product. This reaction was allowed to proceed for up to 10 minutes. Sections were rinsed in running water and then counterstained with Gill's haematoxylin for 30 seconds. After a further wash, Scott's tap water was added for 10 seconds before washing in running water.   Finally, the slides were dehydrated by immersion in an ascending series of ethanol concentrations and mounted using VectaMount™ (Vector Laboratories Ltd.).

2.7 Detection of human neutrophil apoptosis

2.7.1 Preparation of cytocentrifugation slides

Cytocentrifuge slides allow the long-term preservation of neutrophil morphology and therefore assessment of the morphological changes observed during apoptosis. Neutrophils (100 µl of 5×10^6/ml) were removed from culture and added to the chamber of the cytospin apparatus. This consisted of slide holder, microscope slide, filter paper and cytospin chamber. Cells were spun at 300 rpm for 3 minutes in a Cytospin 3 cytocentrifuge (Shandon Life Sciences International Ltd, Runcorn, UK). Slides were allowed to dry before methanol was applied to fix the cells. The cells were then stained with Reastain Quick-Diff (Reagena Ltd, Toivala, Finland), a modified Wright-Geimsa stain. Once dry, slides were cover-slipped and viewed using oil immersion light microscopy (see Figure 2.7-1).
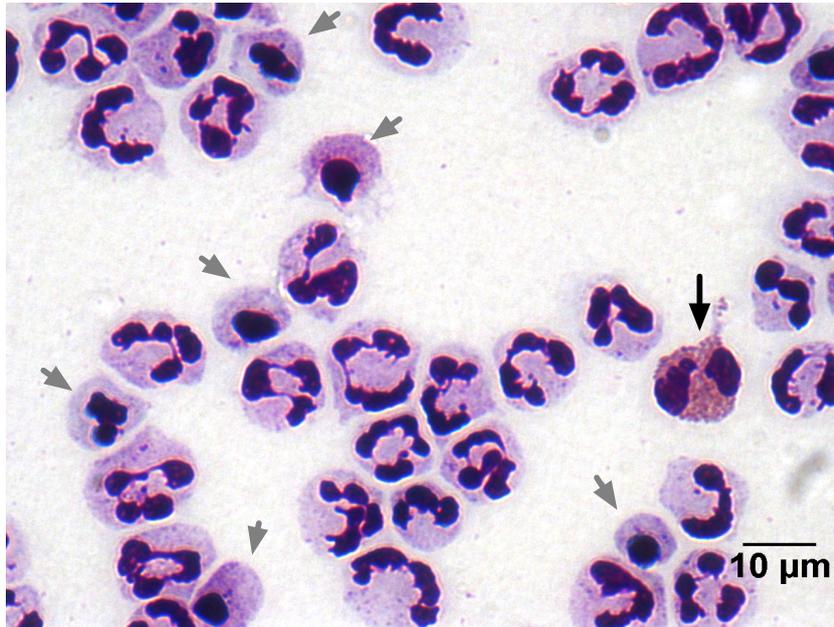
Figure 2.7-1. Apoptotic neutrophils.

Photomicrograph of human neutrophils after 8 hours of culture in normoxic conditions. Neutrophils were spun onto cytocentrifugation slides, fixed with methanol and stained with Reastain Quick-Diff. Grey arrows indicate morphologically apoptotic cells, black arrow indicates an eosinophil. Original magnification x1000.

2.8   Assessment of human neutrophil function

2.8.1   Neutrophil phagocytosis

2.8.1.1   Phagocytosis of opsonized zymosan A

Zymosan A is prepared from the cell wall of *Saccharomyces cerevisiae* (Sigma-Aldrich). Before use, 1 g zymosan should be boiled in 200 ml of sterile PBS for 30 minutes then allowed to cool. Aliquots of this mixture were centrifuged (1200 rpm for 10 minutes at 4°C) and washed three times with sterile PBS. The zymosan was then pooled into a final volume of 20 ml of sterile PBS and aliquots transferred into eppendorf tubes. These aliquots were spun at 3000 rpm for 5 minutes and the supernatant discarded before storing at -20°C. On the day of use the zymosan was opsonized by adding 1 ml of foetal bovine serum to 10 mg of zymosan and agitating for 1 hour at 37°C. Particles were then washed three times in PBS before re-suspending in PBS to give a stock suspension of 50 mg/ml. Prepared in this way zymosan forms a fine suspension of particles around 3 μm in diameter.

Neutrophils were incubated with 0.2 mg/ml or 1 mg/ml of opsonized zymosan A particles for 15 minutes at 37°C. Cytocentrifuge slides were then prepared and uptake of the yeast particles by neutrophils assessed. Phagocytic index (PI) was calculated as follows:

PI = (Mean number of particles per neutrophil) x (% of neutrophils containing particles)

2.8.1.2   Phagocytosis of Escherichia coli

Neutrophils were incubated with heat-inactivated fluorescein isothiocyanate-conjugated *Escherichia coli* (Sigma-Aldrich Company Ltd., Gillingham, UK) at a multiplicity of infection of 1 for 30 minutes at 37°C. The cells were then placed on ice to stop phagocytosis, washed in PBS and re-suspended in fluorescence-activated cell sorting (FACS) buffer (PBS without $Ca2^+/Mg2^+$, 0.25% bovine serum albumin, 0.1 mM HEPES, pH 7.4, filter-sterilized). Samples were processed using a flow cytometer (BD FACSCalibur™, BD Biosciences, Becton Dickinson Ltd.,

Oxford, UK). Results in the FL-1 channel were analysed using FlowJo software (version 9.0,

Tree Star Inc., Ashland, US).

2.8.2 Respiratory burst

Intracellular reactive oxygen species production was assessed using 2',7'-dichlorofluorescein

diacetate (DCF)(Sigma-Aldrich Company Ltd., Gillingham, UK). This cell-permeable compound

fluoresces upon reaction with oxidants (Hempel *et al.*, 1999). Cells were pre-equilibrated for 1

hour then treated with 3% DCF. After 30 minutes cells were stimulated with 100 nM formyl-

methionyl-leucyl-phenylalanine (fMLP) or 0.2 mg/ml opsonised zymosan A for a further 30

minutes. After washing in PBS, the fluorescence of the cells from the FL-1 channel was

recorded by a flow cytometer (BD FACSCalibur™, BD Biosciences, Becton Dickinson Ltd.,

Oxford, UK) and geometric mean fluorescence was subsequently calculated using FlowJo

software (version 9.0, Tree Star Inc., Ashland, US).

2.9 Fish husbandry

The neutrophil specific fluorescent zebrafish line *Tg(mpx:GFP)i114* (Renshaw *et al.*, 2006) was used, subsequently referred to as *mpx*:GFP. Zebrafish were maintained according to standard protocols (Nusslein-Volhard, 2002). Adult fish were maintained on a 14 hour light and 10 hour dark cycle at 28°C in UK Home Office approved facilities in the MRC CDBG aquaria at the University of Sheffield. Fish experiments were kindly performed by Dr Phil Elks.

2.9.1 Inflammation assay

Inflammatory responses were elicited in zebrafish embryos by tail transection as previously described using the neutrophil specific line *mpx*:GFP (Elks *et al.*, 2011; Renshaw *et al.*, 2006). Two days post-fertilization (dpf) embryos were anesthetized by immersion in 0.168 mg/ml Tricaine (Sigma-Aldrich) and transection of the tail was performed as previously described (Elks *et al.*, 2011). Neutrophils were counted at the site of transection at 6, 24 and 48 hpi using a fluorescent dissecting stereomicroscope (Leica Microsystems GmbH, Wetzlar, Germany). Counting was performed blind to experimental conditions.

2.9.2 Zebrafish neutrophil apoptosis assay

Rates of apoptosis were assessed using TUNEL/TSA, by blinded assessors, and by anti-active caspase-3/TSA staining, as previously described (Elks *et al.*, 2011). Apoptotic neutrophils were identified in the tail transection region, imaged on an UltraVIEWVoX spinning disk confocal microscope (Perkin Elmer Inc.) and quantified by the percentage of neutrophils co-labelled with TUNEL.

2.9.3 Wild-type and mutant *epas1* cloning

Zebrafish 2dpf RNA purified using TRIzol (Invitrogen) was used for RT-PCR cloning of zebrafish the *HIF2A* homologue *epas1a* (primer details in Appendix VII) using Pfusion polymerase (Finnzymes, Espoo, Finland). These were initially cloned into the TOPOBlunt vector (Invitrogen) and were subsequently subcloned into the pCS2+ vector (Invitrogen) for RNA synthesis.

Dominant active forms of *epas1a* were generated by successive rounds of site-directed mutagenesis. In each round one of the hydroxylation sites (P347A, P481G, N753A) was mutated into non-hydroxylatable amino acids as previously described in zebrafish *hif1a* (Elks *et al.*, 2011). Additionally, the corresponding zebrafish amino acid to the human HIF-2α G537R and G537W was mutated in the same fashion. Dominant active RNAs were transcribed (mMessageMachine, Ambion, Life Technologies Corp., Carlsbad, CA) and micro-injected into zebrafish embryos at the one cell stage as previously described (Elks *et al.*, 2011).

2.9.4   Determination of *epas1a* signalling activity

To assess the function of overexpressed G487 mutant constructs, *phd3* in situ hybridization was performed using previously described methods 24 hours following injection of *G487R, G487W* or dominant active *epas1a* at the 1 cell stage (Thisse and Thisse, 2008). A dominant negative form of *epas1a* was generated using primers amplifying DNA corresponding to amino acids 1-330 of human HIF-2α (Elks *et al.*, 2011; Manotham *et al.*, 2005).

2.9.5   Morpholino knockdown of *arnt-1*.

The *arnt-1* morpholino (Genetools, Philomath, OR) was used as previously reported (Prasch *et al.*, 2006). A standard control morpholino (5' CCTCTTACCTCAGTTACAATTTATA 3') (Genetools) was used as a negative control.

2.10 Murine colonies

A tissue specific Cre-loxP system was used to delete *Hif1a* or *Hif2a.* Lysozyme M-driven Cre recombinase (LysMCre) was used to target *Hif1a* (*Hif1a*$^{flox/flox}$;LysMCre$^{+/-}$) or *Hif2a* (*Hif2a*$^{flox/flox}$;LysMCre$^{+/-}$) in myeloid lineage cells. Animals were back crossed to a C57BL/6 background (Cramer *et al.*, 2003; Takeda *et al.*, 2010). Breeding pairs of these mice, homozygous for the floxed alleles, were kindly provided by Professor Randall Johnson (University of California, San Diego; now at University of Cambridge, UK) and Professor Celeste Simon (University of Pennsylvania, Philadelphia). C57BL/6 mice (Harlan, Oxon, UK) or littermate *Hif2a*$^{flox/flox}$;LysMCre$^{-/-}$ mice were used as controls. All animal experiments were conducted in accordance with the Home Office Animals (Scientific Procedures) Act of 1986 with local ethics approval.

2.10.1 Extraction of murine DNA

Ear clippings were put into 1.5 ml eppendorf tubes before 180 µl of buffer ATL (Qiagen DNeasy kit, Qiagen Ltd. Crawley, UK) and 20 µl of proteinase K (Qiagen Ltd.) were added to each sample. Samples were then vortexed and placed in a shaking water bath at 56˚C overnight. Following lysis, the samples were vortexed followed by the addition of 200 µl of buffer AL and 200 µl of ethanol. After thorough mixing, each sample was added to a DNeasy mini spin column (Qiagen Ltd.) and spun at 8000 rpm for 1 minute. The flow through was discarded and the column was washed using 500 µl AW1. After spinning at 800 rpm for 1 minute, the wash was repeated with 500 µl buffer AW2 and the samples were spun at 13,400 rpm to dry the column membrane. DNA was then eluted into a fresh collection tube with 100 µl H$_2$O.

2.10.2 Genotyping of murine colonies

Genotyping of the mice was performed by Ian Phillips (Bioserv UK Ltd, Sheffield, UK) using primers, mastermix and cycling conditions detailed in Appendix VIII. An example of the genotyping results for animals from these colonies are shown in Figure 2.10-1.
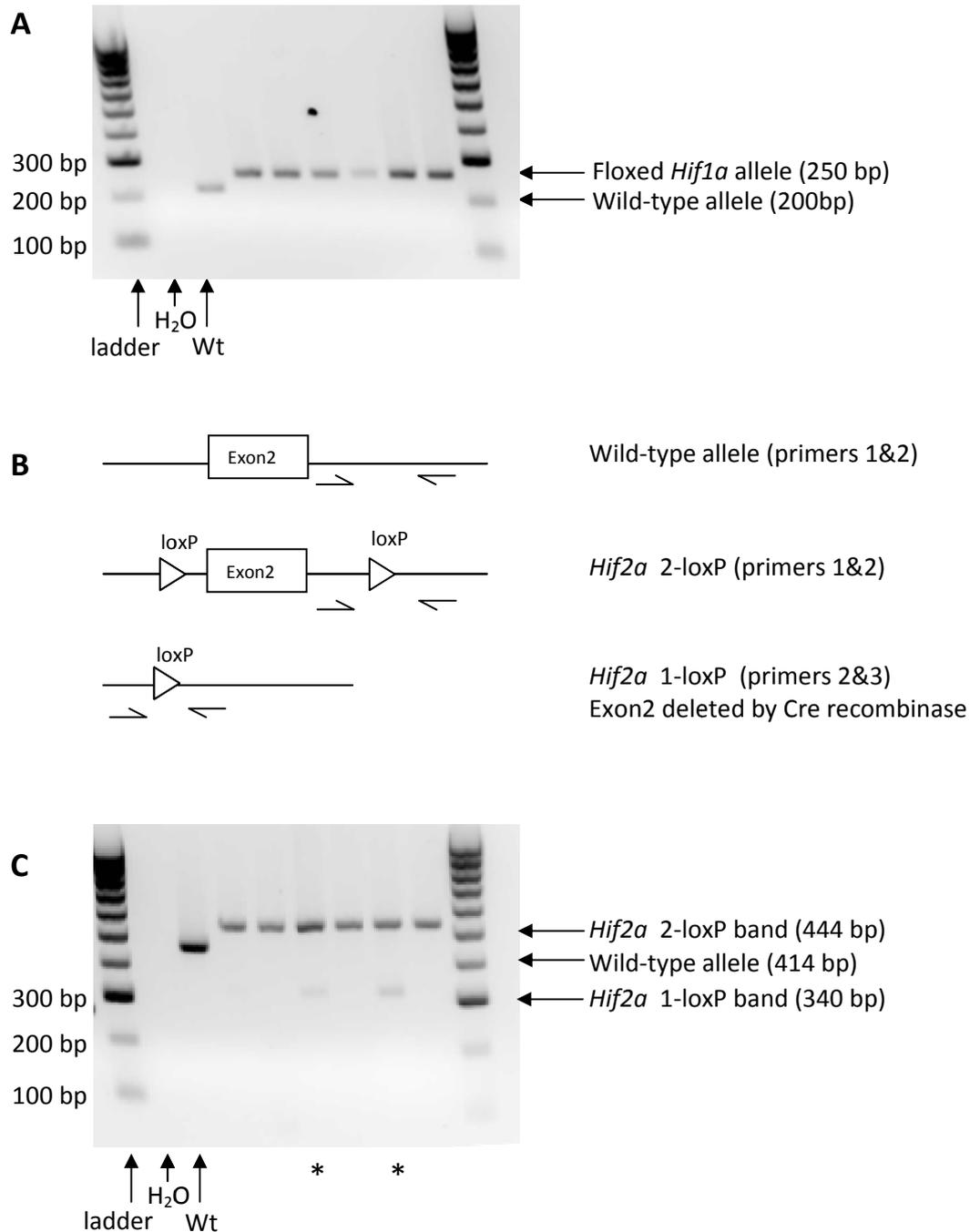
Figure 2.10-1. Genotyping of murine colonies.

(A & C) Representative images of PCR gels performed to detect murine genotypes. DNA was extracted from ear clips of mice and amplified using primers to detect wild-type or floxed (A) *Hif1a* or (C) *Hif2a* alleles. Wild type and floxed allele bands are labelled in each panel. H_2O and wild-type DNA (Wt) were used as controls. (B) A schematic showing the use of 3 primers for *Hif2a* genotyping. This allowed detection of wild-type, floxed and deleted alleles. In Panel C, the multiplex PCR detected the 1-loxP band in ear tissue of animals that possessed the lysozyme M driven Cre transgene (lanes indicated by *). This phenomenon is reported in other tissue-specific Cre-loxP systems (Zhang *et al.*, 2007). The presence or absence of the Cre transgene was confirmed by a further PCR reaction in all animals.

2.11 Murine neutrophil isolation

Peripheral blood or bone marrow murine neutrophils were isolated by negative magnetic selection using commercially available kits. Following leukocyte preparation (described in sections 2.11.1 and 2.11.2), the EasySep® 'neutrophil enrichment kit' from StemCell technologies produced a better yield of neutrophils than the Miltenyi MACS® 'untouched neutrophil isolation kit' and was therefore used as the standard method of isolation for peripheral blood neutrophils. However, when isolating neutrophils for RNA work or from bone marrow, better purity was obtained using the Miltenyi neutrophil isolation kit (see Figure 2.11-1). The standard (EasySep®) neutrophil isolation is described in section 2.11.3 and the highly pure (Miltenyi MACS®) neutrophil isolation is described in section 2.11.4.

2.11.1 Murine peripheral blood leukocyte preparation

Mice were anesthetised using a mixture of xylazine hydrochloride (10 mg/kg, Rompun® 2%, Bayer HealthCare, Kiel, Germany), atropine sulphate (0.02 mg/kg, Atrocare®, Animalcare Ltd., York, UK) and ketamine (200 mg/kg, Ketaset®, Fort Dodge Animal Health Ltd., Southampton, UK). Once adequately anaesthetised, a laparotomy was performed and the inferior vena cava exposed by blunt dissection. Blood was collected using a 23G needle (BD Microlance™3, Becton Dickinson, Fraga, Spain) and 1 ml syringe (BD Plastipak™). Between 0.5 and 1 ml of blood were obtained per mouse and this was transferred into labelled 15 ml falcon tubes. Mice were culled by cervical dislocation following venesection. The erythrocytes were lysed using 9 parts of an ammonium chloride lysis solution (StemCell technologies) to every 1 part blood. The blood and lysis solution were incubated together for 10 minutes at room temperature and out of direct light. The leukocytes were pelleted at 300 g for 10 minutes at 4˚C and the supernatant removed. Pellets were resuspended in 10 ml of a PBS buffer solution containing 2% foetal bovine serum and 5 mM EDTA (RoboSep™ buffer, StemCell technologies) and spun again at 300 g for 10 minutes at 4˚C. Typically leukocytes from 2 or 3 mice were pooled to obtain sufficient numbers for neutrophil isolation.
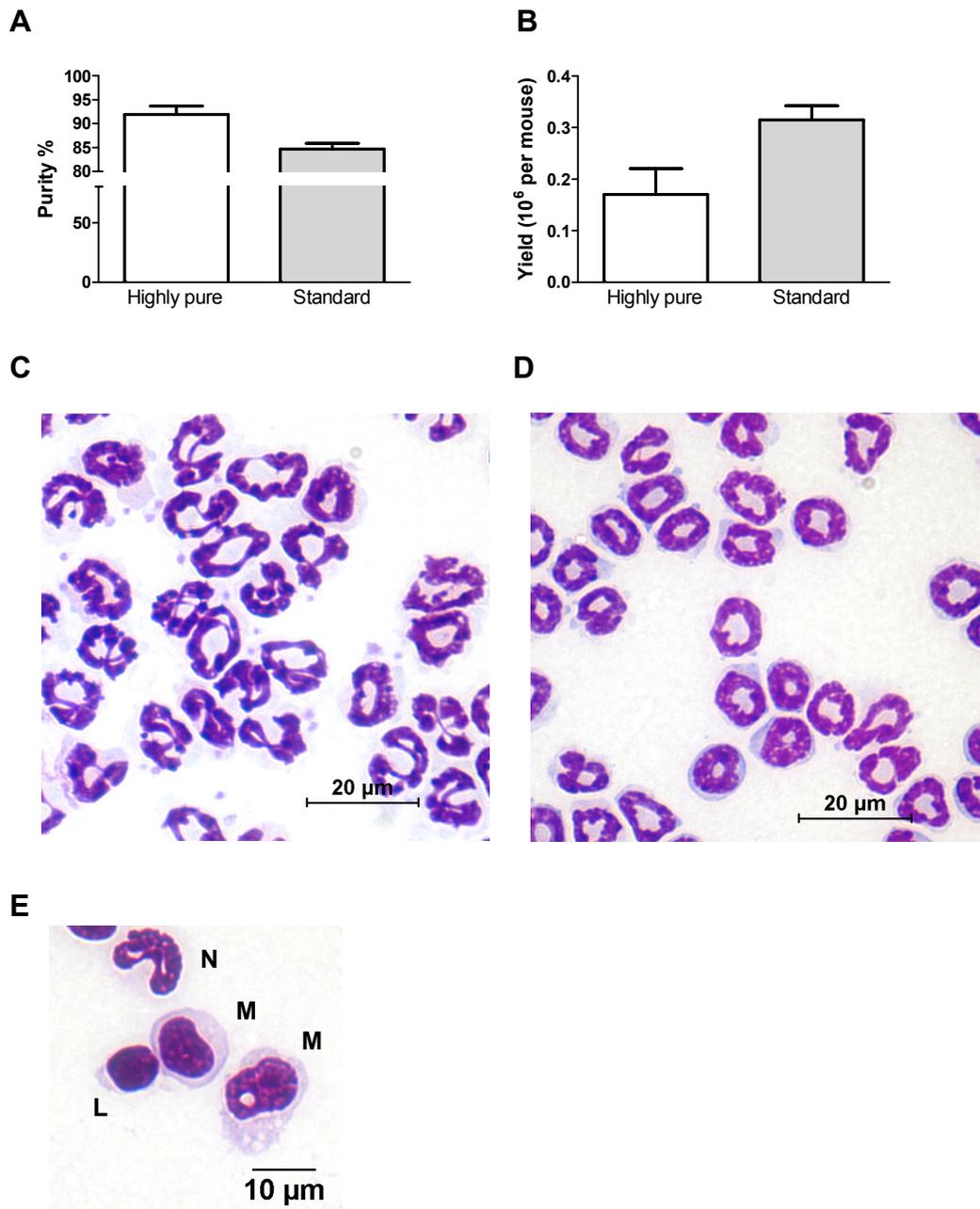
Figure 2.11-1. Isolation of murine neutrophils from peripheral blood and bone marrow.

(A) Purity of peripheral blood neutrophils isolated using either Miltenyi negative selection kit and MACS® LD columns or the EasySep® neutrophil isolation kit with Easyplate® magnet. (B) Yield of neutrophils from peripheral blood using the Miltenyi or EasySep isolation methods expressed as 10^6 cells per mouse. (C & D) Photographs of freshly isolated murine (C) peripheral blood or (D) bone marrow derived neutrophils. Original magnification 1000x. (E) Photograph of a cytocentrifuge slide showing contaminating leukocytes in murine peripheral blood neutrophil isolations. N = neutrophil; M = monocyte; L = lymphocyte. Original magnification 1000x.

2.11.2 Murine bone marrow leukocyte isolation

Mice were killed by cervical dislocation following venesection (2.11.1) and the hind legs de-gloved and removed by cutting at ankle and hip joint. Femurs and tibias were carefully dissected from the surrounding muscle and placed in ice cold HBSS with 0.5% bovine serum albumin (Sigma-Aldrich). Bones were cannulated with 25G needles (BD Microlance™) and the marrow was flushed into falcon tubes using 10 mls of HBSS plus BSA. This cell suspension was passed over a 40 μm cell strainer (BD Falcon™) to remove clumps and other tissue before the cells were pelleted at 350 g for 6 minutes at 4°C. The supernatant was discarded and the cells were resuspended in 20 mls of PBS plus 0.5% BSA. A haemocytometer count was performed before the cells were pelleted again, ready to proceed to negative magnetic selection as described in 2.11.4. Typically 50 x 10^6 leukocytes were obtained per mouse.

2.11.3 Standard murine peripheral blood neutrophil isolation - EasySep® kit

Following peripheral blood leukocyte preparation, leukocyte pellets were resuspended in 150 μl of RoboSep™ buffer and transferred into a 96-well non-tissue culture treated U-bottom plate (BD Falcon Microtest™). The EasySep® neutrophil enrichment antibody cocktail labels a maximum concentration of leukocytes of 100 x 10^6 per ml or 15 million cells per well. Typically blood from 3 mice yielded less than 15 million leukocytes and therefore leukocytes from a maximum of 3 mice were pooled per well. Rat serum (7.5 μl per 150 μl sample) and neutrophil enrichment cocktail (7.5 μl per 150 μl sample) were added and the plate incubated at 4°C for 15 minutes. RoboSep™ buffer (100 μl) was then added to each sample and the plates centrifuged at 300 g for 7 minutes. The supernatant was aspirated and the cell pellets resuspended in 150 μl of RoboSep™ buffer. A biotin selection cocktail was then added (7.5 μl per 150 μl sample) and plates were incubated for a further 15 minutes at 4°C. Magnetic dextran-coated iron particles (D Particles) were added (20 μl per 150 μl sample) and plates incubated for 10 minutes at 4°C. RoboSep™ buffer was added to each well to give a total volume of 250 μl and the plate was placed on an EasyPlate™ EasySep® magnet (StemCell

technologies) for 10 minutes at room temperature. The tetrameric antibody complexes bound to contaminating cells were attracted to the magnet and settled at the bottom of the wells leaving unlabelled neutrophils in the supernatant. This supernatant was carefully transferred into 15 ml falcon tubes and topped up with RoboSep™ buffer to a final volume of 500 µl. A haemocytometer count was performed and the cells were washed in 10 mls of PBS before being spun at 300 g for 10 minutes. The cells were then ready to be suspended in media or the appropriate lysis solution.

2.11.4 Highly pure murine neutrophil isolation – Miltenyi MACS® kit

The volumes of antibody and buffer solutions described for this method apply to the use of the MACS® untouched murine neutrophil isolation kit (Miltenyi Biotec Ltd.) with 50×10^6 or fewer leukocytes. If greater than 50×10^6 leukocytes, buffer and antibody volumes were titrated up accordingly, but if less than 50×10^6 leukocytes the volumes were not reduced. Murine peripheral blood or bone marrow leukocytes were resuspended in 400 µl of a buffer solution (PBS plus 0.5% BSA). Mouse FC receptor blocking reagent (Miltenyi Biotec Ltd.) was added (50 µl per 50×10^6 leukocytes) and the cells incubated for 10 minutes at 4˚C. A biotinylated antibody cocktail was added (50 µl per 50×10^6 leukocytes) and cells were incubated for a further 10 minutes at 4˚C. Cells were washed in 10 ml of the buffer solution and centrifuged at 300g for 10 minutes. The supernatant was removed and cells were resuspended in 400 µl buffer. Anti-Biotin MicroBeads (100 µl per 50×10^6 leukocytes) were added followed by 15 minutes incubation at 4˚C. Cells were washed again in 10 ml of buffer and spun at 300 g for 10 minutes. The supernatant was removed and cells were resuspended in 500 µl buffer. During the final spin a MACS® LD column, placed in a MidiMACS™ magnet, was primed by rinsing with 2 ml of buffer. The cell suspension was applied to the primed column and unlabelled cells were collected in a clean falcon tube. Once the cells had fully penetrated the column matrix, buffer solution (2 x 1 ml aliquots) was used to wash the column. The enriched neutrophils which had passed through the column were washed by topping up the flow through to a total volume of

10 mls, pelleted at 300 g for 10 minutes and resuspended in 500 μl of buffer before being counted. The neutrophils were pelleted at 300 g for 10 minutes and were then ready for use.

2.12 Murine neutrophil culture

Murine neutrophils were cultured at a concentration of $1x10^6$/ml on 96-well non-tissue culture treated polyvinyl chloride plates (BD Falcon™). Normoxic and hypoxic cell culture was carried as described in section 2.3. Cells were also cultured in the presence or absence of 10 ng/ml LPS from *E coli.* (Serotype R515(RE), TLR*grade*™, Alexis® biochemicals, Lausen, Switzerland) or the hydroxylase inhibitor, dimethyloxalylglycine (DMOG 1-1000 μM, Frontier Scientific Europe, Carnforth, UK).

2.13 Murine neutrophil RNA extraction

Murine peripheral blood or bone marrow neutrophil RNA was extracted using the mirVana™ total RNA isolation protocol (Ambion, Austin, USA). Cells ($1x10^6$ per condition) were lysed in 300 μl of mirVana lysis/binding buffer and stored at -80 ˚C if not being extracted immediately. To extract the RNA, miRNA homogenate (1/10th of the lysate volume) was added to the lysate to stabilise the RNA and inactivate RNases. Samples were vortexed (Vortex Genie®2, Scientific Industries, Bohemia, USA) to mix and incubated on ice for 10 minutes. A volume of Acid-Phenol:Chloroform (Ambion) equivalent to that of the initial lysate was added, mixed well using a vortex mixer and spun at 13400 rpm (Eppendorf Mini Spin Hamburg, Germany) for 5 minutes at room temperature. The upper aqueous layer was carefully removed and transferred to a clean RNase-free 1.5 ml eppendorf tube. The volume removed was noted to

enable 1.25 volumes of ethanol to be added. Samples were vortexed and a maximum of 700 μl of this aqueous layer/ethanol mixture was transferred onto a filter cartridge within a labelled mirVana kit collection tube. These tubes were spun for 15 seconds at room temperature at 10000 rpm. The flow through was discarded and any remaining aqueous/ethanol mixture was added to the filter cartridge. Once all the aqueous/ethanol mixture had been spun over the cartridge, 700 μl miRNA wash-solution 1 was added to the filter cartridge. Tubes were again spun for 15 seconds at 10000 rpm, the flow through was discarded and washing of the filter cartridge was repeated a further two times using 500 μl miRNA wash-solution 2/3, discarding the flow through after each wash. After the final wash, the tubes were spun for a further 60 seconds to dry the filter cartridge. Cartridges were then placed into a clean labelled collection tube and 30 μl of RNase free water pre-heated to 95 °C was added to the filter cartridge. Tubes were spun again for 20-30 seconds at 13400 rpm. The flow through containing the RNA was then analysed using a NanoDrop™ 1000 spectrophotometer (Fisher Scientific UK Ltd.). cDNA synthesis was performed as per section 2.4.1 but due to the low numbers of murine neutrophils and low yield of RNA, 500 ng of RNA were used to make each cDNA sample.

2.14 Murine neutrophil protein extraction and immunoblotting

Murine neutrophil lysates were prepared by adding complete protease inhibitor cocktail ($1x10^6$ cells in 30 μl) to cell pellets and boiling in an equal volume of 2xSDS buffer (see Appendix V). Protein separation was performed as described in section 2.5.2 and antibody concentrations are indicated in Appendix VI.

2.15 Murine neutrophil functional assays

2.15.1 Neutrophil chemotaxis

Neutrophil chemotaxis was assessed using Neuro Probe ChemoTx® microplates with a 5 µm filter (Neuro Probe, Inc. Receptor Technologies Ltd., Adderbury, UK). Microplate wells were filled in duplicate with 29 µl of test solutions containing various concentrations of recombinant murine KC (PeproTech EC Ltd., London, UK). A negative control (RPMI 1640) and positive control (25 µl of cells at a concentration of 2×10^6/ml) were also added to the microplate. The framed filter was firmly applied to the microplate so that the fluid in the wells made contact with the filter and no air bubbles were seen. Cells (25 µl) were added to each site on the filter except for over the positive control well and allowed to migrate for 1 hour. A chemokinesis control (cells suspended in 10 nM KC with 10 nM KC in the microplate well below) was also prepared. After incubation, any remaining cells on the top of the filter were removed using a cotton bud and the plates were centrifuged at 350 g for 10 minutes. The filter was carefully removed and cells in the microplate wells were counted using a haemocytometer. The number of cells in the microplate wells is expressed as a percentage of the positive control minus the percent migration of the chemokinesis control:

% chemotaxis = $\dfrac{\text{no. migrated cells} - \text{no. of migrated cells in chemokinesis control}}{\text{no. of cells in positive control well}}$ x 100

2.15.2 Neutrophil cell surface receptor expression

After 4 hours incubation, cells were washed with ice-cold FACS buffer (PBS plus 0.5% BSA) and stained with anti-mouse antibodies at 4°C. Cells were single-stained with PE-anti-CD62L (L-selectin) (8 µg/ml, BD Pharmingen™) and PE-anti-CD11b (8 µg/ml, BD Pharmingen™). Isotype-matched controls (PE-IgG2a and PE-IgG2b respectively) were used to set baselines. Antibody binding was detected using a BD FACSCalibur™ flow cytometer (BD Biosciences, Becton

Dickinson Ltd., Oxford, UK). During analysis specific geometric mean fluorescence was calculated by obtaining geometric mean fluorescence intensity values for each antibody and subtracting the geometric mean fluorescence of the isotype control. Results were processed using FlowJo software (version 9.0, Tree Star Inc., Ashland, US).

2.16 *In vivo* models

2.16.1 Acute lung injury models

2.16.1.1 Intratracheal instillation of lipopolysaccharide (LPS)

Mice were anaesthetised with ketamine (100 mg/kg i.p.; Willows Francis Veterinary, Crawley, U.K.) and acepromazine (5 mg/kg i.p.; C-Vet Veterinary Products, Lancashire, UK) before fur was shaved from their necks. A small (<1 cm) midline incision was made and the trachea exposed through gentle blunt dissection until it could be cannulated under direct vision with a 24G cannula (Jelco® radiopaque cannula, Smiths Medical International Ltd. Rossendale, UK). LPS from *Salmonella minnesota* R595 (TLR*grade*™, Enzo Life Sciences, Exeter, UK) was directly instilled (0.3 µg in 20 µl) via the cannula and the animals recovered for 6 hours in a warmed cage in room air (Rowe *et al.*, 2002).

2.16.1.2 Nebulised lipopolysaccharide

Awake mice were placed in a plastic container which was connected to an oxygen-driven nebuliser. Oxygen was delivered at 6 litres per minute through 3 mg LPS from *Salmonella minnesota* creating a vapour that was delivered into the container. Once all the LPS was delivered, mice were transferred back into their original cages.

2.16.1.3 Bronchoalveolar lavage, blood and tissue collection

At specified time points (6, 24, 48 or 72 hours) mice were anaesthetised with ketamine/atropine/xylazine (as per section 2.11.1) and exsanguinated. The chest wall was exposed by opening the skin in the midline from the initial neck wound down to the abdomen. Pneumothoraces were introduced by carefully puncturing the inferior surface of the diaphragm and then the thorax was opened by carefully cutting along the lateral margins of the rib cage on each side exposing the untouched lungs and heart. The trachea was exposed, cannulated and secured in place with suture before the lungs were instilled with 3.5 ml of ice cold 0.9% saline in 0.5-1.0 ml aliquots. The recovered lavage fluid was maintained on ice before haemocytometer counts were performed and samples spun at 1000 g for 5 minutes. Cell pellets were resuspended in foetal bovine serum prior to cytocentrifugation or directly lysed and RNA extracted using the mirVana™ total RNA isolation protocol (Ambion, Austin, USA). BAL supernatant was stored at -80˚C for cytokine analysis. Cytospins of serum-suspended BAL cells were stained with Reastain Quick-Diff (see section 2.7.1) for differential cell counts and morphologic scoring of apoptosis.

Blood from mice exposed to LPS was used to generate plasma and to isolate peripheral blood neutrophils. Heparinised blood drawn prior to performing bronchoalveolar lavage was spun at 3000 rpm for 5 minutes (Eppendorf, Mini Spin) and the plasma carefully removed and stored at -80˚C. Cell pellets were lysed in ammonium chloride as per section 2.11.1 and the neutrophils isolated using the standard negative selection protocol described in section 2.11.3.

For histological sections, lungs which had not been lavaged were fixed via the trachea with 10% buffered formalin at 20 cm H_2O and paraffin-embedded blocks prepared. Following deparaffinization, serial sections were stained with anti-HIF-2α (clone ep190b) as described in section 2.6.

2.16.1.4 Analysis of IgM in bronchoalveolar lavage fluid

Levels of IgM in bronchoalveolar lavage fluid were determined by enzyme-linked immunosorbent assay (ELISA) using a commercially available kit (Mouse IgM ELISA quantitation set, Bethyl Laboratories Inc, Montgomery, USA). High affinity plates (Costar 96-well EIA plates, Thermo Fisher Scientific, Loughborough, UK) were coated with 100 µl per well of coating antibody diluted 1:100 in coating buffer (see Appendix X). Plates were incubated at room temperature for 60 minutes before being washed 5 times with 200 µl per well of wash solution (see Appendix X). Blocking buffer (200 µl per well) was added and plates incubated for a further 30 minutes at room temperature. Plates were again washed 5 times before 100 µl of neat samples and standards were added in duplicate. Serial dilutions of mouse reference serum were performed to produce a standard curve with an IgM concentration range of 7.8 ng/ml to 1000 ng/ml in 0.9% saline. After 1 hour of incubation, the plates were washed 5 times and 100 µl per well of HRP-conjugated detection antibody, diluted 1: 50,000 in blocking solution, was added. After a further 1 hour of incubation the plates were washed 5 times and 100 µl of tetramethylbenzidine (TMB) substrate solution (eBioscience Ltd., Hatfield, UK) was added to each well. The plate was developed in the dark for 15 minutes before the reaction was stopped by adding 100 µl of 1M sulphuric acid. Plates were read at 450 nm (VarioskanFlash®, Thermo Fisher Scientific) and data were analysed in Microsoft excel.

2.16.2 Pneumococcal pneumonia model

Mice were anaesthetised and the trachea cannulated as described in 2.16.1. Pneumococci (*Streptococcus pneumoniae,* serotype 2, stain D39) were prepared at a concentration of 5×10^{8} per ml in PBS and 20 µl (1×10^{7} cfu) were instilled via the trachea. This strain and concentration of bacteria leads to established pneumonia, induces neutrophilic lung inflammation and is associated with a high rate of mortality in wild-type animals (Dockrell *et al.*, 2003). Following intratracheal administration of bacteria, the mice were allowed to recover and then monitored closely for 9 days. Animals which displayed a pre-determined level of

morbidity (severely ruffled fur, hunched posture and impaired movement) were culled. The individuals making this assessment were not aware of mouse genotype.   On day 9 surviving mice were culled and Kaplan-Meier survival curves plotted.

2.17 Analysis of cytokines in plasma and bronchoalveolar lavage fluid.

Cytokine analysis was performed on plasma and bronchoalveolar lavage fluid from mice exposed to LPS using a multiplex analysis kit, the Meso Scale Discovery mouse proinflammmatory 7-plex assay ultra-sensitive kit (Meso Scale Discovery®. Gaithersburg, USA). This method follows the same principle as enzyme-linked immunosorbent assays (ELISA) but each well of the 96-well Multi-Spot® carbon electrode plate surface contained 7 spatially distinct spots each coated with antibody for a specific protein. This allowed multiple proteins to be detected in a small volume of the same sample.

Standards and samples (25 µl) were added to a pre-coated plate and incubated for 2 hours with vigorous shaking (600 rpm) at room temperature. The plates were washed with PBS containing 0.05% Tween®-20 (Fisher Scientific) before addition of the detection antibody. Plates were incubated for 2 hours with vigorous shaking and then washed again in PBS containing Tween (PBS-T). Read buffer was then added to each well and the plate read using a MSD Sector® Imager 2400 (Meso Scale Discovery). Data were analysed using MSD Discovery Workbench® software (Meso Scale Discovery) and exported into Microsoft Excel for subsequent analysis.

2.18 A model of subcutaneous *Staphylococcus aureus* infection

2.18.1 Preparation of live *Staphylococcus aureus*

Bacterial work was carried out in a class II microbiological safety cabinet (Walker, Glossop, UK). The SH1000 strain of *S. aureus*, derived from the clinical isolate NCTC 8325, was used throughout these experiments. As the NCTC 8325 strain harbours a naturally occurring mutation in the *rsb*U element, the SH1000 strain was generated to restore the lack of this virulence factor (Horsburgh *et al.*, 2002; Kullik *et al.*, 1998). Bacteria were plated on Columbia horse blood agar (Oxoid Ltd.. Basingstoke, UK) and grown overnight at 37°C with 5% CO_2. A single colony was used to inoculate 30 mls of brain heart infusion (BHI, Oxoid Ltd.) in a 50 ml falcon. This was cultured for 15 hours at 37°C to generate bacteria in stationary phase growth (Horsburgh *et al.*, 2001). Bacteria were centrifuged at 5000 g for 10 minutes to pellet the cells and were subsequently washed twice with PBS. Following centrifugation bacteria were resuspended in a final volume of 10 mls and the concentration of colony forming units (cfu) in this stock was calculated using the Miles and Misra method (Miles *et al.*, 1938). A 100 µl sample of stock was diluted in a ten-fold dilution series in sterile PBS, vortexing samples thoroughly between each serial dilution. Three 10 µl drops from each of 7 serial dilutions were incubated overnight on blood agar plates. Viable colonies were counted the following day and from this the original bacterial concentration calculated. The stock was stored at -80°C. Prior to use, stock vials were defrosted, the cells pelleted at 9000 rpm for 3 minutes and washed twice in PBS before being resuspended in a volume which yielded an estimated concentration of 2 x 10^9 cfu/ml. The final bacterial concentration was subsequently confirmed for each experiment using the Miles and Misra method.

2.18.2 Skin lesion model

Wild-type C57BL/6 mice had the fur on their backs shaved with electric hair trimmers and were then injected with 50 µl of SH1000 at a concentration of 2 x 10^9 cfu/ml. Mice were weighed

and a photograph of the injected area was taken. Mice were then checked daily for 7 days and on each day weights were recorded and a photographic image taken of the back using a ruler to indicate scale. On day 7 mice were sacrificed and the skin lesions dissected, weighed, snap frozen in liquid nitrogen and stored at -80˚C.   ImageJ software (version 1.45, National Institutes of Health, USA) was used to trace the circumference of abnormal skin in each photographic image and skin lesion area was calculated.

2.18.3 Exposure of animals infected with *S. aureus* to hypoxia

Mice were prepared as in section 2.18.2 and injected with 50 µl of SH1000 at a concentration of 2 x 10^9 cfu/ml or PBS as a control and injection sites were marked. Following injection mice were either left in room air (normoxia) or placed in a hypoxic chamber (Wolf laboratories, York, UK) which delivered 10% oxygen/90% nitrogen. The oxygen tension in the chamber was reduced gradually to the set point of 10% over 1 hour using an oxygen sensing control unit (Coy Labs, Grass Lake, Michigan, USA). Carbon dioxide was removed with soda lime (Sigma Aldrich). At indicated time points (3-12 hours) mice were taken out of the chamber to be assessed alongside normoxic controls. Routinely temperature was recorded using a rectal thermometer probe (VisualSonics, Toronto, Canada) and sickness severity was assessed (see section 2.19). Following this clinical assessment mice were anaesthetised and exsanguinated via the inferior vena cava. To investigate potential bacterial seeding of organs, spleens and kidneys were harvested and stored at -80˚C and a 4 mm punch biopsy (Decree Thermo Ltd, Sheffield, UK) of the skin at the injection site was taken to be processed as described in section 2.20.

2.19 Mouse sickness scoring

Clinical assessment of mouse sickness behaviour was made by two independent observers blinded as to which oxygen tension the mice had been exposed. Two sickness scores (see Appendix XI) were used based on existing objective scoring systems (Biswas *et al.*, 2002; Lloyd and Wolfensohn, 1999). Scores provided by each observer were averaged for each animal.

2.20 Assessing local response to infection

2.20.1 Skin sections

Skin biopsies of the injection site were placed in 10% buffered formalin prior to processing. Tissue embedding and sectioning was performed by Yvonne Stephenson. In brief, tissue was removed from the formalin and placed in a cassette before being processed into wax using a Leica TP1020 processor (Leica Microsystems, Milton Keynes, UK). Waxed tissue was embedded in paraffin blocks before cutting with a microtome (Leica RM2245) and floating onto glass slides (Superfrost plus, Thermo Fisher Scientific, Loughborough, UK) in a water bath at 45˚C. Slides were dried overnight in an oven at 37˚C.

2.20.1.1 Haematoxylin and eosin staining

Slides were dewaxed and rehydrated by immersing in graded descending concentrations of ethanol. Slides were washed in tap water and stained with Gill's haematoxylin (Leica) for 2 minutes. After a further wash, the sections were covered in Scott's tap water (1000 ml water, 3.5 g sodium bicarbonate, 20 g magnesium sulphate) for 10 seconds before washing and staining with 1% aqueous eosin (Leica) for 5 minutes. This was rinsed with tap water and the sections were dehydrated through ascending ethanol concentrations until in xylene (VWR

International Ltd., Lutterworth, UK) and then mounted using Consul-Mount™ (Thermo Fisher Scientific).

2.20.1.2 Gram's stain

To visualise Gram positive bacteria in tissue sections, the Accustain® Gram stain kit was used (Sigma Aldrich). The kit uses a modified method from Gram's original description (Gram, 1884). Sections were dewaxed in xylene and rehydrated to deionised water as described above. Slides were flooded with Crystal Violet solution and allowed to stand for 1 minute. Slides were washed with water and treated with Gram's iodine solution for 5 minutes followed by a further wash. Excess water was blotted before slides were dipped twice in ethanol to differentiate and checked by light microscopy. A further dip in ethanol could be performed if required. Following a rinse in deionised water, slides were covered in Safranin O solution for 1 minute. This was rinsed, slides were blotted and Tartrazine solution was applied for 5 sections. Excess stain was immediately blotted and the slides rinsed twice in ethanol. Slides were cleared in xylene before mounting.

2.20.1.3 Immunohistochemistry

Immunohistochemical staining of mouse skin sections was performed as described in section 2.6 using an anti-myeloperoxidase antibody. Antibody dilutions are in Appendix IX.

2.20.2 Skin myeloperoxidase activity

Skin biopsies were weighed then immediately frozen in liquid nitrogen and stored at -80˚C for subsequent analysis. Skin was chopped finely with a scalpel blade while defrosting and subsequently homogenised. The chopped skin was placed in 0.5 ml of 5 mg/ml hexadecyltrimethylammonium bromide (Sigma Aldrich) containing 50 mM potassium phosphate (HTAB buffer) at pH 6.0. Homogenisation was performed using either a glass pestle and mortar or with stainless steel beads in a Bullet Blender® (Next Advance, Averill Park, USA). HTAB buffer efficiently extracts myeloperoxidase from skin specimens (Bradley *et al.*, 1982).

The samples were sonicated in a Bioruptor™ iced water bath (Diagenode Europe SA, Liège, Belgium) for 5 minutes using 30 second on/off high power cycles. Samples were then frozen and thawed 4 times before a further 5 minute period of sonication and subsequently centrifuged at 14000 g for 30 minutes at 4˚C. The supernatant was removed and 100 µl of this was added to 1.9 ml O-dianisidine solution (0.167 mg/ml O-dianisidine hydrochloride (Sigma Aldrich), 0.0005% hydrogen peroxide, 50 mM potassium phosphate). O-dianisidine hydrochloride is a chromogenic oxidase substrate and its reaction with myeloperoxidase under the conditions used has been reported to be sensitive enough to detect the myeloperoxidase activity of 10,000 neutrophils (Bradley *et al.*, 1982). Absorbance was read by a spectrophotometer (Jenway 6310, Barloworld Scientific Ltd, Dunmow, UK) at a wavelength of 450 nm. The absorbance change between 30 seconds and 90 seconds of the reaction time gave the relative myeloperoxidase activity.

2.20.3 Bacterial counts in homogenised skin

Skin biopsies were weighed then immediately frozen in liquid nitrogen and stored at -80˚C for subsequent analysis. Skin was homogenised as in section 2.20.2 but PBS was used in place of the HTAB buffer. The numbers of colony forming units in skin homogenates were calculated using the Miles and Misra method and normalised per gram of skin.

2.21 Assessing systemic response to *S. aureus* infection

2.21.1 Plasma cytokine analysis

Blood from mice injected with SH1000 or placebo was harvested at 3, 6 or 12 hours and spun at 3000 rpm for 5 minutes to generate plasma. This was stored at -80˚C until further analysis could be performed. To analyse cytokines, cytometric bead arrays (CBA) were performed by

Susan Newton (Flow cytometry core facility, University of Sheffield) on a FACSarray flow cytometer (Becton Dickinson Ltd., Oxford, UK) using BD™ CBA flex sets (murine Il-1β, Il-6, Il-10, TNF-α, KC, MCP-1) as per manufacturer's instructions.

2.21.2 Serum markers of organ dysfunction

Serum was generated by allowing blood to clot at room temperature before centrifugation at 5000 rpm for 5 minutes (Mini Spin, Eppendorf). Serum was then transported on ice to a veterinary laboratory (Nationwide Veterinary Laboratories, Leeds) and analysed for makers of liver (aspartate transaminase), kidney (creatinine) and pancreatic dysfunction (lipase).

2.21.3 Assessment of lung injury

To assess for possible lung injury in animals injected with SH1000 bacteria, animals were anaesthetised after 12 hours in hypoxia or normoxia. Respiratory rate was counted then bronchoalveolar lavage was performed, while in other animals lungs were fixed by instillation of buffered formalin. Both methods are described in section 2.16.1.3. In separate experiments lungs were harvested, weighed and maintained in a warm room until fully dehydrated. Lung weights were recorded each day until measurements were stable for more than 2 readings giving the dry weight.

2.21.4 Assessment of brain oedema

Mice were injected subcutaneously with *S. aureus* or PBS control and after 12 hours in hypoxia or normoxia were terminally anaesthetised with pentobarbital (20% w/v, JM Loveridge PLC, Southampton, UK). The brains were carefully removed and placed in a warm room to obtain dry weights as described for lungs in Section 2.21.3. In other experiments, mice were injected intraperitoneally with Evan's blue dye (4 ml/kg of 2%) and subsequently infected and either exposed to hypoxia or maintained in normoxia for 12 hours. Mice were then anaesthetised and exsanguinated and the circulation flushed from the left ventricle with 10 mls of ice cold PBS to remove intravascular dye. The brains were harvested and placed in 500 µl of formamide

(Sigma Aldrich) for 48 hours in a dark warm room. The supernatant was then carefully harvested and 100 µl added in duplicate to a flat-bottomed 96-well plate. Plasma collected at the same time as the brain tissue was also added to the plate and optical density was analysed by spectrophotometry at 630 nm. A standard curve of serial dilutions of Evans blue dye was performed and sample concentrations were read against this curve (see Figure 2.21-1). Plasma values were checked to ensure equal absorption of dye in each group and to check that no values exceeded the maximum binding capacity of plasma proteins for the dye (500 µg/ml) (Hafezi-Moghadam *et al.*, 2007; Kakinuma *et al.*, 1998).

2.21.5 Measurement of blood glucose and bicarbonate

Blood glucose levels were measured in infected mice after 12 hours in normoxia or hypoxia using an Optium Xceed blood glucose meter (Abbott Laboratories Ltd, Maidenhead, UK). A single drop of blood was placed on the measurement strip to obtain the reading. Venous bicarbonate levels were obtained from infected mice by drawing 100 µl heparinised blood into a syringe and analysing on a blood gas analyser (ABL5, Radiometer, Copenhagen, Denmark).

2.21.6 Blood pressure and heart rate measurements in awake mice

To obtain readings in awake mice, animals were trained for 7 days to undergo non-invasive blood pressure measurement using a BP-2000 Blood Pressure Analysis System™ (Visitech Systems Inc., Apex, USA). Training involved placing mice in the restraints used by the analysis machine each day, followed by 10 or 20 recordings of blood pressure. This was performed to allow animals to become accustomed to the procedure. After training, these animals were then injected with either SH1000 bacteria or PBS (as per section 2.18.3) and exposed to hypoxia or normoxia for 12 hours after which time blood pressure and heart rate measurements were recorded. A minimum of 10 readings were attempted on each animal.
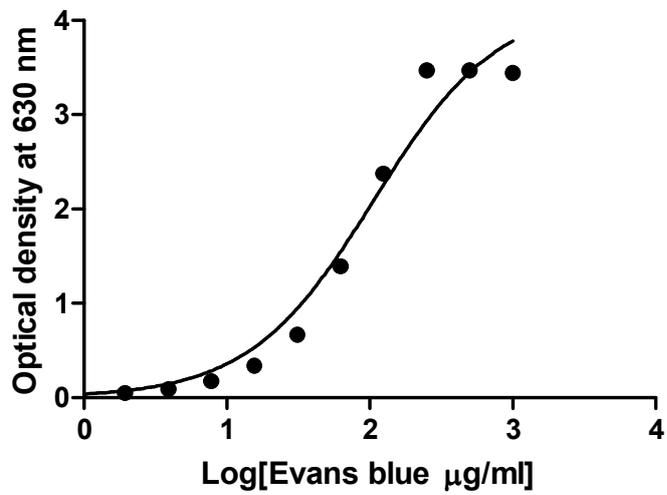
Figure 2.21-1. Optical density of serial dilutions of Evan's blue dye.

A standard curve fitted to values of optical density at 630 nm plotted against the logarithm of Evan's blue dye concentrations.

2.21.7 Echocardiography

Twelve hours after subcutaneous injection of bacteria, hypoxic or normoxic mice were anaesthetised with 5% isoflurane supplied in oxygen at 2 l/min and placed on a warming pad. Mice were secured on the pad lying flat and supine. The fur on the chest was clipped and hair removal cream used to ensure good penetration of ultrasound waves.

Transthoracic echocardiography was performed by an experienced operator (Dr Abdul Hameed, Department of Cardiovascular Sciences, University of Sheffield) using a VisualSonics Vevo® 770 Imaging system and RMV707B scanhead (VisualSonics, Toronto, Canada). Short axis view recordings were made in M-mode at the level of the papillary muscles to enable measurement of left ventricular diameter at end-systole and end-diastole. Using these values, fractional shortening (FS) and left ventricular end-systolic and end-diastolic volumes were calculated allowing subsequent calculation of ejection fraction (EF). Left ventricular volumes were also used to calculate stroke volume and thus cardiac output. For equations used see Table 2.21-1. Cine (2-D) images in the short axis view were acquired and endocardial area traced in systole and diastole from which fractional area change (FAC%) was calculated. Another independent measure of contractility used was pulse wave tissue doppler velocities. These were manually recorded from the endocardial aspect of the posterior left ventricular wall.

Parameter	Equation
Fractional shortening (%)	$((LVIDd - LVIDs)/LVIDd) \times 100$
Left ventricular volume (µl)	$(7/(2.4+LVID)) \times LIVD^3$
Ejection fraction (%)	$((EDV - ESV)/EDV) \times 100$
Fractional area change (%)	$((LVAd - LVAs)/LVAd) \times 100$
Stroke volume (SV) (µl)	$EDV - ESV$
Cardiac output (ml/min)	$SV \times HR / 1000$

Table 2.21-1. Echocardiographic calculations.

Equations used to calculate echocardiographic measurements of left ventricular volume and function. Abbreviations are as follows: LVID = left ventricular internal diameter; d = end-diastole; s = end-systole; EDV = end-diastolic volume; ESV = end-systolic volume; LVAd = left ventricular endocardial area in diastole; LVAs = left ventricular endocardial area in systole; HR = heart rate.

2.21.8 Nitric oxide measurements

Frozen plasma obtained from mice infected with *S. aureus* or injected with PBS was analysed for nitric oxide content by Dr Andrew Cowburn, University of Cambridge. In brief, plasma was defrosted and passed over a 10 kDa filter column. Samples were then analysed on a Sievers Nitric Oxide Analyser NOA 280i (GE Water & Process Technologies, Boulder, USA) following manufacturer instructions. The analyser uses a reducing agent (vanadium chloride in 1M hydrochloric acid) heated to 95 ˚C to convert nitrite, nitrate and S-nitroso compounds into nitric oxide. In the gas phase NO will react with oxygen to form nitric dioxide producing a chemiluminescent signal emitted from electronically excited NO_2. Total NO_x concentration was determined from a calibration curve constructed with readings obtained from serially diluted nitrate solutions.

2.21.9 Malondialdehyde measurements

Malondialdehyde (MDA) is a product of lipid peroxidation, a process that occurs *in vivo* in response to oxidative stress (Ortolani *et al.*, 2000). The reaction of MDA with thiobarbituric acid reactive substances (TBARS) produces an adduct that can be quantified fluorometrically. I used a MDA quantitation kit (OxiSelect™, TBARS assay kit, Cell Biolabs Inc., San Diego, USA) to determine the amount of lipid peroxidation in plasma from mice infected with *S. aureus* and maintained in normoxic or hypoxic conditions for 12 hours. A calibration curve was generated using serial dilutions of MDA in water. Samples and standards (100 µl) were transferred into eppendorf tubes and 100 µl of SDS lysis solution (OxiSelect™ kit) was added. Samples and standards were incubated at room temperature for 5 minutes before 250 µl of TBA reagent was added. The tubes were then heated to 95 ˚C for 60 minutes before being cooled in ice for 5 minutes. Samples were then centrifuged at 3000 rpm for 15 minutes and the supernatant removed for analysis. For fluorimetric analysis, 150 µl of samples and standards were transferred to a black fluorescence microplate (Nunc MicroWell™ plates, Nalge Nunc

International, Rochester, USA) and read using a wavelength of 540 nm for excitation and 590 nm for emission (FLUOstar Galaxy, BMG Labtech Ltd., Aylesbury, UK).

2.22 Statistical analysis

Data were analysed using Prism 5.0 software (GraphPad Software Inc, San Diego, CA). For comparison of two sample means when cells from the same subject were used, paired *t* tests were performed. Unpaired *t* tests were used for comparisons between control and patient or wild type and transgenic sample means. If multiple time points or concentrations were used, repeated measures ANOVA with Tukey post tests were performed and if comparisons between normoxia and hypoxia, controls and patients or wild type and transgenic mice were required in these experiments, two-way ANOVA with Bonferonni post tests were performed. Statistical significance was accepted when $p < 0.05$.

3 The role of HIF-2α in neutrophilic inflammation

3.1 Introduction

Neutrophils are key mediators of tissue injury in acute and chronic inflammatory diseases (Barnes, 2007; Quint and Wedzicha, 2007). Effective treatments to limit the toxic effects of neutrophilic inflammation are currently lacking and thus represent a major unmet clinical need. The therapeutic challenge is to simultaneously preserve key neutrophil anti-microbial effector functions, whilst maximising efficient neutrophil removal to limit persistent and inappropriate inflammation. Timely neutrophil apoptosis, with effective macrophage efferocytosis, ensures resolution of inflammation and protects against the cytotoxic effects of neutrophils (Rossi *et al.*, 2006; Savill *et al.*, 1989; Whyte *et al.*, 1993). As such, targeting neutrophil apoptosis represents an attractive therapeutic strategy.

Recent evidence has revealed the importance of oxygen-sensing pathways in innate immune biology. Accumulation of HIF-α subunits in myeloid cells occurs in hypoxic conditions, as in other cell types, but also in response to bacteria and bacterial products irrespective of the ambient oxygen tension (Peyssonnaux *et al.*, 2005). These recent data demonstrate complex roles for the HIF pathway that go beyond the regulation of hypoxic signalling and implicate HIF in host responses to bacteria (Imtiyaz *et al.*, 2010; Peyssonnaux *et al.*, 2007; Peyssonnaux *et al.*, 2005). Indeed, myeloid-specific deficiency of HIF-1α not only abolished the prolonged survival of neutrophils in hypoxia but also resulted in depletion of intracellular ATP levels and impairment of neutrophil granule protease production, macrophage motility and invasion, and bacterial killing (Cramer *et al.*, 2003; Peyssonnaux *et al.*, 2005; Walmsley *et al.*, 2005). These *in vitro* findings translated into reduced inflammatory cell infiltrates in acute models of inflammation and more severe bacterial skin infections (Cramer *et al.*, 2003; Peyssonnaux *et al.*, 2005). With such profound effects on innate immune cell function, HIF-1α itself is not an attractive therapeutic target for the many inflammatory diseases, e.g. chronic obstructive

pulmonary disease (COPD) and inflammatory bowel disease (IBD), where inflammation and bacteria frequently co-exist. In marked contrast to deficiency of HIF-1α, deficiency of the HIF hydroxylase PHD3 had minimal consequences for the functional status of neutrophils prior to their apoptosis (Walmsley *et al.*, 2011). This raises the possibility that specific targeting of individual components of the HIF hydroxylase pathway, independent of HIF-1α itself, may result in selective regulation of neutrophil survival pathways independent of key host-pathogen responses.

As discussed in Chapter 1, distinct biological roles for HIF-1α and HIF-2α have recently emerged, with HIF-2α regulating a distinct but overlapping set of target genes to HIF-1α and importantly playing a less significant role in regulating glycolytic enzyme expression (Hu *et al.*, 2003; Warnecke *et al.*, 2008). Furthermore, evidence has shown that differential transcriptional activation of HIF-1α and HIF-2α can result in co-ordinated cellular responses, dependent upon the relative abundance of each isoform, with for example HIF-1α and HIF-2α having opposing effects on macrophage nitric oxide formation (Takeda *et al.*, 2010). HIF-2α has also been implicated in the regulation of other macrophage functions, with myeloid-specific HIF-2α deficient mice having reduced macrophage-mediated inflammatory responses to endotoxemia, and reduced tumour-associated macrophage (TAM) infiltration with an associated reduction in tumour cell proliferation and progression (Imtiyaz *et al.*, 2010). Given this evidence of differential functions for HIF-1α and HIF-2α in myeloid cells, and the known dominance of HIF-1α over HIF-2α in the regulation of glycolysis and ATP generation, I hypothesised that HIF-2α deficiency may have a more selective immunomodulatory phenotype than that of HIF-1α deficiency in neutrophils.

Results

3.2 Human neutrophils express *HIF2A* mRNA.

To confirm expression of *HIF2A* in neutrophils, human peripheral blood neutrophils were isolated, purified by negative magnetic selection and *HIF2A* mRNA expression assessed by non quantitative PCR (Figure 3.2-1). Expression of *HIF2A* mRNA was confirmed by sequencing of the PCR products (Figure 3.2-1). Subsequently, using real time PCR, I showed that expression of *HIF2A* mRNA is not significantly altered over time in normoxic or hypoxic culture or with stimulation by heat-killed *S. aureus* or peptidoglycan although some trends were visible that suggested differential expression of *HIF1A* and *HIF2A* (Figure 3.2-2).

A

400 bp   *HIF2A*

t0 N H

B

C

NM_001430.3 Homo sapiens endothelial PAS domain protein 1 (EPAS1), mRNA
Identities = 341/349 (98%), Gaps = 0/349 (0%)

Query 19   CTNAAGCGNCNGCTGGAGTANGAAGAGCAAGCCTTCCNGGACCTGA GCGGGGGGGANCCA   78
             || |||||| | ||||||||| ||||||||||||| ||||||||||||||||| |||
Sbjct 2610 CTGAAGCGACAGCTGGAGTATGAAGAGCAAGCCTTCCAGGACCTGAGCGGGGGGGACCCA   2669

Query 79   CCTGGTGGCAGCACCTCACATTTGATGTGGAAACGGATGAANAACCTCAGGGGTGGGAGC   138
             ||||||||||||||||||||||||||||||||||||||| ||||||||||||||||||||
Sbjct 2670 CCTGGTGGCAGCACCTCACATTTGATGTGGAAACGGATGAAGAACCTCAGGGGTGGGAGC   2729

Query 139   TGCCCTTTGATGCCGGACAAGCCACTGAGCGCAAATGTACCCAATGATAAGTTCACCCAA   198
             ||||||||||||||||||||||||||||||||||||||||||||||||||||||||||||
Sbjct 2730 TGCCCTTTGATGCCGGACAAGCCACTGAGCGCAAATGTACCCAATGATAAGTTCACCCAA   2789

Query 199   AACCCCATGAGGGGCCTGGGCCATCCCCTGAGAC ATCTGCCGCTGCCACAGCCTCCATCT   258
             ||||||||||||||||||||||||||||||||||| ||||||||||||||||||||||||
Sbjct 2790 AACCCCATGAGGGGCCTGGGCCATCCCCTGAGACATCTGCCGCTGCCACAGCCTCCATCT   2849

Query 259   GCCATCAGTCCCGGGGAGAACAGCAAGAGCAGGTTCCCCCCACAGTGCTACNCCAC CCAG   318
             ||||||||||||||||||||||||||||||||||||||||||||||||||||| ||||||||
Sbjct 2850 GCCATCAGTCCCGGGGAGAACAGCAAGAGCAGGTTCCCCCCACAGTGCTACGCCACCCAG   2909

Query 319   TACCAGGACTACAGCCTGTCGTCAGCCCACAAGGTGTCAGGCAT GGCAA   367
             |||||||||||||||||||||||||||||||||||||||||||||||||
Sbjct 2910 TACCAGGACTACAGCCTGTCGTCAGCCCACAAGGTGTCAGGCATGGCAA   2958

Figure 3.2-1. Human neutrophils express *HIF2A* mRNA.

(A) Expression of *HIF2A* in freshly isolated neutrophils (t0) or cells cultured for 4 hours in normoxia (N) or hypoxia (H) was determined by PCR and agarose gel electrophoresis. A representative gel image of n=3 is shown. (B) The PCR product obtained in panel A was run on 1.5% agarose gels, extracted and sequenced. Screenshot from FinchTV showing the sequence of this product. (C) Alignment of the PCR product sequence with that of the *HIF2A* mRNA sequence was verified using NCBI Blast®.

Figure 3.2-2. Expression of *HIF2A* and *HIF1A* mRNA in hypoxia and following stimulation by *S. aureus* or peptidoglycan.

(A) Fold change in expression of *HIF2A* and *HIF1A* following culture of human neutrophils in normoxia (filled bars) or hypoxia (open bars) for 6 or 12 hours. TaqMan analysis of cDNA was performed with data normalized to *ACTB* expression. Data show mean and SEM of fold change with respect to normoxic samples at 6 hours, n=3, analysed by ANOVA. (B) Fold change in expression of *HIF2A* and *HIF1A* following culture with heat killed *S. aureus* (MOI 10:1) (hatched bars) or without (filled bars) for 3 or 5 hours. TaqMan analysis of cDNA was performed with data normalized to *ACTB* expression. Data show mean and SEM fold change with respect to unstimulated samples at 3 hours, n=5. (C) Fold change in expression of *HIF2A* and *HIF1A* following culture with peptidoglycan (10 µg/ml) (shaded bars) or without (filled bars) for 3 or 5 hours. TaqMan analysis of cDNA was performed with data normalized to *ACTB* expression. Data show fold change with respect to unstimulated samples at 3 hours, n=4.

3.3 Human neutrophils express HIF-2α protein.

In contrast to HIF-1α, low levels of HIF-2α protein were detected in neutrophils that were freshly-isolated or cultured in normoxia. Further induction of HIF-2α was seen in hypoxia, with iron chelators or hydroxylase inhibition (Figure 3.3-1). Following culture in the presence of heat-killed bacteria, neutrophils showed induction of both HIF-1α and HIF-2α (Figure 3.3-1).

A

HIF-1α

P38

N   H   Co   DFO   DMOG

4 hrs

B

HIF-1α

P38

N   SA   Spn   H

4 hrs

C

HIF-2α

P38

N   H   Co   DFO   DMOG

4 hrs

D

HIF-2α

P38

N   SA   Spn   H

4 hrs
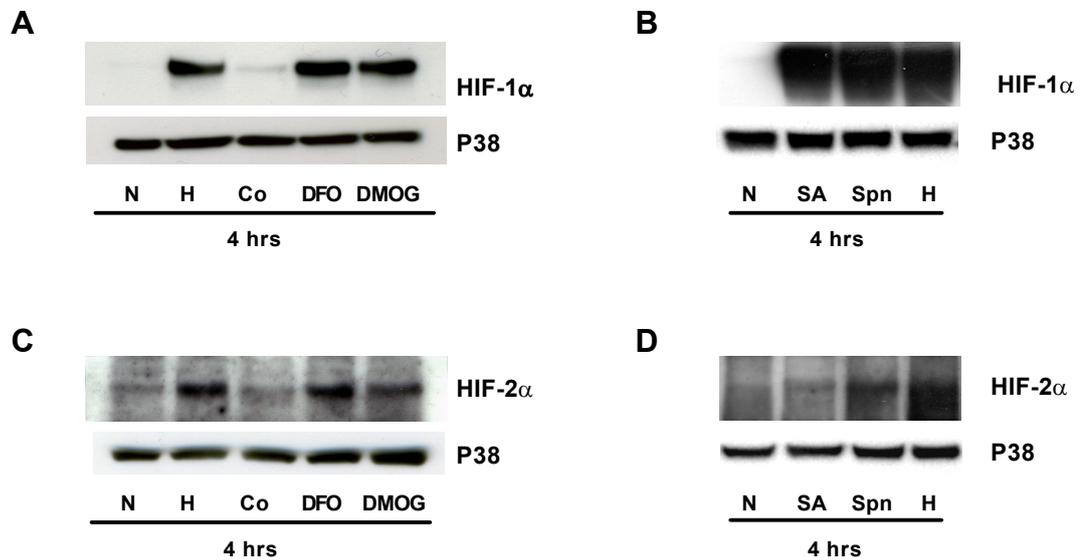
Figure 3.3-1. Expression of HIF-2α is upregulated by hypoxia, hydroxylase inhibition and heat killed bacteria.

(A-D) Expression of HIF-1α and HIF-2α is differentially regulated by hydroxylase inhibitors and upregulated in response to heat killed bacteria. Neutrophils were cultured in normoxia or hypoxia and with (A & C) cobalt chloride [100µM], deferoxamine (DFO) [300µM], dimethyloxalylglycine (DMOG) [100µM] or (B & D) heat killed *S. aureus* or *S. pneumoniae* before being lysed. Proteins were separated using SDS-PAGE and blots probed for HIF-1α (A & B) and HIF-2α (C & D). p38 MAPK was used as a loading control. Blots are representative of n=3.

3.4   Inflammatory neutrophils show enhanced HIF-2α expression.

Peripheral blood neutrophils isolated from patients with active inflammatory arthritis displayed enhanced *HIF1A* and *HIF2A* mRNA expression (Figure 3.4-1).   HIF-2α protein expression was also significantly higher in circulating neutrophils of arthritis patients than of healthy controls (Figure 3.4-1). Interestingly this was selective for HIF-2α, with no increase in HIF-1α protein observed in freshly isolated circulating neutrophils from these patients (data not shown). In order to demonstrate whether transmigrated neutrophils also express HIF-2α in inflamed tissue, lung biopsy sections from patients with COPD were obtained. Neutrophils recruited to the airways in both mild and severe COPD displayed strong HIF-2α staining, in marked contrast to epithelium where no HIF-2α expression was demonstrated (Figure 3.4-2).

A

B

C
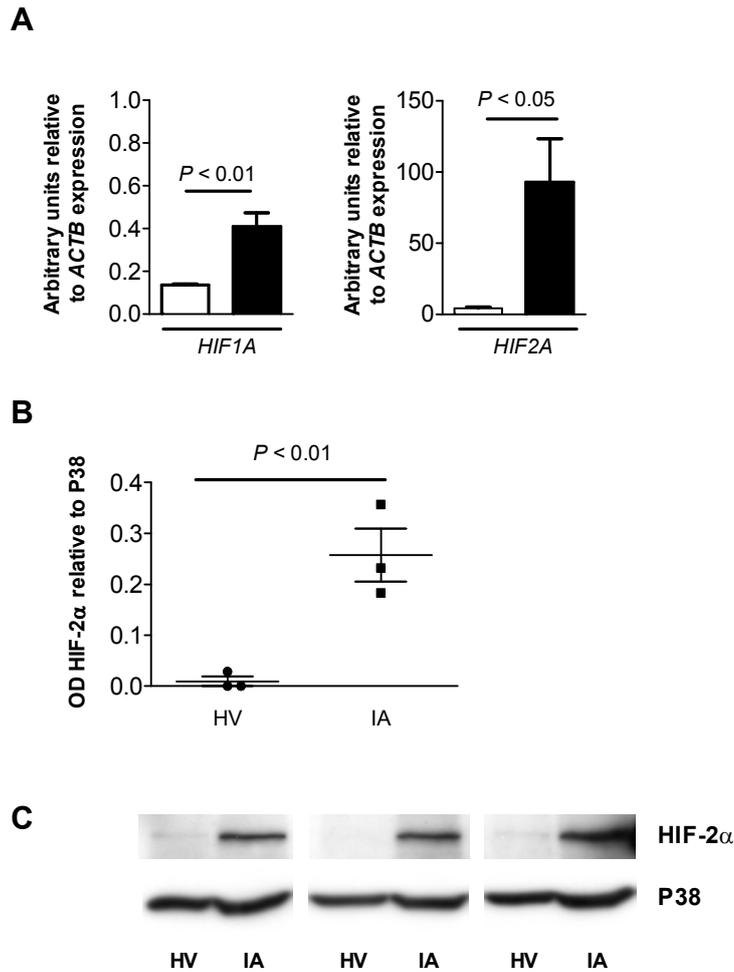
Figure 3.4-1. Expression of HIF-2α is upregulated in neutrophils from patients with active inflammatory arthritis.

(A) Expression of *HIF1A* and *HIF2A* in inflammatory arthritis patients (filled bars) and controls (open bars) was determined by TaqMan analysis of cDNA from freshly isolated peripheral blood neutrophils with data normalized to *ACTB* expression. Data are mean and SEM for n=4. (B & C) HIF-2α protein expression is significantly higher in neutrophils from patients with inflammatory arthritis (IA) than healthy volunteers (HV). Freshly isolated neutrophils were lysed and proteins separated by SDS-PAGE. Blots were probed for HIF-2α and densitometry data were normalised to p38 MAPK. (B) Data are mean and SEM for n=3. (C) HIF-2α blots of circulating neutrophil lysates from 3 healthy volunteers (HV) and 3 patients with inflammatory arthritis (IA).
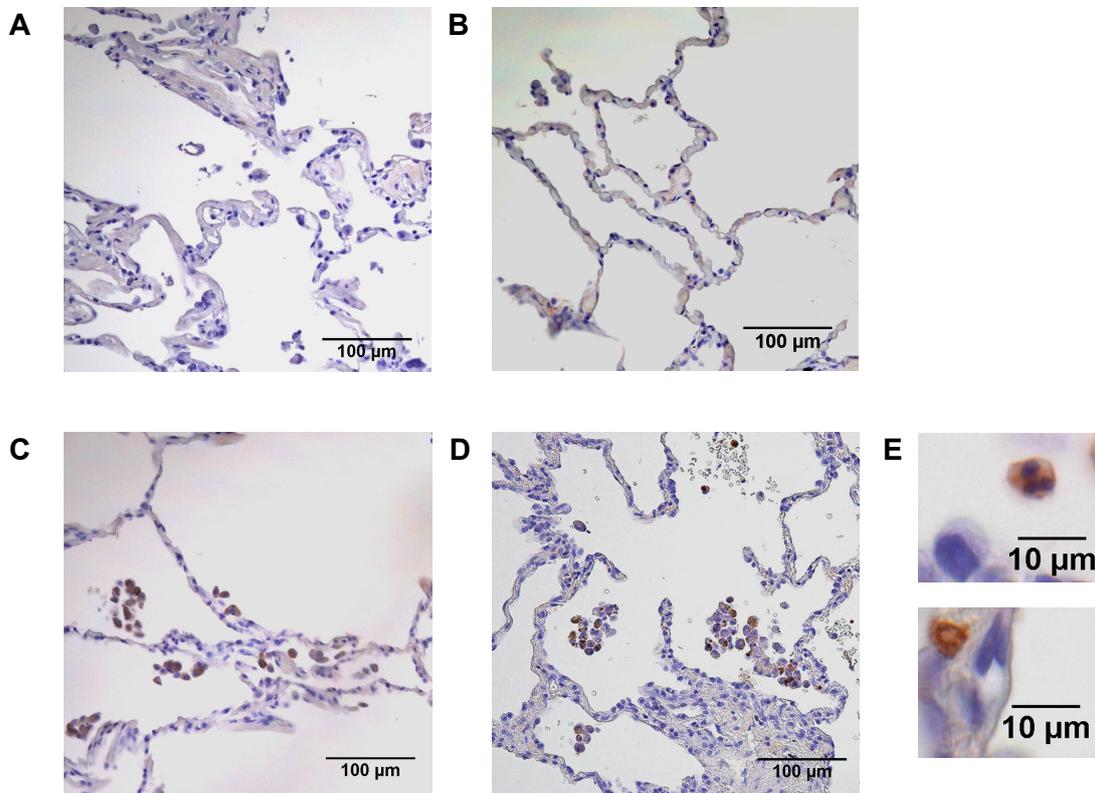
Figure 3.4-2. Expression of HIF-2α is seen in neutrophils within lung biopsies from patients with COPD.

(A-E) Immunohistochemistry showing HIF-2α expression in lung biopsies from a non-smoker (B) and patients with mild (C) or severe COPD (D & E). Images are representative of n=2. Panel A is a section stained with an isotype control. Original magnification (A-D) x200, (E) x1000.

3.5 Overexpression of HIF-2α delays neutrophil apoptosis but does not affect neutrophil function.

Study of idiopathic cases of erythrocytosis with raised serum erythropoietin has resulted in the identification of a rare group of individuals with gain-of-function mutations in the *HIF2A* gene (Percy *et al.*, 2008a; Percy *et al.*, 2008b). I obtained peripheral blood neutrophils from some of these individuals to determine the consequences of HIF-2α overexpression for neutrophil survival and function. Patients with gain-of-function *HIF2A* mutations had lower rates of neutrophil apoptosis compared to controls, but a preserved response to hydroxylase inhibition by the pan hydroxylase inhibitor dimethyloxalylglycine (DMOG) (Figure 3.5-1). Neutrophils from these patients also showed enhanced expression of the HIF-2α target genes *VEGF, PAI-1* and *PHD3* (Figure 3.5-1). Functional assays showed preserved phagocytosis and respiratory burst (Figure 3.5-2) indicating that HIF-2α overexpression resulted in a selective pro-survival phenotype without alteration of key neutrophil functions.
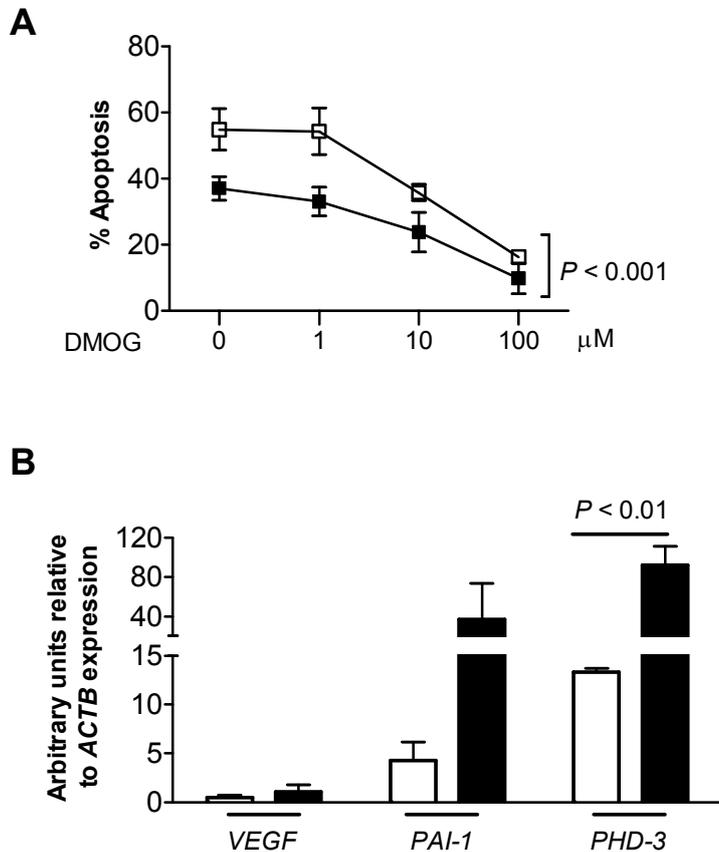
Figure 3.5-1. Neutrophils isolated from patients with gain-of-function *HIF2A* mutations have enhanced survival and altered *HIF2A* target gene expression.

(A) Neutrophils from patients with *HIF2A* mutations (closed squares) or healthy controls (open squares) were cultured for 20 hours with the hydroxylase inhibitor, dimethyloxalylglycine (0-100 µM) and apoptosis determined by morphology. Data are mean ± SEM for n=3, analysed by 2-way ANOVA. (B) Expression of the HIF targets *VEGF, PAI-1* and *PHD3*. TaqMan® quantitative PCR analysis of cDNA prepared from freshly isolated neutrophils from patients with *HIF2A* mutations (filled bars) or healthy controls (open bars). Data are mean and SEM for n=3.
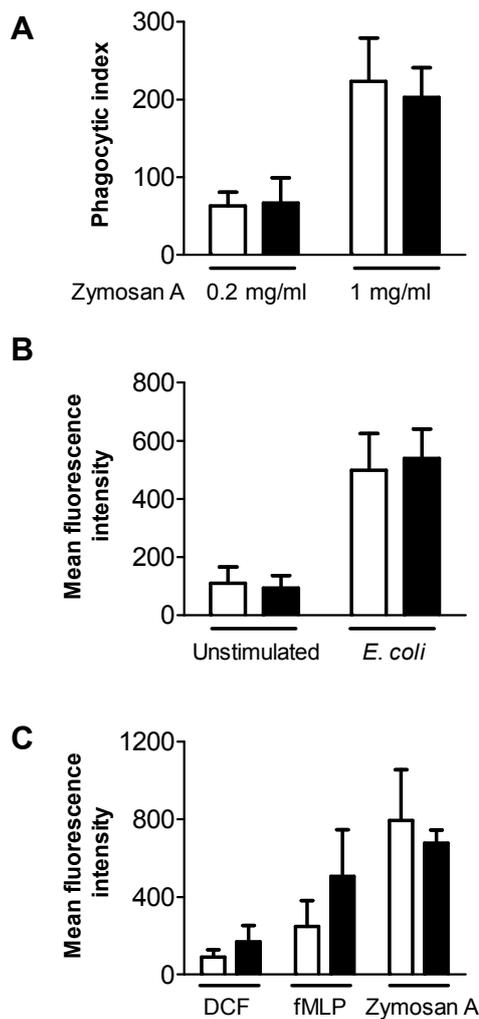
Figure 3.5-2. Neutrophils isolated from patients with gain-of-function *HIF2A* mutations have normal phagocytosis and respiratory burst.

(A) Phagocytic index was calculated from cytospin slides of neutrophils from healthy controls (open bars) and *HIF2A* patients (filled bars) prepared after 30 minutes of culture with opsonised zymosan (0.2-1 mg/ml). (B) Flow cytometry analysis of intracellular Alexa Fluor® 488 *E. coli* was performed after 30 minutes of culture of cells from healthy controls (open bars) and *HIF2A* patients (filled bars). (C) Respiratory burst. Neutrophils from healthy controls (open bars) and *HIF2A* patients (filled bars) were cultured in the presence of DCF only or DCF and fMLP (100 nM) or zymosan A (0.2 mg/ml) and analysed by flow cytometry. Data show mean and SEM for n=3.

3.6 Overexpression of *epas1a* in zebrafish delays resolution of inflammation.

To explore the significance of the reduced rates of apoptosis seen in humans with gain-of-function mutations in *HIF2A*, we mutated the zebrafish orthologue, *epas1a,* to produce a protein with an amino acid substitution at the glycine site corresponding to the mutant human protein. We found that replacing the glycine with either arginine (G487R) or tryptophan (G487W), to replicate the *HIF2A* mutations observed in the patients, did not affect whole body neutrophil counts (Figure 3.6-1). In a well-characterised tail injury model of neutrophilic inflammation (Renshaw *et al.*, 2006), neutrophil recruitment did not differ between wild-type and mutants but the *epas1a* overexpressing fish showed impaired resolution of inflammation (Figure 3.6-1). The magnitude of neutrophil persistence was equivalent to that seen with expression of dominant active *hif1ab* (Figure 3.6-1) or previously reported with caspase inhibition (Renshaw *et al.*, 2006). The increase in neutrophil number at the site of injury after 24 hours was associated with a significant reduction in neutrophil apoptosis (Figure 3.6-1). Corresponding results were obtained when the PHD target sites were mutated into non-hydroxylatable amino acids to create a dominant active form of *epas1a* (Figure 3.6-2). Importantly, all three *epas1a* mutants displayed evidence of upregulation of target genes (Figure 3.6-3). Injection of a morpholino anti-sense oligonucleotide to achieve knock-down of the *epas1a* binding partner, *arnt* (Prasch *et al.*, 2006) restored resolution of inflammation in *epas1a* overexpressing fish, confirming that the phenotype of neutrophil persistence required intact *epas1a* signalling (3.6-2).
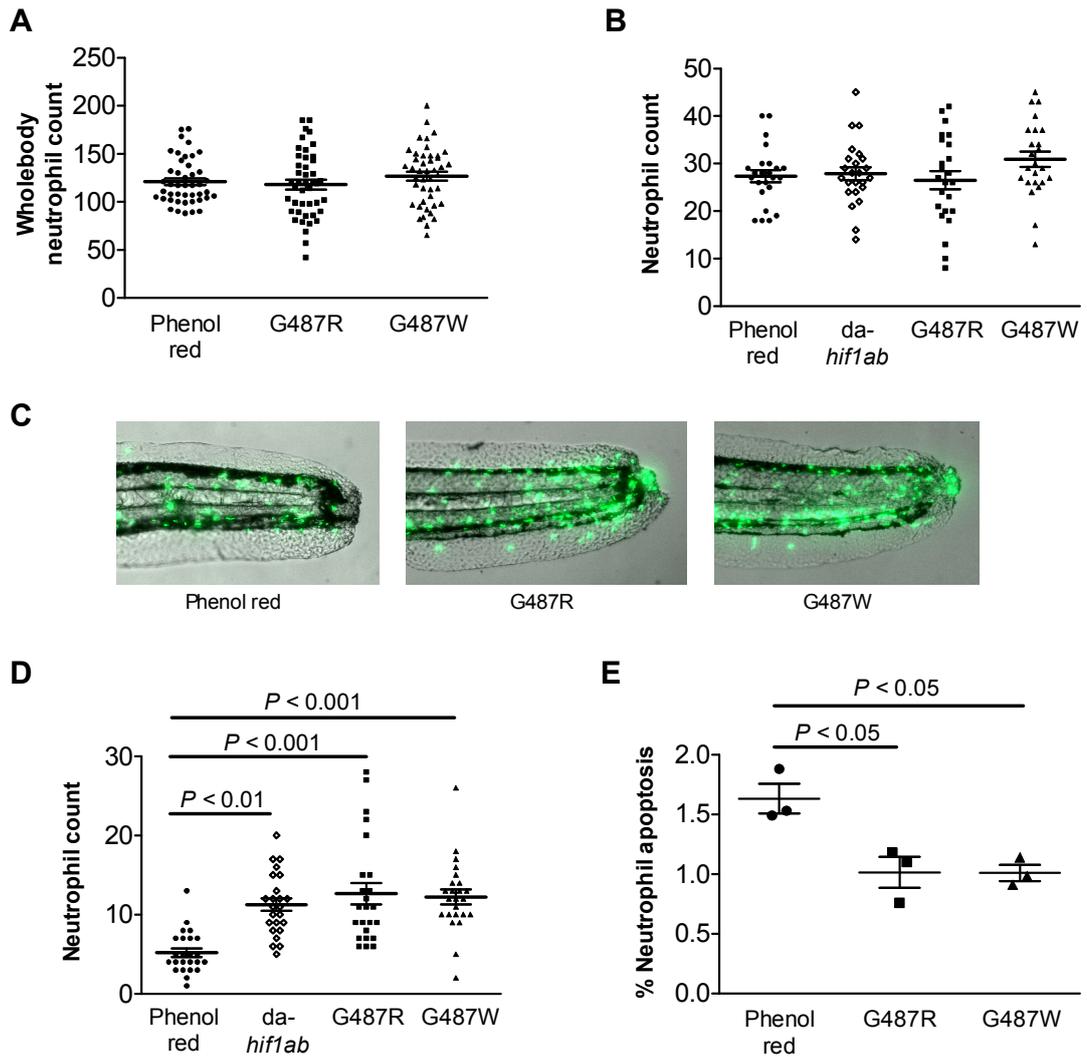
Figure 3.6-1. Gain-of-function mutations in the zebrafish *HIF2A* orthologue *epas1a* delay resolution of neutrophilic inflammation.

epas1a G487R or G487W RNA (177pg) or dominant active (da) *hif1ab* control was injected into 1 cell stage zebrafish *mpx*:GFP embryos. (A) Wholebody total neutrophil numbers at 2 days post fertilization (dpf) were not altered by injection of *epas1a* G487 variants. n=44 performed as 3 independent experiments. (B-D) Tailfin transection was performed at 2dpf, and neutrophils counted at 6 and 24 hours post injury (hpi). Data shown are mean ± SEM. (B) Injection of dominant active *epas1a* variants did not alter the recruitment of neutrophils to the tailfin injury site after 6hpi. n=24 performed as 3 independent experiments. (C & D) *epas1a* G487 mutations caused a significant increase in neutrophil number at 24hpi compared to phenol red injected negative controls. (C) Representative overlaid fluorescence and bright field micrographs (x 4 magnifications). (D) Neutrophil numbers at 24hpi. n=24 performed as 3 independent experiments. (E) Injection of *epas1a* G487 mutations significantly decreased the percentage of neutrophils at the injury site co-labelled with TUNEL apoptosis staining at 12hpi. n=3 performed as independent experiments containing 17-36 embryos per injection group per repeat. These experiments were performed by Dr Phil Elks.
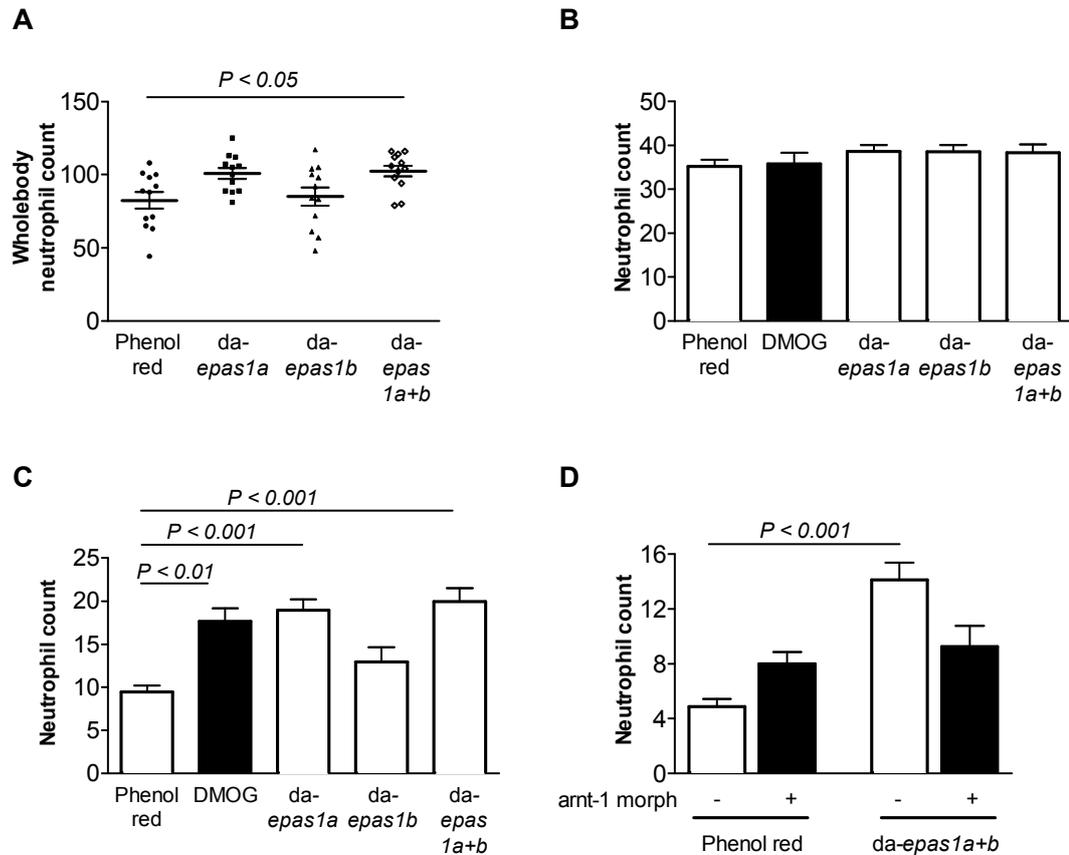
Figure 3.6-2. Dominant active *epas1a* delays resolution of neutrophilic inflammation.

Dominant active (da) forms of *epas1* RNA (177pg) were injected into the 1 cell stage zebrafish *mpx*:GFP embryos, tailfin transection performed at 2dpf, and neutrophils counted at 6 and 24hpi. Data shown are mean and SEM. (A) Injection of individual dominant active *epas1a* variants did not alter wholebody neutrophil numbers at 2dpf. However, injection of dominant active *epas1* variants led to a significant increase in total neutrophil numbers if they were co-injected. n=14-17, performed as 2 independent experiments. (B) The recruitment of neutrophils to the injury site after 6hpi when the tail was transected at 2dpf. Treatment with 100μM DMOG (filled bar) or DMSO vehicle control (open bars) was performed 2 hours before injury. n=14-17, performed as 2 independent experiments. (C) Dominant active *epas1a* caused a significant increase in neutrophil number at 24hpi in the absence of DMOG treatment compared to phenol red injected negative controls. Treatment with 100μM DMOG (filled bar) or DMSO vehicle control (open bars) was performed at 4 hpi. Dominant active *epas1a* alone was able to recapitulate the DMOG phenotype, whilst dominant active *epas1b* homologue did not. n=24, performed as 2 independent experiments. (D) 24hpi neutrophil counts in the *epas1a+b* overexpressing fish at 2dpf following co-injection with control (open bars) and *arnt-1* morpholinos (filled bars). n=8 performed as 2 independent experiments. These experiments were performed by Dr Phil Elks.

A - *phd3*
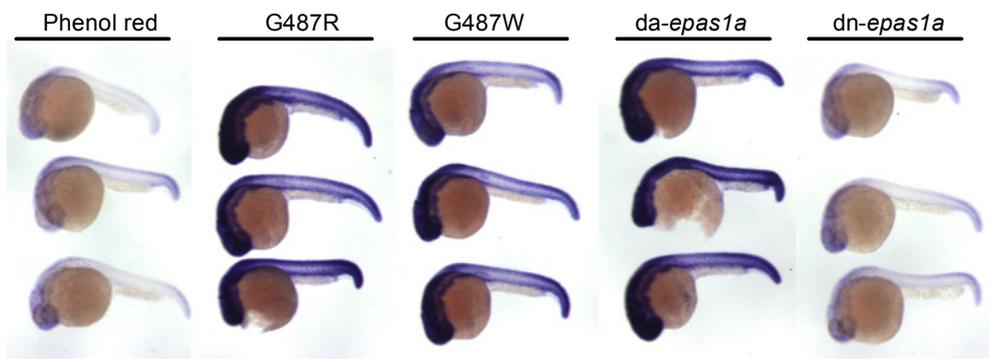
B - *atf4*
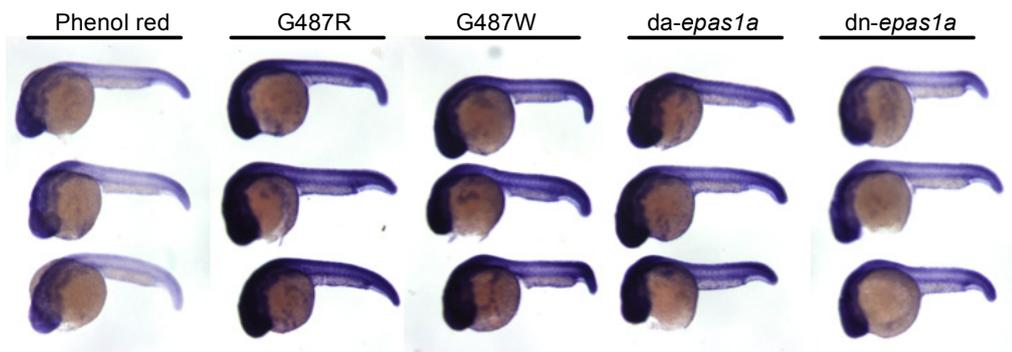
Figure 3.6-3. Gain-of-function mutations in the zebrafish *HIF2A* orthologue *epas1a* upregulate expression of the target genes, *phd3* and *atf4*.

Evidence of *epas1a* target gene activation in zebrafish embryos with overexpressed G487 mutant constructs. Photomicrographs of 24hpf embryos after injection of dominant active forms of *epas1a* RNA (177pg) or dominant negative (dn) *epas1a* at the 1 cell stage. Embryos were stained for (A) *phd3* or (B) *atf4* expression by in situ hybridization as representative *epas1a* target genes. These experiments were performed by Dr Phil Elks.

3.7 Neutrophils from mice with myeloid-specific deficiency of HIF-2α have maintained LPS and hypoxic survival responses and preserved function.

Next the consequences of HIF-2α deficiency for neutrophil survival and function were investigated. Peripheral blood neutrophils were isolated from wild-type mice and the presence of *Hif2a* confirmed by PCR (Figure 3.7-1). In keeping with previous data I was, however, unable to detect *Hif2a* in bone marrow derived neutrophils from wild-type animals (Imtiyaz *et al.*, 2010). Consistent with my findings in human neutrophils and in contrast to HIF-1α, murine neutrophils showed basal expression of HIF-2α protein following normoxic culture with further expression in hypoxia and following lipopolysaccharide (LPS) or DMOG treatment (Figure 3.7-1). To investigate the consequences of HIF-2α deficiency, I used mice with myeloid-specific targeted deletion of *Hif2a* (*Hif2a^{flox/flox};LysMCre^{+/-}*)(Takeda *et al.*, 2010). HIF-2α deficient neutrophils showed preserved rates of apoptosis in normoxia and, in contrast to HIF-1α deficient neutrophils (Walmsley *et al.*, 2011), a delay of apoptosis in hypoxia that was equivalent to wild-type cells (Figure 3.7-2). The survival response to LPS did not differ between wild-type cells and those deficient in HIF-1α or HIF-2α (Figure 3.7-2). Functional assays on HIF-2α deficient neutrophils revealed no deficits in respiratory burst, chemotaxis or phagocytosis (Figure 3.7-3) and these cells also showed preserved changes in receptor expression in response to stimulation with LPS (Figure 3.7-4). Furthermore, an *in vivo* model of pneumococcal pneumonia which is associated with significant neutrophil recruitment to the lungs did not reveal a difference in mortality between HIF-2α deficient and wild-type animals (Figure 3.7-5) indicating preserved ability to control bacterial infection.

A

B

C
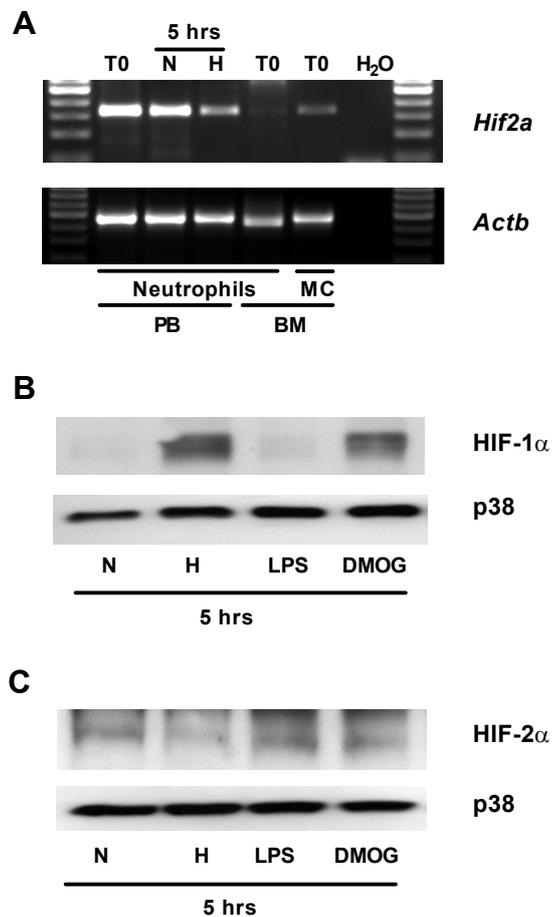
Figure 3.7-1. Murine neutrophils express HIF-2α mRNA and protein.

(A) Expression of *Hif2a* in murine peripheral blood but not bone marrow neutrophils. Neutrophils isolated by magnetic negative selection from peripheral blood (PB) or bone marrow (BM) or bone marrow mononuclear cells (MC) were cultured in normoxia (N) or hypoxia (H) for 5 hours or lysed when freshly isolated (T0). cDNA was amplified using custom *Hif2a* primers and a representative gel image of n=3 is shown. (B & C) Murine neutrophils express HIF-1α (B) and HIF-2α (C). Representative western blots of lysates from neutrophils cultured in normoxia (N) or hypoxia (H) or stimulated in normoxia with LPS (10 ng/ml) or DMOG (100 µM) for 5 hours.
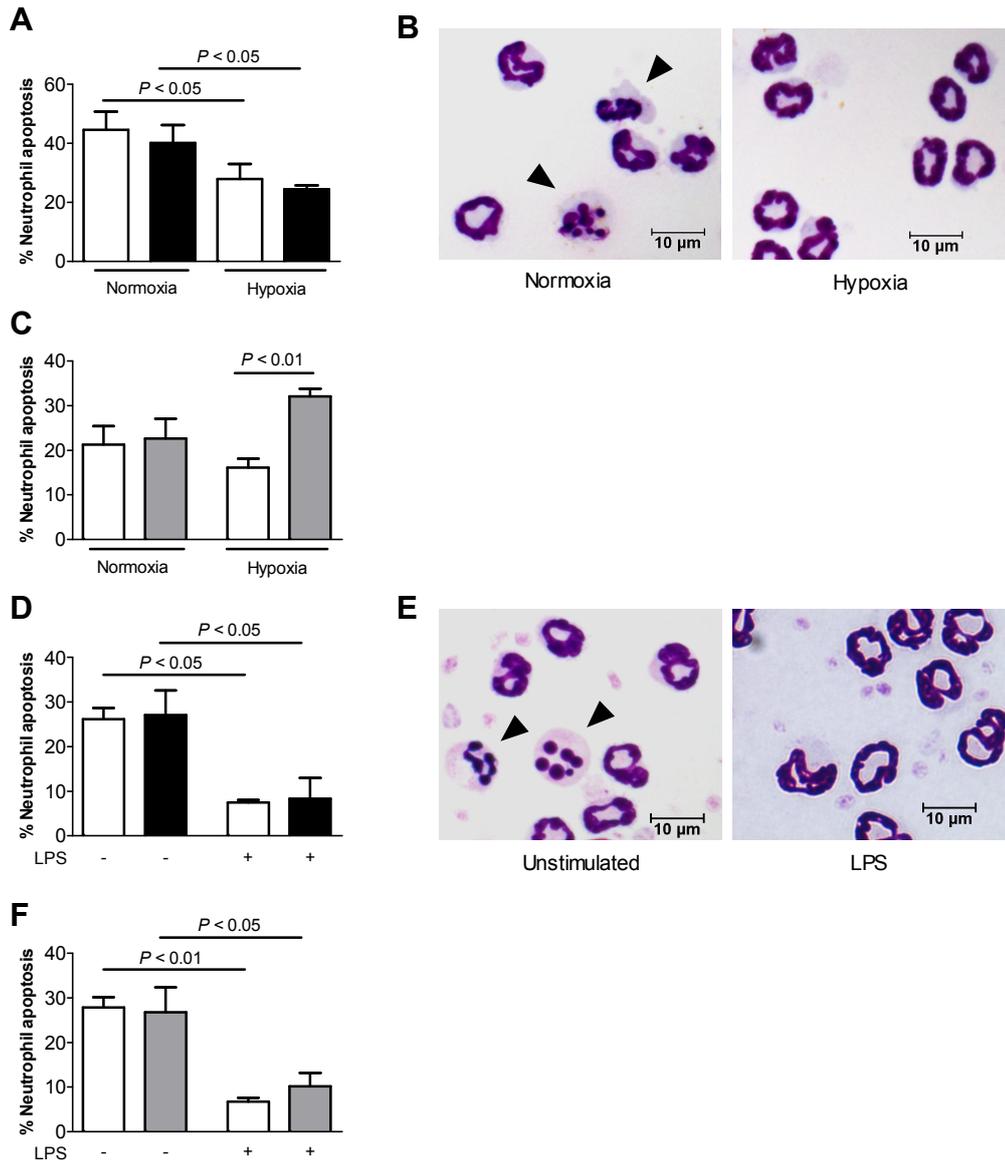
Figure 3.7-2 Myeloid-specific HIF-2α deficiency does not affect *in vitro* apoptosis.

(A & C) Neutrophils from mice with myeloid-specific deletion of (A) *Hif2a* (filled bars), (C) *Hif1a* (grey bars), or littermate controls (open bars) were cultured for (A) 10 hours or (C) 6 hours in normoxia or hypoxia before apoptosis was assessed by morphology. Data are mean and SEM for n=3. (D & F) Neutrophils from mice with myeloid-specific deletion of (D) *Hif2a* (filled bars), (F) *Hif1a* (grey bars), or littermate controls (open bars) were cultured with 10 ng/ml LPS for 5 hours. Apoptosis was assessed by morphology. Data are mean and SEM for n=3 (C) or n=6 (E). (B & E) Representative cytospin images of HIF-2α deficient neutrophils cultured (B) in normoxia or hypoxia for 9 hours or (E) with 10 ng/ml LPS for 5 hours. Arrowheads indicate apoptotic neutrophils. Panel C was redrawn with additional data with permission from S. Walmsley (Walmsley et al. 2011)
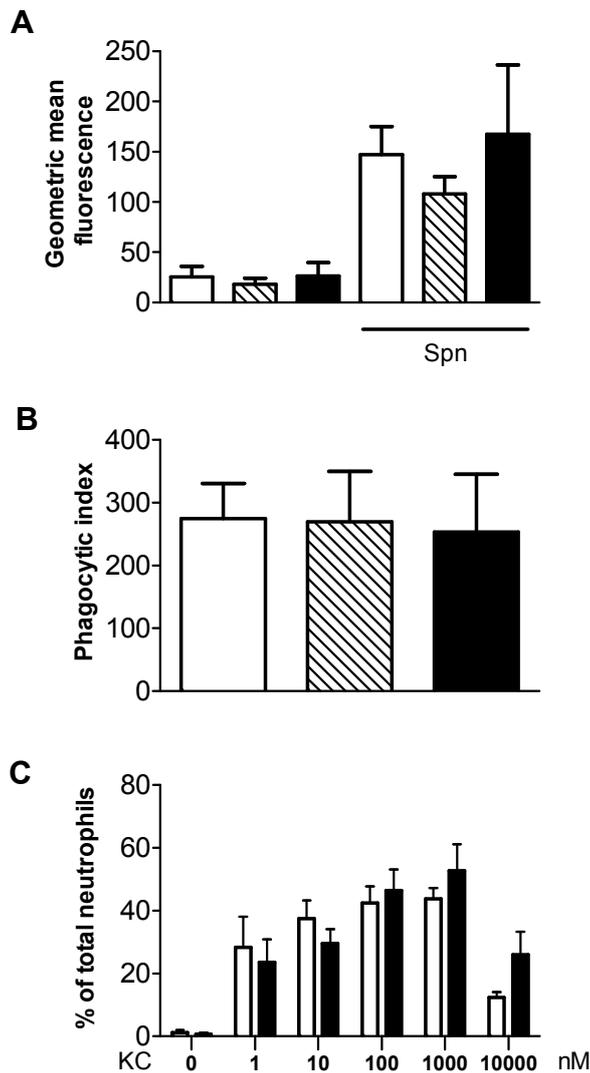
Figure 3.7-3. Murine neutrophils deficient in HIF-2α have normal function and preserved receptor expression.

Functional assays. (A) Respiratory burst: neutrophils from C57BL/6 (open bars), *Hif1a*$^{flox/flox}$*;LysMCre*$^{+/-}$ (hatched bars) and *Hif2a*$^{flox/flox}$*;LysMCre*$^{+/-}$ (filled bars) mice were pre-incubated with 6 μM DCF (30 mins) and stimulated with heat-inactivated *S. pneumoniae* (MOI 10:1) and FL1 geometric mean fluorescence determined by flow cytometry (n=3). (B) Phagocytic index was calculated on cytospins of neutrophils from C57BL/6 (open bars), *Hif1a*$^{flox/flox}$*;LysMCre*$^{+/-}$ (hatched bars) and *Hif2a*$^{flox/flox}$*;LysMCre*$^{+/-}$ (filled bars) mice that were stimulated with opsonised zymosan A (0.2 mg/ml) for 30 minutes. Data are mean and SEM (n=3). (C) Chemotaxis: neutrophil migration to KC (0-10 μM) across a 5 μm filter was assessed in neutrophils from *Hif2a*$^{flox/flox}$*;LysMCre*$^{-/-}$ (open bars) and *Hif2a*$^{flox/flox}$*;LysMCre*$^{+/-}$ (filled bars) mice. Data are mean and SEM (n=3).

A

B
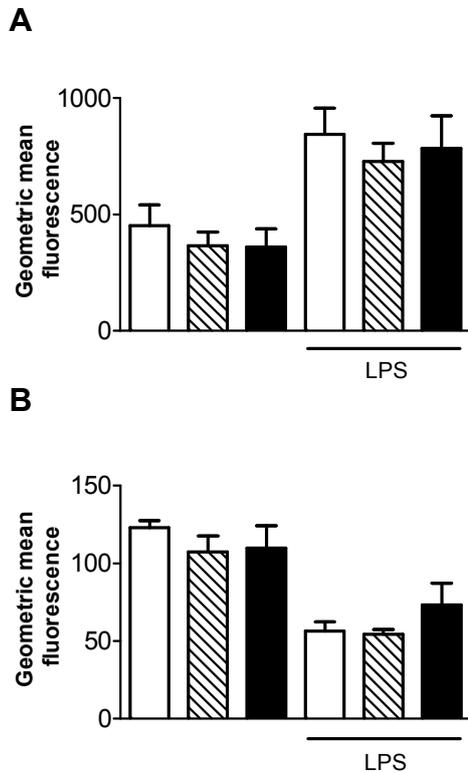
Figure 3.7-4. Murine neutrophils deficient in HIF-2α have preserved receptor expression.

Neutrophils from C57BL/6 (open bars), *Hif1a*$^{flox/flox}$;*LysMCre*$^{+/-}$ (hatched bars) and *Hif2a*$^{flox/flox}$;*LysMCre*$^{+/-}$ (filled bars) mice were cultured in the presence/absence of LPS (10 ng/ml), stained with PE-anti-CD11b (A) or PE-anti-L-selectin (B) and geometric mean fluorescence determined by flow cytometry (n=3).
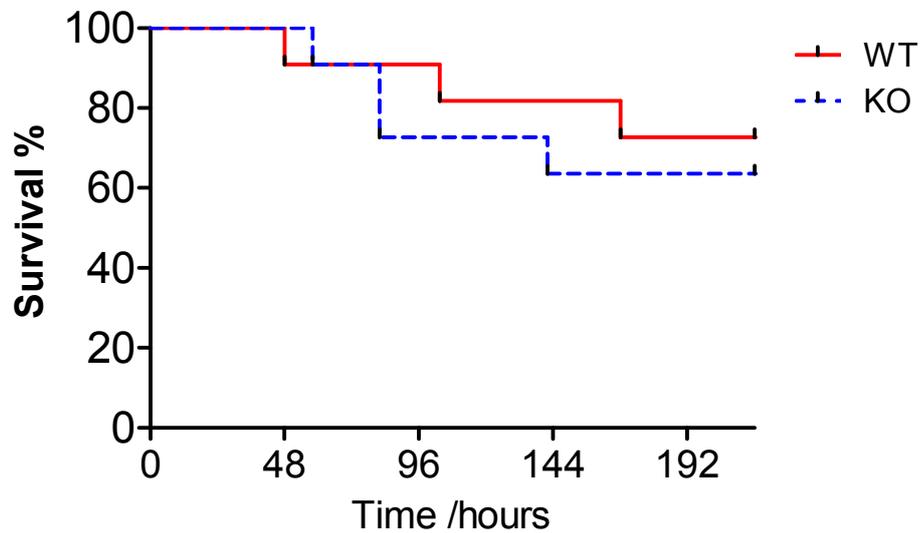
Figure 3.7-5. Mice with myeloid-specific deficiency of HIF-2α have normal survival in bacterial pneumonia.

Mice were challenged with 1×10^7 colony forming units of *Streptococcus pneumoniae* administered via the trachea under anaesthetic. Mice were observed at least twice daily for 9 days and those that reached a pre-determined level of morbidity were culled by an observer blinded to genotype. Kaplan Meier survival curves were analysed and plotted for wild-type *Hif2α*$^{flox/flox}$*;LysMCre*$^{-/-}$ (solid red line, n=10) and *Hif2α*$^{flox/flox}$*;LysMCre*$^{+/-}$ (broken blue line, n=11).

3.8 Loss of HIF-2α enhances resolution of neutrophilic inflammation following an acute lung injury.

To determine the effect of HIF-2α deficiency on neutrophilic inflammation *in vivo*, I utilised a neutrophil-mediated LPS-induced model of acute lung injury. Mice with myeloid-specific deletion of *Hif2a* had normal recruitment of neutrophils to the lung, but enhanced inflammation resolution, with significantly lower bronchoalveolar lavage neutrophil counts than controls at 48 hours, associated with increased neutrophil apoptosis in the HIF-2α deficient mice (Figure 3.8-1). Immunohistochemistry confirmed HIF-2α expression in neutrophils of LPS treated wild-type mice with no staining seen in myeloid cells of HIF-2α deficient mice (Figure 3.8-2). Cytokine and chemokine profiles in plasma and lavage fluid showed no deficit in pro-inflammatory cytokine production between strains, in keeping with their equivalent neutrophil recruitment (Figure 3.8-3). Differential regulation of *Hif1a* and *Hif2a* was also observed in wild type LPS treated animals, with downregulation *Hif1a* mRNA in bronchoalveolar lavage samples over time following LPS challenge (Figure 3.8-4), in marked contrast to *Hif2a* which was maintained during the resolution phase of the acute lung injury (Figure 3.8-4). This also reflected in the selective induction of *Hif2a* but not *Hif1a* mRNA in cells harvested from the bronchoalveolar lavage fluid at 24 hours compared with circulating neutrophil expression (figure 3.8-4), and was subsequently confirmed on flow sorted bronchoalveolar neutrophils (data not shown).
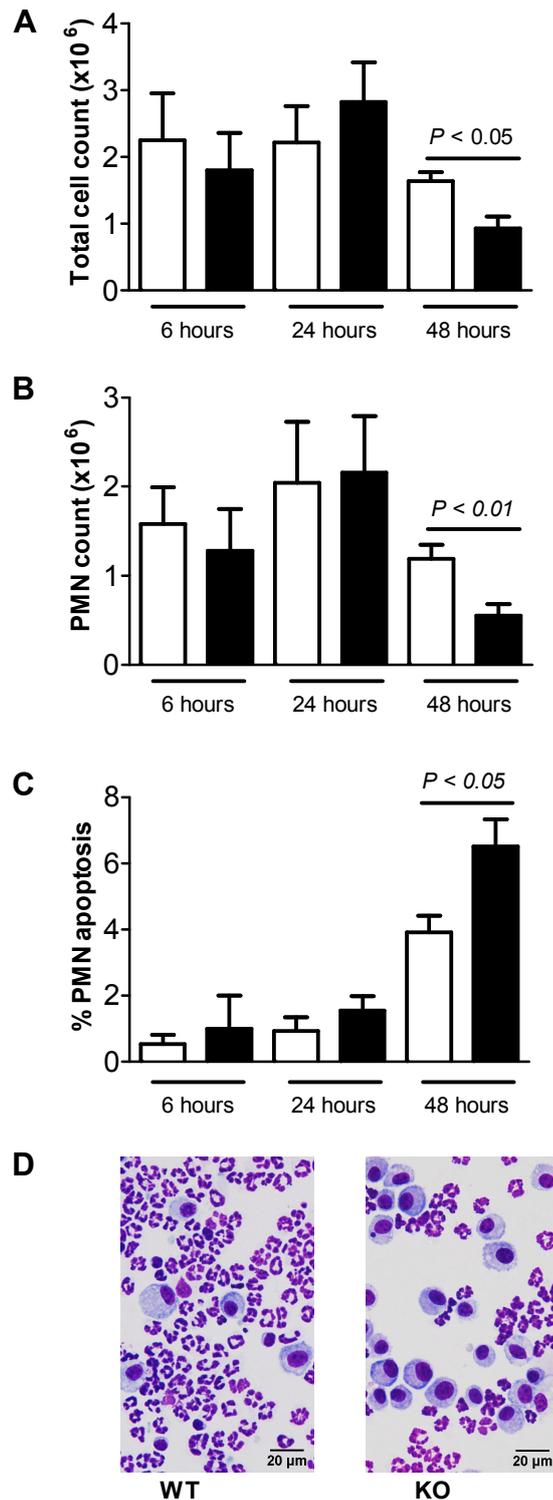
Figure 3.8-1. Enhanced resolution of acute lung inflammation in mice with myeloid-specific deficiency of HIF-2α.

*Hif2a*flox/flox;*LysMCre*+/- mice, littermate *Hif2a*flox/flox;*LysMCre*-/- controls or C57BL/6 mice were instilled with intratracheal LPS (0.3 μg). Bronchoalveolar lavage (BAL) was performed at 6, 24 and 48 hours and (A) total cell counts and (B) neutrophil counts were determined by haemocytometer. (C) Neutrophil apoptosis was assessed by morphology. Data are mean and SEM for controls (open bars), HIF-2α deficient mice (filled bars), n=6. (D) Representative cytospins of BAL from *Hif2a*flox/flox;*LysMCre*-/- (WT) or *Hif2a*flox/flox;*LysMCre*+/- (KO) mice at 48 hours post instillation.
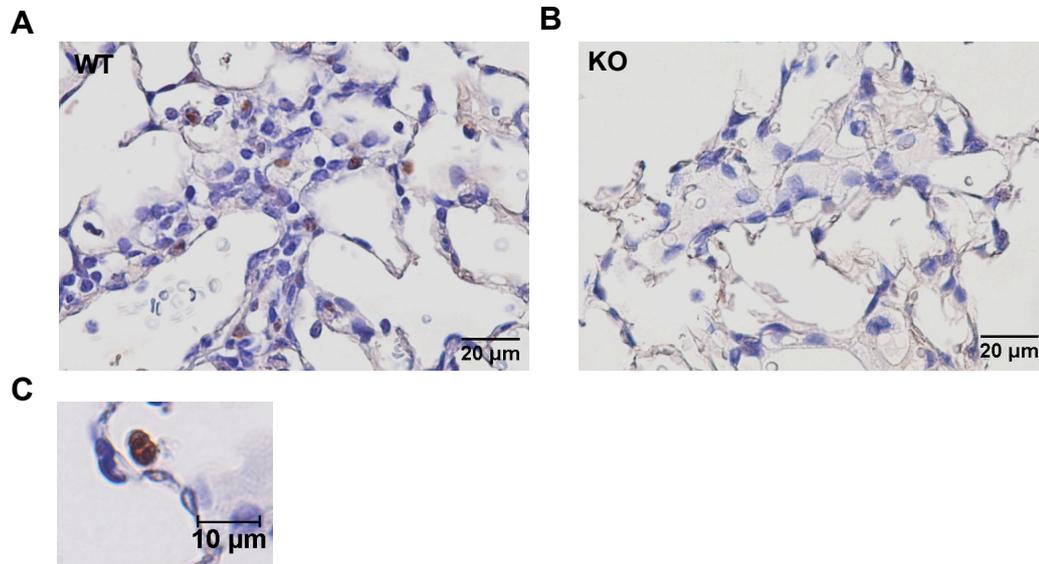
Figure 3.8-2. Expression of HIF-2α in inflammatory murine neutrophils recruited to the lung after intratracheal LPS instillation.

Immunohistochemistry showing expression of HIF-2α in neutrophils of WT (A & C) mice challenged with intratracheal LPS, while in HIF-2α deficient mice (B) no staining was observed. Original magnification (A & B) x400, (C) x1000.
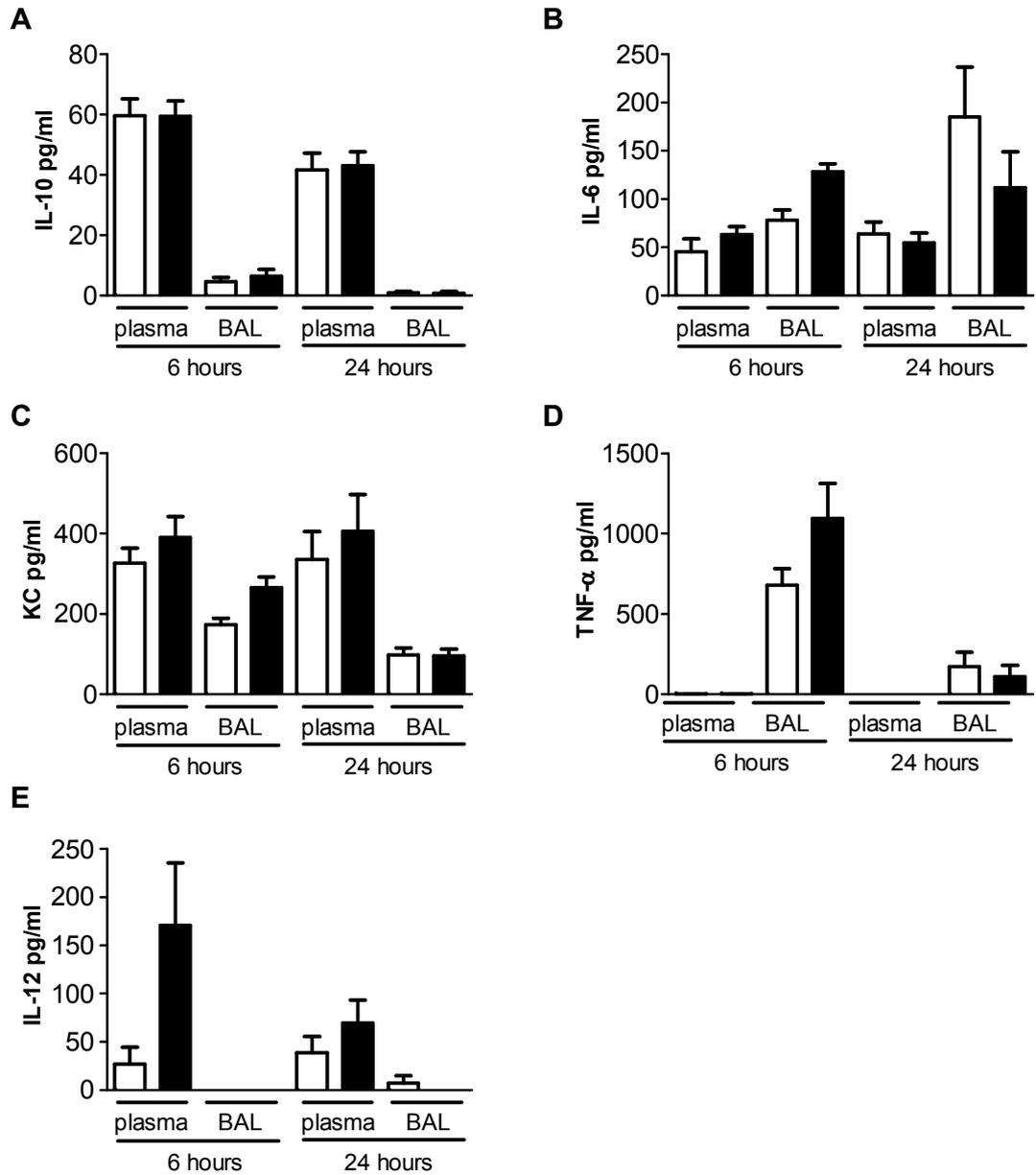
Figure 3.8-3. Mice with myeloid-specific deficiency of HIF-2α have preserved cytokine production following LPS-induced acute lung injury.

Hif2a^{flox/flox};*LysMCre*^{+/-} mice or littermate *Hif2a*^{flox/flox};*LysMCre*^{-/-} controls were instilled with intratracheal LPS (0.3 μg). Bronchoalveolar lavage was performed at 6, 24 and 48 hours. Cytokines in plasma and bronchoalveolar lavage fluid were assessed using a multiplex cytokine kit. Levels of (A) IL-10, (B) IL-6, (C) KC, (D) TNF-α and (E) IL-12 are shown for control (open bars) and Hif-2α deficient mice (filled bars) as mean ± SEM for a minimum n=4.
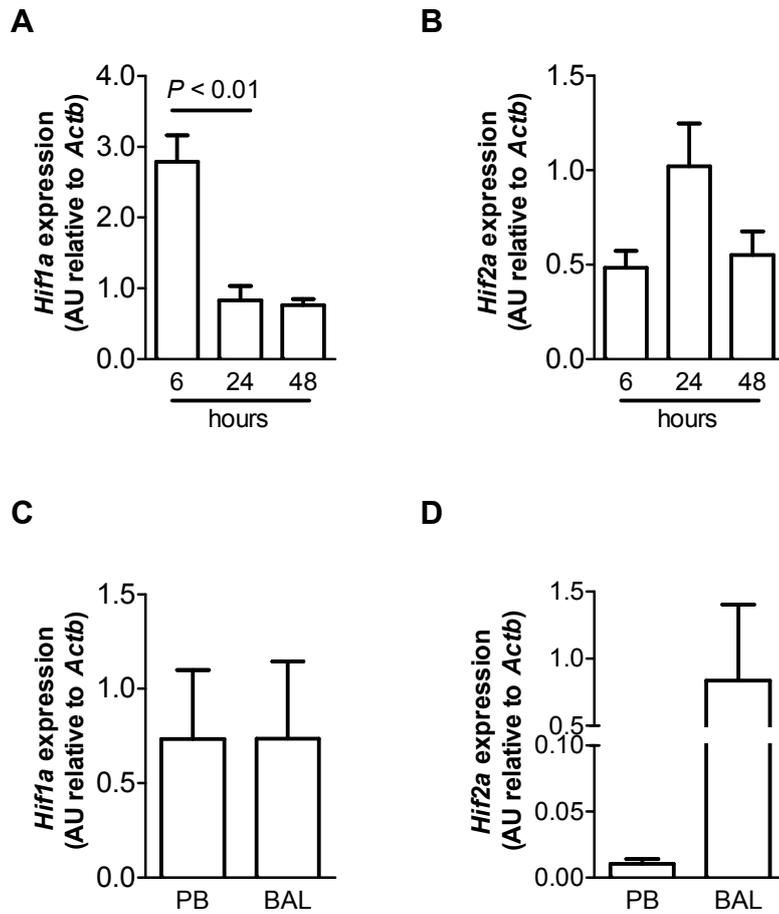
Figure 3.8-4. Expression of *Hif1a* and *Hif2a* in peripheral blood and bronchoalveolar lavage cells during LPS-induced acute lung injury.

C57BL/6 mice were instilled with intratracheal LPS (0.3 µg). Bronchoalveolar lavage (BAL) was performed at 6, 24 and 48 hours. (A) *Hif1a* and (B) *Hif2a* expression in BAL cell lysates from C57BL/6 mice determined by Taqman® and normalised to *Actb*. Data are mean and SEM for n=3. (C) *Hif1a* and (D) *Hif2a* expression in peripheral blood neutrophils (PB) or BAL cells from C57BL/6 mice at 24 hours post LPS instillation. Data are mean and SEM for n=3.

Given the finding of reduced neutrophil counts after 48 hours in mice with myeloid-cell deficiency of HIF-2α, I wished to determine whether this enhanced resolution was associated with a reduction in lung injury. Acute lung injury is characterised by neutrophil-mediated damage to the pulmonary vascular endothelium and alveolar epithelium leading to leak of plasma components into the airspaces (Matthay and Zemans, 2011). I challenged mice with a high dose of nebulised LPS which has been shown to cause significant elevation in IgM in bronchoalveolar lavage fluid. In this model I confirmed the finding of enhanced resolution of inflammation in the HIF-2α deficient animals at 48 and 72 hours following LPS administration (Figure 3.8-5). Associated with the reductions in neutrophil counts in BAL, I found evidence of reduced lung injury with significantly lower levels of IgM in the lavage fluid from HIF-2α deficient mice (Figure 3.8-5).
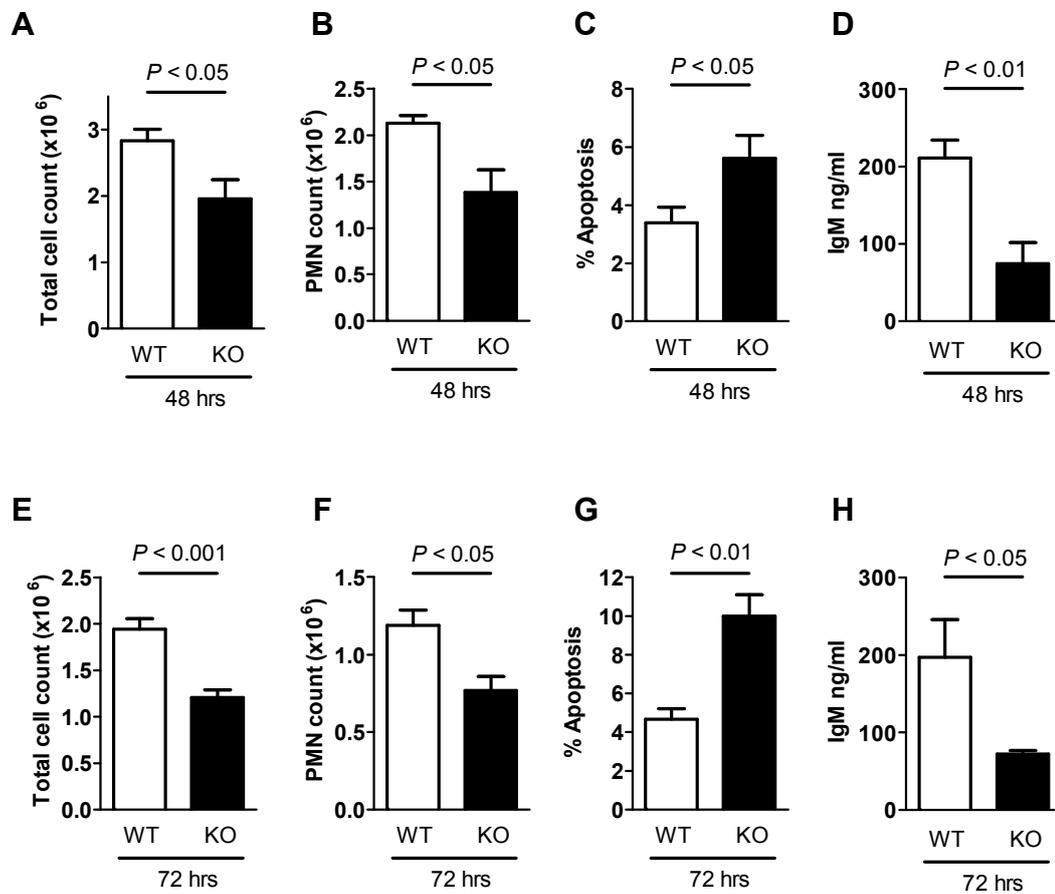
Figure 3.8-5. Reduced lung injury in mice with myeloid cell deficiency of HIF-2α.

C57BL/6 (WT) and $Hif2a^{flox/flox};LysMCre^{+/-}$ (KO) mice were challenged with nebulised LPS (3 mg). Bronchoalveolar lavage (BAL) was performed at 48 and 72 hours. (A & E) Total cell counts and (B & F) neutrophil counts were performed by haemocytometer. (C & G) Neutrophil apoptosis was determined by morphology. (D & H) IgM levels were determined in BAL fluid by ELISA. Data are mean and SEM for n=5.

3.9 Discussion

Innate immune cells must function competently in the hypoxic microenvironment of infected and inflamed tissues and they utilise oxygen sensing transcription factors, notably HIF, to adapt to these conditions. In addition to its key role in cellular oxygen sensing and metabolic adaptation to hypoxia, HIF-1α has been shown to regulate neutrophil survival in hypoxia as well as regulating myeloid cell motility, invasiveness and bacterial killing, in part through its ability to regulate intracellular ATP levels and, in neutrophils, granule protease production (Cramer *et al.*, 2003; Peyssonnaux *et al.*, 2005; Walmsley *et al.*, 2005). HIF-1α expression is itself induced in response to microbial products, even in normoxic conditions (Peyssonnaux *et al.*, 2005). *In vivo* myeloid-specific HIF-1α deficiency therefore results in reduced myeloid cell mediated inflammation, but also increased susceptibility to bacterial infections both locally and systemically (Cramer *et al.*, 2003; Peyssonnaux *et al.*, 2005). Consequently, direct targeting of HIF-1α would not appear to be a desirable anti-inflammatory approach given the potential for rendering the host more susceptible to uncontrolled bacterial infection. This has resulted in the search for more selective regulators of neutrophil function and fate. The data presented in this thesis implicate HIF-2α as a regulator of longevity in inflammatory neutrophils; with conservation of its role across species, and show that overexpression of HIF-2α promotes neutrophil survival in humans and zebrafish whilst its deletion results in enhanced resolution of neutrophilic inflammation in mice. These data imply that upregulation of HIF-2α mediates a distinct survival mechanism in neutrophils at inflamed sites and that this occurs independently of local oxygen availability.

Whilst HIF-1α and HIF-2α display significant sequence homology, a number of unique functions have been ascribed to each protein with HIF-1α exclusively regulating glycolytic enzyme abundance and intracellular ATP generation, and HIF-2α determining the transcription of erythropoietin and the stem cell transcription regulator, Oct4 (Covello *et al.*, 2006; Gruber *et*

al., 2007; Hu *et al.*, 2003). More recently, HIF-2α has been shown to directly regulate macrophage expression of pro-inflammatory cytokines and receptors M-CSFR and CXCR4, with myeloid-specific loss of HIF-2α resulting in resistance to LPS-induced endotoxemia, reduced tumour-associated macrophage infiltration, and reduced hepatocellular tumour progression, but no associated change in intracellular ATP levels (Imtiyaz *et al.*, 2010). Although these data clearly implicate HIF-2α in myeloid cell mediated inflammatory responses and begin to dissociate HIF-1α and HIF-2α functional responses, the work also highlights responses common to both, given the previously described role for HIF-1α in the regulation of LPS-mediated systemic inflammatory response syndrome. I therefore proposed that HIF-2α would also play a critical role in neutrophil biology, and more specifically regulate neutrophil apoptosis in the context of acute inflammation.

In keeping with previous findings from bone marrow derived neutrophils and murine neutrophil cell lines (MPRO) (Imtiyaz *et al.*, 2010), I was unable to detect HIF-2α mRNA or protein in immature murine bone marrow neutrophils. Importantly, however, detectable levels of *HIF2A* mRNA were found in highly pure peripheral blood neutrophils, although previous work had failed to detect it by less sensitive RNase protection assay (Walmsley *et al.*, 2005). Marked differential expression between bone marrow and circulating neutrophils has previously been described for numerous other genes, including BCL-2, which is only detected in immature bone marrow derived cells (Andina *et al.*, 2009; Theilgaard-Monch *et al.*, 2005). Interestingly other transcription factors, for example c-fos, c-jun and members of the C/EBP family, are also induced during late granulopoesis (Bjerregaard *et al.*, 2003). I speculate that *Hif2a* expression is activated upon exit from the bone marrow but the functional consequences of delayed expression remain the subject for future work. Nonetheless, HIF-2α is unlikely to influence neutrophil release from the marrow, given myeloid-specific HIF-2α deficient animals have normal circulating neutrophil numbers, equivalent proportions of

neutrophils in the spleen and bone marrow (Imtiyaz *et al.*, 2010) and that *epas1a* overexpression in zebrafish did not alter whole body neutrophil numbers.

In marked contrast to HIF-1α, constitutive expression of HIF-2α was detected in normoxic culture. Detectable levels of HIF-2α in normoxic macrophages are widely reported but the mechanism by which it evades degradation in myeloid cells is unknown (Fang *et al.*, 2009; Imtiyaz *et al.*, 2010; Rius *et al.*, 2008; Takeda *et al.*, 2010). One proposed mechanism may be through dynamic changes in HIF mRNA expression, as evidenced by work from Takeda et al. (Takeda *et al.*, 2010). They showed *HIF1A* and *HIF2A* mRNA to be differentially expressed in M1- and M2-polarised macrophages, with labile *HIF1A* mRNA displaying a relatively short half-life and conversely *HIF2A* mRNA being much more stable with a lower rate of turnover. Of note, these changes in mRNA expression occurred independently of oxygen availability, and were themselves a strong predictor of protein abundance. In this context, I observed no significant acute changes in mRNA expression of either *HIF1A* or *HIF2A* in healthy volunteer neutrophils but, in neutrophils isolated from patients with an ongoing chronic inflammatory arthritis, a 20-fold induction in *HIF2A* mRNA expression was observed suggesting transcriptional regulation of HIF-2α can occur in a disease context.

While HIF-1α protein was dramatically induced by hypoxia, hydroxylase inhibition and heat killed bacteria, the further modulation of HIF-2α protein expression above constitutive levels was less pronounced *in vitro*. However, much higher levels of expression in freshly isolated neutrophils from patients with inflammatory arthritis were observed compared to healthy control neutrophils and I demonstrated neutrophil expression of HIF-2α protein following recruitment to the lung in patients with mild and severe COPD. This was subsequently mirrored in a more acute setting in a murine model of LPS mediated acute lung injury. In contrast, no HIF-1α expression was detected in circulating inflammatory neutrophils. The

importance of HIF-2α accumulation with respect to disease outcomes is unknown but, through access to three patients with known gain-of-function mutations in the *HIF2A* gene, I was able to assess the functional consequences of HIF-2α overexpression in neutrophils. Baseline rates of constitutive apoptosis were consistently lower in neutrophils from the patients than controls, although further reduction in apoptosis was achieved by stimulation with DMOG. This is consistent with experimental evidence showing only partial activation of HIF-2α in these patients, thus permitting further stabilisation through hydroxylase inhibition, and also the consequent additional stabilisation of HIF-1α (Percy *et al.*, 2008b). Interestingly, neutrophils derived from patients with gain-of-function mutations in *HIF2A* also showed increased target gene expression namely *VEGF, PAI-1* and *PHD-3*. Whilst modulation of target gene mRNA expression by both HIF-1α and HIF-2α cannot be excluded, changes were observed in the specific HIF-2α target gene, *PAI-1*. Unfortunately, this did not reach statistical significance, but this is likely to reflect the limited sample size, given the small number of patients available to study.

Whilst delayed apoptosis has been implicated in animal models of inflammation (Jonsson *et al.*, 2005; Rossi *et al.*, 2006), it is not known whether the increase in HIF-2α expression and associated intrinsic delay of neutrophil apoptosis might predispose these patients to inflammatory disease, not least because of the rarity of the condition and the dominant clinical phenotype of erythrocytosis and its consequences. To address directly the importance of selective HIF-2α stabilisation in the regulation of neutrophil survival and resolution of inflammation the human gain-of-function *HIF2A* mutations were replicated in the genetically tractable zebrafish (Elks *et al.*, 2011; Renshaw *et al.*, 2006). The hydroxylation sites of HIF-α subunits are highly conserved across species (Elks *et al.*, 2011) with an overall amino acid homology of 58% between zebrafish epas1a and human HIF-2α. Using zebrafish RNA, the same glycine residues as are altered in the patients with gain-of-function *HIF2A* mutations were mutated, and these mutant constructs were injected into zebrafish at the one cell stage.

The resulting overexpression of mutant *epas1a* led to impaired resolution of inflammation in a tail injury model that was equivalent to overexpression of dominant active *hif1ab* and of a similar magnitude to previously reported results using the pan-caspase inhibitor, zVD.fmk (Renshaw *et al.*, 2006). These findings highlight that *in vivo epas1a* can modulate neutrophil survival to the same order of magnitude as *hif1ab.*

Given the possibility that HIF-2α may represent a more selective and therefore potentially attractive anti-inflammatory target, I investigated the consequences of HIF-2α deficiency using mice with myeloid-specific deletion of *Hif2a*, as previously described (Takeda *et al.*, 2010). In marked contrast to HIF-1α deficiency (Cramer *et al.*, 2003), I found no impairment of neutrophil chemotaxis, phagocytosis or respiratory burst in HIF-2α deficient neutrophils. The expression profiles of the adhesion molecules CD11b and L-selectin were also preserved following LPS stimulation as was neutrophil trafficking into the lung in response to intratracheal LPS. This highlights important differences in the consequences of HIF-2α deficiency within myeloid cell populations, given myeloid-specific *Hif2a* deletion resulted in reduced macrophage trafficking into tumours and reduced expression of CXCR4 and the extracellular protein, fibronectin-1, in these cells (Imtiyaz *et al.*, 2010). Consistent with my findings of preserved neutrophil function *in vitro* and normal recruitment *in vivo*, I also demonstrated no impairment of host defence against bacterial infection in animals with HIF-2α deficiency in myeloid cells. This was assessed using a pneumococcal pneumonia model at a dose sufficient to overwhelm the defence provided by resident macrophages and result in marked neutrophil infiltration into the lungs (Dockrell *et al.*, 2003). This model produces established pneumonia with a significant mortality rate but the mice with neutrophils deficient in HIF-2α had equivalent rates of survival compared to wild-type controls.

In the light of my findings with HIF-2α overexpression in human and zebrafish neutrophils, it was surprising to find no differences in murine neutrophil apoptosis, either constitutively or in response to hypoxia or LPS *in vitro*. My data, together with previously published data, suggest that while HIF-2α is unable to compensate for loss of HIF-1α and maintain survival in hypoxia the survival response to LPS may be mediated by either transcription factor, or an independent pathway. Nonetheless, evidence suggests that the *in vivo* response to LPS involves both transcription factors given that myeloid-specific loss of either HIF-1α or HIF-2α results in reduced systemic inflammatory responses and mortality following intravenous or intraperitoneal challenges (Imtiyaz *et al.*, 2010; Peyssonnaux *et al.*, 2007). Despite the preserved survival response *in vitro*, in LPS-mediated *in vivo* models of acute lung injury HIF-2α deficiency was associated with enhanced inflammation resolution, with fewer neutrophils in BAL samples at 48 and 72 hours, in association with an increase in morphological neutrophil apoptosis. Neutrophils recruited from the circulation to the lung and the airways following LPS stimulation significantly up-regulated *Hif2a* mRNA but not *Hif1a* mRNA, with persistence of *Hif2a* mRNA in bronchoalveolar lavage cells during inflammation resolution when *Hif1a* mRNA expression had substantially reduced. This would suggest, in a model of neutrophilic inflammation in which oxygen availability is not limited, it is HIF-2α expression that dictates the resolution of the inflammatory process. Importantly the consequences of enhanced resolution of inflammation were evident in the high dose nebulised LPS model, with the reduction in neutrophil count being associated with evidence of reduced lung injury, as assessed by levels of IgM in the bronchoalveolar lavage fluid.

The preservation of neutrophil function *in vitro* and recruitment *in vivo* dissociates HIF-2α neutrophil phenotypes from deficiency of HIF-1α (Cramer *et al.*, 2003). Furthermore the phenotype of enhanced resolution in LPS-mediated acute lung injury contrasts with findings in

PHD3 deficient animals, in which a specific role was demonstrated for PHD3 in regulating inflammation resolution in the context of both whole animal hypoxia in a hypoxic LPS acute lung injury model, and localised tissue hypoxia in a DSS model of colitis (Walmsley *et al.*, 2011). While PHD3 is essential therefore for neutrophil survival and inflammatory responses in hypoxia, I propose that the effects of HIF-2α deficiency in inflammatory neutrophils occur independently of oxygen tension and targeting HIF-2α may therefore be of greater clinical utility in inflammation in tissues such as the lung where oxygen tension may vary widely (Hamedani *et al.*, 2011).

Interestingly, cytokine responses were preserved in myeloid-specific HIF-2α deficient mice when challenged with intratracheal LPS. My data contrast with findings from an intraperitoneal LPS-induced endotoxemia in which HIF-2α deficiency resulted in reduced serum levels of pro-inflammatory cytokines and increased levels of IL-10 (Imtiyaz *et al.*, 2010). However, the two models differ in magnitude of cytokine release and outcome, with lethality in the intraperitoneal model within 48 hours. Furthermore, although *in vitro* data supported a role for HIF-2α mediated regulation of IL-6 in macrophages (Imtiyaz *et al.*, 2010), no differences were seen in serum in either model. These results may reflect differences in the mechanisms by which neutrophils and macrophages upregulate cytokine production or the *in vivo* production of cytokines from non-myeloid cells. Indeed alveolar epithelial cells are a major source of chemokines and IL-6 in the lung (Thorley *et al.*, 2007). During resolution, cytokine levels fell dramatically in both BAL and plasma and there were no differences with HIF-2α deficiency (data not shown), reinforcing that the phenotype of increased neutrophil apoptosis seen in *Hif2α^{flox/flox};LysMCre^{+/-}* mice at 48 hours is independent of a defect in macrophage cytokine production.

In summary, I have described expression of HIF-2α in human and murine neutrophils and showed upregulation in inflammatory neutrophils. I have shown that HIF-2α overexpression leads to an intrinsic delay of neutrophil apoptosis in patients with gain-of-function *HIF2A* mutations and impaired resolution of inflammation in a zebrafish tailfin injury model. Importantly, and in marked contrast to HIF-1α, deficiency of HIF-2α had no effect on neutrophil function but did enhance apoptosis of inflammatory neutrophils *in vivo*. Through modulation of tumour cell apoptosis, HIF-2α has emerged as a potential therapeutic target in cancer biology (Bertout *et al.*, 2008; Raval *et al.*, 2005). I now implicate HIF-2α in neutrophilic inflammation and propose that selective inhibition of HIF-2α may allow effective control of neutrophil-mediated inflammation without compromising host defences.

4 Hypoxia induces hypothermia and sickness behaviour in mice following subcutaneous injection of live *Staphylococcus aureus*

4.1 Introduction

Bacterial infections frequently occur in the context of local and systemic hypoxia. Hypoxaemic patients on critical care commonly succumb to bacterial infections and have a high mortality (Alberti *et al.*, 2003). The acute respiratory distress syndrome, defined by arterial hypoxaemia, has a mortality rate of 40% and the majority of cases are due to infection (Matthay *et al.*, 2003; Sheu *et al.*, 2010). At a tissue level, oxygen tensions measured in healthy subcutaneous tissue of perioperative patients had average values of 7.8 kPa compared to values of less than 3 kPa when infected and inflamed (Hopf *et al.*, 1997; Silver, 1977). The influence of hypoxia on the interaction between host and pathogen, and in particular the host immune response, is therefore of considerable interest.

Outcomes of infection are often worsened by hypoxia. In animal models, infected wound flaps were larger and more necrotic if animals breathed hypoxic gas (12% oxygen) than if they breathed air or were given supplementary oxygen (45% oxygen)(Jonsson *et al.*, 1988). In humans, wound infection rate was inversely proportional to subcutaneous oxygen tension during surgery (Hopf *et al.*, 1997). Furthermore, several randomised controlled clinical trials in patients having surgery under general anaesthetic have shown reduced frequency of surgical wound infection if 80% oxygen rather than 30% oxygen was administered during the perioperative period (Belda *et al.*, 2005; Greif *et al.*, 2000). These observations are consistent with the finding that limitation of molecular oxygen impairs neutrophils' capacity to generate reactive oxygen species (ROS) and reduces neutrophil killing of *Staphylococcus aureus in vitro* (McGovern *et al.*, 2011). Hypoxia, on the other hand, does not impair the ability of *S. aureus* to subvert the host response as it is capable of killing neutrophils in hypoxic culture media (McGovern *et al.*, 2011).

Although hypoxia may compromise elements of the immune response to infection, there is also good evidence that components of cellular oxygen sensing pathways are key regulators of the host's innate immune response. HIF-1α, a master regulator of cellular adaptation to hypoxia and of innate immune function, is stabilised not only by hypoxia but also by bacteria and endotoxin independent of oxygen tension (Peyssonnaux *et al.*, 2005). Studies of bone marrow-derived macrophages from HIF-1α deficient mice showed that killing of both gram positive and gram negative bacteria was reduced (Peyssonnaux *et al.*, 2005). Conversely, macrophages from mice with myeloid cell specific deletion of the VHL gene, and thus activation of HIF-pathways, had increased bactericidal action (Peyssonnaux *et al.*, 2005). Moreover stabilisation of HIF-1α by the HIF-hydroxylase inhibitor, mimosine, enhanced killing of *S. aureus* by neutrophils and monocytes *in vitro* and reduced lesion size when injected locally in a mouse model of *S. aureus* infection skin (Zinkernagel *et al.*, 2008).

The HIF pathway also has a critical role in the development of endotoxin-induced sepsis. Despite the evidence discussed earlier in this thesis of distinct roles for HIF-1α and HIF-2α regulating neutrophil and macrophage phenotypes, deletion of either HIF-1α or HIF-2α in myeloid cells protected mice from the effects of high dose intraperitoneal LPS injection (Imtiyaz *et al.*, 2010; Peyssonnaux *et al.*, 2007). Temperature, haemodynamic indices and overall mortality were improved with myeloid cell deficiency of either HIF-α subunit. Interestingly, in a similar model pre-treatment of mice with the hydroxylase inhibitor, DMOG, improved outcome in endotoxaemic mice in an NF-κB dependent manner but DMOG pre-treatment worsened outcome in response to polymicrobial sepsis (Hams *et al.*, 2011). Therefore, despite the ability of both hypoxia and bacteria to activate the HIF-pathway, the effects of local versus systemic HIF activation appear to be crucial in determining outcome in sepsis and localised infection. I used a model of subcutaneous *S. aureus* infection with the added insult of reduced ambient oxygen tension to investigate the interaction between hypoxia and the host response to bacterial infection *in vivo*.

S. aureus is an important cause of morbidity and mortality in humans (Boucher and Corey, 2008; Laupland *et al.*, 2003). Although 30%-50% of the population may have skin or mucosal colonisation, *S. aureus* has the potential to cause diverse and devastating infections, even in immunocompetent individuals (Lowy, 1998; van Belkum *et al.*, 2009). Local infections include impetigo, folliculitis and cellulitis. Moreover, *S. aureus* is the most common pathogen in community acquired skin and soft tissue infections requiring hospital admission (Dryden, 2010; Zervos *et al.*, 2012). Invasive infections, defined as *S. aureus* isolated from blood, cerebrospinal fluid, pleural fluid, synovial fluid or aseptically obtained tissue samples, had an incidence of 28.4 cases per 100,000 population with a mortality of 19% (Laupland *et al.*, 2003). While certain populations are known to be at high risk of developing invasive infections, for example patients on haemodialysis (Laupland *et al.*, 2003), virulent forms of *S. aureus* expressing the Panton-Valentine leukocidin toxin are responsible for necrotizing pneumonia in previously healthy children and young adults (Gillet *et al.*, 2002).

An important problem for clinicians treating *S. aureus* infections is the emergence of antibiotic resistance. Methicillin resistance is no longer only a feature of nosocomial infection but is increasingly found in community acquired *S. aureus* infections (Boucher and Corey, 2008; Fridkin *et al.*, 2005). Resistance to other antibiotics is also emerging with vancomycin and linezolid resistant strains reported (Rivera and Boucher, 2011) To improve strategies for combating *S. aureus* infection in the face of increasing antibiotic resistance (Hiramatsu, 2001; Rivera and Boucher, 2011) a greater understanding of host-pathogen interactions is required.

S. aureus is a major pathogen in critical care where patients may have profound hypoxaemia (Alberti *et al.*, 2003; Guidet *et al.*, 2005) and at a tissue level, *S. aureus* frequently infects ischaemic wounds (Galkowska *et al.*, 2009). *S. aureus* is therefore a useful tool to model the interaction between pathogens and host responses to infection in the context of hypoxia. I hypothesised that systemic hypoxia might alter the host immune response to a local *S. aureus*

(strain SH1000) infection. Additionally, in this setting of combined systemic hypoxia and bacterial infection which both stabilise HIF-α subunits, I aimed to explore whether myeloid cell deficiency of HIF-1α or HIF-2α would alter the host response.

Results

4.2 Subcutaneous injection of live *S. aureus* induces hypothermia and sickness behaviour in hypoxia but not normoxia.

Injection of 5 x 10^7 cfu SH1000 bacteria into the subcutaneous tissue of normoxic mice consistently produced a skin lesion which increased in size over 7 days (see Figure 4.2-1). Mice had lost weight at 24 hours post-injection but this was regained by day 7 (Figure 4.2-1).

As I wished to determine the interaction between hypoxia and *S. aureus in vivo*, I challenged mice with subcutaneous SH1000 or PBS and placed them in a hypoxic incubator, reducing the oxygen level to 10% (approximately 50% of atmospheric oxygen tension) over 1 hour. This level of oxygen tension is frequently used in mouse models and is normally well tolerated but if mice are maintained in hypoxia for more than 1 week, they develop right ventricular hypertrophy and pulmonary arterial hypertension (Hancher and Smith, 1975; James and Thomas, 1968; Naeye, 1967; Yu *et al.*, 1999). After 6 hours in hypoxia, I observed a slight but significant reduction in control mouse body temperature (39.1˚C +/- 0.56 vs. 37.2˚C +/- 0.43, n=6, p<0.05) consistent with previous studies (Bhatia *et al.*, 1969; Gellhorn and Janus, 1936; Gordon and Fogelson, 1991). There was no evidence of sickness behaviour in these animals. However, after 12 hours I found no difference in temperature between control mice but profound hypothermia in infected hypoxic animals compared to those maintained in normoxia (see Figure 4.2-2). Furthermore the mice appeared clinically unwell and I developed assessment tools to objectively score the sickness behaviour of the mice. Clinical assessment of the mice by independent observers revealed marked sickness behaviour in hypoxic mice injected with SH1000 which was not observed in mice maintained in normoxia or in hypoxic mice injected with PBS (see Figure 4.2-2). On one occasion the time point was extended to 18 hours, but by this time 1 out of 3 hypoxic infected mice was dead and 2 out of 3 were moribund.
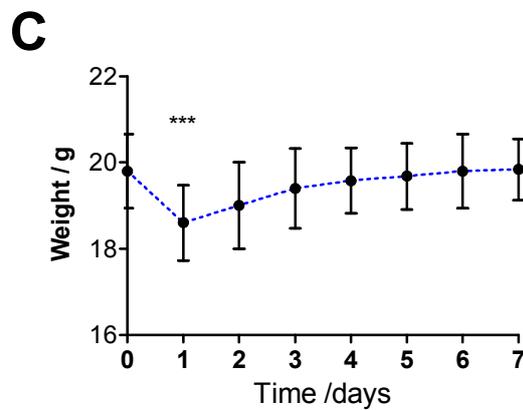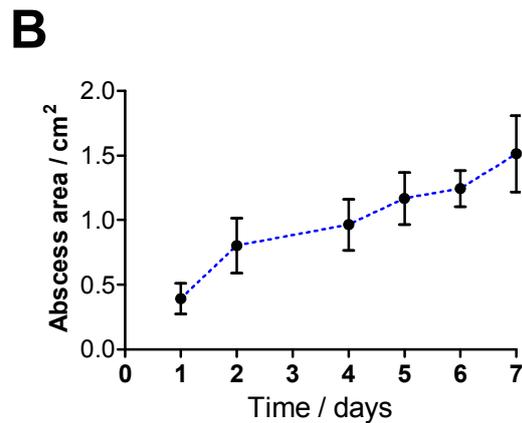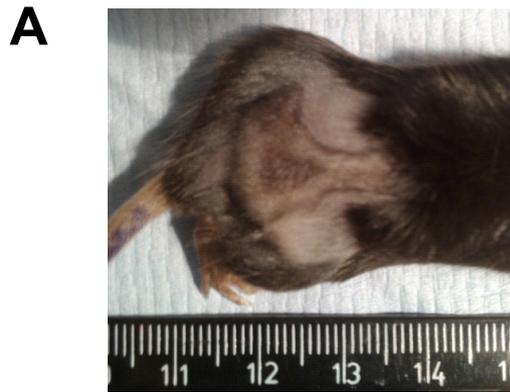
Figure 4.2-1. Subcutaneous injection of 5×10^7 cfu *Staphylococcus aureus* produces a skin lesion in normoxic mice.

C57BL/6 mice were injected with 5×10^7 cfu *S. aureus* (SH1000) then photographed and weighed daily for 7 days. (A) A representative photograph of a skin lesion 7 days post-injection. (B) Skin lesion area calculated using ImageJ software. (C) Mouse body weight in grams. Data are mean +/- SEM n=5. *** $p < 0.001$ versus starting weight analysed by repeated measures ANOVA and Bonferroni's post-test.

A

B

C
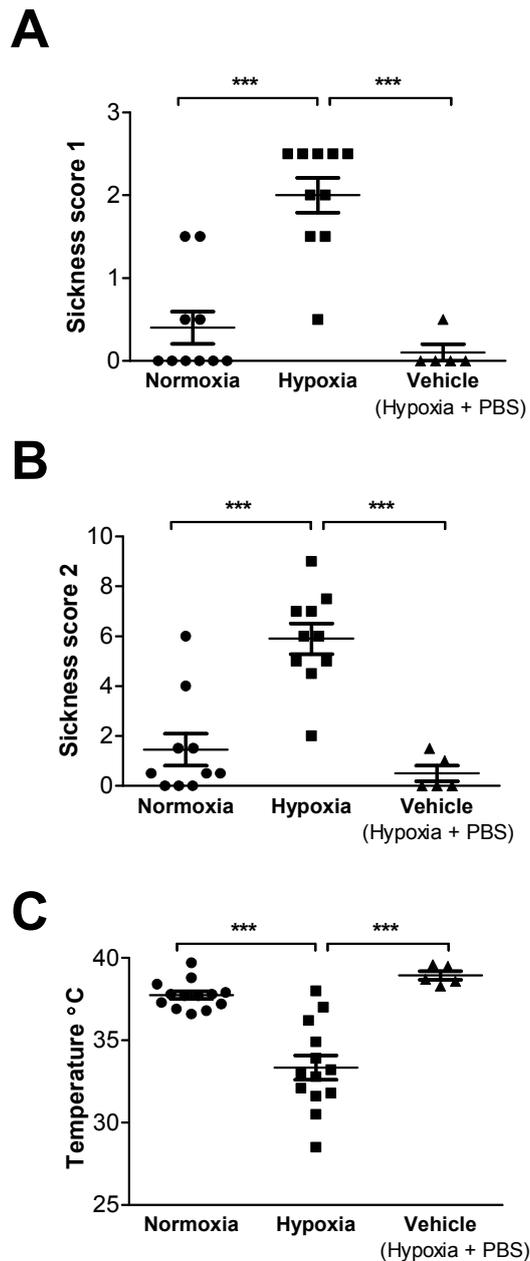
Figure 4.2-2. Hypoxia induces hypothermia and sickness behaviour in mice infected subcutaneously with *Staphylococcus aureus*.

Mice were injected subcutaneously with 5×10^7 colony forming units of SH1000 *S. aureus* or PBS vehicle control and placed in normoxia or hypoxia (10% O_2) for 12 hours. (A & B) Scatter plots of mouse sickness scores assessed by independent observers blinded to experimental condition. (B) Rectal temperatures were also recorded 12 hours following injection. Data are mean +/- SEM. n=10 or n=5 (vehicle). ***p<0.0001 by ANOVA.

To establish whether live bacteria were required to produce the phenotype of hypothermia and sickness behaviour in hypoxic mice, 5×10^7 cfu of heat-killed SH1000 were injected subcutaneously. Unlike live SH1000, the heat-killed bacteria did not lead to a significant increase in sickness score or reduction in body temperature (see Figure 4.2-3).
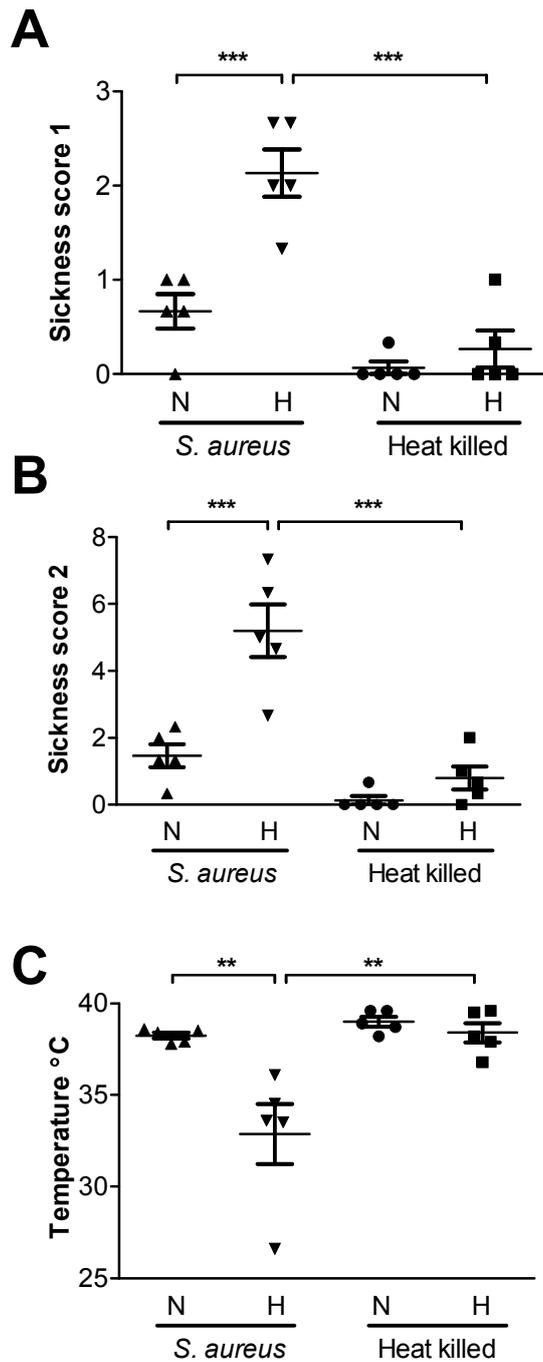
Figure 4.2-3. Live bacteria are required to produce the phenotype of hypothermia and sickness behaviour in hypoxic animals.

Mice were injected with $5x10^7$ cfu of live or heat killed SH1000. (A & B) Sickness scores and (C) rectal temperature were recorded after 12 hours. Data are mean +/- SEM n=5. ***p<0.0001, **p<0.01 by ANOVA. N=normoxia, H=hypoxia.

4.3 Hypoxia does not alter inflammatory cell recruitment or bacterial burden.

To investigate whether hypoxia impaired the local immune response to the subcutaneous bacterial challenge, the skin around the injection site was biopsied 12 hours after injection. Histological sections revealed an inflammatory infiltrate in both normoxic and hypoxic skin but no differences were detected in counts of myeloperoxidase expressing cells (see Figure 4.3-1). Further objective quantification of inflammatory infiltration was performed using an assay of myeloperoxidase activity in homogenised biopsy specimens. No difference in myeloperoxidase activity was detected between infected hypoxic or normoxic skin.

Bacterial counts in the skin were equivalent between normoxic and hypoxic mice in keeping with the evidence of preserved inflammatory cell recruitment in hypoxia (see Figure 4.3-2).
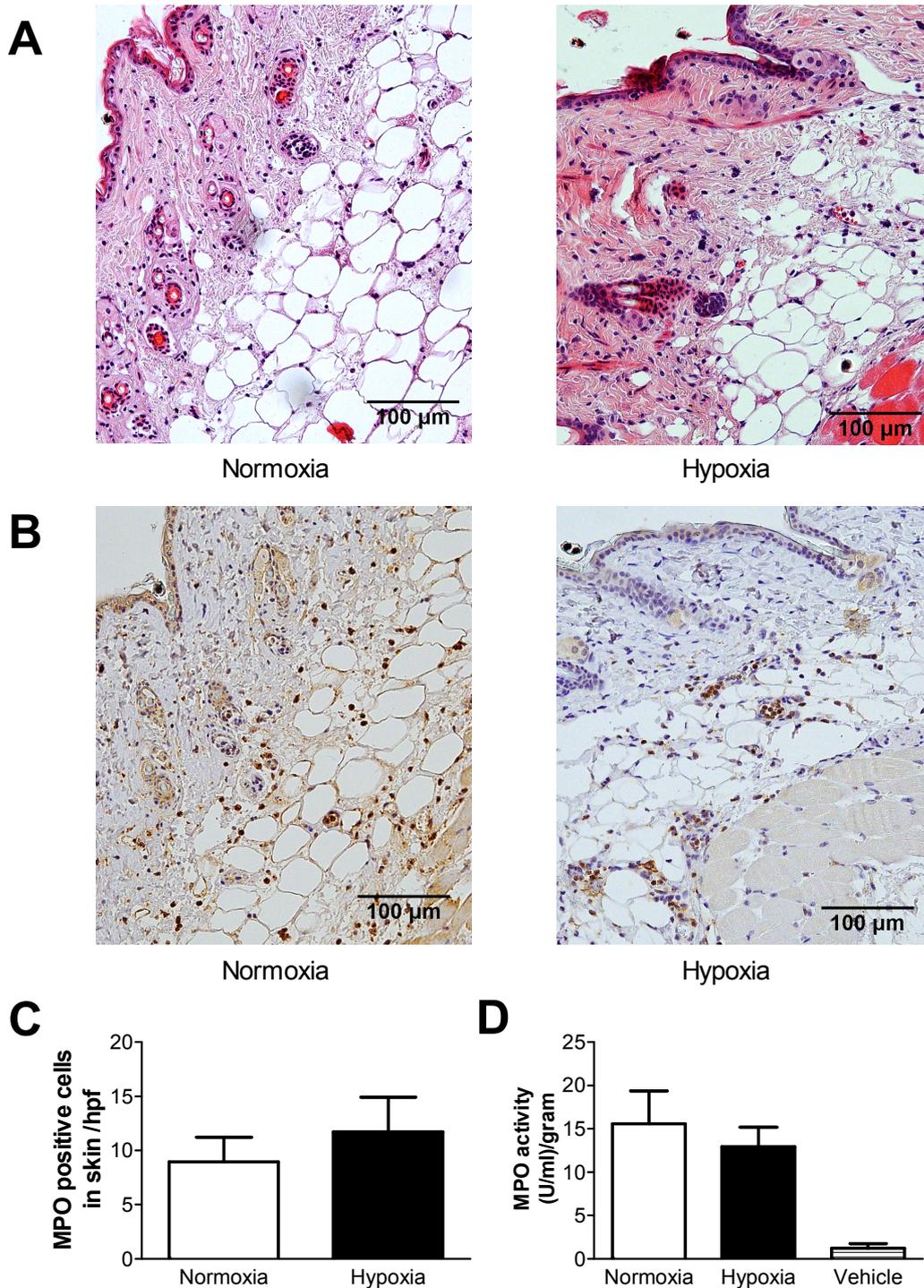
Figure 4.3-1. No differences in local host response to subcutaneous injection of SH1000 bacteria after 12 hours.

Mice were injected subcutaneously with 5×10^7 cfu of SH1000 *S. aureus* or PBS control and placed in hypoxia or normoxia for 12 hours. (A & B) Representative photomicrographs of infected skin biopsy sections stained with (A) haematoxylin and eosin or (B) anti-myeloperoxidase antibody. Original magnification x200. (C) Counts of myeloperoxidase positive cells per high powered field in skin tissue. (D) Skin biopsies were homogenized in HTAB buffer. Myeloperoxidase activity was analysed and normalised per gram of skin tissue. Data are mean +/- SEM for n=5.

A

50 µm
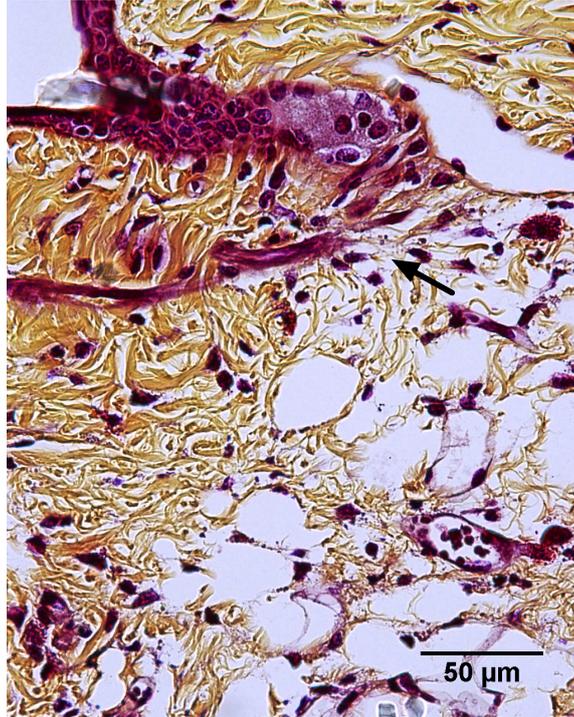
B
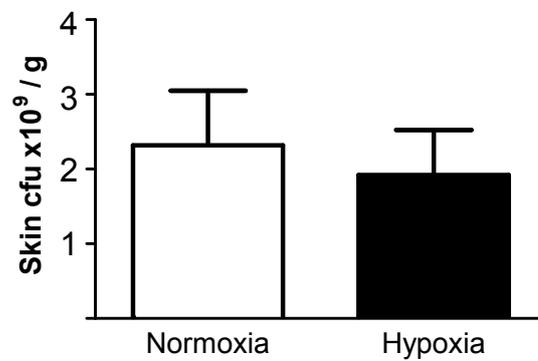
Figure 4.3-2. No differences in bacterial count in skin after 12 hours.

Mice were injected subcutaneously with $5x10^7$ cfu of SH1000 *S. aureus* and placed in hypoxia or normoxia for 12 hours. (A) A photomicrograph of a section of skin tissue stained using a Gram stain kit showing gram positive bacteria within the subcutaneous tissue. The arrowhead marks one example. Original magnification x400. (B) Skin biopsies were weighed and homogenized in PBS before colony forming unit counts were obtained using the Miles and Misra method.

4.4   No detectable bacteraemia in infected animals

Using blood drawn from mice 12 hours following injection of SH1000 I performed serial dilutions and cultured these overnight on blood agar plates. No bacteria were evident in the blood from normoxic or hypoxic animals (n=5). To determine whether a transient bacteraemia had seeded vital organs, as occurs following intravenous injection of *S. aureus* (Jonsson *et al.*, 2004), I isolated kidneys, liver and spleen from animals 12 hours after subcutaneous infection. Again, I observed no detectable gram positive bacteria.

4.5   Cytokine responses in mice infected with SH1000.

Cytokine release was measured in plasma at 3, 6 and 12 hours following injection of *S. aureus*. I found decreased levels of MCP-1 and KC at 3 hours in infected hypoxic mice compared to infected normoxic mice (see Figure 4.5-1). Levels of KC and IL-6 were higher 6 hours after injection but there were no significant differences in levels of these cytokines between hypoxic and normoxic animals at this time point. Twelve hours following injection cytokine levels had reduced from those seen at 6 hours and there were no significant differences between the animals maintained in normoxia versus infected hypoxic animals. At none of the time points was I able to detect IL-1β, TNF-α, IFN-γ, IL-10, IL-4 or IL-13 by cytometric bead array.
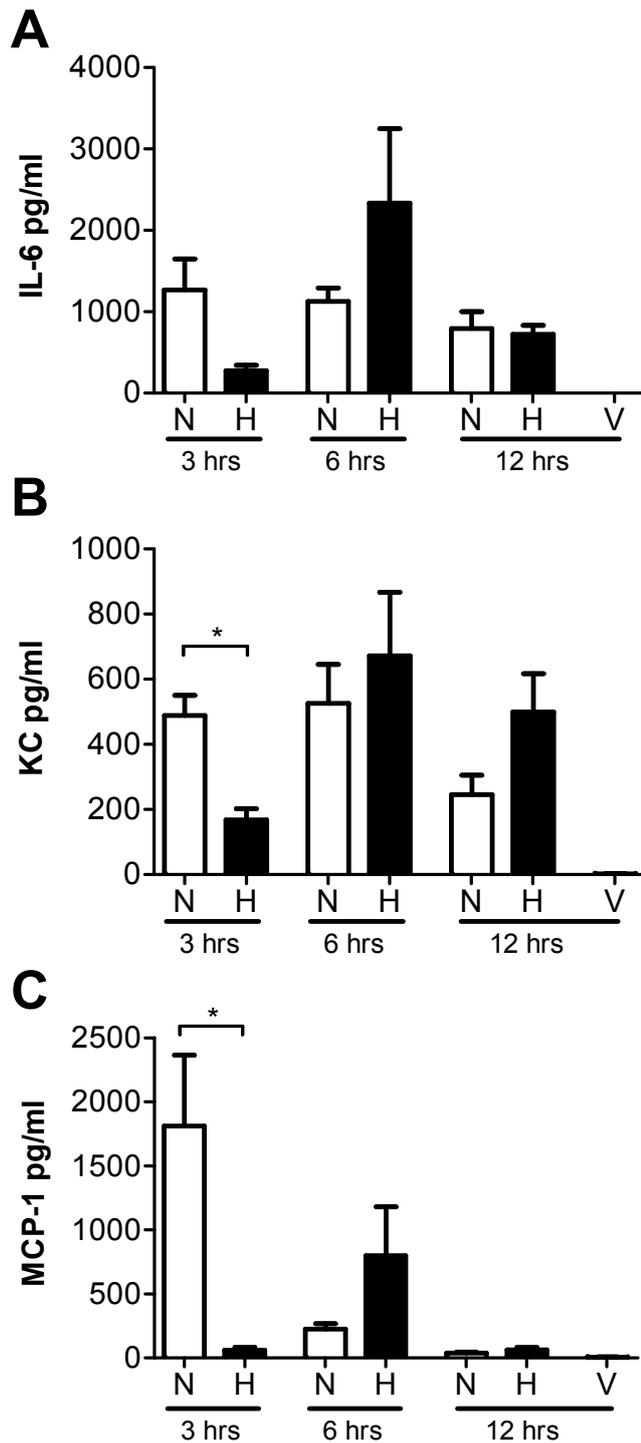
Figure 4.5-1. Circulating cytokine concentrations in normoxic and hypoxic animals infected with *S. aureus*.

Mice were placed in hypoxia or normoxia following infection with SH1000 and sacrificed at either 3, 6 or 12 hours. Plasma was obtained and analysed by cytokine bead array for (A) IL-6, (B) KC and (C) MCP-1. IL-1 and TNF were also analysed but were below the limit of detection at these times. Data are mean +/- SEM of a minimum n=4.

4.6   No evidence of multi-organ dysfunction.

In order to try to establish the cause of the sickness behaviour and hypothermia in infected hypoxic mice, a series of investigations were performed assessing the function of vital organs. Analysis of serum revealed no evidence of either pancreatic or liver dysfunction but there was a significant elevation in serum creatinine (see Figure 4.6-1).

To assess for acute lung injury, bronchoalveolar lavage was performed 12 hours following *S. aureus* injection and this recovered low numbers of cells with no difference in counts between infected hypoxic or normoxic mice (see Figure 4.6-2). Notably there was no evidence of neutrophilic inflammation. Histological samples confirmed the lack of inflammatory infiltration in infected animals (see Figure 4.6-2).   There was also no evidence of increased pulmonary oedema in hypoxic animals compared to normoxic mice determined by wet to dry lung weight ratios. Consistent with these findings, the infected mice had similar respiratory rates in hypoxia and normoxia (see Figure 4.6-3).

Given the precedent of cerebral oedema in the context of hypobaric hypoxia (Houston and Dickinson, 1975; Schoch *et al.*, 2002), I analysed wet and dry brain weights and found no evidence of cerebral oedema in either normoxic or hypoxic infected mice (see Figure 4.6-4). In a separate experiment, mice were injected with Evan's blue dye to assess for fluid leak across the blood brain barrier. This method has been used to show cerebral oedema following ischaemic tissue injury (Aoki *et al.*, 2002; Manaenko *et al.*, 2011). I did not detect any dye in the brain tissue of hypoxic or normoxic mice.

To investigate for evidence of significant acidosis or hypoglycaemia contributing to the phenotype of hypothermia and sickness behaviour in hypoxic mice, blood glucose and bicarbonate levels were measured, but no differences were detected compared to normoxic infected mice (see Figure 4.6-5).

A

B

C
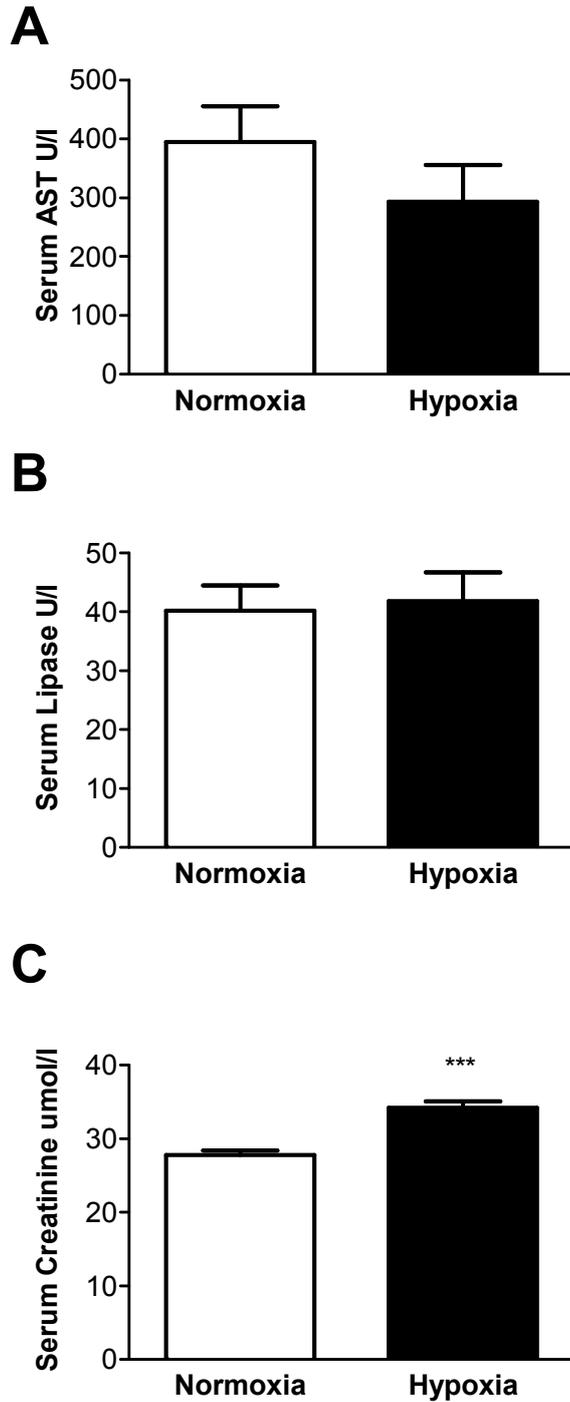
Figure 4.6-1. Elevated serum creatinine in hypoxic mice infected with *S. aureus* but no evidence of pancreatic or liver dysfunction.

Mice were injected subcutaneously with 5×10^7 cfu of SH1000 *S. aureus* and placed in hypoxia or normoxia for 12 hours. Serum was obtained and analysed for (A) aspartate transaminase, (B) lipase and (C) creatinine. Data are mean +/- SEM, n=5. *** $p < 0.001$ by unpaired t test.

Figure 4.6-2. Injection of subcutaneous *S. aureus* does not induce acute lung injury.

Mice were placed in hypoxia or normoxia for 12 hours following infection with SH1000. Bronchoalveolar lavage was performed in anaesthetised animals and (A) total cell count and (B) neutrophil counts were calculated. Data are mean and SEM, n=5. (C) Representative photographs of lung tissue sections from infected normoxic and hypoxic mice stained with haematoxylin and eosin. Original magnification x200.

Figure 4.6-3. No evidence of increased pulmonary oedema or respiratory distress in hypoxic animals infected with *S. aureus*.

Mice were placed in hypoxia or normoxia for 12 hours following infection with SH1000. (A) Lung oedema was assessed by wet to dry lung weight ratio. (B) Respiratory rate of infected animals was counted. Data are mean and SEM, n=5.
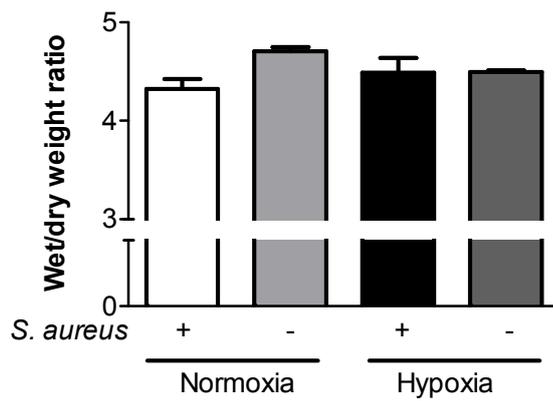
Figure 4.6-4. Injection of subcutaneous *S. aureus* does not precipitate cerebral oedema in hypoxia.

Mice were placed in hypoxia or normoxia for 12 hours following infection with SH1000. Brain oedema was assessed by wet to dry brain weight ratio. Data are mean and SEM, n=3.
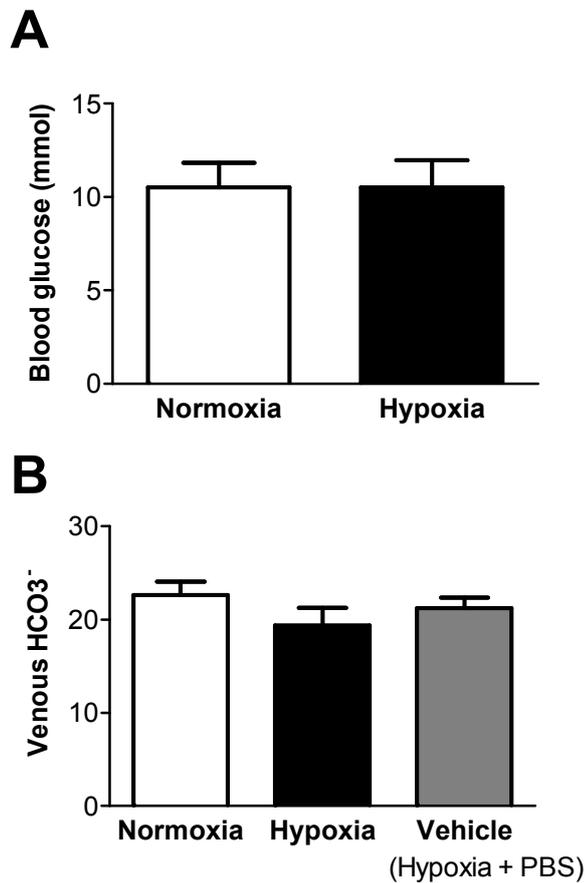
Figure 4.6-5. Blood glucose levels and venous bicarbonate are not significantly altered in infected hypoxic mice.

Mice were placed in hypoxia or normoxia for 12 hours following subcutaneous injection with *S. aureus*. (A) Blood glucose levels were measured using an Optium Xceed blood glucose meter. Animals were not fasted during this experiment. (B) Venous bicarbonate was obtained with a blood gas analyser. Data are from a minimum n=4 and are mean and SEM.

4.7 Evidence of circulatory dysfunction.

Further non-invasive assessment of awake mice displaying sickness behaviour revealed significant systolic hypotension and bradycardia (see Figure 4.7-1). Echocardiographic assessment of infected hypoxic and normoxic animals was therefore performed under light anaesthetic 12 hours after injection of bacteria.

Several markers of left ventricular contractility were assessed. For comparison, data from non-infected normoxic mice of equivalent weight but assessed at a different time are shown alongside infected animals. Representative M-mode images of the left ventricle in the short axis view are shown in Figure 4.7-2. These M-mode images revealed fractional shortening, calculated from the change in diameter of the left ventricle between diastole and systole, was reduced in hypoxic infected animals (see Figure 4.7-3). 2-dimensional measurements of left ventricular area were used to calculate fractional area change (see Figure 4.7-3). This was significantly reduced in infected hypoxic animals compared to normoxic animals. Furthermore, tissue doppler measurements of left ventricular anterior wall velocity provided additional evidence of reduced left ventricular contractility in the hypoxic infected mice (see Figure 4.7-3).

Left ventricular volumes were estimated from the internal diameter of the left ventricle measured in M-mode. End-systolic volume was significantly greater in the injected hypoxic mice, with no significant change in diastolic volume (see Figure 4.7-4). Using these volumes to calculate ejection fraction, stroke volume index and cardiac index revealed a significant reduction in left ventricular function in hypoxic infected mice (see Figure 4.7-4).
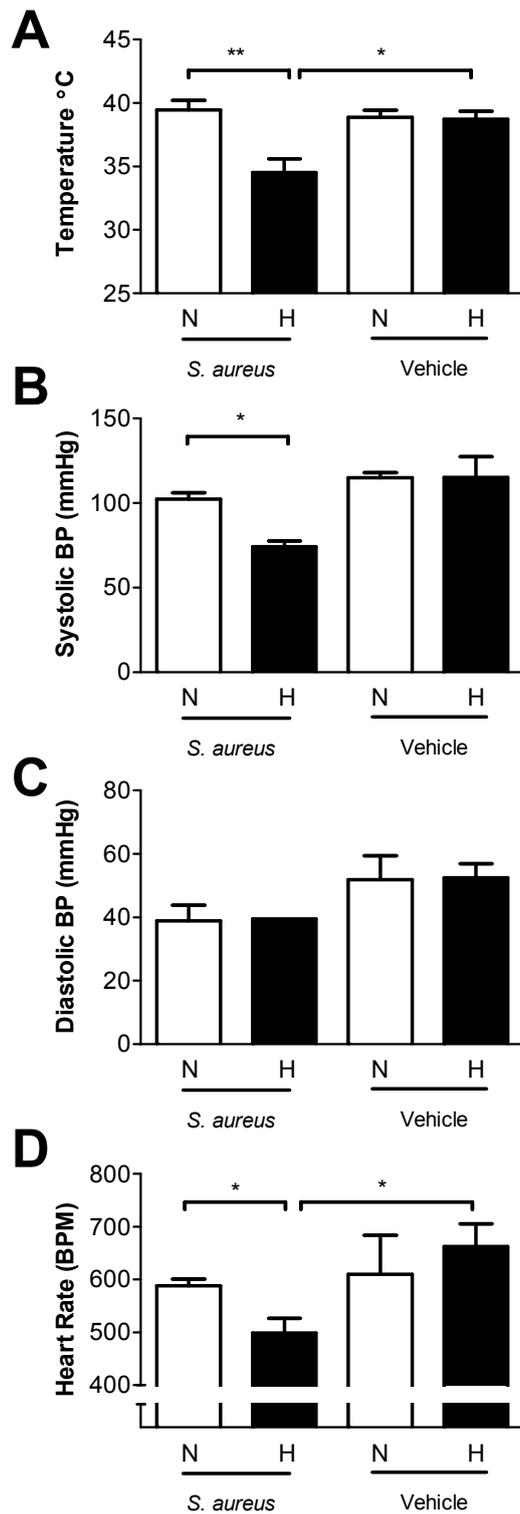
Figure 4.7-1. Hypoxic mice infected with *S. aureus* are hypotensive and bradycardic.

Mice were trained to undergo non-invasive measurement of blood pressure and heart rate. 12 hours following subcutaneous injection of SH1000 or PBS control, animals maintained in either hypoxic or normoxic conditions had measurements of (A) rectal temperature, (B) systolic blood pressure, (C) diastolic blood pressure and (D) heart rate performed. Data are mean and SEM of a minimum n=3. * p<0.05, ** p<0.01

A
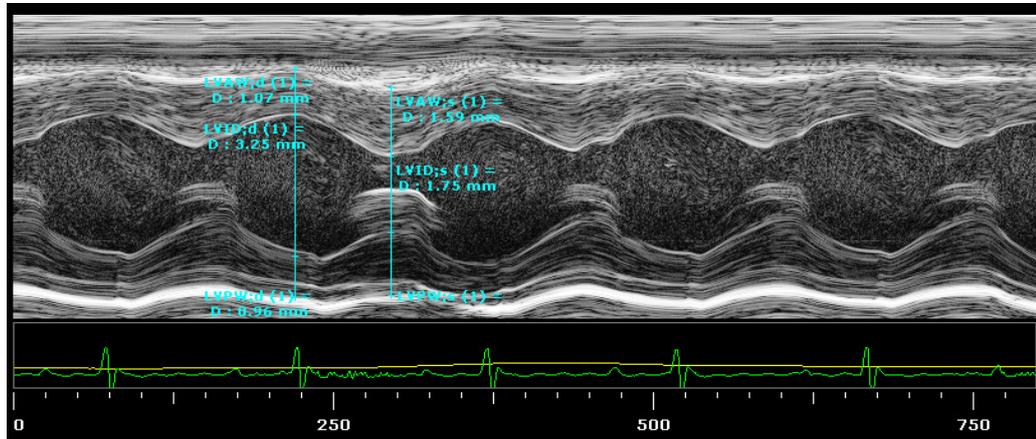
B
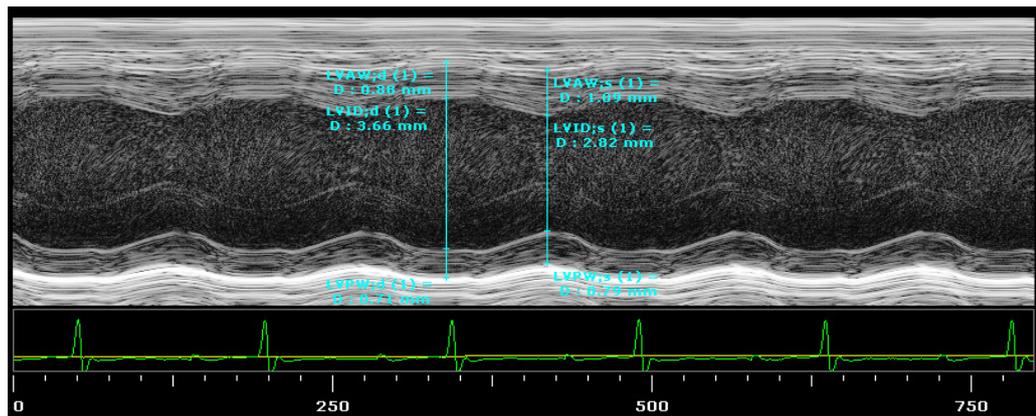
Figure 4.7-2. M mode images of the left ventricle showing impaired left ventricular function.

Echocardiography was performed by Dr Abdul Hameed on anaesthetised mice 12 hours after infection with SH1000. Representative M mode images were captured in the short axis view of mice maintained in (A) normoxia or (B) hypoxia. These images were used to measure left ventricular diameters in systole (LVID;s) and diastole (LVID;d).
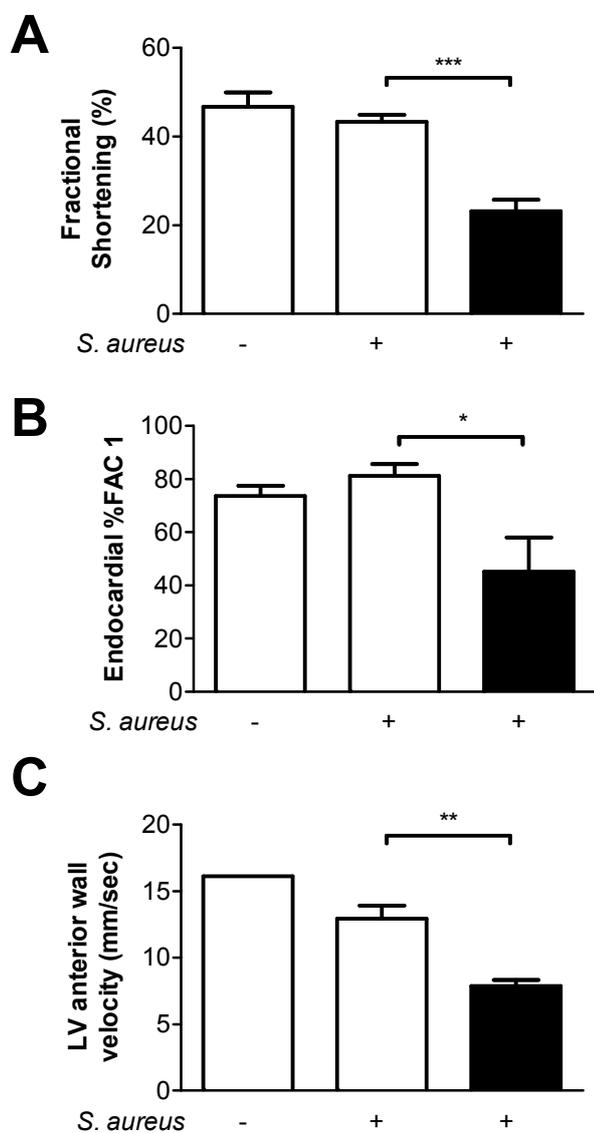
Figure 4.7-3. Measurements of left ventricular contractility in mice 12 hours after subcutaneous *S. aureus* injection.

Echocardiography was performed by Dr Abdul Hameed on anaesthetised mice 12 hours after infection with SH1000. Data from non-infected normoxic mice are shown for comparison. (A) Fractional shortening, calculated from the change in left ventricular internal diameter between end-diastole and end-systole. (B) Fractional area change, calculated from the 2-dimensional measurement of left ventricular area in systole and diastole. (C) Left ventricular anterior wall velocity measured by tissue doppler. Data are mean and SEM of n=3 or 4. * p <0.05, ** p <0.01, *** p<0.001 by ANOVA.
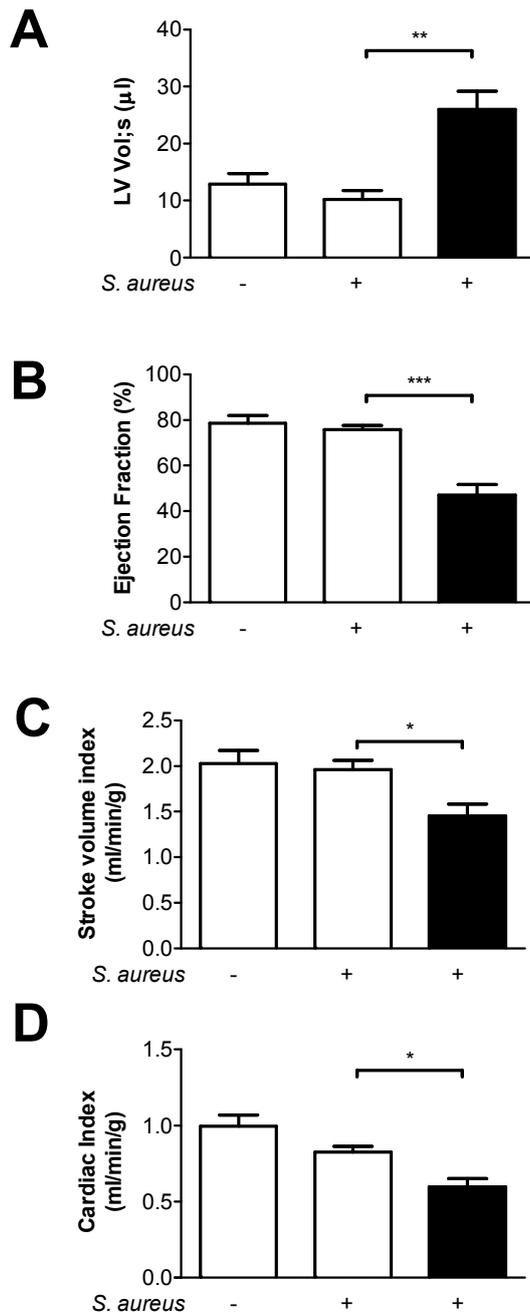
Figure 4.7-4. Impaired left ventricular function in hypoxic mice 12 hours after subcutaneous *S. aureus* injection.

Echocardiography was performed by Dr Abdul Hameed on anaesthetised mice 12 hours after infection with SH1000. Data from non-injected normoxic mice are shown for comparison. (A) Left ventricular end-systolic volumes calculated from left ventricular internal diameter. (B) Ejection fraction calculated from the measurements of left ventricular volume at end-systole and end-diastole. (C) Stroke volume index calculated as the change in left ventricular volume between systole and diastole and corrected for mouse body weight. (D) Cardiac index. Cardiac output was calculated as the product of stroke volume and heart rate then corrected for size by dividing by the body weight of each animal. Data are mean and SEM of n=4. * $p < 0.05$, ** $p < 0.01$, *** $p < 0.001$ by ANOVA.

4.8 No significant increases in oxidative stress or plasma nitric oxide levels in infected hypoxic animals.

Nitric oxide has been implicated as a cause of both hypotension and cardiac dysfunction in the context of sepsis (Boyle *et al.*, 2000; Flierl *et al.*, 2008). Nitric oxide in plasma samples were kindly analysed by Dr Andrew Cowburn, University of Cambridge. No significant differences were found between infected hypoxic animals and normoxic animals (Figure 4.8-1).

Hypoxia paradoxically leads to increased levels of oxidative stress, potentially contributing to cardiac dysfunction (Fink, 2002; Flierl *et al.*, 2008). Malondialdehyde (MDA), a marker of lipid peroxidation, was measured in plasma but there were no differences between levels in normoxic infected and hypoxic infected mice (Figure 4.8-1). Grouped analysis using 2-way ANOVA revealed higher levels of MDA in hypoxia versus normoxia.
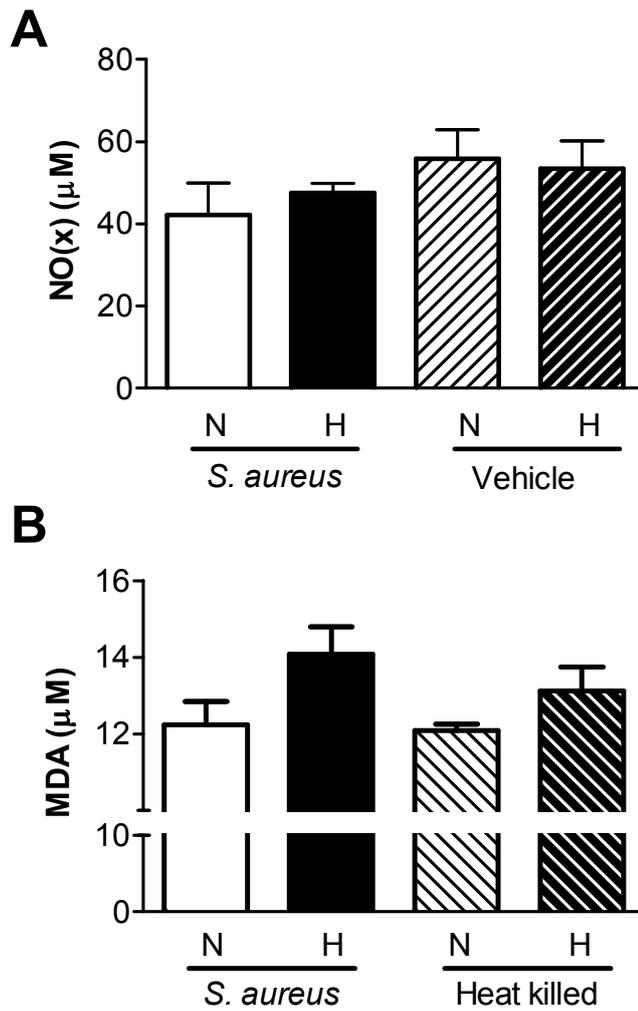
Figure 4.8-1. No significant differences in nitric oxide levels or oxidative stress in hypoxic infected animals.

(A) Plasma was harvested from mice injected with *S. aureus* or PBS (vehicle) and maintained in normoxia or hypoxia (10% O_2) for 6 hours. Nitric oxide (NO_X) analysis was performed by Dr Andrew Cowburn. Data are mean +/- SEM, minimum n = 3. (B) Mice were infected with live or heat killed *S. aureus* and plasma harvested after 12 hours in normoxia or hypoxia. Malondialdehyde levels were measured using the OxiSelect[TM] TBARS assay kit (Cell Biolabs Inc., San Diego). Data are mean +/- SEM, n = 4.

4.9 Myeloid-specific deletion of *Hif1a* or *Hif2a* protects infected animals from hypoxia-induced hypothermia and sickness behaviour.

In order to assess whether host innate immune responses played an important role in the development of sickness behaviour and hypothermia, myeloid-specific knockout mice were challenged with subcutaneous *S. aureus* and exposed to normoxia or hypoxia for 12 hours. Deletion of either *Hif1a* (see Figure 4.9-1) or *Hif2a* (see Figure 4.9-2) in myeloid cells significantly protected mice from the adverse effects of infection in hypoxia. No significant differences were observed in skin bacterial count at 12 hours despite deficiency of HIF-1α or HIF-2α (see Figure 4.9-3).
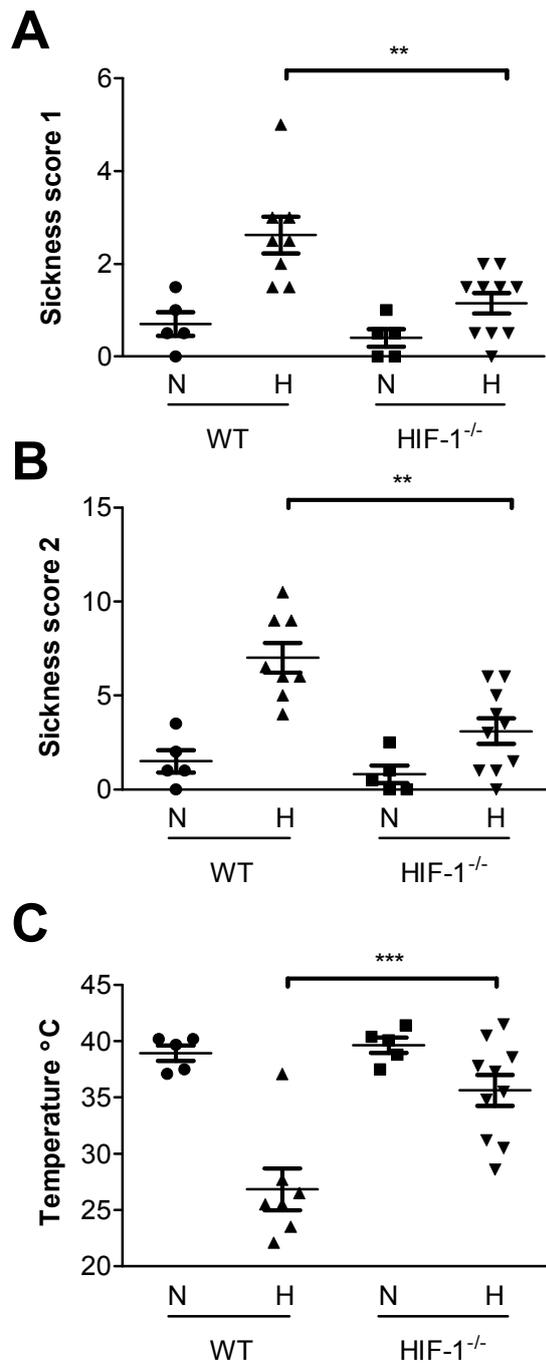
Figure 4.9-1. Myeloid-specific deletion of *Hif1a* protects infected hypoxic mice from the phenotype of hypothermia and sickness behaviour.

Wild-type C57BL/6 and *Hif1a^flox/flox*;LysMCre^+/- mice were assessed 12 hours following subcutaneous injection of SH1000. (A & B) Sickness scores and (C) rectal temperature were recorded. Data are mean and SEM of a minimum n=5. * $p<0.05$, ** $p<0.01$, *** $p<0.001$ analysed by 2-way ANOVA.
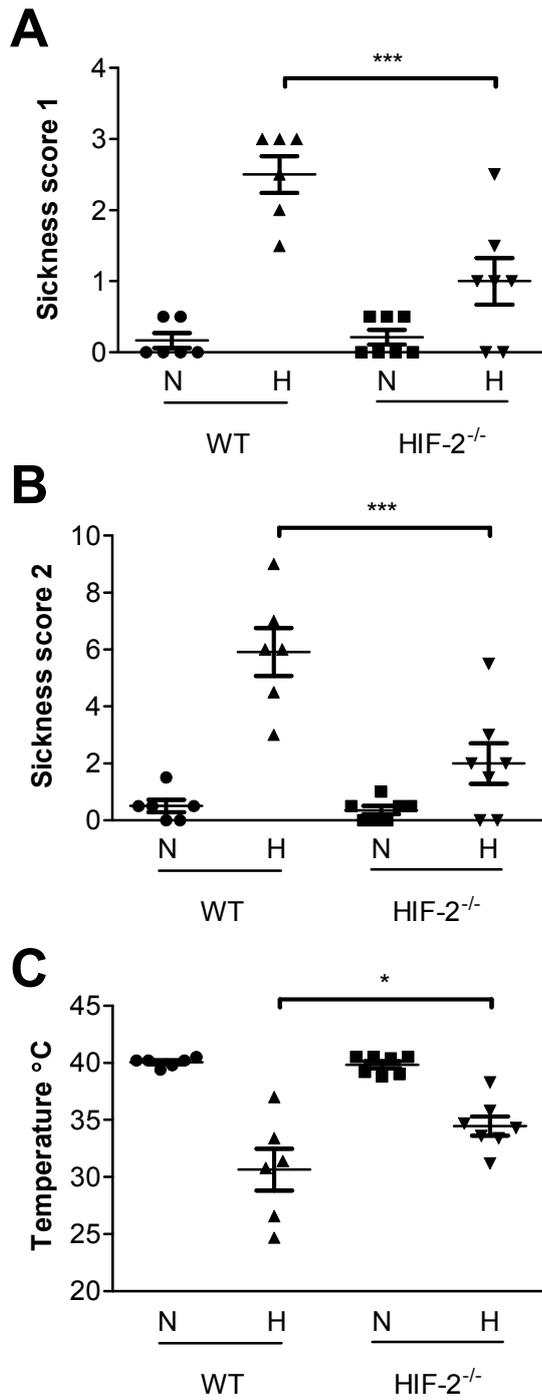
Figure 4.9-2. Myeloid-specific deletion of *Hif2a* provides protection against hypothermia and sickness behaviour in infected hypoxic mice.

Wild-type *Hif2a^{flox/flox};LysMCre^{-/-}* and *Hif2a^{flox/flox};LysMCre^{+/-}* mice were assessed 12 hours following subcutaneous injection of SH1000. (A & B) Sickness scores and (C) rectal temperature were recorded. Data are mean and SEM of a minimum n=6. * $p<0.05$, *** $p<0.001$ analysed by 2-way ANOVA.

A

B
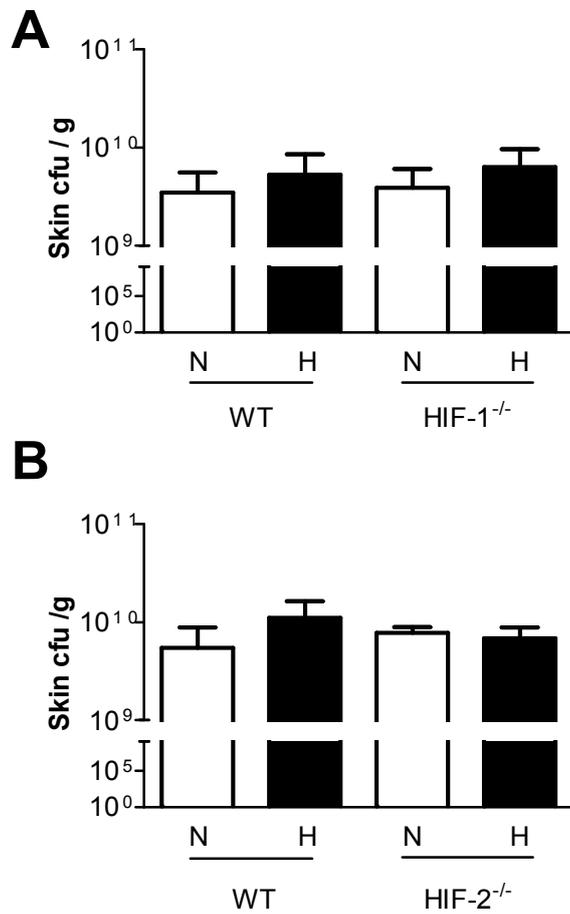
Figure 4.9-3. No significant differences in skin bacterial burden of HIF-deficient animals 12 hours following subcutaneous injection of SH1000.

Skin of infected animals was biopsied after 12 hours in normoxia or hypoxia. (A) Bacterial colony forming units per gram of skin in wild-type C57BL/6 and *Hif1a^flox/flox^;LysMCre^+/-^* mice. (B) Skin bacterial counts in wild type *Hif2a^flox/flox^;LysMCre^-/-^* and *Hif2a^flox/flox^;LysMCre^+/-^* mice. Data are mean and SEM of a minimum n=5 analysed by 2-way ANOVA.

4.10 Discussion

Hypoxia frequently complicates bacterial infection at a tissue or systemic level. Oxygen sensors, particularly HIF-1α, are essential for a normal innate immune response to infection (Cramer *et al.*, 2003) yet studies have also shown compromised host defence in hypoxic conditions (Belda *et al.*, 2005; McGovern *et al.*, 2011). I investigated the effects of an ambient reduction in oxygen tension on the host response to a local *S. aureus* infection. Surprisingly, I found that hypoxia modified a low dose subcutaneous *S. aureus* challenge from a minor to severe insult, with severe hypothermia, sickness behaviour, hypotension and impaired cardiac function occurring within 12 hours of injection in hypoxic mice. The mechanism behind this phenotype remains unknown but I show that it is independent of acute lung injury, bacteraemia or a typical cytokine response to sepsis. Interestingly, deficiency of either HIF-1α or HIF-2α in myeloid cells protected mice from the effects of the challenge strongly implicating the host innate immune response in the pathogenesis of the phenotype. These findings imply that subcutaneous bacterial infection may cause severe systemic effects in hypoxic patients and that in such a setting modulation of the HIF pathway may be a possible therapeutic option.

Subcutaneous injection of *S. aureus* produced a cutaneous lesion in wild-type mice maintained in room air for 7 days. No adverse systemic effects, with the exception of transient weight loss, were observed. This model is a good correlate of the commonest manifestations of *S. aureus* in humans, namely soft tissue and skin infections (Lowy, 1998). Similar models using gram-positive group A *Streptococcus* and a different strain of *S. aureus* (ATCC 33591) have been used to demonstrate the dependence of the innate immune response on HIF-1α (Peyssonnaux *et al.*, 2005; Zinkernagel *et al.*, 2008). Given the data showing impaired immune responses in hypoxic wounds and the possibility that *S. aureus* may infect patients with alveolar hypoxia in the setting of lung disease and critical care, I investigated the combined challenge of *S. aureus* and alveolar hypoxia.

When mice were infected with *S. aureus* and placed in a hypoxic chamber with 10% ambient oxygen they developed a profound phenotype of sickness behaviour and hypothermia. Previous reports suggesting impaired *in vitro* (McGovern *et al.*, 2011) and *in vivo* (Jonsson *et al.*, 1988) immune responses to *S. aureus* in hypoxia implicated reduced host defence as the likely mechanism behind the phenotype. Indeed, antibody-mediated depletion of myeloid cells has previously been shown to lead to bacteraemia, increased skin lesion size and increased weight loss in an intradermal *S. aureus* model (Molne *et al.*, 2000). Surprisingly, however, I was unable to detect evidence of *S. aureus* bacteraemia from cultures of blood or homogenates of tissues which would be seeded by circulating *S. aureus* (Jonsson *et al.*, 2004). Furthermore, despite reduced levels of the chemoattractant cytokines, KC and MCP-1 at 3 hours post-injection of *S.* aureus in hypoxic mice, at 12 hours post-injection there were no differences in numbers of recruited myeloid cells to the site of infection. There was also no increase in bacterial burden, suggesting that host responses to infection were preserved.

Whilst there was no evidence of bacteraemia or of differences in the local response to infection, the systemic effects may have been mediated by circulating factors released by the host or pathogen during infection. Implicating the bacteria in the pathogenesis was the finding that live *S. aureus* were required to produce the hypoxic phenotype. The strain of *S. aureus* used in these experiments was a derivative of the 8325-4 strain, which descends from a clinical isolate (Novick, 1967). SH1000 corrects a mutation in the *rsbU* gene of the parent strain (Horsburgh *et al.*, 2002). Restoration of *rsbU* function normalized expression of the sigma B accessory factor (σ^B), a regulator of virulence-associated loci such as *agr* (accessory gene regulator) and *sarA* (staphylococcal accessory regulator)(Giachino *et al.*, 2001; Horsburgh *et al.*, 2002). Phenotypically, SH1000 mirrors clinical strains such as UAMS-1 and UAMS-601 because it produces lower amounts of proteases than the 8325-4 strain and has lower expression of the α-haemolysin exotoxin (Blevins *et al.*, 2002; Horsburgh *et al.*, 2002). Nonetheless, SH1000 produces a variety of virulence factors in addition to α-haemolysin,

including the other pore-forming toxins, β- and γ-haemolysin; enzymes such as catalase, lipase, staphylokinase and serine proteases; and the pigment staphyloxanthine (Horsburgh *et al.*, 2002; Ziebandt *et al.*, 2004). The surface proteins, protein A and fibronectin binding proteins, FnBPA and FnBPB are also expressed, but notably the parent strain 8325-4 does not produce enterotoxins or toxic shock syndrome toxin-1 (Nilsson *et al.*, 1999; Shinji *et al.*, 2011; Tamber *et al.*, 2010). However, it is possible that hypoxia altered the virulence profile of SH1000. In order to adapt to its surroundings, *S. aureus* is capable of sensing changes in nutrient availability, including the capacity to respond to changes in oxygen tension (Fuchs *et al.*, 2007; Novick, 1967). Importantly *S. aureus* possesses the metabolic machinery to respire both aerobically and anaerobically although it predominantly uses glycolysis to metabolise carbohydrates (Somerville and Proctor, 2009). Several two-component oxygen-sensing systems have been described which subsequently regulate virulence factor expression (Schlag *et al.*, 2008; Somerville and Proctor, 2009; Sun *et al.*, 2012; Worlitzsch *et al.*, 2002). For example, AirS is a sensor kinase containing a 2Fe-2S cluster that is sensitive to oxidation and reduction. In aerobic conditions, AirS has an oxidised $[2Fe-2S]^{2+}$ cluster, the kinase is active and phosphorylates AirR while in anaerobic conditions the $[2Fe-2S]^{+}$ form is inactive. The consequences of reduced AirR activity in anaerobic conditions were examined using a strain with a mutation of the a*irR* gene. These studies revealed that AirR regulates expression of numerous virulence factors and surface proteins (Sun *et al.*, 2012).

Given the phenotype of hypotension and sickness behaviour, secreted mediators from *S. aureus* might be involved in the pathogenesis and pyrogenic-toxin superantigens are plausible candidates. Toxic shock syndrome toxin-1 (TSST-1) typically causes fever, hypotension and multiple organ failure in humans, usually in the absence of bacteraemia (Lin and Peterson, 2010). In a rabbit model of toxic shock syndrome, subcutaneous infusion of TSST-1 produced a transient fever, sickness behaviour and hypothermia preceding death (Parsonnet *et al.*, 1987). However, mice are resistant to the effects of gram-positive exotoxins unless sensitised with,

for example, endotoxin (Lavoie *et al.*, 1999; Miethke *et al.*, 1992). Furthermore, studies have suggested that TSST-1 production is downregulated in hypoxia (Pragman *et al.*, 2004; Wong and Bergdoll, 1990).

Although it is possible that bacterial virulence may have been altered in hypoxia, using mice deficient in HIF-1α and HIF-2α I was able to demonstrate that the host immune response is critical to the development of the sickness phenotype. With selective deficiency of HIF-1α or HIF-2α in myeloid cells, mice were protected from the adverse effects of the subcutaneous bacterial challenge in hypoxia. Whilst surprising that deficiency of either HIF-α subunit protected the mice, this finding is consistent with the protection conferred by HIF deficiency in response to lethal doses of LPS or gram-positive stimuli (Imtiyaz *et al.*, 2010; Mahabeleshwar *et al.*, 2012; Peyssonnaux *et al.*, 2007). The putative mechanism proposed in those studies was a dampening of the exaggerated inflammatory response and shock that occurs in severe sepsis. Mediators produced by myeloid cells may therefore be important in the infected hypoxic phenotype.

Numerous studies have demonstrated the importance of cytokines on outcome in models of sepsis (Leon, 2002). For example, 6 hours following caecal ligation and puncture plasma levels of IL-6 over 3000 pg/ml were associated with higher mortality (Stearns-Kurosawa *et al.*, 2011). Although IL-6 was significantly elevated at 6 hours following *S. aureus* injection, I found no significant difference between infected normoxic and hypoxic mice. Studies have implicated TNF-α in the pathology of severe sepsis, particularly with reference to the hypothermic response of mice, with injection of TNF-α exacerbating hypothermia and antagonism using soluble TNF receptor attenuating hypothermia (Kozak *et al.*, 1995). Furthermore, mice lacking TNF receptors had a blunted hypothermic response in a caecal ligation and puncture sepsis model (Leon *et al.*, 1998). Interestingly, the male TNF receptor knockout mice had improved survival compared to wild-type controls. However, consistent with the lack of evidence of

circulating bacteraemia, I observed no detectable TNF-α in plasma in either normoxia or hypoxia. Indeed, the lower levels of IL-6 and complete lack of detectable IL-1β, TNF-α and IL-10 distinguish the cytokine profile in this model from that of a typical sepsis response (Cohen, 2002; Dinarello, 1997).

Nitric oxide (NO) is a potent bactericidal agent produced by macrophages and necessary for normal immune responses in mice (Wei *et al.*, 1995). NO has been implicated in local vasodilatory responses to intradermal LPS and is released from macrophages in response to gram positive stimuli (Cunha *et al.*, 1993; Pons *et al.*, 1993). Peripheral vasodilation is an important regulator of heat loss and NO is a key regulator of vessel tone in this setting (Bertuglia and Giusti, 2005; Kottke *et al.*, 1948; Simmons *et al.*, 2011; Taylor and Bishop, 1993). Thus increases in NO production due to the combination of hypoxia and *S. aureus* infection could exacerbate heat loss through the skin, leading to the observed hypothermic phenotype. However, whilst alveolar hypoxia is a global stimulus resulting in systemic alterations in vessel tone, the local injection of *S. aureus* may not have provoked a body-wide alteration in the peripheral vascular tone. Indeed plasma levels of NO were not different between infected and non-infected hypoxic animals. Furthermore, the fact that HIF-1α and HIF-2α differentially regulate macrophage NO production in response to LPS would argue against it being the mediator of the hypoxic phenotype (Takeda *et al.*, 2010).

In the setting of severe sepsis or lethal endotoxaemia, acute lung injury may occur (Reutershan and Ley, 2004). Given the combined stimulus of alveolar hypoxia, the consequences of such injury would be exacerbated, plausibly causing sickness behaviour and eventual death. However, I did not observe any evidence of respiratory distress, lung oedema or inflammatory cell infiltration in the lungs of hypoxic animals. Despite evidence of systemic hypotension, organ function was also remarkably preserved, with only a slight increase in creatinine differentiating renal, liver and pancreatic plasma markers between hypoxic and normoxic

mice. Severe sepsis or endotoxaemia tend to lead to more profound organ damage and are assumed to be the cause of death in those conditions (Cohen, 2002). Therefore, the mechanism behind sickness behaviour in hypoxic infected animals appears to be distinct from that of sepsis.

A further potential cause of sickness behaviour that I examined was that of cerebral oedema. As discussed in Chapter 1, alveolar hypoxia can lead to life-threatening pathology in previously healthy humans at high altitude through cerebral oedema (Hackett and Roach, 2001). Interestingly, previous studies have suggested that hypoxia may induce vascular permeability and lead to a degree of oedema in the brain and other organs (Eltzschig *et al.*, 2005; Schoch *et al.*, 2002). However, I observed no evidence of vascular leak in the brains of infected mice as assessed by extravasation of Evan's blue dye and no evidence of brain oedema as assessed by wet/dry weight ratio.

Notably, in the absence of other major organ dysfunction, I found evidence of significantly impaired cardiac function. Cardiac dysfunction is an important feature of sepsis (Parker *et al.*, 1984). The haemodynamic changes observed in the hypoxic infected mice mirror the sepsis phenotype prior to volume resuscitation with reduced ejection fraction and increased left-ventricular end-systolic volume (Buys *et al.*, 2009; Jianhui *et al.*, 2010). Both gram negative (LPS) and gram positive (lipoteichoic acid) stimuli may induce cardiac suppression, mediated at least in part by cytokines and NO (Kumar *et al.*, 1996; Natanson *et al.*, 1989; Ullrich *et al.*, 2000). The lack of plasma cytokines or elevation in plasma NO levels in hypoxic animals count against these factors as the mechanism. Importantly, I observed no infiltration of inflammatory cells in the myocardium, but it would be interesting to assess local expression of cytokines and NO within the heart to exclude autocrine and paracrine-mediated effects. Other potential mechanisms of cardiac dysfunction require consideration. First, coronary vasoconstriction has been observed in isolated perfused rat heats in response to purified

staphylococcal α-haemolysin (Sibelius *et al.*, 2000). Whether this occurs in the hypoxic infected mice requires further examination. Secondly, myocardial metabolism may also be impaired. In sepsis, glucose and fatty acid uptake may be reduced, plasma lactate rises and abnormalities in myocardial oxygen extraction have also been described (Dhainaut *et al.*, 1987; Herbertson *et al.*, 1995). I found no reduction in plasma bicarbonate levels making a significant lactic acidosis unlikely but have not examined myocardial oxygen or glucose uptake. Finally, related to impaired metabolism, mitochondrial dysfunction in human skeletal muscle is associated with mortality and severity of sepsis (Brealey *et al.*, 2002). The putative mediators of mitochondrial dysfunction in this context are nitric oxide and reactive oxygen species (Brealey *et al.*, 2002; Flierl *et al.*, 2008). Indeed, anti-oxidants targeted to the mitochondria alleviate cardiac dysfunction in a rat endotoxin model (Supinski *et al.*, 2009). Hypoxia could exacerbate mitochondrial dysfunction as it is known to provoke oxidative stress at cellular and systemic levels (Baillie *et al.*, 2007; Guzy and Schumacker, 2006). However, I found no evidence of increased oxidative stress in hypoxic infected animals compared to hypoxic vehicle controls.

A further factor which may have contributed to impaired cardiac function is hypothermia. Hypothermia was profound in hypoxic infected mice and is known to induce bradycardia and hypotension (Goodyer, 1965; Prec *et al.*, 1949). The mechanisms behind temperature regulation in mammals are complex and changes in body temperature are highly dependent on the stimulus and ambient temperature. Below the thermoneutral ambient temperature (31°C for C57BL/6 mice, (Rudaya *et al.*, 2005)), animals employ thermogenic mechanisms to maintain body temperature (T_b). Involuntary or autonomic mechanisms include piloerection and peripheral vasoconstriction to minimise heat loss and an increase in metabolic rate and shivering to generate heat (IUPS, 1987; Landsberg *et al.*, 1984). In hypoxia, experimental evidence suggests that these mechanisms are blunted (Kottke *et al.*, 1948; Mortola *et al.*, 1999; Rohlicek *et al.*, 1998). Indeed, consistent with published studies conducted on mice and other mammals, there was a slight but significant reduction in T_b in non-infected mice placed

in hypoxia after 6 hours (Bhatia *et al.*, 1969; Gellhorn and Janus, 1936; Gordon and Fogelson, 1991; Wood and Stabenau, 1998). This phenomenon, known as anapyrexia, is a regulated reduction in T_b and has been proposed to be an adaptive response reducing the oxygen requirements of tissues sensitive to hypoxia and facilitating oxygen uptake in the lungs by shifting the oxyhaemoglobin dissociation curve leftwards (Buchan and Pulsinelli, 1990; Busto *et al.*, 1987; Wood, 1991). Animals also display behavioural temperature regulation, moving to warmer or cooler thermal ambience, wetting body surfaces and huddling (IUPS, 1987). Consistent with the hypoxic reduction in T_b being adaptive is the observation that hypoxic animals permitted to regulate temperature through behaviour surprisingly seek lower ambient temperatures to facilitate the reduction in body temperature (Gordon and Fogelson, 1991). In more extreme hypoxia (2-5%), data from rodents showed that a reduction in T_b is associated with longer survival (Artru and Michenfelder, 1981; Minard and Grant, 1982; Wood and Stabenau, 1998).

Outwith the context of hypoxia, there is debate as to whether hypothermia in severe sepsis may also constitute a protective host response. Lui et al. found that rats challenged with either a sub-lethal dose of LPS or *E. coli,* had higher survival rates in cool environments (with a hypothermic response) compared to those in a warm environment that responded with fever (Liu *et al.*, 2012). Nonetheless, other studies have shown that reductions in T_b, in sepsis and lethal endotoxaemia are highly predictive of poor outcome (Leon *et al.*, 1998; Vlach *et al.*, 2000). Furthermore, hypothermia (<36°C) in humans admitted to critical care with sepsis is associated with higher risk of mortality (Brun-Buisson *et al.*, 1995; Peres Bota *et al.*, 2004). The development of hypothermia described here occurred in response to a low dose of subcutaneous *S.* aureus that did not induce any temperature change in normoxic animals. Furthermore the hypoxic infected animals displayed sickness behaviour with lack of interest in their surroundings, hunched postures, reduced and uncoordinated movements and often

exudative accumulation around the eyes, strongly suggesting that the response observed in infected hypoxic mice is dysregulated and pathological.

By 12 hours T_b in control, PBS-injected mice was not significantly lower in hypoxia than normoxia but profound differences were detected between infected groups. These data contrast with those of Kozak et al. who found that 12% hypoxia led to persistent hypothermia in mice without any additional stimuli (Kozak *et al.*, 1995). In that particular model, hypoxia was induced aggressively by reducing the ambient oxygen tension to 11% in 15 minutes and the nadir in T_b was reached at 4 hours. Although T_b then increased and diurnal variation was restored the mice remained mildly hypothermic, with body temperatures around 2°C lower than normoxic mice, for the duration of the 7 day hypoxic exposure. A notable difference between the experimental findings was the elevation in IL-6 detected in plasma which contrasts with my finding of undetectable levels in non-infected hypoxic mice (Kozak *et al.*, 1995). Surprisingly, given data showing the direct relationship between ambient temperature and the reduction in body temperature in hypoxic rats (Bhatia *et al.*, 1969), the ambient temperature was higher (28°C) in Kozak et al's model compared to 21°C in my experiments. However, the temperature within the hypoxic chamber was not reported (Kozak *et al.*, 1995). Interestingly, intraperitoneal injection of low dose LPS (80 µg/kg) led to a fever in normoxic mice but exacerbated the hypoxia-induced hypothermia whereas I observed no pyrexia in infected mice maintained in normoxia compared to control mice, but profound hypothermia was induced in the infected hypoxic mice. These data suggest that either the difference in ambient temperature between the two protocols may have influenced the thermoregulatory response or the mechanisms of temperature regulation involved in the response to LPS are distinct from those in subcutaneous *S. aureus* infection.

Several other potential mechanisms for the phenotype observed in hypoxia deserve mention. Spontaneous activity can contribute to thermogenesis in mice (Humphries and Careau, 2011;

Mount and Willmott, 1967). Diurnal variations in temperature correlate with fluctuations in activity (Mount and Willmott, 1967; Nautiyal *et al.*, 2009). However, following either injection of inflammatory stimuli or a reduction in ambient oxygen tension, activity is depressed (Kozak *et al.*, 1995; Nautiyal *et al.*, 2009). However, studies have demonstrated dissociation between temperature responses and activity, with reduced activity evident despite normalization of body temperature and in the presence of fever (Kozak *et al.*, 1995; Nautiyal *et al.*, 2009). Therefore, although I have not yet formally monitored activity counts, I believe that the hypothermia observed in hypoxia is not simply due to reduced activity.

Finally, alveolar hypoxia results in a reduction in oxygen consumption in small mammals and this has been linked to hypoxic inhibition of thermogenic responses (Gautier, 1996). This is not thought to be solely due to a reduction in oxygen availability because oxygen consumption in hypoxic conditions can be increased in response to cold stress or pharmacologically (Mortola *et al.*, 1999; Rohlicek *et al.*, 1998). However, it is possible that the added stimulus of bacterial infection reduced the potential to increase oxygen consumption leading to a further impairment of thermogenesis in infected mice. Indeed in the setting of sepsis, as discussed above, utilisation of oxygen is compromised due to impaired mitochondrial respiration (Brealey *et al.*, 2002; Singer *et al.*, 2004). Therefore, measurements of oxygen consumption or other markers of global metabolism may provide insight into the mechanism behind the phenotype of hypothermia and sickness behaviour.

In conclusion, hypoxic mice infected with *S. aureus* develop a phenotype of sickness behaviour, hypothermia and cardiac dysfunction. The data suggest that even localised *S. aureus* infection could have multiple and profound adverse systemic effects in hypoxaemic patients. Indeed, in the setting of invasive *S. aureus* infection in humans, underlying lung disease increased the relative risk of infection by nearly 4 times and patients with a respiratory focus were over 3

times more likely to die (Laupland *et al.*, 2003). These data suggest that this murine model is relevant in human disease and could provide insight into why hypoxia may potentiate the virulence of *S. aureus* infection.

The cause of the hypoxic phenotype is not yet known but I have shown that it is not due to excessive cytokine production, impaired local immune responses, or early multi-organ failure. Although bacterial viability is required for the development of hypothermia and sickness behaviour, I also showed that the host myeloid cell response is critical to this mechanism. Animals with myeloid-cell deficiency of either HIF-1α or HIF-2α were protected from the adverse consequences of bacterial infection in hypoxia and therefore these transcription factors may represent future therapeutic targets. Interestingly, given that myeloid cell HIF-1α deficiency has been shown to impair immune responses and bacterial killing (Cramer *et al.*, 2003; Peyssonnaux *et al.*, 2005), I observed no increase in local bacterial burden. However, this assessment was made at an early time point, before the development of a visible skin lesion. Crucially, consistent with my data from Chapter 3 suggesting that HIF-2α deficient neutrophils have preserved bactericidal activity, there was also no increase in skin bacterial counts in the HIF-2α deficient animals. Therefore, to avoid potential compromise of host defences, HIF-2α may be the preferred target for potential therapeutic intervention in this model.

S. aureus is a common pathogen leading to diverse and life-threatening illnesses. Understanding the interaction between pathogen and host is vital to develop new treatments. This model reveals a novel role for hypoxia in promoting virulence of *S. aureus* infection in a manner dependent upon the host response. While further work is needed to explore whether the phenotype observed is precipitated by other pathogens, I identify host myeloid-cell oxygen sensing pathways as key mediators of the adverse response to subcutaneous infection in hypoxia.

5 Discussion

Responses to injury and infection necessitate highly regulated and co-ordinated machinery to limit damage, resolve inflammation and repair tissue. The host immune system, microenvironment and pathogens all influence such responses. I have shown that HIF-2α plays a key role in neutrophils as they respond to infection or to inflammatory stimuli and that hypoxia may profoundly alter the host response to a minor subcutaneous bacterial challenge.

5.1 Summary of key findings

Neutrophils are vital effector cells, critical for defence against bacterial and fungal infections, but their antimicrobial arsenal is capable of damaging healthy tissue. Neutrophil-mediated damage is implicated in both acute and chronic inflammatory settings, with inhibition of neutrophil apoptosis contributing to pathology by preventing timely resolution of the inflammatory response. Neutrophil survival at sites of inflammation is promoted not only by inflammatory stimuli but also by hypoxia, a feature of inflamed tissue. Hypoxic survival of neutrophils is dependent upon HIF-1α which has emerged as a master regulator of innate immune cell function. Myeloid cells lacking HIF-1α have impaired function probably due to the important role HIF-1α plays in regulating glycolytic enzymes, utilised in neutrophils as the predominant pathway for energy production. Thus the finding that HIF-2α plays a role in neutrophil persistence at sites of inflammation is important for future development of therapeutic anti-inflammatory strategies. Importantly, I have shown that HIF-2α is expressed in neutrophils in the setting of human chronic inflammatory diseases and is upregulated in a murine model of acute lung injury. Overexpression of HIF-2α was associated with reduced rates of constitutive apoptosis in human neutrophils and delayed resolution of inflammation in a zebrafish tail injury model. On the other hand myeloid-cell deficiency of HIF-2α enhanced

resolution of inflammation and reduced tissue injury in a neutrophil-mediated model of acute lung injury without any evidence of host defences being compromised.

Whilst targeting HIF-2α may be a possibility for treating inflammatory diseases, work demonstrating that local HIF-α stabilisation improved anti-bacterial defences raised the question of what effect systemic hypoxia would have on host-pathogen interactions. My work begins to dissect this by using a murine model of subcutaneous *S. aureus* infection in the setting of ambient hypoxia. Surprisingly hypoxia transformed this local bacterial challenge into a phenotype of sickness behaviour and hypothermia. The mechanism responsible for this phenotype remains unknown but I found no evidence of bacteraemia, excessive cytokine production or lung injury in the hypoxic infected mice. However, there was significant circulatory dysfunction, with hypotension, bradycardia and impaired left ventricular function. These findings imply that in a hypoxic host, minor bacterial challenges may result in systemic pathology.

5.2   Limitations

Although I have demonstrated a role for HIF-2α in neutrophils that is conserved across three species, a number of limitations require discussion. First, the purity of peripheral blood murine neutrophils used for *in vitro* experiments was not 100 %. Contaminating mononuclear cells are known to influence human neutrophil responses to lipopolysaccharide (Sabroe *et al.*, 2002). However, I did not attempt to quantify the cytokine production of these cells and purity was sufficiently high to accept protein and RNA expression data. The influence of contaminating cells was less important in assessing *in vitro* apoptosis as I was primarily interested in whether known survival signals remained intact in HIF-2α deficient neutrophils. Secondly, the lysozyme M-driven Cre recombinase results in deletion of *Hif2a* in all myeloid cells. Therefore it could be argued that the *in vivo* responses observed in HIF-2α deficient mice

were at least in part mediated by monocytes and macrophages. To minimize this potential issue, I chose models that depended principally on neutrophil function. For example, the LPS-induced acute lung injury is characterized by an intense neutrophil infiltration, often with neutrophils constituting 90% of cells in BAL 24 hours following LPS administration. Similarly, the model of pneumococcal infection was one in which the initial macrophage containment of infection has been overwhelmed and recruited neutrophils are required to prevent excessive mortality (Dockrell *et al.*, 2003). Thirdly, recapitulation of the human gain-of-function *HIF2A* mutations was possible in the zebrafish but was achieved through injection of mutant constructs at the one cell stage. Therefore, *epas1a* was overexpressed in all cells in the fish and therefore it may have been overexpression of the gene in other cells that contributed to delayed resolution of inflammation and reduced neutrophil apoptosis. This issue can be addressed by generating a zebrafish line with neutrophil-specific upregulation of *epas1a*. Furthermore, I cannot exclude that the effects on neutrophil constitutive apoptosis were not due to the expression of the protein during granulopoesis. The data from immature bone marrow neutrophils suggests that expression during the early stages of maturation would be abnormal. However, in the patients with gain-of-function mutations in the *HIF2A* gene I observed the same phenotype of reduced apoptosis. In these neutrophils, upregulation of HIF-2α expression reflects impaired post-translational degradation; mRNA expression should not have been altered during cell development. Finally, the data showing impaired resolution of inflammation in the zebrafish with *epas1a* overexpression would be strengthened if there was evidence that patients with gain-of-function mutations in the *HIF2A* gene were more prone to developing chronic inflammatory conditions. Unfortunately such evidence does not exist because of the extreme rarity of the mutation and the fact that patients may die prematurely from other complications of their polycythaemia.

The limitations of the work using *S. aureus* relate mainly to how widely applicable the findings are. This is a murine model and the phenotype may not translate into human disease. For

example, the experiments were performed outside the thermoneutral zone for C57BL/6 mice and impairment of thermogenesis by the combined stimuli of hypoxia and bacteria may be the primary mediator of the phenotype. Given species differences in temperature control, this phenomenon may not occur in humans. However, the cardiac dysfunction observed may be independent of body temperature and is not only a common finding in humans in the context of sepsis but could also be exacerbated by hypoxia. Nonetheless, even in the mouse it remains to be shown that this phenotype would be recapitulated in other settings, for example with different bacteria or with systemic hypoxaemia due to underlying lung disease rather than normobaric hypoxia.

5.3 Future work

Multiple avenues of future work can be pursued in light of the findings described in this thesis. Regarding the role of HIF-2α in neutrophils further work is needed on how HIF-2α regulates neutrophil apoptosis at sites of inflammation. As HIF-2α deficient neutrophils showed no loss of enhanced survival in response to LPS, impaired responses to other mediators of neutrophil survival (e.g. GM-CSF) or enhanced pro-apoptotic (e.g. TNF-α) signalling compared to wild type cells must have contributed to the enhanced resolution of inflammation in the mouse acute lung injury model. Future work could examine the effects of modulators of apoptosis on HIF-2α deficient neutrophils. For example, the survival pathways that may operate in response to stimuli present in the inflammatory microenvironment, such as damage associated molecular patterns (DAMPS), could be explored by microarray analysis of key apoptotic pathway components in wild type and HIF-2α deficient neutrophils.

The mechanism by which HIF-2α is upregulated also deserves further investigation. I have shown upregulation of *Hif2a* mRNA in neutrophils as they transmigrate into the lungs from the circulation in mice, but I also found upregulation of HIF-2α expression in circulating neutrophils

of patients with inflammatory arthritis. These data suggest that upregulation could occur in response to either a circulating mediator or a signal during the process of endothelial transmigration. Identifying such factors may provide potential targets for preventing inappropriate upregulation of HIF-2α expression. These questions may be answered by investigating the regulation of HIF-2α expression in COPD patients from whom it would be possible to obtain neutrophils from the circulation, bronchoalveolar lavage and sputum. It would be of great interest to discover whether HIF-2α expression correlates with disease severity and whether alterations in expression occur during infective exacerbations.

The work in this thesis would be strengthened by investigating the role of HIF-2α in other models of neutrophil-mediated inflammatory disease. For example, whether the enhanced resolution of inflammation seen in the models of acute lung injury in HIF-2α deficient mice was evident in models of chronic inflammation could be investigated. Chronic models in which neutrophil apoptosis has been implicated include bleomycin induced lung inflammation and passively induced arthritis (Jonsson *et al.*, 2005; Rossi *et al.*, 2006).

Further work is also required to elucidate the mechanism behind the phenotype of hypothermia and sickness behaviour in the *S. aureus* infected hypoxic mice. Both host and pathogen have been implicated in the phenotype and both require further investigation. Host factors to explore include other circulating mediators and the neuroendocrine response to inflammation. Several circulating factors implicated in sepsis have not been measured. One example is macrophage inhibitory factor (MIF), a pro-inflammatory cytokine implicated in cardiac dysfunction and mortality in sepsis models (Calandra *et al.*, 2000; Chagnon *et al.*, 2005). Interestingly, inhibition of MIF in TNF-α knockout mice improved survival in a model of lethal peritonitis suggesting that it may play a role in pathogenic host responses independently of TNF-α (Calandra *et al.*, 2000), which I did not detect in plasma.

The neuroendocrine system not only encompasses autonomic control of temperature, heart, vasculature and inflammation, but includes hormonal modulators of stress responses (Tracey, 2002). In response to stress or inflammatory stimuli, catecholamines and glucocorticoids are released and these regulate vessel tone as well as inflammatory cell production of cytokines (Rittirsch *et al.*, 2008). Autonomic responses are also vital in the context of sepsis with vagal tone contributing to the control cytokine production and disease severity (Borovikova *et al.*, 2000; Huston *et al.*, 2007). Hypoxia also impacts upon autonomic tone, with many of the cardiovascular responses to acute and chronic hypoxia mediated through sympathetic activation (Morrison, 2001). However, dampening of responses to catecholamines in hypoxia has also been demonstrated in the context of thermogenesis and cardiac rate control (Bicego *et al.*, 2007; Richalet *et al.*, 1988). Therefore, dysregulation of neuroendocrine responses to the inflammatory stimulus in hypoxia could provoke systemic consequences contributing to the phenotype of sickness behaviour, cardiac dysfunction and hypothermia. Indeed, loss of sympathetic tone leading to reduced thermogenesis in brown adipose tissue and skeletal muscle, inappropriate cutaneous vasodilation and reduced heart rate and contractility would be in keeping with the observed phenotypic changes in hypoxic infected animals. Thus, it would be interesting to assess autonomic tone and adrenal hormone levels. Furthermore as phagocytes are known to produce catecholamines (Flierl *et al.*, 2007), if it could be demonstrated that myeloid cell production of catecholamines was regulated by HIF, impaired production would constitute a potential mechanism by which deficiency of HIF-1α or HIF-2α conferred protection in the model. Counting against this hypothesis is the evidence that stimuli known to induce macrophage secretion of catecholamines and upregulate thermogenesis would differentially activate HIF-2α (Nguyen *et al.*, 2011). However, one could argue that in view of their distinct roles, it remains possible that different mechanisms are responsible for protection observed with deficiency of either HIF-1α or HIF-2α subunits in the model of *S. aureus* infection.

Given that live bacteria were required to invoke the hypoxic phenotype, it is possible that bacterial virulence was altered in the hypoxic conditions. However, it may be that the effect was mediated by the host response to a critical threshold of bacterial burden and that the dose of injected heat-killed bacteria was not a sufficient stimulus. Further studies could therefore involve different doses of bacteria and the use of different *S. aureus* strains to establish which virulence factors are involved in mediating the phenotype. As mentioned above, use of alternative bacterial species would also be interesting to determine the wider applicability of this phenotype. Equally, performing this infection when animals are hypoxaemic due to a lung injury will be important to more closely recapitulate a situation that may occur in human patients.

Monitoring of activity and temperature using telemetry would potentially provide useful and more detailed information regarding the time course of the sickness phenotype. Additionally, extending the protocol to document mortality and confirm the level of protection conferred by myeloid-specific deficiency of HIF-1α and HIF-2α will be important.

5.4 Therapeutic targeting of the HIF pathway

To date, the majority of work to modify HIF pathways therapeutically has focussed on enhancing HIF signalling. Clinical trials using hydroxylase inhibitors are already underway for the treatment of anaemia in renal patients (Semenza, 2009). Upregulation of HIF-2α in this context will not only promote EPO production but increase iron absorption through its actions on DMT1 (Gruber *et al.*, 2007; Mastrogiannaki *et al.*, 2009). Activation of the HIF pathway may also benefit inflammatory bowel disease, where HIF-1α is involved in protecting the barrier function of the gut epithelium (Cummins *et al.*, 2008). Furthermore, the study by Zinkernagel *et al.* provided evidence that HIF stabilisation could reduce tissue damage caused by bacterial infection (Zinkernagel *et al.*, 2008).

However, studies on patients with Chuvash polycythaemia, who have systemic HIF activation, revealed potentially detrimental effects on cardiopulmonary physiology and metabolism during exercise (Formenti *et al.*, 2010; Smith *et al.*, 2008). Furthermore given the evidence, presented here and elsewhere, that targeting HIF-2α in myeloid cells may be of benefit in the context of chronic inflammation and maladaptive host responses such as those observed in the models of hypoxic *S. aureus* infection or high-dose endotoxaemia (Imtiyaz *et al.*, 2010), the potential adverse consequences of activating HIF signalling need to be considered. Indeed the model of infected hypoxic mice may be a useful platform on which to test the effects of both activators and inhibitors of HIF signalling on host responses to infection.

A number of challenges exist with regard to the development of HIF-2α inhibitors. Currently available HIF pathway inhibitors lack target specificity (Kung *et al.*, 2004). With the potential for disruption of HIF-1α signalling to compromise myeloid cell function it will be important to identify more selective HIF-2α inhibitors. As HIF-1α and HIF-2α are structurally and biologically similar, understanding the mechanisms by which they can differentially regulate target genes will be important in the process of identifying potential candidate molecules for indirect therapeutic manipulation. Given the widespread expression of HIF-2α and its important function in non-myeloid cell types, targeting such inhibition to neutrophils is also challenging. However, it may be feasible to develop drugs that could be applied locally, for example to lungs or skin, to minimise the potential for systemic side-effects.

5.5 Conclusions

The balance of maintaining host defence while suppressing inappropriate persistent inflammation presents a therapeutic conundrum. Therefore understanding of the pathways involved in controlling inflammation and infection has obvious potential benefits for patients. Oxygen sensing pathways have now been heavily implicated in the control of the innate immune system but work is needed to dissect out specific roles for the key members of these pathways. This work provides evidence of a role for HIF-2α in persistent neutrophilic inflammation and of an adverse host response to bacterial infection in hypoxia, which may also be ameliorated by targeting HIF-2α. Further investigation of this transcription factor may lead to the identification of therapeutic targets that may regulate host responses in inflammatory sites and in the context of systemic hypoxaemia.

6 Bibliography

Acker, T., Fandrey, J., and Acker, H. (2006). The good, the bad and the ugly in oxygen-sensing: ROS, cytochromes and prolyl-hydroxylases. Cardiovasc Res *71*, 195-207.

Agusti, A.G., Noguera, A., Sauleda, J., Sala, E., Pons, J., and Busquets, X. (2003). Systemic effects of chronic obstructive pulmonary disease. Eur Respir J *21*, 347-360.

Ahmad, A., Ahmad, S., Glover, L., Miller, S.M., Shannon, J.M., Guo, X., Franklin, W.A., Bridges, J.P., Schaack, J.B., Colgan, S.P.*, et al.* (2009). Adenosine A2A receptor is a unique angiogenic target of HIF-2alpha in pulmonary endothelial cells. Proc Natl Acad Sci U S A *106*, 10684-10689.

Alberti, C., Brun-Buisson, C., Burchardi, H., Martin, C., Goodman, S., Artigas, A., Sicignano, A., Palazzo, M., Moreno, R., Boulme, R.*, et al.* (2002). Epidemiology of sepsis and infection in ICU patients from an international multicentre cohort study. Intensive Care Med *28*, 108-121.

Alberti, C., Brun-Buisson, C., Goodman, S.V., Guidici, D., Granton, J., Moreno, R., Smithies, M., Thomas, O., Artigas, A., and Le Gall, J.R. (2003). Influence of systemic inflammatory response syndrome and sepsis on outcome of critically ill infected patients. Am J Respir Crit Care Med *168*, 77-84.

Andina, N., Conus, S., Schneider, E.M., Fey, M.F., and Simon, H.U. (2009). Induction of Bim limits cytokine-mediated prolonged survival of neutrophils. Cell Death Differ *16*, 1248-1255.

Ang, S.O., Chen, H., Hirota, K., Gordeuk, V.R., Jelinek, J., Guan, Y., Liu, E., Sergueeva, A.I., Miasnikova, G.Y., Mole, D.*, et al.* (2002). Disruption of oxygen homeostasis underlies congenital Chuvash polycythemia. Nat Genet *32*, 614-621.

Anning, P.B., Sair, M., Winlove, C.P., and Evans, T.W. (1999). Abnormal tissue oxygenation and cardiovascular changes in endotoxemia. Am J Respir Crit Care Med *159*, 1710-1715.

Aoki, T., Sumii, T., Mori, T., Wang, X., and Lo, E.H. (2002). Blood-brain barrier disruption and matrix metalloproteinase-9 expression during reperfusion injury: mechanical versus embolic focal ischemia in spontaneously hypertensive rats. Stroke *33*, 2711-2717.

Appelhoff, R.J., Tian, Y.M., Raval, R.R., Turley, H., Harris, A.L., Pugh, C.W., Ratcliffe, P.J., and Gleadle, J.M. (2004). Differential function of the prolyl hydroxylases PHD1, PHD2, and PHD3 in the regulation of hypoxia-inducible factor. J Biol Chem *279*, 38458-38465.

Aprelikova, O., Wood, M., Tackett, S., Chandramouli, G.V., and Barrett, J.C. (2006). Role of ETS transcription factors in the hypoxia-inducible factor-2 target gene selection. Cancer Res *66*, 5641-5647.

ARDSN (2000). Ventilation with lower tidal volumes as compared with traditional tidal volumes for acute lung injury and the acute respiratory distress syndrome. The Acute Respiratory Distress Syndrome Network. N Engl J Med *342*, 1301-1308.

Arruda, M.A., Barcellos-de-Souza, P., Sampaio, A.L., Rossi, A.G., Graca-Souza, A.V., and Barja-Fidalgo, C. (2006). NADPH oxidase-derived ROS: key modulators of heme-induced mitochondrial stability in human neutrophils. Exp Cell Res *312*, 3939-3948.

Arteel, G.E., Thurman, R.G., Yates, J.M., and Raleigh, J.A. (1995). Evidence that hypoxia markers detect oxygen gradients in liver: pimonidazole and retrograde perfusion of rat liver. Br J Cancer *72*, 889-895.

Artru, A.A., and Michenfelder, J.D. (1981). Influence of hypothermia or hyperthermia alone or in combination with pentobarbital or phenytoin on survival time in hypoxic mice. Anesth Analg *60*, 867-870.

Bae, S.H., Jeong, J.W., Park, J.A., Kim, S.H., Bae, M.K., Choi, S.J., and Kim, K.W. (2004). Sumoylation increases HIF-1alpha stability and its transcriptional activity. Biochem Biophys Res Commun *324*, 394-400.

Baillie, J.K., Bates, M.G., Thompson, A.A., Waring, W.S., Partridge, R.W., Schnopp, M.F., Simpson, A., Gulliver-Sloan, F., Maxwell, S.R., and Webb, D.J. (2007). Endogenous urate production augments plasma antioxidant capacity in healthy lowland subjects exposed to high altitude. Chest *131*, 1473-1478.

Ban, K., Ikeda, U., Takahashi, M., Kanbe, T., Kasahara, T., and Shimada, K. (1994). Expression of intercellular adhesion molecule-1 on rat cardiac myocytes by monocyte chemoattractant protein-1. Cardiovasc Res *28*, 1258-1262.

Barnes, P.J. (2007). New molecular targets for the treatment of neutrophilic diseases. J Allergy Clin Immunol *119*, 1055-1062; quiz 1063-1054.

Bartsch, P. (1999). High altitude pulmonary edema. Med Sci Sports Exerc *31*, S23-27.

Basnyat, B., and Murdoch, D.R. (2003). High-altitude illness. Lancet *361*, 1967-1974.

Belaaouaj, A., McCarthy, R., Baumann, M., Gao, Z., Ley, T.J., Abraham, S.N., and Shapiro, S.D. (1998). Mice lacking neutrophil elastase reveal impaired host defense against gram negative bacterial sepsis. Nat Med *4*, 615-618.

Belaiba, R.S., Bonello, S., Zahringer, C., Schmidt, S., Hess, J., Kietzmann, T., and Gorlach, A. (2007). Hypoxia up-regulates hypoxia-inducible factor-1alpha transcription by involving phosphatidylinositol 3-kinase and nuclear factor kappaB in pulmonary artery smooth muscle cells. Mol Biol Cell *18*, 4691-4697.

Belda, F.J., Aguilera, L., Garcia de la Asuncion, J., Alberti, J., Vicente, R., Ferrandiz, L., Rodriguez, R., Company, R., Sessler, D.I., Aguilar, G.*, et al.* (2005). Supplemental perioperative oxygen and the risk of surgical wound infection: a randomized controlled trial. JAMA *294*, 2035-2042.

Bell, E.L., Klimova, T.A., Eisenbart, J., Moraes, C.T., Murphy, M.P., Budinger, G.R., and Chandel, N.S. (2007). The Qo site of the mitochondrial complex III is required for the transduction of hypoxic signaling via reactive oxygen species production. J Cell Biol *177*, 1029-1036.

Berchner-Pfannschmidt, U., Tug, S., Kirsch, M., and Fandrey, J. (2010). Oxygen-sensing under the influence of nitric oxide. Cell Signal *22*, 349-356.

Berra, E., Benizri, E., Ginouves, A., Volmat, V., Roux, D., and Pouyssegur, J. (2003). HIF prolyl-hydroxylase 2 is the key oxygen sensor setting low steady-state levels of HIF-1alpha in normoxia. EMBO J *22*, 4082-4090.

Bertout, J.A., Patel, S.A., and Simon, M.C. (2008). The impact of O2 availability on human cancer. Nat Rev Cancer *8*, 967-975.

Bertuglia, S., and Giusti, A. (2005). Role of nitric oxide in capillary perfusion and oxygen delivery regulation during systemic hypoxia. Am J Physiol Heart Circ Physiol *288*, H525-531.

Bhatia, B., George, S., and Rao, T.L. (1969). Hypoxic poikilothermia in rats. J Appl Physiol *27*, 583-586.

Bianchi, S.M., Dockrell, D.H., Renshaw, S.A., Sabroe, I., and Whyte, M.K. (2006). Granulocyte apoptosis in the pathogenesis and resolution of lung disease. ClinSci(Lond) *110*, 293-304.

Bicego, K.C., Barros, R.C., and Branco, L.G. (2007). Physiology of temperature regulation: comparative aspects. Comp Biochem Physiol A Mol Integr Physiol *147*, 616-639.

Biswas, B., Adhya, S., Washart, P., Paul, B., Trostel, A.N., Powell, B., Carlton, R., and Merril, C.R. (2002). Bacteriophage therapy rescues mice bacteremic from a clinical isolate of vancomycin-resistant Enterococcus faecium. Infect Immun *70*, 204-210.

Bjerregaard, M.D., Jurlander, J., Klausen, P., Borregaard, N., and Cowland, J.B. (2003). The in vivo profile of transcription factors during neutrophil differentiation in human bone marrow. Blood *101*, 4322-4332.

Blevins, J.S., Beenken, K.E., Elasri, M.O., Hurlburt, B.K., and Smeltzer, M.S. (2002). Strain-dependent differences in the regulatory roles of sarA and agr in Staphylococcus aureus. Infect Immun *70*, 470-480.

Bone, R.C., Balk, R.A., Cerra, F.B., Dellinger, R.P., Fein, A.M., Knaus, W.A., Schein, R.M., and Sibbald, W.J. (1992). Definitions for sepsis and organ failure and guidelines for the use of innovative therapies in sepsis. The ACCP/SCCM Consensus Conference Committee. American College of Chest Physicians/Society of Critical Care Medicine. Chest *101*, 1644-1655.

Borovikova, L.V., Ivanova, S., Zhang, M., Yang, H., Botchkina, G.I., Watkins, L.R., Wang, H., Abumrad, N., Eaton, J.W., and Tracey, K.J. (2000). Vagus nerve stimulation attenuates the systemic inflammatory response to endotoxin. Nature *405*, 458-462.

Borregaard, N., Sorensen, O.E., and Theilgaard-Monch, K. (2007). Neutrophil granules: a library of innate immunity proteins. Trends Immunol *28*, 340-345.

Boucher, H.W., and Corey, G.R. (2008). Epidemiology of methicillin-resistant Staphylococcus aureus. Clin Infect Dis *46 Suppl 5*, S344-349.

Boyle, W.A., 3rd, Parvathaneni, L.S., Bourlier, V., Sauter, C., Laubach, V.E., and Cobb, J.P. (2000). iNOS gene expression modulates microvascular responsiveness in endotoxin-challenged mice. Circ Res *87*, E18-24.

Bracken, C.P., Fedele, A.O., Linke, S., Balrak, W., Lisy, K., Whitelaw, M.L., and Peet, D.J. (2006). Cell-specific regulation of hypoxia-inducible factor (HIF)-1alpha and HIF-2alpha stabilization and transactivation in a graded oxygen environment. J Biol Chem *281*, 22575-22585.

Bracken, C.P., Whitelaw, M.L., and Peet, D.J. (2005). Activity of hypoxia-inducible factor 2alpha is regulated by association with the NF-kappaB essential modulator. J Biol Chem *280*, 14240-14251.

Bradley, P.P., Priebat, D.A., Christensen, R.D., and Rothstein, G. (1982). Measurement of cutaneous inflammation: estimation of neutrophil content with an enzyme marker. J Invest Dermatol *78*, 206-209.

Brahimi-Horn, M.C., Chiche, J., and Pouyssegur, J. (2007). Hypoxia and cancer. J Mol Med *85*, 1301-1307.

Brealey, D., Brand, M., Hargreaves, I., Heales, S., Land, J., Smolenski, R., Davies, N.A., Cooper, C.E., and Singer, M. (2002). Association between mitochondrial dysfunction and severity and outcome of septic shock. The Lancet *360*, 219-223.

Bruick, R.K., and McKnight, S.L. (2001). A conserved family of prolyl-4-hydroxylases that modify HIF. Science *294*, 1337-1340.

Brun-Buisson, C., Doyon, F., Carlet, J., Dellamonica, P., Gouin, F., Lepoutre, A., Mercier, J.C., Offenstadt, G., and Regnier, B. (1995). Incidence, risk factors, and outcome of severe sepsis and septic shock in adults. A multicenter prospective study in intensive care units. French ICU Group for Severe Sepsis. JAMA *274*, 968-974.

British Thoracic Society (2006). The burden of lung disease: a statistical report from the British Thoracic Society 2nd edition (London).

Buchan, A., and Pulsinelli, W.A. (1990). Hypothermia but not the N-methyl-D-aspartate antagonist, MK-801, attenuates neuronal damage in gerbils subjected to transient global ischemia. J Neurosci *10*, 311-316.

Busto, R., Dietrich, W.D., Globus, M.Y., Valdes, I., Scheinberg, P., and Ginsberg, M.D. (1987). Small differences in intraischemic brain temperature critically determine the extent of ischemic neuronal injury. J Cereb Blood Flow Metab *7*, 729-738.

Buys, E.S., Cauwels, A., Raher, M.J., Passeri, J.J., Hobai, I., Cawley, S.M., Rauwerdink, K.M., Thibault, H., Sips, P.Y., Thoonen, R.*, et al.* (2009). sGC(alpha)1(beta)1 attenuates cardiac dysfunction and mortality in murine inflammatory shock models. Am J Physiol Heart Circ Physiol *297*, H654-663.

Calandra, T., Echtenacher, B., Roy, D.L., Pugin, J., Metz, C.N., Hultner, L., Heumann, D., Mannel, D., Bucala, R., and Glauser, M.P. (2000). Protection from septic shock by neutralization of macrophage migration inhibitory factor. Nat Med *6*, 164-170.

Carrero, P., Okamoto, K., Coumailleau, P., O'Brien, S., Tanaka, H., and Poellinger, L. (2000). Redox-regulated recruitment of the transcriptional coactivators CREB-binding protein and SRC-1 to hypoxia-inducible factor 1alpha. Mol Cell Biol *20*, 402-415.

Cassin, S., Dawes, G.S., Mott, J.C., Ross, B.B., and Strang, L.B. (1964). THE VASCULAR RESISTANCE OF THE FOETAL AND NEWLY VENTILATED LUNG OF THE LAMB. J Physiol *171*, 61-79.

Chagnon, F., Metz, C.N., Bucala, R., and Lesur, O. (2005). Endotoxin-induced myocardial dysfunction: effects of macrophage migration inhibitory factor neutralization. Circ Res *96*, 1095-1102.

Chen, H., Yoshioka, H., Kim, G.S., Jung, J.E., Okami, N., Sakata, H., Maier, C.M., Narasimhan, P., Goeders, C.E., and Chan, P.H. (2011). Oxidative stress in ischemic brain damage: mechanisms of cell death and potential molecular targets for neuroprotection. Antioxid Redox Signal *14*, 1505-1517.

Chen, L., Uchida, K., Endler, A., and Shibasaki, F. (2007). Mammalian tumor suppressor Int6 specifically targets hypoxia inducible factor 2 alpha for degradation by hypoxia- and pVHL-independent regulation. J Biol Chem *282*, 12707-12716.

Cheng, J., Kang, X., Zhang, S., and Yeh, E.T. (2007). SUMO-specific protease 1 is essential for stabilization of HIF1alpha during hypoxia. Cell *131*, 584-595.

Cockman, M.E., Webb, J.D., and Ratcliffe, P.J. (2009). FIH-dependent asparaginyl hydroxylation of ankyrin repeat domain-containing proteins. Ann N Y Acad Sci *1177*, 9-18.

Cohen, J. (2002). The immunopathogenesis of sepsis. Nature *420*, 885-891.

Colgan, S.P., Dzus, A.L., and Parkos, C.A. (1996). Epithelial exposure to hypoxia modulates neutrophil transepithelial migration. J ExpMed *184*, 1003-1015.

Colotta, F., Re, F., Polentarutti, N., Sozzani, S., and Mantovani, A. (1992). Modulation of granulocyte survival and programmed cell death by cytokines and bacterial products. Blood *80*, 2012-2020.

Compernolle, V., Brusselmans, K., Acker, T., Hoet, P., Tjwa, M., Beck, H., Plaisance, S., Dor, Y., Keshet, E., Lupu, F.*, et al.* (2002). Loss of HIF-2alpha and inhibition of VEGF impair fetal lung maturation, whereas treatment with VEGF prevents fatal respiratory distress in premature mice. Nat Med *8*, 702-710.

Covello, K.L., Kehler, J., Yu, H., Gordan, J.D., Arsham, A.M., Hu, C.J., Labosky, P.A., Simon, M.C., and Keith, B. (2006). HIF-2alpha regulates Oct-4: effects of hypoxia on stem cell function, embryonic development, and tumor growth. Genes Dev *20*, 557-570.

Cramer, T., Yamanishi, Y., Clausen, B.E., Forster, I., Pawlinski, R., Mackman, N., Haase, V.H., Jaenisch, R., Corr, M., Nizet, V.*, et al.* (2003). HIF-1alpha is essential for myeloid cell-mediated inflammation. Cell *112*, 645-657.

Cross, A., Barnes, T., Bucknall, R.C., Edwards, S.W., and Moots, R.J. (2006). Neutrophil apoptosis in rheumatoid arthritis is regulated by local oxygen tensions within joints. J Leukoc Biol *80*, 521-528.

Cummins, E.P., Seeballuck, F., Keely, S.J., Mangan, N.E., Callanan, J.J., Fallon, P.G., and Taylor, C.T. (2008). The hydroxylase inhibitor dimethyloxalylglycine is protective in a murine model of colitis. Gastroenterology *134*, 156-165.

Cunha, F.Q., Moss, D.W., Leal, L.M., Moncada, S., and Liew, F.Y. (1993). Induction of macrophage parasiticidal activity by Staphylococcus aureus and exotoxins through the nitric oxide synthesis pathway. Immunology *78*, 563-567.

D'Angelo, G., Duplan, E., Boyer, N., Vigne, P., and Frelin, C. (2003). Hypoxia up-regulates prolyl hydroxylase activity: a feedback mechanism that limits HIF-1 responses during reoxygenation. J Biol Chem *278*, 38183-38187.

Dhainaut, J.F., Huyghebaert, M.F., Monsallier, J.F., Lefevre, G., Dall'Ava-Santucci, J., Brunet, F., Villemant, D., Carli, A., and Raichvarg, D. (1987). Coronary hemodynamics and myocardial metabolism of lactate, free fatty acids, glucose, and ketones in patients with septic shock. Circulation *75*, 533-541.

Dinarello, C.A. (1997). Proinflammatory and anti-inflammatory cytokines as mediators in the pathogenesis of septic shock. Chest *112*, 321S-329S.

Dinauer, M.C. (2005). Chronic granulomatous disease and other disorders of phagocyte function. Hematology Am Soc Hematol Educ Program, 89-95.

Dockrell, D.H., Marriott, H.M., Prince, L.R., Ridger, V.C., Ince, P.G., Hellewell, P.G., and Whyte, M.K. (2003). Alveolar macrophage apoptosis contributes to pneumococcal clearance in a resolving model of pulmonary infection. J Immunol *171*, 5380-5388.

Doege, K., Heine, S., Jensen, I., Jelkmann, W., and Metzen, E. (2005). Inhibition of mitochondrial respiration elevates oxygen concentration but leaves regulation of hypoxia-inducible factor (HIF) intact. Blood *106*, 2311-2317.

Dorward, D.A., Thompson, A.A., Baillie, J.K., MacDougall, M., and Hirani, N. (2007). Change in plasma vascular endothelial growth factor during onset and recovery from acute mountain sickness. Respir Med *101*, 587-594.

Dransfield, I., and Rossi, A.G. (2004). Granulocyte apoptosis: who would work with a 'real' inflammatory cell? Biochem Soc Trans *32*, 447-451.

Dryden, M.S. (2010). Complicated skin and soft tissue infection. J Antimicrob Chemother *65 Suppl 3*, iii35-44.

Elizur, A., Cannon, C.L., and Ferkol, T.W. (2008). Airway inflammation in cystic fibrosis. Chest *133*, 489-495.

Elks, P.M., van Eeden, F.J., Dixon, G., Wang, X., Reyes-Aldasoro, C.C., Ingham, P.W., Whyte, M.K., Walmsley, S.R., and Renshaw, S.A. (2011). Activation of hypoxia-inducible factor-1alpha (Hif-1alpha) delays inflammation resolution by reducing neutrophil apoptosis and reverse migration in a zebrafish inflammation model. Blood *118*, 712-722.

Eltzschig, H.K., Abdulla, P., Hoffman, E., Hamilton, K.E., Daniels, D., Schonfeld, C., Loffler, M., Reyes, G., Duszenko, M., Karhausen, J*., et al.* (2005). HIF-1-dependent repression of equilibrative nucleoside transporter (ENT) in hypoxia. J Exp Med *202*, 1493-1505.

Elvidge, G.P., Glenny, L., Appelhoff, R.J., Ratcliffe, P.J., Ragoussis, J., and Gleadle, J.M. (2006). Concordant regulation of gene expression by hypoxia and 2-oxoglutarate-dependent dioxygenase inhibition: the role of HIF-1alpha, HIF-2alpha, and other pathways. J Biol Chem *281*, 15215-15226.

Ema, M., Taya, S., Yokotani, N., Sogawa, K., Matsuda, Y., and Fujii-Kuriyama, Y. (1997). A novel bHLH-PAS factor with close sequence similarity to hypoxia-inducible factor 1alpha regulates the VEGF expression and is potentially involved in lung and vascular development. Proc Natl Acad Sci U S A *94*, 4273-4278.

Engstad, C.S., Gutteberg, T.J., and Osterud, B. (1997). Modulation of blood cell activation by four commonly used anticoagulants. Thromb Haemost *77*, 690-696.

Epstein, A.C., Gleadle, J.M., McNeill, L.A., Hewitson, K.S., O'Rourke, J., Mole, D.R., Mukherji, M., Metzen, E., Wilson, M.I., Dhanda, A*., et al.* (2001). C. elegans EGL-9 and mammalian homologs define a family of dioxygenases that regulate HIF by prolyl hydroxylation. Cell *107*, 43-54.

Erecińska, M., and Silver, I.A. (2001). Tissue oxygen tension and brain sensitivity to hypoxia. Respir Physiol *128*, 263-276.

Eul, B., Rose, F., Krick, S., Savai, R., Goyal, P., Klepetko, W., Grimminger, F., Weissmann, N., Seeger, W., and Hanze, J. (2006). Impact of HIF-1alpha and HIF-2alpha on proliferation and migration of human pulmonary artery fibroblasts in hypoxia. FASEB J *20*, 163-165.

Fahling, M. (2009). Surviving hypoxia by modulation of mRNA translation rate. J Cell Mol Med *13*, 2770-2779.

Fang, H.Y., Hughes, R., Murdoch, C., Coffelt, S.B., Biswas, S.K., Harris, A.L., Johnson, R.S., Imityaz, H.Z., Simon, M.C., Fredlund, E*., et al.* (2009). Hypoxia-inducible factors 1 and 2 are important transcriptional effectors in primary macrophages experiencing hypoxia. Blood *114*, 844-859.

Fink, M.P. (2002). Bench-to-bedside review: Cytopathic hypoxia. Crit Care *6*, 491-499.

Flamme, I., Frohlich, T., von Reutern, M., Kappel, A., Damert, A., and Risau, W. (1997). HRF, a putative basic helix-loop-helix-PAS-domain transcription factor is closely related to hypoxia-inducible factor-1 alpha and developmentally expressed in blood vessels. Mech Dev *63*, 51-60.

Flierl, M.A., Rittirsch, D., Huber-Lang, M.S., Sarma, J.V., and Ward, P.A. (2008). Molecular events in the cardiomyopathy of sepsis. Mol Med *14*, 327-336.

Flierl, M.A., Rittirsch, D., Nadeau, B.A., Chen, A.J., Sarma, J.V., Zetoune, F.S., McGuire, S.R., List, R.P., Day, D.E., Hoesel, L.M*., et al.* (2007). Phagocyte-derived catecholamines enhance acute inflammatory injury. Nature *449*, 721-725.

Flugel, D., Gorlach, A., Michiels, C., and Kietzmann, T. (2007). Glycogen synthase kinase 3 phosphorylates hypoxia-inducible factor 1alpha and mediates its destabilization in a VHL-independent manner. Mol Cell Biol *27*, 3253-3265.

Formenti, F., Constantin-Teodosiu, D., Emmanuel, Y., Cheeseman, J., Dorrington, K.L., Edwards, L.M., Humphreys, S.M., Lappin, T.R., McMullin, M.F., McNamara, C.J.*, et al.* (2010). Regulation of human metabolism by hypoxia-inducible factor. Proc Natl Acad Sci U S A *107*, 12722-12727.

Francois, S., El Benna, J., Dang, P.M., Pedruzzi, E., Gougerot-Pocidalo, M.A., and Elbim, C. (2005). Inhibition of neutrophil apoptosis by TLR agonists in whole blood: involvement of the phosphoinositide 3-kinase/Akt and NF-kappaB signaling pathways, leading to increased levels of Mcl-1, A1, and phosphorylated Bad. J Immunol *174*, 3633-3642.

Freitas, M., Porto, G., Lima, J.L., and Fernandes, E. (2008). Isolation and activation of human neutrophils in vitro. The importance of the anticoagulant used during blood collection. Clin Biochem *41*, 570-575.

Fridkin, S.K., Hageman, J.C., Morrison, M., Sanza, L.T., Como-Sabetti, K., Jernigan, J.A., Harriman, K., Harrison, L.H., Lynfield, R., and Farley, M.M. (2005). Methicillin-resistant Staphylococcus aureus disease in three communities. N Engl J Med *352*, 1436-1444.

Fuchs, S., Pane-Farre, J., Kohler, C., Hecker, M., and Engelmann, S. (2007). Anaerobic gene expression in Staphylococcus aureus. J Bacteriol *189*, 4275-4289.

Galkowska, H., Podbielska, A., Olszewski, W.L., Stelmach, E., Luczak, M., Rosinski, G., and Karnafel, W. (2009). Epidemiology and prevalence of methicillin-resistant Staphylococcus aureus and Staphylococcus epidermidis in patients with diabetic foot ulcers: Focus on the differences between species isolated from individuals with ischemic vs. neuropathic foot ulcers. Diabetes Res Clin Pract *84*, 187-193.

Gautier, H. (1996). Interactions among metabolic rate, hypoxia, and control of breathing. J Appl Physiol *81*, 521-527.

Geering, B., and Simon, H.U. (2011). Peculiarities of cell death mechanisms in neutrophils. Cell Death Differ *18*, 1457-1469.

Gellhorn, E., and Janus, A. (1936). THE INFLUENCE OF PARTIAL PRESSURE OF O2 ON BODY TEMPERATURE. American Journal of Physiology -- Legacy Content *116*, 327-329.

Gharaee-Kermani, M., Gyetko, M.R., Hu, B., and Phan, S.H. (2007). New insights into the pathogenesis and treatment of idiopathic pulmonary fibrosis: a potential role for stem cells in the lung parenchyma and implications for therapy. Pharm Res *24*, 819-841.

Giachino, P., Engelmann, S., and Bischoff, M. (2001). Sigma(B) activity depends on RsbU in Staphylococcus aureus. J Bacteriol *183*, 1843-1852.

Gillet, Y., Issartel, B., Vanhems, P., Fournet, J.C., Lina, G., Bes, M., Vandenesch, F., Piemont, Y., Brousse, N., Floret, D.*, et al.* (2002). Association between Staphylococcus aureus strains carrying gene for Panton-Valentine leukocidin and highly lethal necrotising pneumonia in young immunocompetent patients. Lancet *359*, 753-759.

Goodyer, A.V.N. (1965). Effects of hypothermia and pyrexia on left ventricular function in the intact animal. The American Journal of Cardiology *15*, 206-212.

Gordon, C.J., and Fogelson, L. (1991). Comparative effects of hypoxia on behavioral thermoregulation in rats, hamsters, and mice. Am J Physiol *260*, R120-125.

Gram, H.C. (1884). Über die isolierte Färbung der Schizomyceten in Schnitt- und Trockenpräparaten. Fortschr Med *2*, 185-189.

Green, D.R., and Kroemer, G. (2004). The pathophysiology of mitochondrial cell death. Science *305*, 626-629.

Greif, R., Akca, O., Horn, E.P., Kurz, A., and Sessler, D.I. (2000). Supplemental perioperative oxygen to reduce the incidence of surgical-wound infection. N Engl J Med *342*, 161-167.

Gruber, M., Hu, C.J., Johnson, R.S., Brown, E.J., Keith, B., and Simon, M.C. (2007). Acute postnatal ablation of Hif-2alpha results in anemia. Proc Natl Acad Sci U S A *104*, 2301-2306.

Guidet, B., Aegerter, P., Gauzit, R., Meshaka, P., and Dreyfuss, D. (2005). Incidence and Impact of Organ Dysfunctions Associated With Sepsis*. CHEST Journal *127*, 942-951.

Guzy, R.D., Hoyos, B., Robin, E., Chen, H., Liu, L., Mansfield, K.D., Simon, M.C., Hammerling, U., and Schumacker, P.T. (2005). Mitochondrial complex III is required for hypoxia-induced ROS production and cellular oxygen sensing. Cell Metab *1*, 401-408.

Guzy, R.D., and Schumacker, P.T. (2006). Oxygen sensing by mitochondria at complex III: the paradox of increased reactive oxygen species during hypoxia. Exp Physiol *91*, 807-819.

Hackett, P.H., and Roach, R.C. (2001). High-altitude illness. N Engl J Med *345*, 107-114.

Hafezi-Moghadam, A., Thomas, K.L., and Wagner, D.D. (2007). ApoE deficiency leads to a progressive age-dependent blood-brain barrier leakage. Am J Physiol Cell Physiol *292*, C1256-1262.

Hagen, T., Taylor, C.T., Lam, F., and Moncada, S. (2003). Redistribution of intracellular oxygen in hypoxia by nitric oxide: effect on HIF1alpha. Science *302*, 1975-1978.

Hamedani, H., Kadlecek, S.J., Emami, K., Kuzma, N.N., Xu, Y., Xin, Y., Mongkolwisetwara, P., Rajaei, J., Barulic, A., Wilson Miller, G.*, et al.* (2011). A multislice single breath-hold scheme for imaging alveolar oxygen tension in humans. Magn Reson Med.

Hampton-Smith, R.J., and Peet, D.J. (2009). From polyps to people: a highly familiar response to hypoxia. Ann N Y Acad Sci *1177*, 19-29.

Hams, E., Saunders, S.P., Cummins, E.P., O'Connor, A., Tambuwala, M.T., Gallagher, W.M., Byrne, A., Campos-Torres, A., Moynagh, P.M., Jobin, C.*, et al.* (2011). The hydroxylase inhibitor dimethyloxallyl glycine attenuates endotoxic shock via alternative activation of macrophages and IL-10 production by B1 cells. Shock *36*, 295-302.

Hancher, C.W., and Smith, L.H. (1975). A normobaric hypoxia facility for preparing polycythemic mice for assay of erythropoietin. Lab Anim Sci *25*, 39-44.

Hannah, S., Mecklenburgh, K., Rahman, I., Bellingan, G.J., Greening, A., Haslett, C., and Chilvers, E.R. (1995). Hypoxia prolongs neutrophil survival in vitro. FEBS Lett *372*, 233-237.

Haslett, C. (1999). Granulocyte apoptosis and its role in the resolution and control of lung inflammation. Am J Respir Crit Care Med *160*, S5-11.

Haslett, C., Guthrie, L.A., Kopaniak, M.M., Johnston, R.B., Jr., and Henson, P.M. (1985). Modulation of multiple neutrophil functions by preparative methods or trace concentrations of bacterial lipopolysaccharide. Am J Pathol *119*, 101-110.

Healthcare Commission (2006). Clearing the air: a national study of chronic obstructive pulmonary disease.   Commission for Healthcare Audit and Inspection, (London).

Hempel, S.L., Buettner, G.R., O'Malley, Y.Q., Wessels, D.A., and Flaherty, D.M. (1999). Dihydrofluorescein diacetate is superior for detecting intracellular oxidants: comparison with 2',7'-dichlorodihydrofluorescein diacetate, 5(and 6)-carboxy-2',7'-dichlorodihydrofluorescein diacetate, and dihydrorhodamine 123. Free Radic Biol Med *27*, 146-159.

Herbertson, M.J., Werner, H.A., Russell, J.A., Iversen, K., and Walley, K.R. (1995). Myocardial oxygen extraction ratio is decreased during endotoxemia in pigs. J Appl Physiol *79*, 479-486.

Hiramatsu, K. (2001). Vancomycin-resistant Staphylococcus aureus: a new model of antibiotic resistance. Lancet Infect Dis *1*, 147-155.

Holmquist-Mengelbier, L., Fredlund, E., Lofstedt, T., Noguera, R., Navarro, S., Nilsson, H., Pietras, A., Vallon-Christersson, J., Borg, A., Gradin, K.*, et al.* (2006). Recruitment of HIF-1alpha and HIF-2alpha to common target genes is differentially regulated in neuroblastoma: HIF-2alpha promotes an aggressive phenotype. Cancer Cell *10*, 413-423.

Honig, C.R., and Tenney, S.M. (1957). Determinants of the circulatory response to hypoxia and hypercapnia. Am Heart J *53*, 687-698.

Hopf, H.W., Hunt, T.K., West, J.M., Blomquist, P., Goodson, W.H., 3rd, Jensen, J.A., Jonsson, K., Paty, P.B., Rabkin, J.M., Upton, R.A.*, et al.* (1997). Wound tissue oxygen tension predicts the risk of wound infection in surgical patients. Arch Surg *132*, 997-1004; discussion 1005.

Horsburgh, M.J., Aish, J.L., White, I.J., Shaw, L., Lithgow, J.K., and Foster, S.J. (2002). sigmaB modulates virulence determinant expression and stress resistance: characterization of a functional rsbU strain derived from Staphylococcus aureus 8325-4. J Bacteriol *184*, 5457-5467.

Horsburgh, M.J., Ingham, E., and Foster, S.J. (2001). In Staphylococcus aureus, fur is an interactive regulator with PerR, contributes to virulence, and Is necessary for oxidative stress resistance through positive regulation of catalase and iron homeostasis. J Bacteriol *183*, 468-475.

Houston, C.S., and Dickinson, J. (1975). Cerebral form of high-altitude illness. Lancet *2*, 758-761.

Hsu, L.C., Enzler, T., Seita, J., Timmer, A.M., Lee, C.Y., Lai, T.Y., Yu, G.Y., Lai, L.C., Temkin, V., Sinzig, U.*, et al.* (2011). IL-1beta-driven neutrophilia preserves antibacterial defense in the absence of the kinase IKKbeta. Nat Immunol *12*, 144-150.

Hu, C.J., Iyer, S., Sataur, A., Covello, K.L., Chodosh, L.A., and Simon, M.C. (2006). Differential regulation of the transcriptional activities of hypoxia-inducible factor 1 alpha (HIF-1alpha) and HIF-2alpha in stem cells. Mol Cell Biol *26*, 3514-3526.

Hu, C.J., Sataur, A., Wang, L., Chen, H., and Simon, M.C. (2007). The N-terminal transactivation domain confers target gene specificity of hypoxia-inducible factors HIF-1alpha and HIF-2alpha. Mol Biol Cell *18*, 4528-4542.

Hu, C.J., Wang, L.Y., Chodosh, L.A., Keith, B., and Simon, M.C. (2003). Differential roles of hypoxia-inducible factor 1alpha (HIF-1alpha) and HIF-2alpha in hypoxic gene regulation. Mol Cell Biol *23*, 9361-9374.

Humphries, M.M., and Careau, V. (2011). Heat for nothing or activity for free? Evidence and implications of activity-thermoregulatory heat substitution. Integr Comp Biol *51*, 419-431.

Huston, J.M., Gallowitsch-Puerta, M., Ochani, M., Ochani, K., Yuan, R., Rosas-Ballina, M., Ashok, M., Goldstein, R.S., Chavan, S., Pavlov, V.A.*, et al.* (2007). Transcutaneous vagus nerve stimulation reduces serum high mobility group box 1 levels and improves survival in murine sepsis. Crit Care Med *35*, 2762-2768.

Imamura, T., Kikuchi, H., Herraiz, M.T., Park, D.Y., Mizukami, Y., Mino-Kenduson, M., Lynch, M.P., Rueda, B.R., Benita, Y., Xavier, R.J.*, et al.* (2009). HIF-1alpha and HIF-2alpha have divergent roles in colon cancer. Int J Cancer *124*, 763-771.

Imtiyaz, H.Z., Williams, E.P., Hickey, M.M., Patel, S.A., Durham, A.C., Yuan, L.J., Hammond, R., Gimotty, P.A., Keith, B., and Simon, M.C. (2010). Hypoxia-inducible factor 2alpha regulates macrophage function in mouse models of acute and tumor inflammation. J Clin Invest *120*, 2699-2714.

IUPS (1987). Glossary of terms for thermal physiology. Second edition. Revised by The Commission for Thermal Physiology of the International Union of Physiological Sciences (IUPS Thermal Commission). Pflugers Arch *410*, 567-587.

Ivan, M., Kondo, K., Yang, H., Kim, W., Valiando, J., Ohh, M., Salic, A., Asara, J.M., Lane, W.S., and Kaelin, W.G., Jr. (2001). HIFalpha targeted for VHL-mediated destruction by proline hydroxylation: implications for O2 sensing. Science *292*, 464-468.

Jaakkola, P., Mole, D.R., Tian, Y.M., Wilson, M.I., Gielbert, J., Gaskell, S.J., Kriegsheim, A., Hebestreit, H.F., Mukherji, M., Schofield, C.J.*, et al.* (2001). Targeting of HIF-alpha to the von Hippel-Lindau ubiquitylation complex by O2-regulated prolyl hydroxylation. Science *292*, 468-472.

James, W.R., and Thomas, A.J. (1968). The effect of hypoxia on the heart and pulmonary arterioles of mice. Cardiovasc Res *2*, 278-283.

Jamieson, D., and van den Brenk, H.A. (1965). Electrode size and tissue pO2 measurement in rats exposed to air or high pressure oxygen. J Appl Physiol *20*, 514-518.

Jianhui, L., Rosenblatt-Velin, N., Loukili, N., Pacher, P., Feihl, F., Waeber, B., and Liaudet, L. (2010). Endotoxin impairs cardiac hemodynamics by affecting loading conditions but not by reducing cardiac inotropism. Am J Physiol Heart Circ Physiol *299*, H492-501.

Jonsson, H., Allen, P., and Peng, S.L. (2005). Inflammatory arthritis requires Foxo3a to prevent Fas ligand-induced neutrophil apoptosis. Nat Med *11*, 666-671.

Jonsson, I.M., Arvidson, S., Foster, S., and Tarkowski, A. (2004). Sigma factor B and RsbU are required for virulence in Staphylococcus aureus-induced arthritis and sepsis. Infect Immun *72*, 6106-6111.

Jonsson, K., Hunt, T.K., and Mathes, S.J. (1988). Oxygen as an isolated variable influences resistance to infection. Ann Surg *208*, 783-787.

Kaelin, W.G., Jr., and Ratcliffe, P.J. (2008). Oxygen sensing by metazoans: the central role of the HIF hydroxylase pathway. Mol Cell *30*, 393-402.

Kakinuma, Y., Hama, H., Sugiyama, F., Yagami, K., Goto, K., Murakami, K., and Fukamizu, A. (1998). Impaired blood-brain barrier function in angiotensinogen-deficient mice. Nat Med *4*, 1078-1080.

Karhausen, J., Furuta, G.T., Tomaszewski, J.E., Johnson, R.S., Colgan, S.P., and Haase, V.H. (2004). Epithelial hypoxia-inducible factor-1 is protective in murine experimental colitis. J Clin Invest *114*, 1098-1106.

Kasahara, Y., Iwai, K., Yachie, A., Ohta, K., Konno, A., Seki, H., Miyawaki, T., and Taniguchi, N. (1997). Involvement of reactive oxygen intermediates in spontaneous and CD95 (Fas/APO-1)-mediated apoptosis of neutrophils. Blood *89*, 1748-1753.

Kawakami, Y., Kishi, F., Yamamoto, H., and Miyamoto, K. (1983). Relation of oxygen delivery, mixed venous oxygenation, and pulmonary hemodynamics to prognosis in chronic obstructive pulmonary disease. N Engl J Med *308*, 1045-1049.

Kaynar, A.M., Houghton, A.M., Lum, E.H., Pitt, B.R., and Shapiro, S.D. (2008). Neutrophil elastase is needed for neutrophil emigration into lungs in ventilator-induced lung injury. Am J Respir Cell Mol Biol *39*, 53-60.

Kelly, M., Hwang, J.M., and Kubes, P. (2007). Modulating leukocyte recruitment in inflammation. J Allergy Clin Immunol *120*, 3-10.

Kempf, V.A., Lebiedziejewski, M., Alitalo, K., Walzlein, J.H., Ehehalt, U., Fiebig, J., Huber, S., Schutt, B., Sander, C.A., Muller, S.*, et al.* (2005). Activation of hypoxia-inducible factor-1 in bacillary angiomatosis: evidence for a role of hypoxia-inducible factor-1 in bacterial infections. Circulation *111*, 1054-1062.

Kessler, R., Faller, M., Fourgaut, G., Mennecier, B., and Weitzenblum, E. (1999). Predictive factors of hospitalization for acute exacerbation in a series of 64 patients with chronic obstructive pulmonary disease. Am J Respir Crit Care Med *159*, 158-164.

Keys, A., Stapp, J.P., and Violante, A. (1943). RESPONSES IN SIZE, OUTPUT AND EFFICIENCY OF THE HUMAN HEART TO ACUTE ALTERATION IN THE COMPOSITION OF INSPIRED AIR. American Journal of Physiology -- Legacy Content *138*, 763-771.

Kim, W.Y., Perera, S., Zhou, B., Carretero, J., Yeh, J.J., Heathcote, S.A., Jackson, A.L., Nikolinakos, P., Ospina, B., Naumov, G.*, et al.* (2009). HIF2alpha cooperates with RAS to promote lung tumorigenesis in mice. J Clin Invest *119*, 2160-2170.

Knighton, D., Hunt, T., Scheuenstuhl, H., Halliday, B., Werb, Z., and Banda, M. (1983). Oxygen tension regulates the expression of angiogenesis factor by macrophages. Science *221*, 1283-1285.

Knowles, H.J., Mole, D.R., Ratcliffe, P.J., and Harris, A.L. (2006). Normoxic stabilization of hypoxia-inducible factor-1alpha by modulation of the labile iron pool in differentiating U937 macrophages: effect of natural resistance-associated macrophage protein 1. Cancer Res *66*, 2600-2607.

Knowles, H.J., Raval, R.R., Harris, A.L., and Ratcliffe, P.J. (2003). Effect of ascorbate on the activity of hypoxia-inducible factor in cancer cells. Cancer Res *63*, 1764-1768.

Koivunen, P., Tiainen, P., Hyvarinen, J., Williams, K.E., Sormunen, R., Klaus, S.J., Kivirikko, K.I., and Myllyharju, J. (2007). An endoplasmic reticulum transmembrane prolyl 4-hydroxylase is induced by hypoxia and acts on hypoxia-inducible factor alpha. J Biol Chem *282*, 30544-30552.

Kong, T., Eltzschig, H.K., Karhausen, J., Colgan, S.P., and Shelley, C.S. (2004). Leukocyte adhesion during hypoxia is mediated by HIF-1-dependent induction of beta2 integrin gene expression. Proc Natl Acad Sci U S A *101*, 10440-10445.

Kothakota, S., Azuma, T., Reinhard, C., Klippel, A., Tang, J., Chu, K., McGarry, T.J., Kirschner, M.W., Koths, K., Kwiatkowski, D.J.*, et al.* (1997). Caspase-3-generated fragment of gelsolin: effector of morphological change in apoptosis. Science *278*, 294-298.

Kottke, F.J., Phalen, J.S., and et al. (1948). Effect of hypoxia upon temperature regulation of mice, dogs, and man. Am J Physiol *153*, 10-15.

Kozak, W., Conn, C.A., Klir, J.J., Wong, G.H., and Kluger, M.J. (1995). TNF soluble receptor and antiserum against TNF enhance lipopolysaccharide fever in mice. Am J Physiol *269*, R23-29.

Kullik, I., Giachino, P., and Fuchs, T. (1998). Deletion of the alternative sigma factor sigmaB in Staphylococcus aureus reveals its function as a global regulator of virulence genes. J Bacteriol *180*, 4814-4820.

Kumar, A., Thota, V., Dee, L., Olson, J., Uretz, E., and Parrillo, J.E. (1996). Tumor necrosis factor alpha and interleukin 1beta are responsible for in vitro myocardial cell depression induced by human septic shock serum. J Exp Med *183*, 949-958.

Kung, A.L., Zabludoff, S.D., France, D.S., Freedman, S.J., Tanner, E.A., Vieira, A., Cornell-Kennon, S., Lee, J., Wang, B., Wang, J.*, et al.* (2004). Small molecule blockade of transcriptional coactivation of the hypoxia-inducible factor pathway. Cancer Cell *6*, 33-43.

Lando, D., Peet, D.J., Whelan, D.A., Gorman, J.J., and Whitelaw, M.L. (2002). Asparagine hydroxylation of the HIF transactivation domain a hypoxic switch. Science *295*, 858-861.

Landsberg, L., Saville, M.E., and Young, J.B. (1984). Sympathoadrenal system and regulation of thermogenesis. Am J Physiol *247*, E181-189.

Lang, K.J., Kappel, A., and Goodall, G.J. (2002). Hypoxia-inducible factor-1alpha mRNA contains an internal ribosome entry site that allows efficient translation during normoxia and hypoxia. Mol Biol Cell *13*, 1792-1801.

Lau, K.W., Tian, Y.M., Raval, R.R., Ratcliffe, P.J., and Pugh, C.W. (2007). Target gene selectivity of hypoxia-inducible factor-alpha in renal cancer cells is conveyed by post-DNA-binding mechanisms. Br J Cancer *96*, 1284-1292.

Laughner, E., Taghavi, P., Chiles, K., Mahon, P.C., and Semenza, G.L. (2001). HER2 (neu) signaling increases the rate of hypoxia-inducible factor 1alpha (HIF-1alpha) synthesis: novel mechanism for HIF-1-mediated vascular endothelial growth factor expression. Mol Cell Biol *21*, 3995-4004.

Laupland, K.B., Church, D.L., Mucenski, M., Sutherland, L.R., and Davies, H.D. (2003). Population-based study of the epidemiology of and the risk factors for invasive Staphylococcus aureus infections. J Infect Dis *187*, 1452-1459.

Lavoie, P.M., Thibodeau, J., Erard, F., and Sekaly, R.P. (1999). Understanding the mechanism of action of bacterial superantigens from a decade of research. Immunol Rev *168*, 257-269.

Lee, F.S. (2008). Genetic causes of erythrocytosis and the oxygen-sensing pathway. Blood Rev *22*, 321-332.

Lee, W.L., and Downey, G.P. (2001). Leukocyte elastase: physiological functions and role in acute lung injury. Am J Respir Crit Care Med *164*, 896-904.

Leon, L.R. (2002). Invited review: cytokine regulation of fever: studies using gene knockout mice. J Appl Physiol *92*, 2648-2655.

Leon, L.R., White, A.A., and Kluger, M.J. (1998). Role of IL-6 and TNF in thermoregulation and survival during sepsis in mice. Am J Physiol *275*, R269-277.

Levene, P., and Meyer, G. (1912). The action of leucocytes on glucose. J Biol Chem *11*, 361-370.

Levy, D.E., Brierley, J.B., Silverman, D.G., and Plum, F. (1975). Brief hypoxia-ischemia initially damages cerebral neurons. Arch Neurol *32*, 450-456.

Li, Z., Wang, D., Messing, E.M., and Wu, G. (2005). VHL protein-interacting deubiquitinating enzyme 2 deubiquitinates and stabilizes HIF-1alpha. EMBO Rep *6*, 373-378.

Lieb, M.E., Menzies, K., Moschella, M.C., Ni, R., and Taubman, M.B. (2002). Mammalian EGLN genes have distinct patterns of mRNA expression and regulation. Biochem Cell Biol *80*, 421-426.

Lin, Y.C., and Peterson, M.L. (2010). New insights into the prevention of staphylococcal infections and toxic shock syndrome. Expert Rev Clin Pharmacol *3*, 753-767.

Liu, E., Lewis, K., Al-Saffar, H., Krall, C.M., Singh, A., Kulchitsky, V.A., Corrigan, J.J., Simons, C.T., Petersen, S.R., Musteata, F.M.*, et al.* (2012). Naturally occurring hypothermia is more advantageous than fever in severe forms of lipopolysaccharide- and Escherichia coli-induced systemic inflammation. American Journal of Physiology - Regulatory, Integrative and Comparative Physiology *302*, R1372-R1383.

Liu, Y.V., Baek, J.H., Zhang, H., Diez, R., Cole, R.N., and Semenza, G.L. (2007). RACK1 competes with HSP90 for binding to HIF-1alpha and is required for O(2)-independent and HSP90 inhibitor-induced degradation of HIF-1alpha. Mol Cell *25*, 207-217.

Lloyd, M.H., and Wolfensohn, S.E. (1999). Practical use of distress scoring systems in the application of humane endpoints. In Humane Endpoints in Animal Experiments for Biomedical Research - Proceedings of the International Conference, C.F.M. Hendriksen, and D.B. Morton, eds. (London, The Royal Society of Medicine Press Limited), pp. 48-53.

Lowy, F.D. (1998). Staphylococcus aureus infections. N Engl J Med *339*, 520-532.

Luo, W., Zhong, J., Chang, R., Hu, H., Pandey, A., and Semenza, G.L. (2009). HSP70 and CHIP selectively mediate Ubiquitination and degradation of hypoxia-inducible factor (HIF)-1alpha but not HIF-2alpha. J Biol Chem, [Epub ahead of print].

Mahabeleshwar, G.H., Qureshi, M.A., Takami, Y., Sharma, N., Lingrel, J.B., and Jain, M.K. (2012). A myeloid hypoxia-inducible factor 1alpha-Kruppel-like factor 2 pathway regulates gram-positive endotoxin-mediated sepsis. J Biol Chem *287*, 1448-1457.

Maianski, N.A., Geissler, J., Srinivasula, S.M., Alnemri, E.S., Roos, D., and Kuijpers, T.W. (2004a). Functional characterization of mitochondria in neutrophils: a role restricted to apoptosis. Cell Death Differ *11*, 143-153.

Maianski, N.A., Roos, D., and Kuijpers, T.W. (2004b). Bid truncation, bid/bax targeting to the mitochondria, and caspase activation associated with neutrophil apoptosis are inhibited by granulocyte colony-stimulating factor. J Immunol *172*, 7024-7030.

Manaenko, A., Chen, H., Kammer, J., Zhang, J.H., and Tang, J. (2011). Comparison Evans Blue injection routes: Intravenous versus intraperitoneal, for measurement of blood-brain barrier in a mice hemorrhage model. J Neurosci Methods *195*, 206-210.

Manotham, K., Tanaka, T., Ohse, T., Kojima, I., Miyata, T., Inagi, R., Tanaka, H., Sassa, R., Fujita, T., and Nangaku, M. (2005). A biologic role of HIF-1 in the renal medulla. Kidney Int *67*, 1428-1439.

Mansfield, K.D., Guzy, R.D., Pan, Y., Young, R.M., Cash, T.P., Schumacker, P.T., and Simon, M.C. (2005). Mitochondrial dysfunction resulting from loss of cytochrome c impairs cellular oxygen sensing and hypoxic HIF-alpha activation. Cell Metab *1*, 393-399.

Martin, G.S., Mannino, D.M., Eaton, S., and Moss, M. (2003). The epidemiology of sepsis in the United States from 1979 through 2000. N Engl J Med *348*, 1546-1554.

Martin, S.J., Reutelingsperger, C.P., McGahon, A.J., Rader, J.A., van Schie, R.C., LaFace, D.M., and Green, D.R. (1995). Early redistribution of plasma membrane phosphatidylserine is a general feature of apoptosis regardless of the initiating stimulus: inhibition by overexpression of Bcl-2 and Abl. J Exp Med *182*, 1545-1556.

Masson, N., Willam, C., Maxwell, P.H., Pugh, C.W., and Ratcliffe, P.J. (2001). Independent function of two destruction domains in hypoxia-inducible factor-alpha chains activated by prolyl hydroxylation. EMBO J *20*, 5197-5206.

Mastrogiannaki, M., Matak, P., Keith, B., Simon, M.C., Vaulont, S., and Peyssonnaux, C. (2009). HIF-2alpha, but not HIF-1alpha, promotes iron absorption in mice. J Clin Invest *119*, 1159-1166.

Matthay, M.A., and Zemans, R.L. (2011). The acute respiratory distress syndrome: pathogenesis and treatment. Annu Rev Pathol *6*, 147-163.

Matthay, M.A., Zimmerman, G.A., Esmon, C., Bhattacharya, J., Coller, B., Doerschuk, C.M., Floros, J., Gimbrone, M.A., Jr., Hoffman, E., Hubmayr, R.D.*, et al.* (2003). Future research directions in acute lung injury: summary of a National Heart, Lung, and Blood Institute working group. Am J Respir Crit Care Med *167*, 1027-1035.

Maxwell, A.P., MacManus, M.P., and Gardiner, T.A. (1989). Misonidazole binding in murine liver tissue: a marker for cellular hypoxia in vivo. Gastroenterology *97*, 1300-1303.

Maxwell, P.H. (2005). Hypoxia-inducible factor as a physiological regulator. Exp Physiol *90*, 791-797.

Maxwell, P.H., Wiesener, M.S., Chang, G.W., Clifford, S.C., Vaux, E.C., Cockman, M.E., Wykoff, C.C., Pugh, C.W., Maher, E.R., and Ratcliffe, P.J. (1999). The tumour suppressor protein VHL targets hypoxia-inducible factors for oxygen-dependent proteolysis. Nature *399*, 271-275.

McGovern, N.N., Cowburn, A.S., Porter, L., Walmsley, S.R., Summers, C., Thompson, A.A., Anwar, S., Willcocks, L.C., Whyte, M.K., Condliffe, A.M.*, et al.* (2011). Hypoxia selectively inhibits respiratory burst activity and killing of Staphylococcus aureus in human neutrophils. J Immunol *186*, 453-463.

Metzen, E., Berchner-Pfannschmidt, U., Stengel, P., Marxsen, J.H., Stolze, I., Klinger, M., Huang, W.Q., Wotzlaw, C., Hellwig-Burgel, T., Jelkmann, W.*, et al.* (2003). Intracellular localisation of human HIF-1 alpha hydroxylases: implications for oxygen sensing. J Cell Sci *116*, 1319-1326.

Meyer, S., Z'Graggen, B.R., Blumenthal, S., Borgeat, A., Ganter, M.T., Reyes, L., Booy, C., Neff, T.A., Spahn, D.R., and Beck-Schimmer, B. (2007). Hypoxia attenuates effector-target cell interaction in the airway and pulmonary vascular compartment. ClinExpImmunol *150*, 358-367.

Miethke, T., Wahl, C., Heeg, K., Echtenacher, B., Krammer, P.H., and Wagner, H. (1992). T cell-mediated lethal shock triggered in mice by the superantigen staphylococcal enterotoxin B: critical role of tumor necrosis factor. J Exp Med *175*, 91-98.

Miles, A.A., Misra, S.S., and Irwin, J.O. (1938). The estimation of the bactericidal power of the blood. J Hyg (Lond) *38*, 732-749.

Minard, F.N., and Grant, D.S. (1982). Hypothermia as a mechanism for drug-induced resistance to hypoxia. Biochem Pharmacol *31*, 1197-1203.

Mole, D.R. (2009). Iron Homeostasis and Its Interaction with Prolyl Hydroxylases. Antioxid Redox Signal, [Epub ahead of print].

Mole, D.R., Blancher, C., Copley, R.R., Pollard, P.J., Gleadle, J.M., Ragoussis, J., and Ratcliffe, P.J. (2009). Genome-wide association of hypoxia-inducible factor (HIF)-1alpha and HIF-2alpha DNA binding with expression profiling of hypoxia-inducible transcripts. J Biol Chem *284*, 16767-16775.

Mole, D.R., and Ratcliffe, P.J. (2008). Cellular oxygen sensing in health and disease. Pediatr Nephrol *23*, 681-694.

Molne, L., Verdrengh, M., and Tarkowski, A. (2000). Role of neutrophil leukocytes in cutaneous infection caused by Staphylococcus aureus. Infect Immun *68*, 6162-6167.

Morrison, S.F. (2001). Differential control of sympathetic outflow. Am J Physiol Regul Integr Comp Physiol *281*, R683-698.

Mortola, J.P., Merazzi, D., and Naso, L. (1999). Blood flow to the brown adipose tissue of conscious young rabbits during hypoxia in cold and warm conditions. Pflugers Arch *437*, 255-260.

Mount, L.E., and Willmott, J.V. (1967). The relation between spontaneous activity, metabolic rate and the 24 hour cycle in mice at different environmental temperatures. The Journal of Physiology *190*, 371-380.

MRC (1981). Long term domiciliary oxygen therapy in chronic hypoxic cor pulmonale complicating chronic bronchitis and emphysema. Report of the Medical Research Council Working Party. Lancet *1*, 681-686.

Muller, P.K., Krohn, K., and Muhlradt, P.F. (1989). Effects of pyocyanine, a phenazine dye from Pseudomonas aeruginosa, on oxidative burst and bacterial killing in human neutrophils. Infect Immun *57*, 2591-2596.

Naeye, R.L. (1967). Polycythemia and hypoxia. Individual effects on heart and pulmonary arteries. Am J Pathol *50*, 1027-1033.

Nakayama, K., Frew, I.J., Hagensen, M., Skals, M., Habelhah, H., Bhoumik, A., Kadoya, T., Erdjument-Bromage, H., Tempst, P., Frappell, P.B.*, et al.* (2004). Siah2 regulates stability of prolyl-hydroxylases, controls HIF1alpha abundance, and modulates physiological responses to hypoxia. Cell *117*, 941-952.

Natanson, C., Danner, R.L., Elin, R.J., Hosseini, J.M., Peart, K.W., Banks, S.M., MacVittie, T.J., Walker, R.I., and Parrillo, J.E. (1989). Role of endotoxemia in cardiovascular dysfunction and mortality. Escherichia coli and Staphylococcus aureus challenges in a canine model of human septic shock. J Clin Invest *83*, 243-251.

Nautiyal, K.M., McKellar, H., Silverman, A.J., and Silver, R. (2009). Mast cells are necessary for the hypothermic response to LPS-induced sepsis. Am J Physiol Regul Integr Comp Physiol *296*, R595-602.

Ng, C.T., Biniecka, M., Kennedy, A., McCormick, J., Fitzgerald, O., Bresnihan, B., Buggy, D., Taylor, C.T., O'Sullivan, J., Fearon, U.*, et al.* (2010). Synovial tissue hypoxia and inflammation in vivo. Ann Rheum Dis *69*, 1389-1395.

Nguyen, K.D., Qiu, Y., Cui, X., Goh, Y.P., Mwangi, J., David, T., Mukundan, L., Brombacher, F., Locksley, R.M., and Chawla, A. (2011). Alternatively activated macrophages produce catecholamines to sustain adaptive thermogenesis. Nature *480*, 104-108.

Nilsson, I.M., Hartford, O., Foster, T., and Tarkowski, A. (1999). Alpha-toxin and gamma-toxin jointly promote Staphylococcus aureus virulence in murine septic arthritis. Infect Immun *67*, 1045-1049.

NOTT (1980). Continuous or nocturnal oxygen therapy in hypoxemic chronic obstructive lung disease: a clinical trial. Nocturnal Oxygen Therapy Trial Group. Ann Intern Med *93*, 391-398.

Nourshargh, S., and Williams, T.J. (1995). Molecular and cellular interactions mediating granulocyte accumulation in vivo. Semin Cell Biol *6*, 317-326.

Novick, R. (1967). Properties of a cryptic high-frequency transducing phage in Staphylococcus aureus. Virology *33*, 155-166.

Nusslein-Volhard, C. (2002). Zebrafish: a Practical Approach., 1st edition edn (Oxford, Oxford University Press).

O'Malley, Y.Q., Reszka, K.J., Spitz, D.R., Denning, G.M., and Britigan, B.E. (2004). Pseudomonas aeruginosa pyocyanin directly oxidizes glutathione and decreases its levels in airway epithelial cells. Am J Physiol Lung Cell Mol Physiol *287*, L94-103.

O'Rourke, J.F., Tian, Y.M., Ratcliffe, P.J., and Pugh, C.W. (1999). Oxygen-regulated and transactivating domains in endothelial PAS protein 1: comparison with hypoxia-inducible factor-1alpha. J Biol Chem *274*, 2060-2071.

Ortolani, O., Conti, A., De Gaudio, A.R., Moraldi, E., Cantini, Q., and Novelli, G. (2000). The effect of glutathione and N-acetylcysteine on lipoperoxidative damage in patients with early septic shock. Am J Respir Crit Care Med *161*, 1907-1911.

Park, S.K., Dadak, A.M., Haase, V.H., Fontana, L., Giaccia, A.J., and Johnson, R.S. (2003). Hypoxia-induced gene expression occurs solely through the action of hypoxia-inducible factor 1alpha (HIF-1alpha): role of cytoplasmic trapping of HIF-2alpha. Mol Cell Biol *23*, 4959-4971.

Parker, M.M., Shelhamer, J.H., Bacharach, S.L., Green, M.V., Natanson, C., Frederick, T.M., Damske, B.A., and Parrillo, J.E. (1984). Profound but reversible myocardial depression in patients with septic shock. Ann Intern Med *100*, 483-490.

Parsonnet, J., Gillis, Z.A., Richter, A.G., and Pier, G.B. (1987). A rabbit model of toxic shock syndrome that uses a constant, subcutaneous infusion of toxic shock syndrome toxin 1. Infect Immun *55*, 1070-1076.

Patel, S.A., and Simon, M.C. (2008). Biology of hypoxia-inducible factor-2alpha in development and disease. Cell Death Differ *15*, 628-634.

Peng, J., Zhang, L., Drysdale, L., and Fong, G.H. (2000). The transcription factor EPAS-1/hypoxia-inducible factor 2alpha plays an important role in vascular remodeling. Proc Natl Acad Sci U S A *97*, 8386-8391.

Percy, M.J., Beer, P.A., Campbell, G., Dekker, A.W., Green, A.R., Oscier, D., Rainey, M.G., van Wijk, R., Wood, M., Lappin, T.R.*, et al.* (2008a). Novel exon 12 mutations in the HIF2A gene associated with erythrocytosis. Blood *111*, 5400-5402.

Percy, M.J., Furlow, P.W., Lucas, G.S., Li, X., Lappin, T.R., McMullin, M.F., and Lee, F.S. (2008b). A gain-of-function mutation in the HIF2A gene in familial erythrocytosis. N Engl J Med *358*, 162-168.

Peres Bota, D., Lopes Ferreira, F., Melot, C., and Vincent, J.L. (2004). Body temperature alterations in the critically ill. Intensive Care Med *30*, 811-816.

Perlman, J.M. (2007). Pathogenesis of hypoxic-ischemic brain injury. J Perinatol *27*, S39-S46.

Peyssonnaux, C., Cejudo-Martin, P., Doedens, A., Zinkernagel, A.S., Johnson, R.S., and Nizet, V. (2007). Cutting edge: Essential role of hypoxia inducible factor-1alpha in development of lipopolysaccharide-induced sepsis. J Immunol *178*, 7516-7519.

Peyssonnaux, C., Datta, V., Cramer, T., Doedens, A., Theodorakis, E.A., Gallo, R.L., Hurtado-Ziola, N., Nizet, V., and Johnson, R.S. (2005). HIF-1alpha expression regulates the bactericidal capacity of phagocytes. J Clin Invest *115*, 1806-1815.

Pons, F., Williams, T.J., and Warren, J.B. (1993). Nitric oxide, but not interleukin-1, mediates the local blood flow response to lipopolysaccharide in rabbit skin. Eur J Pharmacol *239*, 23-30.

Pore, N., Jiang, Z., Shu, H.K., Bernhard, E., Kao, G.D., and Maity, A. (2006). Akt1 activation can augment hypoxia-inducible factor-1alpha expression by increasing protein translation through a mammalian target of rapamycin-independent pathway. Mol Cancer Res *4*, 471-479.

Pragman, A.A., Yarwood, J.M., Tripp, T.J., and Schlievert, P.M. (2004). Characterization of virulence factor regulation by SrrAB, a two-component system in Staphylococcus aureus. J Bacteriol *186*, 2430-2438.

Prasch, A.L., Tanguay, R.L., Mehta, V., Heideman, W., and Peterson, R.E. (2006). Identification of zebrafish ARNT1 homologs: 2,3,7,8-tetrachlorodibenzo-p-dioxin toxicity in the developing zebrafish requires ARNT1. Mol Pharmacol *69*, 776-787.

Prec, O., Rosenman, R., Braun, K., Rodbard, S., and Katz, L.N. (1949). THE CARDIOVASCULAR EFFECTS OF ACUTELY INDUCED HYPOTHERMIA 12. The Journal of Clinical Investigation *28*, 293-300.

Prince, L.R., Bianchi, S.M., Vaughan, K.M., Bewley, M.A., Marriott, H.M., Walmsley, S.R., Taylor, G.W., Buttle, D.J., Sabroe, I., Dockrell, D.H.*, et al.* (2008). Subversion of a lysosomal pathway

regulating neutrophil apoptosis by a major bacterial toxin, pyocyanin. J Immunol *180*, 3502-3511.

Quint, J.K., and Wedzicha, J.A. (2007). The neutrophil in chronic obstructive pulmonary disease. J Allergy Clin Immunol *119*, 1065-1071.

Rahn, H., and Otis, A.B. (1949). Continuous analysis of alveolar gas composition during work, hyperpnea, hypercapnia and anoxia. J Appl Physiol *1*, 717-724.

Raval, R.R., Lau, K.W., Tran, M.G., Sowter, H.M., Mandriota, S.J., Li, J.L., Pugh, C.W., Maxwell, P.H., Harris, A.L., and Ratcliffe, P.J. (2005). Contrasting properties of hypoxia-inducible factor 1 (HIF-1) and HIF-2 in von Hippel-Lindau-associated renal cell carcinoma. Mol Cell Biol *25*, 5675-5686.

Renshaw, S.A., Loynes, C.A., Trushell, D.M., Elworthy, S., Ingham, P.W., and Whyte, M.K. (2006). A transgenic zebrafish model of neutrophilic inflammation. Blood *108*, 3976-3978.

Renshaw, S.A., Timmons, S.J., Eaton, V., Usher, L.R., Akil, M., Bingle, C.D., and Whyte, M.K. (2000). Inflammatory neutrophils retain susceptibility to apoptosis mediated via the Fas death receptor. J Leukoc Biol *67*, 662-668.

Reszka, K.J., O'Malley, Y., McCormick, M.L., Denning, G.M., and Britigan, B.E. (2004). Oxidation of pyocyanin, a cytotoxic product from Pseudomonas aeruginosa, by microperoxidase 11 and hydrogen peroxide. Free Radic Biol Med *36*, 1448-1459.

Reutershan, J., and Ley, K. (2004). Bench-to-bedside review: acute respiratory distress syndrome - how neutrophils migrate into the lung. Crit Care *8*, 453-461.

Richalet, J.P., Larmignat, P., Rathat, C., Keromes, A., Baud, P., and Lhoste, F. (1988). Decreased cardiac response to isoproterenol infusion in acute and chronic hypoxia. J Appl Physiol *65*, 1957-1961.

Rittirsch, D., Flierl, M.A., and Ward, P.A. (2008). Harmful molecular mechanisms in sepsis. Nat Rev Immunol *8*, 776-787.

Rius, J., Guma, M., Schachtrup, C., Akassoglou, K., Zinkernagel, A.S., Nizet, V., Johnson, R.S., Haddad, G.G., and Karin, M. (2008). NF-kappaB links innate immunity to the hypoxic response through transcriptional regulation of HIF-1alpha. Nature *453*, 807-811.

Rivera, A.M., and Boucher, H.W. (2011). Current concepts in antimicrobial therapy against select gram-positive organisms: methicillin-resistant Staphylococcus aureus, penicillin-resistant pneumococci, and vancomycin-resistant enterococci. Mayo Clin Proc *86*, 1230-1243.

Rohlicek, C.V., Saiki, C., Matsuoka, T., and Mortola, J.P. (1998). Oxygen transport in conscious newborn dogs during hypoxic hypometabolism. J Appl Physiol *84*, 763-768.

Roos, D., van Bruggen, R., and Meischl, C. (2003). Oxidative killing of microbes by neutrophils. Microbes Infect *5*, 1307-1315.

Rossi, A.G., Sawatzky, D.A., Walker, A., Ward, C., Sheldrake, T.A., Riley, N.A., Caldicott, A., Martinez-Losa, M., Walker, T.R., Duffin, R.*, et al.* (2006). Cyclin-dependent kinase inhibitors

enhance the resolution of inflammation by promoting inflammatory cell apoptosis. Nat Med *12*, 1056-1064.

Rotstein, O.D., Fiegel, V.D., Simmons, R.L., and Knighton, D.R. (1988). The deleterious effect of reduced pH and hypoxia on neutrophil migration in vitro. J SurgRes *45*, 298-303.

Rowe, S.J., Allen, L., Ridger, V.C., Hellewell, P.G., and Whyte, M.K. (2002). Caspase-1-deficient mice have delayed neutrophil apoptosis and a prolonged inflammatory response to lipopolysaccharide-induced acute lung injury. J Immunol *169*, 6401-6407.

Rudaya, A.Y., Steiner, A.A., Robbins, J.R., Dragic, A.S., and Romanovsky, A.A. (2005). Thermoregulatory responses to lipopolysaccharide in the mouse: dependence on the dose and ambient temperature. Am J Physiol Regul Integr Comp Physiol *289*, R1244-1252.

Ryan, H.E., Lo, J., and Johnson, R.S. (1998). HIF-1 alpha is required for solid tumor formation and embryonic vascularization. EMBO J *17*, 3005-3015.

Sabroe, I., Jones, E.C., Usher, L.R., Whyte, M.K., and Dower, S.K. (2002). Toll-like receptor (TLR)2 and TLR4 in human peripheral blood granulocytes: a critical role for monocytes in leukocyte lipopolysaccharide responses. J Immunol *168*, 4701-4710.

Sanchez, M., Galy, B., Muckenthaler, M.U., and Hentze, M.W. (2007). Iron-regulatory proteins limit hypoxia-inducible factor-2alpha expression in iron deficiency. Nat Struct Mol Biol *14*, 420-426.

Savill, J. (1997). Apoptosis in resolution of inflammation. J Leukoc Biol *61*, 375-380.

Savill, J.S., Wyllie, A.H., Henson, J.E., Walport, M.J., Henson, P.M., and Haslett, C. (1989). Macrophage phagocytosis of aging neutrophils in inflammation. Programmed cell death in the neutrophil leads to its recognition by macrophages. J Clin Invest *83*, 865-875.

Sbarra, A.J., and Karnovsky, M.L. (1959). The biochemical basis of phagocytosis. I. Metabolic changes during the ingestion of particles by polymorphonuclear leukocytes. J Biol Chem *234*, 1355-1362.

Scheel-Toellner, D., Wang, K., Craddock, R., Webb, P.R., McGettrick, H.M., Assi, L.K., Parkes, N., Clough, L.E., Gulbins, E., Salmon, M*., et al.* (2004). Reactive oxygen species limit neutrophil life span by activating death receptor signaling. Blood *104*, 2557-2564.

Schlag, S., Fuchs, S., Nerz, C., Gaupp, R., Engelmann, S., Liebeke, M., Lalk, M., Hecker, M., and Gotz, F. (2008). Characterization of the oxygen-responsive NreABC regulon of Staphylococcus aureus. J Bacteriol *190*, 7847-7858.

Schoch, H.J., Fischer, S., and Marti, H.H. (2002). Hypoxia-induced vascular endothelial growth factor expression causes vascular leakage in the brain. Brain *125*, 2549-2557.

Schoene, R.B. (2008). Illnesses at high altitude. Chest *134*, 402-416.

Schofield, C.J., and Ratcliffe, P.J. (2004). Oxygen sensing by HIF hydroxylases. Nat Rev Mol Cell Biol *5*, 343-354.

Selak, M.A., Armour, S.M., MacKenzie, E.D., Boulahbel, H., Watson, D.G., Mansfield, K.D., Pan, Y., Simon, M.C., Thompson, C.B., and Gottlieb, E. (2005). Succinate links TCA cycle dysfunction to oncogenesis by inhibiting HIF-alpha prolyl hydroxylase. Cancer Cell *7*, 77-85.

Semenza, G.L. (2009). Involvement of oxygen-sensing pathways in physiologic and pathologic erythropoiesis. Blood *114*, 2015-2019.

Semenza, G.L., Jiang, B.H., Leung, S.W., Passantino, R., Concordet, J.P., Maire, P., and Giallongo, A. (1996). Hypoxia response elements in the aldolase A, enolase 1, and lactate dehydrogenase A gene promoters contain essential binding sites for hypoxia-inducible factor 1. J Biol Chem *271*, 32529-32537.

Semenza, G.L., and Wang, G.L. (1992). A nuclear factor induced by hypoxia via de novo protein synthesis binds to the human erythropoietin gene enhancer at a site required for transcriptional activation. Mol Cell Biol *12*, 5447-5454.

Sergeyeva, A., Gordeuk, V.R., Tokarev, Y.N., Sokol, L., Prchal, J.F., and Prchal, J.T. (1997). Congenital polycythemia in Chuvashia. Blood *89*, 2148-2154.

Serhan, C.N., Brain, S.D., Buckley, C.D., Gilroy, D.W., Haslett, C., O'Neill, L.A., Perretti, M., Rossi, A.G., and Wallace, J.L. (2007). Resolution of inflammation: state of the art, definitions and terms. FASEB J *21*, 325-332.

Sheu, C.C., Gong, M.N., Zhai, R., Bajwa, E.K., Chen, F., Thompson, B.T., and Christiani, D.C. (2010). The influence of infection sites on development and mortality of ARDS. Intensive Care Med *36*, 963-970.

Shinji, H., Yosizawa, Y., Tajima, A., Iwase, T., Sugimoto, S., Seki, K., and Mizunoe, Y. (2011). Role of fibronectin-binding proteins A and B in in vitro cellular infections and in vivo septic infections by Staphylococcus aureus. Infect Immun *79*, 2215-2223.

Shohet, I., Yellin, A., Meyerovitch, J., and Rubinstein, E. (1987). Pharmacokinetics and therapeutic efficacy of gentamicin in an experimental pleural empyema rabbit model. Antimicrob Agents Chemother *31*, 982-985.

Sibelius, U., Grandel, U., Buerke, M., Mueller, D., Kiss, L., Kraemer, H.J., Braun-Dullaeus, R., Haberbosch, W., Seeger, W., and Grimminger, F. (2000). Staphylococcal alpha-toxin provokes coronary vasoconstriction and loss in myocardial contractility in perfused rat hearts: role of thromboxane generation. Circulation *101*, 78-85.

Sigma-Aldrich (1998a). Product Information - Percoll   (Saint Louis, Missouri).

Sigma-Aldrich (1998b). Product Information - Zymosan A from Saccharomyces cerevisiae (Saint Louis, Missouri).

Silver, I.A. (1977). Tissue PO2 changes in acute inflammation. Adv Exp Med Biol *94*, 769-774.

Simmons, G.H., Barrett-O'Keefe, Z., Minson, C.T., and Halliwill, J.R. (2011). Cutaneous vascular and core temperature responses to sustained cold exposure in hypoxia. Exp Physiol *96*, 1062-1071.

Simms, H.H., and D'Amico, R. (1994). Regulation of whole blood polymorphonuclear leukocyte phagocytosis following hypoxemia and hypoxemia/reoxygenation. Shock *1*, 10-18.

Simpson, H.K., Clancy, M., Goldfrad, C., and Rowan, K. (2005). Admissions to intensive care units from emergency departments: a descriptive study. Emergency Medicine Journal *22*, 423-428.

Singer, M., De Santis, V., Vitale, D., and Jeffcoate, W. (2004). Multiorgan failure is an adaptive, endocrine-mediated, metabolic response to overwhelming systemic inflammation. Lancet *364*, 545-548.

Smith, T.G., Brooks, J.T., Balanos, G.M., Lappin, T.R., Layton, D.M., Leedham, D.L., Liu, C., Maxwell, P.H., McMullin, M.F., McNamara, C.J.*, et al.* (2008). Mutation of the von Hippel-Lindau gene alters human cardiopulmonary physiology. Adv Exp Med Biol *605*, 51-56.

Somerville, G.A., and Proctor, R.A. (2009). At the crossroads of bacterial metabolism and virulence factor synthesis in Staphylococci. Microbiol Mol Biol Rev *73*, 233-248.

Spronk, P.E., Zandstra, D.F., and Ince, C. (2004). Bench-to-bedside review: sepsis is a disease of the microcirculation. Crit Care *8*, 462-468.

Stearns-Kurosawa, D.J., Osuchowski, M.F., Valentine, C., Kurosawa, S., and Remick, D.G. (2011). The pathogenesis of sepsis. Annu Rev Pathol *6*, 19-48.

Stroka, D.M., Burkhardt, T., Desbaillets, I., Wenger, R.H., Neil, D.A., Bauer, C., Gassmann, M., and Candinas, D. (2001). HIF-1 is expressed in normoxic tissue and displays an organ-specific regulation under systemic hypoxia. FASEB J *15*, 2445-2453.

Sun, F., Ji, Q., Jones, M.B., Deng, X., Liang, H., Frank, B., Telser, J., Peterson, S.N., Bae, T., and He, C. (2012). AirSR, a [2Fe-2S] cluster-containing two-component system, mediates global oxygen sensing and redox signaling in Staphylococcus aureus. J Am Chem Soc *134*, 305-314.

Supinski, G.S., Murphy, M.P., and Callahan, L.A. (2009). MitoQ administration prevents endotoxin-induced cardiac dysfunction. American Journal of Physiology - Regulatory, Integrative and Comparative Physiology *297*, R1095-R1102.

Takeda, N., O'Dea, E.L., Doedens, A., Kim, J.W., Weidemann, A., Stockmann, C., Asagiri, M., Simon, M.C., Hoffmann, A., and Johnson, R.S. (2010). Differential activation and antagonistic function of HIF-{alpha} isoforms in macrophages are essential for NO homeostasis. Genes Dev *24*, 491-501.

Tamber, S., Reyes, D., Donegan, N.P., Schwartzman, J.D., Cheung, A.L., and Memmi, G. (2010). The staphylococcus-specific gene rsr represses agr and virulence in Staphylococcus aureus. Infect Immun *78*, 4384-4391.

Tamura, D.Y., Moore, E.E., Partrick, D.A., Johnson, J.L., Offner, P.J., and Silliman, C.C. (2002). Acute hypoxemia in humans enhances the neutrophil inflammatory response. Shock *17*, 269-273.

Taylor, C.T. (2008). Interdependent roles for hypoxia inducible factor and nuclear factor-kappaB in hypoxic inflammation. J Physiol *586*, 4055-4059.

Taylor, C.T., and Colgan, S.P. (2007). Hypoxia and gastrointestinal disease. J Mol Med *85*, 1295-1300.

Taylor, C.T., and McElwain, J.C. (2010). Ancient atmospheres and the evolution of oxygen sensing via the hypoxia-inducible factor in metazoans. Physiology (Bethesda) *25*, 272-279.

Taylor, W.F., and Bishop, V.S. (1993). A role for nitric oxide in active thermoregulatory vasodilation. Am J Physiol *264*, H1355-1359.

Theilgaard-Monch, K., Jacobsen, L.C., Borup, R., Rasmussen, T., Bjerregaard, M.D., Nielsen, F.C., Cowland, J.B., and Borregaard, N. (2005). The transcriptional program of terminal granulocytic differentiation. Blood *105*, 1785-1796.

Thisse, C., and Thisse, B. (2008). High-resolution in situ hybridization to whole-mount zebrafish embryos. Nat Protoc *3*, 59-69.

Thorley, A.J., Ford, P.A., Giembycz, M.A., Goldstraw, P., Young, A., and Tetley, T.D. (2007). Differential regulation of cytokine release and leukocyte migration by lipopolysaccharide-stimulated primary human lung alveolar type II epithelial cells and macrophages. J Immunol *178*, 463-473.

Tian, H., Hammer, R.E., Matsumoto, A.M., Russell, D.W., and McKnight, S.L. (1998). The hypoxia-responsive transcription factor EPAS1 is essential for catecholamine homeostasis and protection against heart failure during embryonic development. Genes Dev *12*, 3320-3324.

Tian, H., McKnight, S.L., and Russell, D.W. (1997). Endothelial PAS domain protein 1 (EPAS1), a transcription factor selectively expressed in endothelial cells. Genes Dev *11*, 72-82.

Tracey, K.J. (2002). The inflammatory reflex. Nature *420*, 853-859.

Ullrich, R., Scherrer-Crosbie, M., Bloch, K.D., Ichinose, F., Nakajima, H., Picard, M.H., Zapol, W.M., and Quezado, Z.M. (2000). Congenital deficiency of nitric oxide synthase 2 protects against endotoxin-induced myocardial dysfunction in mice. Circulation *102*, 1440-1446.

van Belkum, A., Melles, D.C., Nouwen, J., van Leeuwen, W.B., van Wamel, W., Vos, M.C., Wertheim, H.F., and Verbrugh, H.A. (2009). Co-evolutionary aspects of human colonisation and infection by Staphylococcus aureus. Infect Genet Evol *9*, 32-47.

van Uden, P., Kenneth, N.S., and Rocha, S. (2008). Regulation of hypoxia-inducible factor-1alpha by NF-kappaB. Biochem J *412*, 477-484.

Vaupel, P. (2004). Tumor microenvironmental physiology and its implications for radiation oncology. Semin Radiat Oncol *14*, 198-206.

Vaupel, P., Schlenger, K., Knoop, C., and Hockel, M. (1991). Oxygenation of human tumors: evaluation of tissue oxygen distribution in breast cancers by computerized O2 tension measurements. Cancer Res *51*, 3316-3322.

Viault, F. (1890). Sur l'augmentation considérable du nombre des globules rouges dans le sang chez les habitants des hauts plateaux de 1'Amérique du Sud. Comptes Rendus Hebdomaires des Seances de l'Académie des Sciences, Paris *111*, 917-918.

Vissers, M.C., and Wilkie, R.P. (2007). Ascorbate deficiency results in impaired neutrophil apoptosis and clearance and is associated with up-regulation of hypoxia-inducible factor 1alpha. J Leukoc Biol *81*, 1236-1244.

Vlach, K.D., Boles, J.W., and Stiles, B.G. (2000). Telemetric evaluation of body temperature and physical activity as predictors of mortality in a murine model of staphylococcal enterotoxic shock. Comp Med *50*, 160-166.

Wagner, P.D., and West, J.B. (2005). Ventilation, blood flow and gas exchange. In Murray and Nadel's Textbook of Respiratory Medicine, J.F. Murray, R.J. Mason, V.C. Broaddus, and J.A. Nadel, eds. (Philadelphia, Elsevier Saunders), pp. 51-86.

Walmsley, S.R., Chilvers, E.R., Thompson, A.A., Vaughan, K., Marriott, H.M., Parker, L.C., Shaw, G., Parmar, S., Schneider, M., Sabroe, I*., et al.* (2011). Prolyl hydroxylase 3 (PHD3) is essential for hypoxic regulation of neutrophilic inflammation in humans and mice. J Clin Invest *121*, 1053-1063.

Walmsley, S.R., Cowburn, A.S., Clatworthy, M.R., Morrell, N.W., Roper, E.C., Singleton, V., Maxwell, P., Whyte, M.K., and Chilvers, E.R. (2006). Neutrophils from patients with heterozygous germline mutations in the von Hippel Lindau protein (pVHL) display delayed apoptosis and enhanced bacterial phagocytosis. Blood *108*, 3176-3178.

Walmsley, S.R., Print, C., Farahi, N., Peyssonnaux, C., Johnson, R.S., Cramer, T., Sobolewski, A., Condliffe, A.M., Cowburn, A.S., Johnson, N*., et al.* (2005). Hypoxia-induced neutrophil survival is mediated by HIF-1alpha-dependent NF-kappaB activity. J Exp Med *201*, 105-115.

Wang, G.L., Jiang, B.H., Rue, E.A., and Semenza, G.L. (1995). Hypoxia-inducible factor 1 is a basic-helix-loop-helix-PAS heterodimer regulated by cellular O2 tension. Proc Natl Acad Sci U S A *92*, 5510-5514.

Wang, G.L., and Semenza, G.L. (1995). Purification and characterization of hypoxia-inducible factor 1. J Biol Chem *270*, 1230-1237.

Wang, J.S., and Liu, H.C. (2009). Systemic hypoxia enhances bactericidal activities of human polymorphonuclear leuocytes. Clin Sci (Lond) *116*, 805-817.

Ward, C., Chilvers, E.R., Lawson, M.F., Pryde, J.G., Fujihara, S., Farrow, S.N., Haslett, C., and Rossi, A.G. (1999). NF-kappaB activation is a critical regulator of human granulocyte apoptosis in vitro. J Biol Chem *274*, 4309-4318.

Warnecke, C., Weidemann, A., Volke, M., Schietke, R., Wu, X., Knaup, K.X., Hackenbeck, T., Bernhardt, W., Willam, C., Eckardt, K.U*., et al.* (2008). The specific contribution of hypoxia-inducible factor-2alpha to hypoxic gene expression in vitro is limited and modulated by cell type-specific and exogenous factors. Exp Cell Res *314*, 2016-2027.

Webb, J.D., Coleman, M.L., and Pugh, C.W. (2009). Hypoxia, hypoxia-inducible factors (HIF), HIF hydroxylases and oxygen sensing. Cell Mol Life Sci, [Epub ahead of print].

Wei, X.-q., Charles, I.G., Smith, A., Ure, J., Feng, G.-j., Huang, F.-p., Xu, D., MullersWerner, Moncada, S., and Liew, F.Y. (1995). Altered immune responses in mice lacking inducible nitric oxide synthase. Nature *375*, 408-411.

Welsh, S.J., and Powis, G. (2003). Hypoxia inducible factor as a cancer drug target. Curr Cancer Drug Targets *3*, 391-405.

Whyte, M.K., Meagher, L.C., MacDermot, J., and Haslett, C. (1993). Impairment of function in aging neutrophils is associated with apoptosis. J Immunol *150*, 5124-5134.

Wiesener, M.S., Jurgensen, J.S., Rosenberger, C., Scholze, C.K., Horstrup, J.H., Warnecke, C., Mandriota, S., Bechmann, I., Frei, U.A., Pugh, C.W.*, et al.* (2003). Widespread hypoxia-inducible expression of HIF-2alpha in distinct cell populations of different organs. FASEB J *17*, 271-273.

Wiesener, M.S., Turley, H., Allen, W.E., Willam, C., Eckardt, K.U., Talks, K.L., Wood, S.M., Gatter, K.C., Harris, A.L., Pugh, C.W.*, et al.* (1998). Induction of endothelial PAS domain protein-1 by hypoxia: characterization and comparison with hypoxia-inducible factor-1alpha. Blood *92*, 2260-2268.

Witko-Sarsat, V., Pederzoli-Ribeil, M., Hirsch, E., Sozzani, S., and Cassatella, M.A. (2011). Regulating neutrophil apoptosis: new players enter the game. Trends Immunol *32*, 117-124.

Wong, A.C., and Bergdoll, M.S. (1990). Effect of environmental conditions on production of toxic shock syndrome toxin 1 by Staphylococcus aureus. Infect Immun *58*, 1026-1029.

Wood, S.C. (1991). Interactions between hypoxia and hypothermia. Annu Rev Physiol *53*, 71-85.

Wood, S.C., and Stabenau, E.K. (1998). Effect of gender on thermoregulation and survival of hypoxic rats. Clin Exp Pharmacol Physiol *25*, 155-158.

Worlitzsch, D., Tarran, R., Ulrich, M., Schwab, U., Cekici, A., Meyer, K.C., Birrer, P., Bellon, G., Berger, J., Weiss, T.*, et al.* (2002). Effects of reduced mucus oxygen concentration in airway Pseudomonas infections of cystic fibrosis patients. J Clin Invest *109*, 317-325.

Wyllie, A.H., Kerr, J.F., and Currie, A.R. (1980). Cell death: the significance of apoptosis. Int Rev Cytol *68*, 251-306.

Yan, Q., Bartz, S., Mao, M., Li, L., and Kaelin, W.G., Jr. (2007). The hypoxia-inducible factor 2alpha N-terminal and C-terminal transactivation domains cooperate to promote renal tumorigenesis in vivo. Mol Cell Biol *27*, 2092-2102.

Ye, J., Wang, S., Leonard, S.S., Sun, Y., Butterworth, L., Antonini, J., Ding, M., Rojanasakul, Y., Vallyathan, V., Castranova, V.*, et al.* (1999). Role of reactive oxygen species and p53 in chromium(VI)-induced apoptosis. J Biol Chem *274*, 34974-34980.

Yoon, D., Pastore, Y.D., Divoky, V., Liu, E., Mlodnicka, A.E., Rainey, K., Ponka, P., Semenza, G.L., Schumacher, A., and Prchal, J.T. (2006). Hypoxia-inducible factor-1 deficiency results in dysregulated erythropoiesis signaling and iron homeostasis in mouse development. J Biol Chem *281*, 25703-25711.

Yu, A.Y., Shimoda, L.A., Iyer, N.V., Huso, D.L., Sun, X., McWilliams, R., Beaty, T., Sham, J.S., Wiener, C.M., Sylvester, J.T.*, et al.* (1999). Impaired physiological responses to chronic hypoxia in mice partially deficient for hypoxia-inducible factor 1alpha. J Clin Invest *103*, 691-696.

Zernecke, A., Bot, I., Djalali-Talab, Y., Shagdarsuren, E., Bidzhekov, K., Meiler, S., Krohn, R., Schober, A., Sperandio, M., Soehnlein, O.*, et al.* (2008). Protective role of CXC receptor 4/CXC ligand 12 unveils the importance of neutrophils in atherosclerosis. Circ Res *102*, 209-217.

Zervos, M.J., Freeman, K., Vo, L., Haque, N., Pokharna, H., Raut, M., and Kim, M. (2012). Epidemiology and outcomes of complicated skin and soft tissue infections in hospitalized patients. J Clin Microbiol *50*, 238-245.

Zhang, J., Liu, W., Ye, P., and D'Ercole, A.J. (2007). Pitfalls of PCR-based strategy for genotyping cre-loxP mice. Biotechniques *42*, 281, 283.

Ziebandt, A.K., Becher, D., Ohlsen, K., Hacker, J., Hecker, M., and Engelmann, S. (2004). The influence of agr and sigmaB in growth phase dependent regulation of virulence factors in Staphylococcus aureus. Proteomics *4*, 3034-3047.

Zinkernagel, A.S., Peyssonnaux, C., Johnson, R.S., and Nizet, V. (2008). Pharmacologic augmentation of hypoxia-inducible factor-1alpha with mimosine boosts the bactericidal capacity of phagocytes. J Infect Dis *197*, 214-217.

7 Appendices

7.1 Appendix I – Mastermix constituents by application

7.1.1 cDNA synthesis

All reagents were from Promega (Promega UK, Southampton). For every 1 μg of human RNA or 500 ng of murine RNA in water, made up to a total volume of 12.4 μl, the following mastermix was added to generate cDNA:

8μl	5x AMV RT buffer
16μl	10mM dNTPs
1.2μl	RNasin®
1.2μl	random primers
1.2μl	AMV reverse transcriptase

7.1.2 Polymerase chain reaction – human and murine cDNA samples

All reagents were from Promega with the exception of the primers (see Appendix II). 2 μl of each sample was added to the following mastermix giving a total volume of 25 μl per reaction:

5 μl	5x GoTaq® flexi green buffer
1.5 μl	magnesium chloride
1 μl	10 mM dNTPs
0.7 μl	10 μM forward primer
0.7 μl	10 μM reverse primer
0.25 μl	GoTaq® flexi DNA polymerase
13.85 μl	dH$_2$O

7.1.3 Real time polymerase chain reaction – human and murine cDNA

For Applied Biosystems primer/probe sets, 1 μl of cDNA was added to 19 μl of mastermix per reaction. The real time PCR mastermix consisted of:

10 μl	2x qPCR MasterMix Plus (Eurogentec Ltd.)
8 μl	H$_2$O
1 μl	primer/probe mix

Mastermix for Sigma-Aldrich custom made primers and probes per reaction using 1 μl of cDNA:

10 μl	2x 1PCR MasterMix Plus
0.1 μl	sense primer
0.1 μl	anti-sense primer
0.02 μl	probe
8.78 μl	H$_2$O

7.2 Appendix II - Primer and probe sequences

7.2.1 Primers for standard polymerase chain reaction – Human

Custom primers were designed for the following targets and supplied by Eurogentec (Eurogentec Ltd., Southampton, UK):

Target gene name	Sequence (5'->3')	Product size
Hypoxia inducible factor 2 (*HIF2A*)	F- CCAGACGTGCTGAGTCCGGC R- GGCTTGCCATGCCTGACACCTT	400 bp
Glyceraldehyde-3-phosphate dehydrogenase (*GAPDH*)	F- ACTTTGGTATCGTGGAAGGAC R- TGGTCGTTGAGGGCAATG	418 bp

7.2.2 Primers for standard polymerase chain reaction – Murine

Custom primers were designed for the following targets and supplied by Eurogentec (Eurogentec Ltd., Southampton, UK):

Target gene name	Sequence (5'->3')	Product size
Hypoxia inducible factor 2 (*Hif2a*)	F- TAAAGCGGCAGCTGGAGTAT R- AGCTCCTGGAGGACCGTAGT	326 bp
Beta-actin (*Actb*)	F- TTCTTTGCAGCTCCTTCGTTGCCG R- TGGATGGCTACGTACATGGCTGGG	457 bp

7.2.3 Primers for real time polymerase chain reaction - Human

Commercially available primer probe sets were obtained from Applied Biosystems (Applied Biosystems, Foster, USA) for the following target transcripts:

Target gene name	TaqMan assay ID
Hypoxia inducible factor 1, alpha subunit (*HIF1A*)	HS00153153_m1
Plasminogen activator inhibitor type 1 (*PAI-1*)	HS01126606_m1
Vascular endothelial growth factor A (*VEGF*)	HS00900054_m1
Beta-actin (*ACTB*)	HS99999903_m1

Primers and 6-FAM labelled probes were designed for the following targets and obtained from Sigma-Aldrich (Sigma-Aldrich Company Ltd., Gillingham, UK):

Target gene name		Sequence
Prolyl hydroxylase 3	Sense	5' AGTCCGGAAACGGGTCGTGGAG 3
(*PHD3*)	Antisense	5' AGCGTCGGGGACAAGGGAAAGTT 3'
	Probe	5' TCCGCACCACTCCCGCTGGTTCCCGAAG 3'
Hypoxia inducible factor 2	Sense	5' CTCCCACGGCTGTACGGACAC 3'
(*HIF2A*)	Antisense	5' AGTGCTCCCGCTGAATGACTCCACT 3'
	Probe	5'CTCGGATTGTCACACCTATGGCAT 3'

7.2.4 Primers for real time polymerase chain reaction - Murine

Commercially available primer probe sets were obtained from Applied Biosystems (Applied Biosystems, Foster, USA) for the following target transcripts:

Target gene name	TaqMan assay ID
Hypoxia inducible factor 1, alpha subunit (*Hif1a*)	Mm00468869_m1
Hypoxia inducible factor 2, alpha subunit (*Hif2a*)	Mm00438717_m1
Beta actin (*Actb*)	Mm00607939_s1

7.3 Appendix III - Polymerase chain reaction cycling conditions

Polymerase chain reactions were carried out using a DNA *Engine*™(PTC-200, MJ Research, Watertown, USA). Conditions were as follows:

Step 1   94˚C   for 5 minutes

Step 2   35 cycles of
                    94˚C   for 30 seconds
                    *Annealing temperature   for 60 seconds
                    72˚C   for 30 seconds

Step 3   72˚C   for 2 minutes

*Optimal annealing temperatures for the primers in Appendix II are shown below:

HIF2A   57˚C
GAPDH   50˚C
Hif2a   50˚C
Actb   50˚C

7.4 Appendix IV – Cell lysis buffers

7.4.1 Sonication lysis buffer (made up in water)

Ingredient	Molarity
1M Tris-HCl pH 7.8 (Bio-Rad Laboratories, Hemel Hempstead, UK)	0.1
EDTA (Sigma-Aldrich Company Ltd., Gillingham, UK)	0.0015
Potassium Chloride (Sigma-Aldrich Company Ltd., Gillingham, UK)	0.01
1,4-Dithio-DL-threitol (DTT) (Fluka Chemie, Buchs, Switzerland)	0.0005
Sodium orthovanadate (Sigma-Aldrich Company Ltd., Gillingham, UK)	0.001
Tetramisole (Sigma-Aldrich Company Ltd., Gillingham, UK)	0.002

Immediately before use the following were added:

Ingredient	Molarity
Complete mini EDTA-free protease inhibitor cocktail tablets (1 tablet in 1 ml water) (Roche Applied Science, Mannheim, Germany)	1:20
Phenylmethanesulfonyl fluoride (PMSF) (Sigma-Aldrich Company Ltd., Gillingham, UK)	1:100

7.4.2 2X SDS lysis buffer (made up in water)

Ingredient	Concentration
1,4-Dithio-DL-threitol (DTT)	0.2 M
20% Sodium dodecyl sulphate (SDS) solution (Fisher Bioreagents®, Fisher Scientific)	4%
Glycerol bi-distilled (AnalaR NORMAPUR, VWR International, Leuven, Belgium)	20%
0.5 M Tris-HCl buffer pH 6.8 (Bio-Rad Laboratories, Hemel Hempstead, UK)	0.1 M
Bromophenol Blue (Fissons scientific equipment, Loughborough, UK)	0.04%
Complete mini EDTA-free protease inhibitor cocktail tablets (1 tablet in 1 ml water)	2%

7.5   Appendix V – Western blot buffers

7.5.1   Resolving Gel – 8% (makes 2 x 1.5 mm gels)

Water	12ml
40% Acrylamide	4.5ml
(AccuGel™ 29:1, Geneflow Ltd, Fradley, UK)	
1.5 M Tris-HCl buffer pH 8.0	5.7ml
(Bio-Rad Laboratories, Hemel Hempstead, UK)	
20% Sodium dodecyl sulphate (SDS) solution	112.5μl
20% Ammonium persulphate (APS)	225μl
(Fisher Bioreagents®, Fisher Scientific)	
Tetramethyl-ethylenediamine (TEMED)	9μl
(Fisher Bioreagents®, Fisher Scientific)	

7.5.2   Stacking Gel (makes 2 x 1.5 mm gels)

Water	6ml
40% Acrylamide	1240μl
0.5 M Tris-HCl buffer pH 6.8	2520μl
(Bio-Rad Laboratories, Hemel Hempstead, UK)	
20% SDS	50μl
20% APS	100μl
TEMED	10μl

7.5.3   Running buffer (10 X)

Glycine	190g
(AnalaR NORMAPUR VWR International, Leuven, Belgium)	
TRIS-(hydroxymethyl) aminomethane	30.3g
(AnalaR NORMAPUR, VWR International, Leuven, Belgium)	
20% SDS	50ml
Water	to 1 litre

7.5.4   Transfer buffer (10 X)

Glycine	14.5g
TRIS-(hydroxymethyl) aminomethane	29g
20% SDS	9.25ml
Water	to 400ml

7.5.5   Transfer Buffer (1 X)

Made immediately before use

10 X Transfer Buffer	10ml
Methanol	20ml
Water	70ml

7.5.6   Tris-buffered saline (TBS) (10 X)

1M Tris-HCl pH 8.0   100ml
(Bio-Rad Laboratories, Hemel Hempstead, UK)
 Sodium Chloride   97.3g
(Sigma-Aldrich Company Ltd., Gillingham, UK)
 Water   to 1000ml

7.5.7   TBS with Tween (10 X)

As for TBS with 5 ml Electran Tween®-20
(VWR International, Haasrode Belgium)

7.5.8   Blocking Solution

 Skimmed Milk Powder (Marvel)   5g
 (Premier International Foods, Spalding, UK)
 TBS   100ml

7.6   Appendix VI - Antibody concentrations used for Western blotting

Target	Size (kDa)	Dilution	Secondary	Dilution
HIF-1α Mouse monoclonal Clone 54, 250 µg/ml (BD transduction laboratories™)	120	1:200	Horse anti-mouse IgG, HRP-linked antibody (#7076, Cell Signaling Technology®, New England Biolabs UK Ltd, Hitchin, UK)	1:2000
HIF-2α Mouse monoclonal Clone ep190b, 1.6 mg/ml (Novus biologicals, Cambridge, UK)	120	1:200	Horse anti-mouse IgG, HRP-linked antibody	1:2000
Anti-p38 MAPK Rabbit polyclonal (Cell signalling Technology®)	40	1:1000	Goat anti-rabbit HRP-linked antibody (P0448, Dako UK Ltd, Ely, UK)	1:2000

7.7 Appendix VII – Zebrafish primer and probe sequences

Primers used to PCR amplify zebrafish *epas1a, epas1b* and the dominant constructs.

Product	Sequence (5'->3')
epas1a	F- CACACCTGGACAAAGCCTCT
	R- CTGATTGCTCACCCCTGTTT
epas1b	F- AGAGCGGCGTAAGGAGAAAT
	R- GGATGAAGAGGGTGAATGGA
epas1a Δ330	F- TCATGAGACTGGCTATCAGC
	R- ATCGATTCAGGAGTTGCGGCTGTTGTA
epas1b Δ330	F- TCATGAGACTGGCTATCAGC
	R- ATCGATTCAGGAGTTGCGGCTGTTGTA
epas1a P347A	F- TAGCGCAGTTAGCGGCTATGCCAGGAGAC
	R- GTCTCCTGGCATAGCCGCTAACTGCGCTA
epas1a P481G	F- CCTGGAGACTCTCGCTGGATACATCCCAATGGAC
	R- GTCCATTGGGATGTATCCAGCGAGAGTCTCCAGG
epas1a N753A	F- GCGATATGACTGTGAGGTAGCCATGCCTCTACAAGGAAAC
	R- GTTTCCTTGTAGAGGCATGGCTACCTCACAGTCATATCGC
epas1b P343A	F- ACGCAGCTGGCAGCTACACCTGGGG
	R- CCCCAGGTGTAGCTGCCAGCTGCGT
epas1b P469G	F- ACTTGGAGACACTGGCTGGCTATATCCCCATGGATG
	R- CATCCATGGGGATATAGCCAGCCAGTGTCTCCAAGT
epas1b N755A	F- TTACGACTGCGAGGTCGCTGTCCCGTTGCAAGGC
	R- GCCTTGCAACGGGACAGCGACCTCGCAGTCGTAA
epas1a G487R	F- ACATCCCAATGGACCGCGAGGACTTCCAG
	R- CTGGAAGTCCTCGCGGTCCATTGGGATGT
epas1a G487W	F- ATACATCCCAATGGACTGGGAGGACTTCCAGCTGC
	R- GCAGCTGGAAGTCCTCCCAGTCCATTGGGATGTAT

7.8 Appendix VIII – Murine genotyping

7.8.1 Primers used to genotype transgenic murine colonies.

Target	Sequence (5'->3')	Product sizes
Hif1a^{flox/flox}	F- GCAAAGAGCACTAGTTG	200 bp (wild type allele)
	R- GGAGCTATCTCTCTAGACC	250 bp (floxed allele)
LysMCre recombinase	F- TGCAAGTTGAATAACCGGAAA	250 bp
	R- CTAGAGCCTGTTTTGCACGTT C	
Hif2a^{flox/flox}	1- CAGGCAGTATGCCTGGCTAATTCCAGTT	410 bp (wild type allele)
	2- CTTCTTCCATCATCTGGGATCTGGGACT	444 bp (2-loxP band)
	3- GCTAACACTGTACTGTCTGAAAGAGTAGC	340 bp (1-loxP band)

7.8.2 Mastermix for PCR reaction – murine genomic DNA.

1 µl of cDNA was diluted in 4 µl H_2O. This was added to 15 µl of the following mastermix:

2 µl	10x PCR buffer (Bioline reagents Ltd., London, UK)
0.8 µl	50 mM magnesium chloride
0.16 µl	25 mM dNTP mix (Bioline reagents Ltd.)
0.4 µl	10 µM forward primer
0.4 µl	10 µM reverse primer
0.3 µl	5u/µl Taq DNA polymerase (Bioline reagents Ltd.)
10.54 µl	dH_2O

7.8.3 PCR cycling conditions.

94°C	5 min	
94°C	30 sec	⎤
58°C	30 sec	⎬ x 35 cycles
72°C	1 min	⎦
72°C	10 min	
4°C	hold	

7.9 Appendix IX – Primary antibodies used for immunohistochemistry

Target	Tissues	Dilution
HIF-2α	Human lung	1:50
Mouse monoclonal	Mouse lung	1:50
Clone ep190b, 1.6 mg/ml		
(Novus biologicals, Cambridge, UK)		
Myeloperoxidase	Mouse skin	1:50
Rabbit polyclonal	Mouse lung	1:50
(Abcam, Cambridge, UK)		
Ly6G	Mouse heart	1:150
Rat monoclonal		
Clone RB6-8C5, 0.5mg/ml		
(BB Pharmingen, Oxford, UK)		

7.10 Appendix X – Mouse IgM ELISA buffers

7.10.1 Coating buffer

0.05 M Carbonate-Bicarbonate, pH 9.6
(Sigma-Aldrich Company Ltd., Gillingham, UK)

7.10.2 Wash solution

50 mM Tris HCl, pH 8.0
(Bio-Rad Laboratories, Hemel Hempstead, UK)
0.14 M NaCl
0.05% Tween 20

7.10.3 Blocking solution

50 mM Tris HCl, pH 8.0
0.14 M NaCl
1% bovine serum albumin
(Sigma-Aldrich Company Ltd., Gillingham, UK)

7.11 Appendix XI – Mouse sickness scoring

7.11.1 Sickness score 1

A single score was applied to each animal as follows:

A normal and unremarkable condition = 0

Slight illness, defined as lethargy and ruffled fur = 1

Moderate illness, defined as severe lethargy, ruffled fur,
and hunched back = 2

Severe illness, with the above signs plus exudative
accumulation around partially closed eyes = 3

Moribund state = 4

Death = 5

7.11.2 Sickness score 2

Several aspects of appearance and behaviour were assessed and the scores for each category

totalled to provide the final value.

Score	0	1	2	3
Coat	Normal	Rough/Lack of grooming	Unkempt, thin, wounds Staring coat	Loss of fur
Activity	Normal	Isolated, abnormal posture	Huddled/inactive OR overactive	Moribund or fitting
Breathing	Normal	Rapid, shallow	Rapid, abdominal	Laboured, blue
Dehydration	Nil	Skin less elastic	Skin tents	Skin tents, eyes sunken
Movement	Normal	Slight uncoordination / abnormality	Uncoordinated, reluctant to move	Staggering, paralysis, limb dragging